UNDERSTANDING THE SENSORY PERCEPTION OF HYDROCOLLOID THICKENED SYSTEMS BASED ON FLOW AND LUBRICATION BEHAVIOUR

By

Qi He, MSc.

Thesis submitted to the University of Nottingham
for the degree of Doctor of Philosophy

Division of Food Sciences
School of Biosciences
University of Nottingham
Loughborough
LE12 5RD

November 2013

ACKNOWLEDGEMENT

My first and sincere appreciation goes to my supervisors: Dr. Bettina Wolf and Professor Joanne Hort, for their help, patience, support and encouragement through my PhD study. This thesis would not have been possible without their help. I would like to thank Professor Joanne Hort for her kindness guidance for sensory studies. Special thanks go to Dr Bettina Wolf for teaching me so many things in Rheology and kindness answers for all my silly questions. It was such a wonderful experience for me to have this opportunity to work with both of you.

I would like to thank Dr Louise Hewson for her help with the sensory studies and valuable discussions. I also would like to thank Dr Rob Linforth for his help in teaching me using the APCI-MS and also statistical software. I would also like to thank Chi Zhang for her valuable discussions. I also must thank Helen Allen for her support during the sensory study and also the hard work from external panels, without whom, this thesis would not have been possible.

I must express my gratitude to the friends in Food Science: Candy, Nicole, Steve, Nathalie, Henghui, Zarani, Amit thanks for your encouragement and support!

Finally I would like give my greatest thanks to my family: thanks to my parents and my brother for their endless love and support! Special thanks to my Fiancée Qian Liu for always be there cheering me up and stood by me through the good times and bad!

ABSTRACT

This thesis seeks for a better understanding of the sensory properties of hydrocolloid thickened foods during oral processing through studying both flow and lubrication behaviours. In addition, during oral processing, saliva plays an important part through mixing with samples, and it is therefore the mixture of foods and saliva that is perceived. However, the role of saliva in sensory perception is not fully elucidated. This research also features a preliminary study on both flow and lubrication properties of saliva in presence of the 5 basic tastants and also how lubrication properties of hydrocolloids are changed when mixing with saliva.

Two groups of five samples were designed to have either similar viscosity at a shear rate of 50 s^{-1} or 10^5 s^{-1} by varying the concentrations of xanthan and dextran with the aim to find out which shear rate(s) is related to mouthfeel perceptions. Samples had the same levels of sucrose and banana flavour (isoamyl acetate) added to them and the flavour release and in mouth perceptions measured. The flow behaviour of samples were further characterised in small amplitude dynamic oscillatory shear and stretch flow. A trained sensory panel generated and evaluated mouthfeel, aroma and taste attributes of these solutions. Sensory results indicated that both low and high shear viscosity were related to mouthfeel perceptions. Models including both low and high shear viscosity values predicted the 'Thickness' perceptions better

than the models including a single shear viscosity. Stickiness and mouthcoating perceptions were better predicted through models including both low shear viscosity and extensional viscosity. Mouthfeel perceptions were also found to be related to complex viscosity at angular frequency of 100 rad.s^{-1}. In terms of sweetness perception, it was affected by the low shear viscosity. However, for samples having similar low shear viscosity, higher scores of overall sweetness were given to samples that were less shear thinning.

The high shear viscosity of hydrocolloid samples determines the lubrication properties. Samples with higher viscosity at high shear rate were found to have lower friction in mixed regime but higher in hydrodynamic regime. The mouthfeel perceptions were found to be correlated with friction coefficient at speed of 40-100 mm/s and flavour and aroma were negatively correlated with friction coefficient at speed of 10-30 mm/s.

The flow and lubrication behaviour of saliva is changed significantly when stimulated by five basic tastes. The presence of saliva mixed with hydrocolloid samples reduced the friction by up to two orders in boundary and mixed regime but did not affect the friction in hydrodynamic regime which is more related to mouthfeel perceptions.

1 INTRODUCTION

1.1 Objectives

Hydrocolloids are widely used in the food industry serving many different functions such as thickening, gelling, emulsifying, stabilization, coating and so on (Foster, 2010, Funami, 2011). The purpose of their application is ultimately to formulate stable foods with acceptable mouthfeel perceptions. For this reason, researchers try to understand the mouthfeel perceptions of hydrocolloid thickened foods using sensory and instrumental methods. The use of instrumental methods to predict sensory perceptions is most common as they tend to be cheaper, more reproducible and quicker (Wood, 1968, Kokini et al., 1977, Chen et al., 2008, Hollowood et al., 2008, Koliandris et al., 2008, Terpstra et al., 2009). As hydrocolloid thickened foods are often semi-liquid or liquid, it is sensible to relate rheological properties to their sensory perception. Indeed rheological properties have been studied widely in this context with the aim to explore the most relevant parameter that relates to sensory perceptions (Wood, 1968, Pangborn et al., 1973, Pangborn and Szczesniak, 1974, Kokini et al., 1977, Christensen, 1979). In the early studies, the rheological properties of liquid and semi-solid foods were studied mainly in shear flow and at a relatively low rate which is widely accepted to be relevant to the oral processing of foods (Wood, 1968, Kokini et al., 1977, Christensen, 1979, Morris and Taylor, 1982, Cutler et al., 1983, Baines and Morris, 1987, Hill et al., 1995). With an increasing number of studies involving oral processing, it has become clear that oral processing is a very

dynamic process involving large scale changes and also different types of flow, shear and extension and combination thereof, at varied flow rates. Despite the many studies based on shear flow and shear viscosity analysis, there is little known about which range of shear rate is related to sensory perceptions. Values as high as 10^5 s^{-1} could be relevant based on numerical analysis (Nicosia and Robbins, 2001). Moreover, during oral processing, the hydrocolloid thickened foods are mixed with saliva and undergo confinement into thin films where the lubrication properties of both hydrocolloids and saliva may play an important role in mouthfeel perceptions (de Vicente et al., 2006, Dresselhuis et al., 2008b, Stokes et al., 2011, Selway and Stokes, 2013, Stokes et al., 2013).

Therefore, the ultimate objective of this research was to explore the relevance of a range of flow properties of hydrocolloid solutions as well as lubrication behaviour to their sensory perceptions. In addition, the aim was to build models that included relevant physical parameters in order to predict the sensory perceptions of hydrocolloids thickened samples. In the course of this research, the impact of interaction with saliva was considered to be another important aspect. Thus preliminary work on the impact of the presence of saliva on the rheological and lubrication properties of hydrocolloid solutions has been conducted. To achieve the research aims, several specific objectives were undertaken and these included:

1. To design two groups of hydrocolloid samples that have specific rheological properties with either: similar shear viscosity at low shear rate or at high shear rate, and to explore the extensional and dynamic viscosities of the designed samples.

2. To select and train a sensory panel to evaluate the sensory properties of the designed samples and to investigate the *in vivo* release of the designed samples during consumption.

3. To explore the relationship between rheological properties of the designed samples and their sensory perceptions, and furthermore, to build models using the rheological parameters to predict the sensory perceptions.

4. To validate the predictive models with three other types of hydrocolloids thickened samples.

5. To investigate the relationship between the friction behaviour of the designed samples and their sensory perceptions.

6. To explore the role of saliva during oral processing by analysing the rheological and lubrication properties of saliva in response to different stimuli and how these properties are affected for hydrocolloid solutions intimately mixed with saliva. .

1.2 Structure of the thesis

In the next chapter of the thesis, Chapter 2, a comprehensive literature review of the three major topics: rheology and tribology, oral processing and sensory perceptions are presented. Current knowledge is reviewed, linking flow and lubrication related

material properties of liquid and semi-liquid foods to sensory perceptions. In addition, the physicochemical properties of the hydrocolloids used in this research are briefly reviewed. In Chapter 3, the materials and methods are described. For the materials, preparation methods for the hydrocolloids samples and also the collection methods of saliva samples are outlined. In the subchapter of the rheological methods, the measurement protocols selected for shear rheology, thin-film shear rheology, extensional rheology as well as oscillatory shear rheology are described. In the case of thin film rheology the methods used to correct for gap error and non-Newtonian behaviour are reported. In the subchapter describing the tribology methods, the tribology cell and details of the method development including development of the contacting surface as well as steps undertaken to improve the data reproducibility are conveyed. The *in vivo* flavour release method is then introduced, followed by the sensory methods section including the training process and the data analysis methods.

The results and discussion chapter, Chapter 4, is comprised of six subchapters that present the data collected in all the experiments and the discussion of these. In the first subchapter 4.1, the investigation of the relationship between hydrocolloid concentration and shear viscosity behaviour using a series of samples to build a model that can be used to generate designed samples is reported. The non-steady shear rheological properties of the designed samples are also presented and discussed. In subchapter 4.2, results from the *in vivo* flavour release of the designed

samples during consumption are presented followed by subchapter 4.3 reporting the results from the sensory methods. In subchapter 4.4, the relationship between the rheological properties of the designed samples and their sensory perceptions is discussed and models that include relevant rheological parameters are presented. Furthermore, the attempt to validate these models using other hydrocolloid solutions and the results are discussed. In subchapter 4.5, the relationship between the friction behaviour of the designed samples and their sensory perceptions are discussed. The final subchapter investigates the role of saliva. The rheological and lubrication properties of saliva samples and saliva samples mixed with hydrocolloid solutions acquired on selected samples are presented and discussed in the context of the overall aim of this research.

Finally, the conclusions of this research are summarized in Chapter 5. Some suggestions for the further work are discussed in this chapter.

2 FUNDAMENTALS AND LITERATURE REVIEW

2.1 Rheology and Tribology

2.1.1 Flow behaviour and viscosity

By definition, rheology is the study of flow and deformation of material (Barnes et al., 1989). A brief introduction to the rheology as relevant to this research is described in this chapter. For more in-depth information on the subject matter the reader is referred to classical textbooks such as *Rheology: concepts, methods and applications* (Malkin and Isayev, 2012) and *Rheology: principle measurements and applications* (Macosko, 1994). Rheological properties are based on the flow and deformation response to a stress applied to materials. Viscous flow is an irreversible deformation which means that the material does not return to its original form when the stress is removed. To better understand the fundamental rheological parameters, the Two-Plate-Model shown in Figure 2.1 is commonly used.

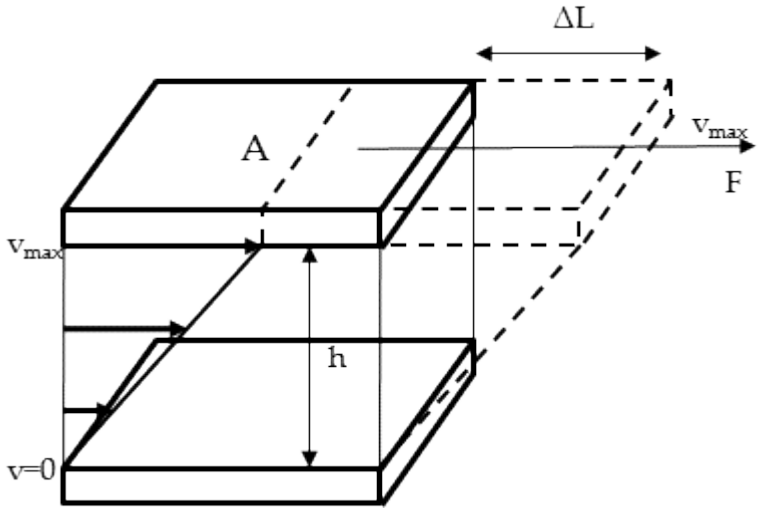

Figure 2.1: Two-Plate-Model: A is the area of the plate [m²]; h is the distance between the two plates [m]; F is the force applied [N]; ΔL is the deflection [m]; v is the velocity [m/s]

A liquid confined between the two plates will be sheared upon application of a force F to the upper plate as indicated in Figure 2.1. The bottom plate is assumed to be fixed, so the velocity profile is linear from zero at the bottom plate to maximum at the top plate. The force F is applied in the plane of the upper plate, thus a shear stress (τ) defined according to Equation 2.1 is acting on the liquid.

$$\tau = \frac{F}{A} \tag{2.1}$$

where τ is the stress [Pa], F is the force [N] and A is the area [m²]

The deformation of the liquid is referred to as shear strain (γ) defined by Equation 2.2.

$$\gamma = \frac{\Delta L}{h} \tag{2.2}$$

where γ is the shear strain, ΔL is the deflection path [m] and h is the distance between two plates [m].

The time derivative of the shear strain corresponds to the shear rate ($\dot{\gamma}$) or the slope of the velocity profile. In the case of the linear velocity profile between two parallel plates the shear rate is constant and can simply be calculated as the ratio of the velocity of the upper plate to the gap height, see Equation 2.3.

$$\dot{\gamma} = \frac{v_{max}}{h} \tag{2.3}$$

where v_{max} is the velocity of the upper plate [m/s] and h is the distance between the two plates [m].

In the case of Newtonian liquids shear stress and shear rate are proportional and the constant of proportionality is termed shear viscosity (η), see Equation 2.4.

$$\eta = \frac{\tau}{\dot{\gamma}} \tag{2.4}$$

where η is the shear viscosity [Pa.s], τ is the shear stress [Pa] and $\dot{\boldsymbol{\gamma}}$ is the shear rate [1/s].

Liquids with shear rate dependent viscosity are referred to as non-Newtonian liquids. The viscosity behaviour of most food materials is non-Newtonian and the different types encountered are illustrated in Figure 2.2.

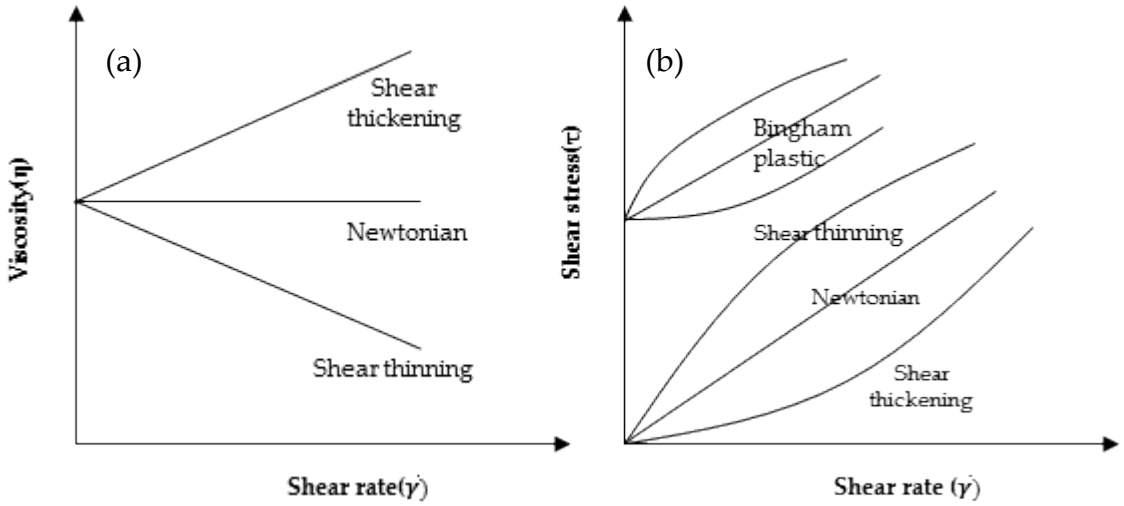

Figure 2.2: Types of viscosity behaviour presented (a) as viscosity curves $\eta(\dot{\gamma})$ and (b) as flow curves $\tau(\dot{\gamma})$

As can be seen in Figure 2.2(a), there are three main types of viscosity behaviour: shear thickening where the viscosity increases with increasing shear rate; shear thinning where the viscosity decreases with increasing shear rate; Newtonian where viscosity is independent of the shear rate. There is also one type of material known as Bingham plastic that requires a minimum stress (known as yield stress) before the onset of flow. This type of flow can be better illustrated in the form of a flow curve and has been included in Figure 2.2(b).

Experimental data are often fitted with rheological models to describe the flow curve $\tau(\dot{\gamma})$ or the viscosity curve $\eta(\dot{\gamma})$. Since there are a lot of fitting functions, it is only possible to mention the most commonly used models here.

Newtonian

Newtonian liquids follow the relationship already shown in Equation 2.4 and have constant viscosity. Water, fruit juice, vegetable oil, honey and dilute polymer solutions show this behaviour over a wide range of shear rates.

Ostwald de Waele (Power –law)

The Ostwald de Waele or Power-law model considers shear rate dependence of the flow behaviour, see Equation 2.5.

$$\tau = k \cdot \dot{\gamma}^n \tag{2.5}$$

where k denotes consistency and n is the flow behaviour index.

For n=1 the power law model describes Newtonian viscosity behaviour, the behaviour is shear-thinning for n < 1 and shear thickening for n > 1.

Bingham

The Bingham model, see Equation 2.6 is valid for Newtonian flow behaviour with yield stress (τ_0)

$$\tau = \tau_0 + k \cdot \dot{\gamma} \tag{2.6}$$

where τ_0 is the yield stress and k is the flow coefficient.

Bingham behaviour may be encountered in concentrated suspensions and colloids.

Cross

In addition to the simplistic models mentioned so far, the following more complex model Cross model is often applied to structured liquids such as hydrocolloid solutions. It is valid only in absence of yield behaviour as it considers a finite viscosity at very low shear rates, the so-called zero-shear viscosity (η_0) as showed in Equation 2.7.

$$\eta = \eta_\infty + \frac{\eta_0 - \eta_\infty}{1 + (C \cdot \dot{\gamma})^p} \tag{2.7}$$

where η_∞ is the infinite-shear viscosity, η_0 is the zero-shear viscosity, C is the time constant related to the relaxation times of the material and p is a dimensionless exponent related to the slope of the shear thinning domain.

Carreau

Carreau model can also be used to describe flow behaviour including both low and high shear rate and can be described as Equation 2.8.

$$\eta = \eta_\infty + \frac{\eta_0 - \eta_\infty}{[1 + (C \cdot \dot{\gamma})^2]^p} \tag{2.8}$$

where η_∞ and C are the time constant related to the relaxation times is the infinite-shear viscosity, η_0 is the zero-shear viscosity, and p is a dimensionless exponent related to the slope of the shear thinning domain

The aforementioned models describe the relationship between shear viscosity and shear rate. Factors other than shear rate affecting the viscosity behaviour of materials include time, temperature, pressure, concentration and molecular weight of the materials.

2.1.2 Measuring rheological properties

The instruments that are employed to measure rheological properties are called rheometers and there are many different types. Among these different types, rotational and capillary rheometers are the most popular ones. In this research both rotational and extensional types were used. Several measuring systems are available and the choice depends on the material tested and the measurement sensitivity of the instrument. The most widely used measuring systems are cone and plate, parallel plate and concentric cylinders. The measurement protocols of this research only included cone and plate and parallel plate. The concentric cylinders methods are not used in this research due to the requirement of high shear rate which is normally not capable for concentric cylinder geometries.

2.1.2.1 Cone and plate

As can be seen in Figure 2.3, the cone and plate geometry consists of a circular cone with a very small cone angle and a plate. In this research a cone and plate with an angle of 2° was used. In practice the apex of the cone is truncated by several ten

micrometers to eliminate the tip of the cone touching the plate. The truncation is considered when setting the geometry at the rheometer. The shear stress (τ) and circumferential shear rate ($\dot{\gamma}_R$) can be calculated with Equations 2.9 and 2.10 respectively.

$$\tau = \frac{3M}{2\pi R^3} \tag{2.9}$$

$$\dot{\gamma}_R = \frac{v_{max}}{h_{max}} = \frac{\omega \cdot R}{R \cdot \tan\alpha} = \frac{\omega}{\tan\alpha} \tag{2.10}$$

where M is the torque [N.m], ω is the angular velocity [rad/s], R is the outer radius of the cone and plate [m], v_{max} is the velocity at rim [m/s] and h_{max} is the maximum gap at the rim [m].

The advantage of the cone and plate geometry is that the shear rate is constant across the gap for sufficiently small cone angles (less than 6°) (Malkin and Isayev, 2012).

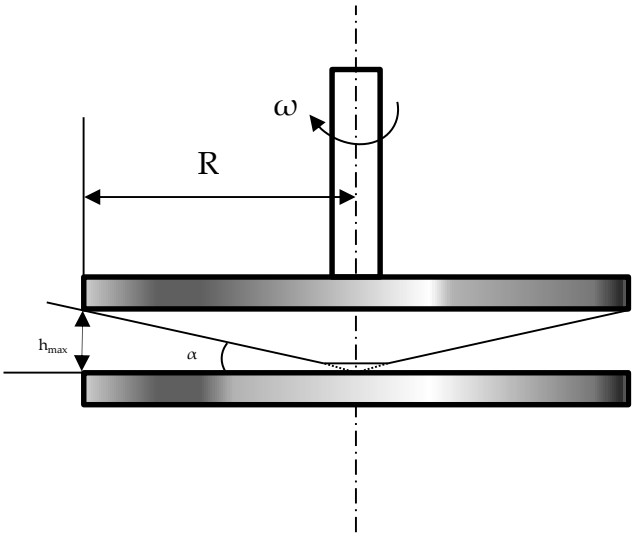

Figure 2.3: Schematic diagram of a cone and plate geometry.

2.1.2.2 Parallel plate

Figure 2.4 depicts a parallel plate geometry consisting of two plates with a radius of R separated by a gap the size of H. With reference to the outer rim of the geometry, the shear stress and the shear rate for the parallel plate are given by Equation 2.11 and 2.12 respectively.

$$\tau = \frac{2M}{\pi R^3} \tag{2.11}$$

$$\dot{\gamma}_R = \frac{v_{max}}{H} = \frac{\omega R}{H} \tag{2.12}$$

Across the gap the shear rate depends on the radial distance from the centre and it is zero at the centre and maximum at the outer rim. The shear stress also varies across the gap from minimum to maximum from centre to the edge but in a fashion that depends on the properties of the fluids. Therefore the Equation 2.11 is the shear stress at the rim for a Newtonian fluid.

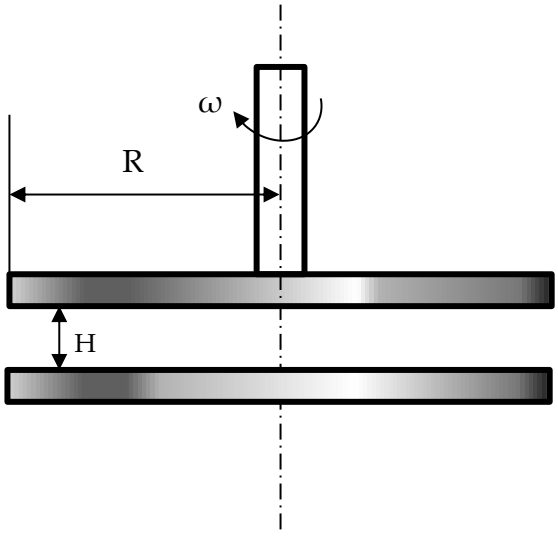

Figure 2.4: Schematic diagram of a parallel plate geometry

2.1.3 Viscoelasticity

Many phenomena cannot be described by the viscosity behaviour alone and elastic behaviour must be taken into consideration (Steffe, 1996). When an ideal solid is deformed, it regains its original form on removal of the stress. This is referred to as ideal elastic deformation. In contrast, when an ideal viscous fluid is deformed, motion ceases as soon as the stress is removed and it remains deformed. A viscoelastic material shows a degree of both types of material behaviour. If the elastic properties dominate material behaviour, the material will be referred to as a viscoelastic solid. In the case of a viscoelastic liquid, the viscous material behaviour dominates. The viscoelasticity of materials can be measured using both first normal stress difference and oscillatory tests.

2.1.3.1 First normal stress difference

When viscoelastic materials are deformed, the forces and stresses applied are never one dimensional but actually a state of three-dimensional deformation. To help understanding this, a three dimensional tensor description is used; see Equation 2.13.

$$\tau_{ij} = \begin{vmatrix} \tau_{xx} & \tau_{xy} & \tau_{xz} \\ \tau_{yx} & \tau_{yy} & \tau_{yz} \\ \tau_{zx} & \tau_{zy} & \tau_{zz} \end{vmatrix} \tag{2.13}$$

The first index of each stress tensor value indicates the position of the area on which the stress is acting and the second index indicates the direction of stress. The three-

dimensional stress tensor can be visualised with the cube model represented in Figure 2.5.

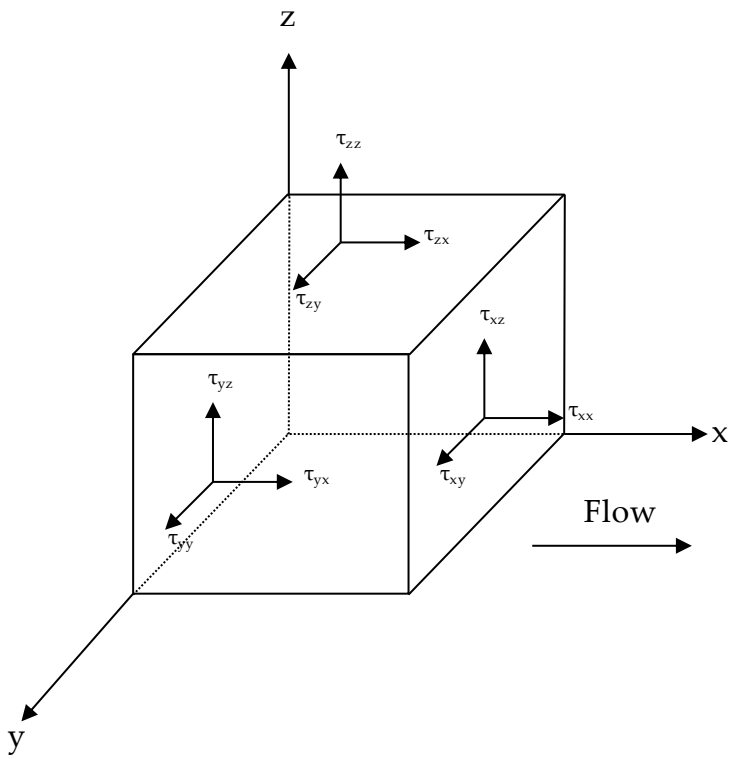

Figure 2.5: Cube model of thethree-dimensional stress tensor.

The components of the stress tensor with the same two indices represent normal stresses, namely τ_{xx}, τ_{yy} and τ_{zz}. They are equal to zero for Newtonian fluids but can be of appreciable magnitude for non-Newtonian fluids (Macosko, 1994). The first normal stress difference (N_1) and the second normal stress difference (N_2) are defined by Equations 2.14 and 2.15.

$$N_1 = \tau_{xx} - \tau_{yy} \tag{2.14}$$

$$N_2 = \tau_{yy} - \tau_{zz} \tag{2.15}$$

N_1 is the first normal stress difference and N_2 is the second normal stress difference.

For viscoelastic fluids, the generation of unequal normal stress components and hence non-zero values of N_1 and N_2 arises from the fact that in a flow process the microstructure of the liquid becomes anisotropic. Typical examples are diluted polymer solutions and emulsions. In the flow field, polymer molecules and emulsion droplets change from a spherical shape at rest to an anisotropic structure and restoring forces are generated. Since the structures are anisotropic, the restoring forces are also anisotropic. As when the spherical shape changed into ellipsoids in the same direction of flow, the restoring force is greater in this direction than the other two orthogonal directions (Barnes et al., 1989).

N_1 increases with shear rate and generally follows power-law behaviour over a range of shear rates. The ratio of N_1 to shear stress, which is known as recoverable shear strain (Kokini and Surmay, 1994), is often used as a measure of how elastic a fluid is.

2.1.3.2 Oscillatory tests

Oscillatory tests also allow quantification of the viscoelastic behaviour of materials. While normal stress differences develop in large shear deformation, oscillatory tests

are conducted within the linear viscoelastic limit of regime that is under very small deformation. Thus, the dynamic structure properties of a material are probed rather than flow-induced behaviour. Oscillatory testing also allows accessing different time scales by changing angular frequency. Normally a sinusoidal strain is applied to the samples, and the magnitude and phase shift of the stress response of the material will depend on its viscoelastic properties. In the case of ideal viscous material behaviour, the stress is dissipated by friction, whereas the stress is fully transmitted in the case of ideal elastic behaviour. The two plate model is also used to explain oscillatory shear deformation, see Figure 2.6, and to derive the relevant equations.

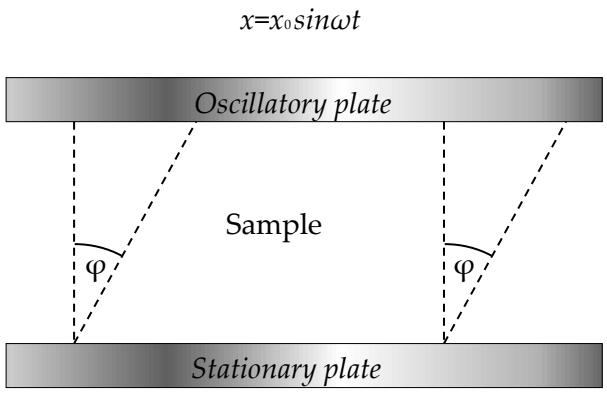

Figure 2.6: Two-plates-model for oscillatory testing: x is the position of the plate at the time t and x_0 is the amplitude of the plate oscillation.

At time t the position of the upper plate sketched in Figure 2.6 is given by Equation 2.16.

$$x = x_0 \sin \omega t \tag{2.16}$$

where x is the position of the plate at time t and x_0 is the amplitude of the oscillation and ω is the angular frequency [rad/s]

The sinusoidal shear strain follows the deformation and is given by Equation 2.17. :

$$\gamma = \gamma_0 \sin \omega t \tag{2.17}$$

where γ is the shear strain and γ_0 is the shear strain amplitude.

For a viscoelastic material the stress response lags somewhat behind the strain imposed (equally the strain response lags behind for applied stress), see Equation 2.18.

$$\tau = \tau_0 \sin(\omega t + \delta) \tag{2.18}$$

where τ_0 is the shear stress amplitude and δ is the phase lag. This equation can be rewritten as Equation 2.19.

$$\tau = \tau_0 \cos \delta \sin \omega t + \tau_0 \sin \delta \cos \omega t \tag{2.19}$$

The stress response can therefore be considered as being composed of two components, the storage modulus G′ and the loss modulus G″, see Equations 2.20 and 2.21.

$$G' = \frac{\tau_0 \cos \delta}{\gamma_0} = \frac{in\ phase\ stress\ amplitude}{strain\ amplitude} \tag{2.20}$$

$$G'' = \frac{\tau_0 \sin \delta}{\gamma_0} = \frac{out\ of\ phase\ stress\ amplitude}{strain\ amplitude} \tag{2.21}$$

Therefore the stress response can be written as Equation 2.22 showing that the storage modulus is an indicator of the degree of the elasticity of the material and the loss modulus is a measure of the degree of viscous behaviour.

$$\tau = G'\gamma_0 \sin \omega t + G"\gamma_0 \cos \omega t \tag{2.22}$$

For a perfectly elastic material (Hookean solids) all the energy is stored, therefore G″ is zero and the stress and the strain will be in phase. In contrast, for an ideal viscous fluid, all energy is dissipated as heat, therefore G′ is zero and the stress and strain will be out of phase by 90°.

The phase angle is then given by Equation 2.23. It is directly related to the energy lost divided by energy stored and it ranges between 0° to 90°. 0° indicates purely elastic behaviour and (no phase lag) and 90° indicates purely viscous material behaviour (out of phase).

$$\tan \delta = \frac{G"}{G'} \tag{2.23}$$

A notation using complex variables can be used to define the complex modulus G* with Equation 2.24.

$$|G^*| = \sqrt{(G')^2 + (G")^2} \tag{2.24}$$

The analysis can also be conducted based on viscosity. The complex viscosity η* and the complex modules G* are linked by Equation 2.25.

$$\eta^* = \frac{G^*}{\omega} = \sqrt{(\eta')^2 + (\eta'')^2} \tag{2.25}$$

2.1.4 Extensional rheology

Oral processing of food is not pure shear deformation but includes some elements of stretching flow and squeeze flow. Therefore, the extensional rheological behaviour of the samples used in this research was studied. There are three main types of extensional flow: uniaxial, biaxial and planar shear extension, see Figure 2.7. In extensional flow, the molecules are orientated and stretched and therefore cause the maximum resistance to deformation due to the chain tension. Thus extensional flows are much more sensitive than shear flows in terms of polymer presence and polymer structure.

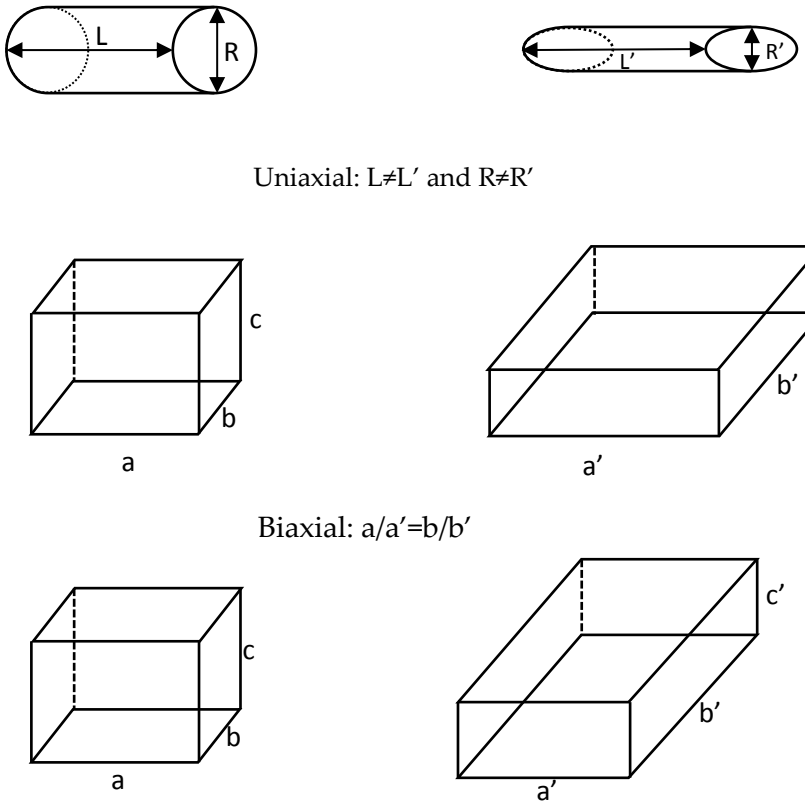

Figure 2.7: Uniaxial, biaxial and planar extension.

Extensional viscosity, unlike the shear viscosity, has no meaning unless the type of extensional deformation is clarified (Denson, 1973). In this research, if not otherwise stated, extensional viscosity means 'uniaxial extensional viscosity'. The concept of extensional viscosity was first mentioned by Trouton in 1906 with the rule that uniaxial extension is three times the shear viscosity for Newtonian fluids, and the ratio between extensional viscosity and shear viscosity is named the Trouton ratio (Trouton, 1906, Petrie, 2006), see Equation 2.26.

$$T_r = \frac{Extensional\ viscosity}{shear\ viscosity} \tag{2.26}$$

Since extensional and shear viscosities are functions of different strain rates, it is necessary to use a conversion method to calculate the Trouton ratio. Jones et al (1987) suggested that the shear viscosity is taken at a shear rate equal to $\sqrt{3} \cdot \dot{\varepsilon}$ for uniaxial extension and therefore the Trouton ratio for uniaxial extensional can be expressed as shown in Equation 2.27.

$$T_r = \frac{\eta_E(\dot{\varepsilon})}{\eta_s(\sqrt{3} \cdot \dot{\varepsilon})} \tag{2.27}$$

where η_E is the extensional viscosity and η_s is the shear viscosity.

2.1.4.1 Filament breakup

There are many ways to measure extensional viscosity such as the tensile test, fibre spinning, stagnation point flows, converging flows and contraction flows (James and Walters, 1993, Petrie, 2006). Here, the filament breakup method was applied using a capillary breakup extensional rheometer. This method has become widely used for measuring the transient extensional viscosity of non-Newtonian fluids such as biopolymer solutions, food dispersions, etc. (Rodd et al., 2005). The principle of the technique is explained in Figure 2.8.

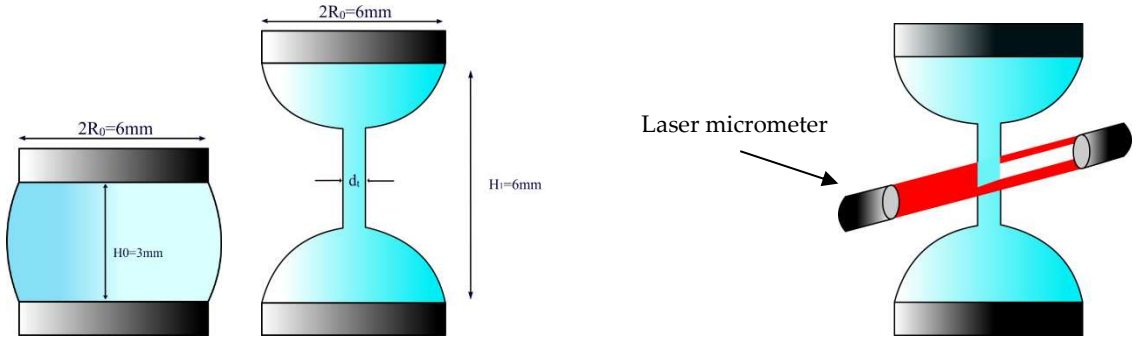

Figure 2.8: Schematic diagram of a capillary breakup extensional rheometer (CaBER) experiment.

As shown in Figure 2.8, initially a nearly cylindrical fluid sample is placed between two concentric spherical plates and the plates are rapidly separated to a certain distance forming a filament from the initial gap size H_0 to the final gap size of H_1. Capillary thinning of the liquid filament formed between the two plates is followed at its midpoint using a laser micrometer. The midpoint may not always correspond to the thinnest diameter and the diameter at which the filament will break. This is a well-recognised draw-back of this equipment when used without additional visualisation of the filament dynamics as was the case in this research. The thinning and leading to the breakup of the fluid filament is driven by capillary stresses and resisted by the extensional stresses developed within the flow.

For Newtonian fluids with extensional viscosity η_E , the filament diameter decreases linearly with time (Bazilevsky et al., 1990, Papageorgiou, 1995, McKinley and

Tripathi, 2000, Anna and McKinley, 2001, Miller et al., 2009), which can be described with Equation 2.28.

$$D_{mid}(t) = \alpha(\frac{2\sigma}{\eta_s})(t_b - t) \tag{2.28}$$

where D_{mid} is the diameter of filament at time t, η_s is the shear viscosity and σ the surface tension of the fluid, t_b is the filament breakup time, α is the numerical pre-factor.

For viscoelastic fluids, it is found that the thinning of the midpoint filament diameter is characterised by a rapid initial viscous dominated phase, then there is an intermediate time scale in which the dynamics of the filament drainage are governed by a balance between surface tension and elasticity, rather than fluid. In this regime, the filament radius decreases exponentially as a function of time as shown in Equation 2.29 (Bousfield et al., 1986, Bazilevsky et al., 1990, Entov and Hinch, 1997, Anna and McKinley, 2001).

$$D_{mid}(t) = D_0 \left(\frac{GD_0}{\sigma}\right)^{\frac{1}{3}} e^{\frac{-t}{3\lambda_c}} \tag{2.29}$$

where λ_c is a characteristic relaxation time governing capillary breakup, G is the elastic modulus of the filament and D_0 is the filament diameter at time zero.

Entov and Hinch (1997) showed that the diameter will approach linear behaviour at late times. This behaviour results when the polymers chains become fully stretched

and the elastic stresses can no longer grow to resist the increasing capillary pressure. In this regime, the fluid behaves as a very viscous anisotropic Newtonian fluid with a viscosity equal to the steady state extensional viscosity of the fluid. The apparent steady state extensional viscosity can be obtained through this regime (Stelter and Brenn, 2000) as shown in Equation 2.30.

$$\eta_E = \frac{\sigma/R_{mid}(t)}{\dot{\varepsilon}(t)} = \frac{-\sigma}{dD_{mid}/dt} \tag{2.30}$$

where $\dot{\varepsilon}$ is the strain rate.

To mimic the expected diameter behaviour in the linear and exponential regime, Anna and McKinley (2001) used the function shown in Equation 2.31:

$$\frac{D_{mid}(t)}{D_l} = ae^{-bt} - ct + d \tag{2.31}$$

where *a, b, c,* and *d* are fitting parameters. The value of b^{-1} is clearly related to the longest relaxation time of the fluid, and the steady state extensional viscosity is related to the value of c^{-1} (Anna and McKinley, 2001).

2.1.5 Tribology

Tribology is the study of friction and lubrication between interacting surfaces in relative motion. These properties have been intensively studied in modern machinery due to their importance in contacting parts of breaks, clutches and gears

etc. (Bhushan, 1999). However, friction and lubrication properties can be very important during oral processing as well due to a number of interacting surfaces in the mouth during food consumption such as teeth-teeth, tongue-palate, tongue-teeth, teeth-food, tongue-food, tongue-bolus, lips, lips-food, bolus-plate and food particles-oral surfaces (Stokes et al., 2013).

The study of tribology in food research is rational as the tongue and hard plates act like two contacting surfaces in relative motion that are lubricated by a film of food and saliva. During oral processing, the food is masticated, sheared and squeezed between the tongue, the hard palate and the teeth where its deformation mainly depends on its bulk rheological and mechanical properties. However, as the oral processing of food continues, the particles are further broken down and thus a thin film is developed. At this stage, mechanical and rheological properties have been hypothesised to be less important in determining mouthfeel perception and friction and lubrication properties may be more important (Chen and Stokes, 2012). Details of how friction and lubrication relate to oral sensory perceptions are discussed in sections 2.3, while in the subsequent two sections the principles that relate to food tribology study are reviewed.

2.1.5.1 Friction

Friction is the force that resists motion and must be overcome before any motion is initiated. The resistive force which is at the tangential direction of motion is called friction force, as illustrated in Figure 2.9.

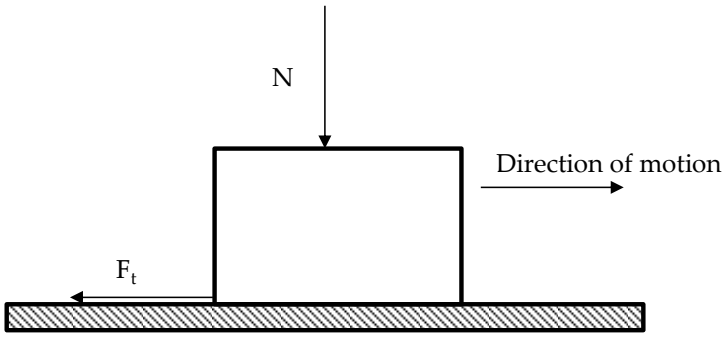

Figure 2.9: Schematic illustration of a body sliding on a surface. N is the normal load and Ft is the friction force.

Friction is a system property rather than a material property, therefore it is inappropriate to state that one material is more frictional than another. Friction is caused by a combination of factors. These factors are the forces required to overcome the adhesion between surfaces, rheological losses due to flow in the lubricant and hysteresis losses due to significant deformation of surfaces such as elastomers (Bhushan and Ebrary, 2013). Friction should only be discussed in the context of every parameter that is involved such as surface material, relative speed and loading (Prinz et al., 2007). There are two types of friction: dry friction and fluid friction. In dry friction, two basic rules are generally obeyed which are known as Amonton's 1st and 2nd laws (Bhushan and Ebrary, 2013). The first law states that friction force is

independent of the apparent area of contact between two contacting bodies. The second law states that the friction force is directly proportional to the normal load. From the second law, a dimensionless coefficient of friction can be defined Equation 2.32.

$$\mu = \frac{F_t}{N} \tag{2.32}$$

where μ is the friction coefficient, F_t is the tangential friction force and N is the normal load.

2.1.5.2 Lubrication

As soon as a liquid is present between the two contacting surfaces one refers to lubrication rather than friction behaviour despite the fact that the friction coefficient is still used as system property. In principle, the characteristics of the film situated between contacting bodies and the consequences of its failure or absence are studied (Stokes, 2012b). Results of friction or lubrication studies are generally presented as a plot of friction coefficient versus the logarithms of a control parameter in the form of a Stribeck curve as shown in Figure 2.10. The two control parameters frequently encountered are film thickness or ηU/W (viscosity × entrainment speed/normal load)

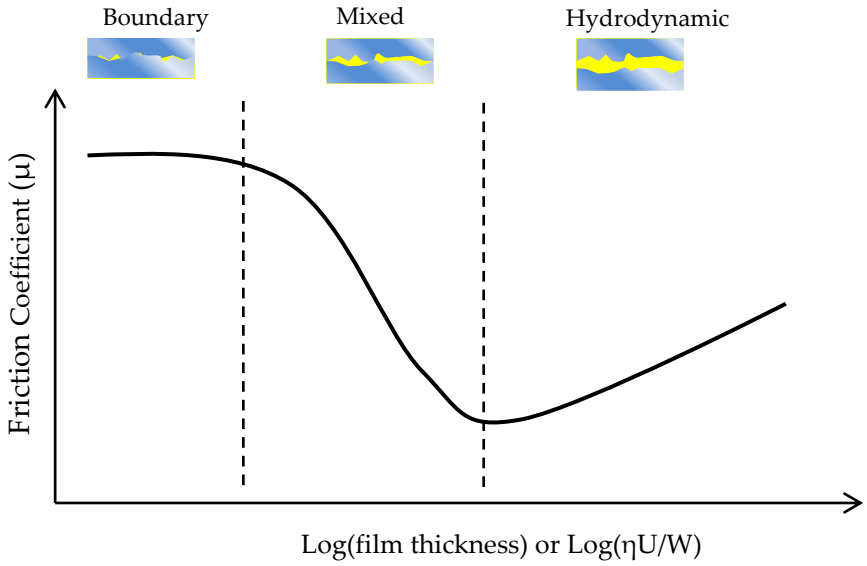

Figure 2.10: A typical Stribeck curve as a function of film thickness or the parameter of ηU/W (η is the viscosity ,U is the entrainment speed and W is the load) with three regime of lubrication: Boundary regime, mixed regime and hydrodynamic regime where the two interfaces are in full contact, partial separation and full separation respectively. Note that the x-axis parameter is plotted as logarithm.

As indicated in Figure 2.10, in the Stribeck curve three regimes of lubrication can be identified.

The boundary regime occurs at very low speed where there is negligible fluid entrainment into the contact and therefore the surface asperities could cause the surfaces to lock up which may result in sever surface wear. The friction coefficient is high and independent of entrainment speed. It is worth stressing that the friction coefficient in this regime only depends on the surface properties. Therefore by using

surface absorbing materials such as mucin, one could significantly change the surface properties and hence change the boundary lubrication properties (Cassin et al., 2001). With increased entrainment speed, the two surfaces enter the mixed regime in which they are separated by a thin fluid layer but just about to touch. A reduced friction coefficient is observed due to the surface separation caused by increased lubrication pressure. In this regime, the friction coefficient reaches the minimum and the system is maximal lubricated. Both surface and lubricant properties affect the system behaviour. A further increase of entrainment speed causes an increase of film thickness which increases friction due to the viscosity of the entrained fluid. This is referred to as the hydrodynamic regime and the friction coefficient is entirely dependent on the rheological properties of the lubricant and independent of surface properties.

2.2 Oral processing and sensory perceptions

2.2.1 Oral physiology

In the past few decades, the anatomy and physiology of the oral cavity has been extensively studied mainly for medical and dental reasons. However, food researchers have become more and more interested in how food and drink are processed in the mouth and also in the interplay between oral processing and sensory perception. Thus the anatomy and physiology of the oral cavity have also been increasingly studied by food researches. As shown in Figure 2.11, the oral

cavity is roughly the void space between the lips and the velum (Chen, 2009). More accurately and scientifically, Stedman's Medical Dictionary (Stedman, 2005) defines the oral cavity as "the region consisting of the vestibulum oris, the narrow cleft between the lips and cheeks, and the teeth and gums, and the cavitas oris propria". In the oral cavity, there are two important organs needed for processing foods, namely the teeth and the tongue, as well as a certain amount of saliva. The presence of saliva is extremely crucial for the management of food and drink in the mouth. Teeth play a key role in mastication, which action by teeth is the major oral operation for consuming solid and semi-solid foods. Foods are transported from the incisors to the molars for size reduction. Once there is no further size reduction needed, the foods are transported to the back of oral cavity for bolus formation before they are swallowed (Lucas et al., 2002, Hiiemae, 2004). This two-phase oral food management model describes a complex physiological process involving decision making, often unconsciously, and preparation of a safe-to-swallow bolus occurring simultaneously with information being transmitted to and from the central nervous system (Koc et al., 2013).

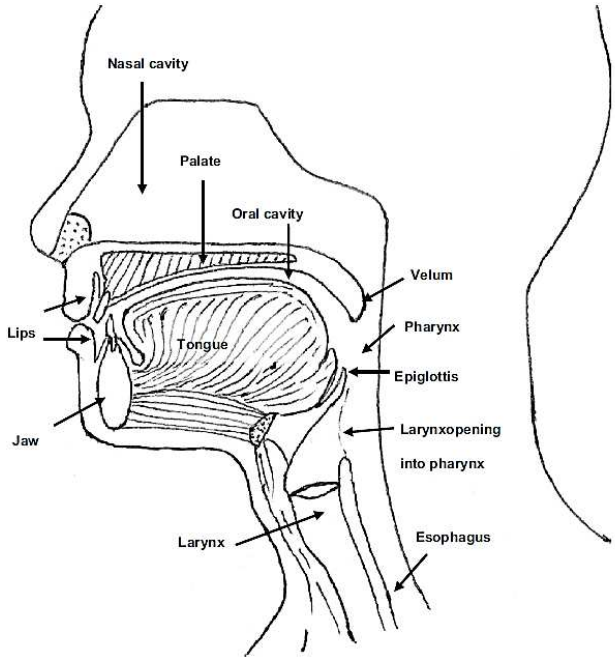

Figure 2.11 The anatomic structure of human oral organ (Chen, 2009)

The research described in this thesis focussed on thickened hydrocolloid solutions and these do not require mastication. Most of the manipulation of this sort of food is conducted by the tongue, so the structure of the tongue and its food manipulating function is addressed as follows.

The tongue consists of striated muscle and occupies the floor of the mouth. It functions as a sensory organ to sense temperature, to taste flavour and to perceive texture, and more importantly, as a digestive organ or mechanical device by facilitating the movement of food during mastication and assisting swallowing by aiding bolus formation (Imai et al., 1995, Heath, 2002, du Toit, 2003). The dorsal mucosal surface of the tongue contains stratified squamous epithelium with

numerous papillae and taste buds, which will be discussed further in section 2.2.2.1. It has been proven that the sensation of virtually all food and drink flavours and mouthfeel attributes requires at least some tongue movement, as these manipulations mix food with saliva hence enhancing mechanical and chemical breakdown, and position the food to the relevant sensing organs (de Wijk et al., 2003). Tongue movements influence flavour sensation by increasing flavour release during food breakdown and redistribution of the food over a larger area of the tongue, thus pumping the volatile flavour compounds into the nose to enhance flavour perception (Baek et al., 1999). More details about sensory perceptions will be discussed in section 2.2.2.

The crucial role of saliva in oral processing and sensory perceptions as well as its physical properties will be addressed in section 2.2.3.

2.2.2 Sensory perceptions

In this section, the fundamentals of sensory perception, including taste, aroma and texture are reviewed. It has become well accepted that food sensory perception is multimodal and each component e.g. visual, tactile, auditory, gustatory and olfactory etc, interacts with the others to affect the final perception. However, in order to better understand the cross-modality between the individual components, it is essential to understand the basic mechanism behind each component.

2.2.2.1 Taste perception

The basic functions of taste are to identify nutritious food and to prevent ingestion of toxic substances. There are five basic tastes: sour, sweet, bitter, salty and umami (monosodium glutamate), although some researchers suggest that fat may be counted as another taste (Khan and Besnard, 2009). The sensation of taste is mediated by specialised neuroepithelial cells that are clustered into onion-shaped end organs called taste buds. These are present at high density on the tongue and at low density in the soft palate, larynx, pharynx and upper part of the oesophagus (Gilbertson et al., 2000). As can be seen from Figure 2.12, there are three different types of taste buds located on different parts of the tongue: fungiform, foliate and circumvallate. Fungiform are located at the anterior part of the tongue and containone or a few taste buds. Foliate are located at the posterior edge of the tongue and contain up to hundreds of taste buds. Circumvallate papillae contain thousands of taste buds and are located at the back of the tongue. In each taste bud, there are about 50-150 taste receptor cells (TRCs) representing all five basic tastes. These TRCs within the taste buds are responsible for detecting soluble chemicals that come into contact with the tongue (Kinnamon and Margolskee, 1996).

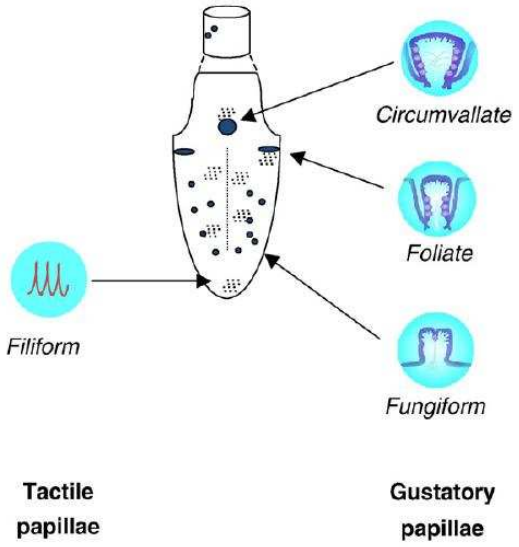

Figure 2.12: Localization of the different taste buds on the tongue (Adapted from Khan and Besnard, 2009).

Taste transduction involves several different processes and each basic taste uses one or more of these mechanisms. Some tastes sensed through direct interaction with ion channels such as salty (Na^+), sour (H^+) and some bitter compounds (e.g. K^+). However, for the taste of sweet, umami and most bitter compounds, specific membrane receptors are required for the transduction process (Kinnamon, 1996, Kinnamon and Margolskee, 1996).

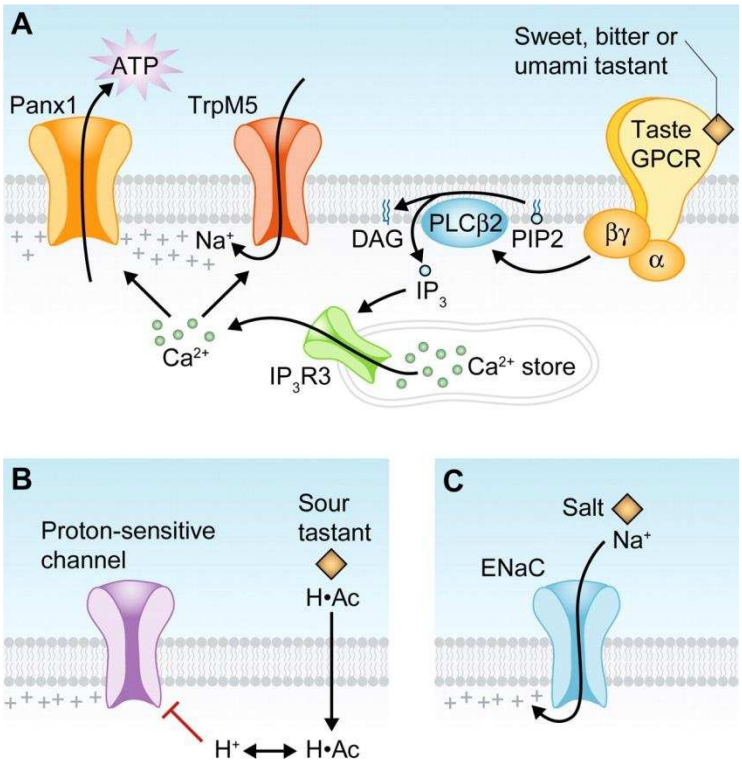

Figure 2.13: Three types of receptor cells by which tastes are transduced: (A) sweet, bitter or umami; (B) sour; (C) salt (Adapted from Chaudhari and Roper, 2010).

According to Chaudhari and Roper (2010), there are three types of taste receptors that are responsible for different taste transduction and the mechanisms for the three types of receptors are shown in Figure 2.13. Type 1 receptors are responsible for the taste of sweet, bitter and umami as showed in Figure 2.13 (A). In type 1 receptors, sweet, bitter and umami taste substances bind to G-protein coupled receptors (GPCRs) and activate a phosphoinositide pathway that elevates cytoplasmic Ca^{2+} and depolarises the membrane via a cation channel, TrpM5. The combined effect of elevated Ca^{2+} level and depolarized membrane causes the large pores of gap junction hemichannels to open and release of ATP (Chaudhari and Roper, 2010).

Type 2 receptors are responsible for the taste of sour, as showed in Figure 2.13 (B). Organic acid (e.g. HAc) can penetrate through the plasma membrane and acidify the cytoplasm where they dissociate to acidify the cytosol. However the membrane receptor or ion channels that transduce acid stimuli are still not identified. It was reported that PKD2L1, a polycystic kidney-disease like ion channel was likely to be a candidate mammalian sour taste sensor (Huang et al., 2006). For the taste of saltiness, receptor type 3 is responsible for the transduction (Figure 2.13 C). Taste buds detect Na^+ by directly allowing Na^+ pass through apical ion channels, known as Epithelial Sodium Channel (ENaC). After passing through the channels, the Na^+ ions then depolarize the taste cells (Roper, 2007).

2.2.2.2 Aroma perception

Aroma compounds can be sensed orthonasally and retronasally (Rozin, 1982), see Figure 2.14. In the orthonasal pathway, the aroma compounds enter the nostrils with the air flow during sniffing and are transported to the olfactory receptors. In the retronasal pathway the aroma compounds are released during oral processing in oral cavity and are then transported to the pharynx and olfactory receptors (Negoias et al., 2008).

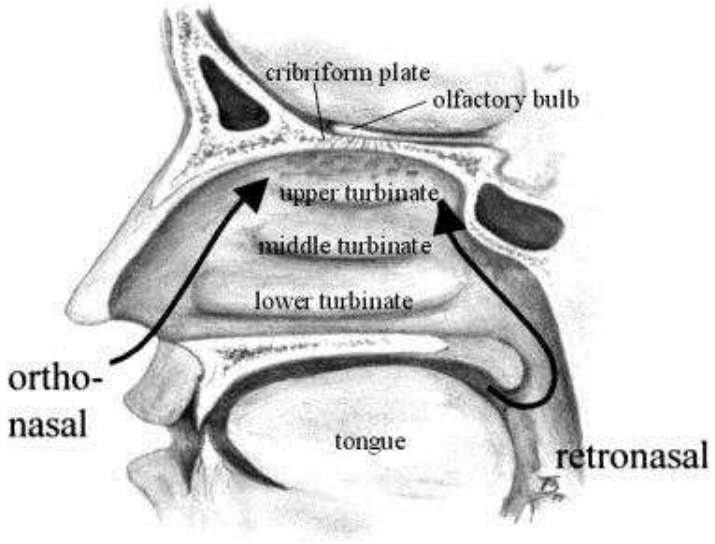

Figure 2.14: Schematic of the nasal cavity showing the orthonasal and retronasal pathways of aroma perception (Negoias et al., 2008).

When the aroma compounds from either pathway reach the nasal cavity, they are detected by the olfactory receptor neurons (ORNs) located in the olfactory epithelium. An ORN is a bipolar neuron with two pathways occurring at either pole. One process is a thin unmyelinated axon that connects to the olfactory bulb and from the other pole a dendrite arises that ends in a knob with 6-12 cilia. These cilia protrude into a layer of mucus which is secreted by the supporting cells of the olfactory epithelium and by Bowman's glands. The mucus contains a large number of soluble aroma compound binding proteins and therefore contributes to the concentration or removal of aroma (Engelen, 2012). The aroma transduction is initiated in the cilia when the aroma compounds interact with specialised ORNs within the ciliary membrane. The interaction of aroma compounds with the ORNs within the ciliary membrane elicits a cascade of transduction events that ultimately

lead to an increase in membrane conductance. The resulting generator potential is converted to a distinct frequency of action potentials which are conveyed to the olfactory bulb and therefore the strength, duration and quality of the aroma stimuli are encoded into patterns of neuronal signals. These signals are further conveyed to the brain and the process of aroma perception starts (Breer, 2003).

2.2.2.3 Texture and mouthfeel perception

The term texture was first used to describe foods by Matz (1963) as the overall experience of sensation derived from oral mucous while sampling food or beverage, and the related physical properties of the material such as density, viscosity, and surface tension etc. Later based on a wide range of previous research, Szczesniak (2002) recapitulated texture as "the sensory and functional manifestation of the structural, mechanical and surface properties of foods detected through the senses of vision, hearing, touch and kinesthetics." As can be seen from the evolution of the definition of texture, it corresponds more to a multidimensional perception rather than a single in-mouth perception. Compared with texture, mouthfeel perception is related to all tactile perceptions from the time point when a food is placed onto the tongue until it has been fully cleared from the oral cavity. Therefore, attributes that are perceived after swallowing such as mouthcoating are still categorised as mouthfeel.

According to Guinard and Mazzucchelli (1996), sensory modalities that are responsible for texture and mouthfeel perceptions can be divided into three groups: (1) mechanoreceptors in the superficial structures of the mouth such as hard and soft palate tongue and gums; (2) mechanoreceptors in the periodontal membrane surrounding the roots of the teeth; (3) mechanoreceptors of the muscles and tendons involved in the mastication. These mechanoreceptors are important in transducing signals of pressure, vibration, and movement taking place in the mouth. Therefore they are very important in texture perception and safe manipulation of food. In addition to mechanoreceptors, there are also proprioceptors and periodontal receptor in the mouth which are indispensable in texture perception. Proprioceptors such as muscle spindles and Golgi tendon organs are crucial in terms of sensing changes in muscle length and tension, respectively. Periodontal receptors by which teeth are equipped , can provide information about the direction forces are applied on the teeth, and therefore very important in the motor control of jaw actions associated with biting, interoral manipulation and chewing of food (Trulsson and Johansson, 1996, Trulsson, 2006). When food is placed into the mouth, all of the information that is sensed by the receptors due to the oral processing is transmitted to the central nervous system through the trigeminal somatic sensory system. The signal will be eventually transmitted to the postcentral gyrus of the primary somatosensory cortex where the texture is perceived.

As already mentioned, texture and mouthfeel perception represent multidimensional perceptions indicating that other factors such as visual, sound, flavour and temperature have an impact (Szczesniak ,2002). There are numerous texture or mouthfeel attributes that food researchers have tried to quantify by using instrumental techniques involving rheological and tribological methods, see section 2.3.

2.2.3 The role of saliva in oral processing and sensory perceptions

2.2.3.1 Saliva

Human saliva is produced by three pairs of organs: the parotid, submandibular and sublingual salivary glands which work simultaneously to produce almost 90% of the saliva in the oral cavity (Matsuo, 2000). Figure 2.15 illustrates the location of major salivary glands. Parotid glands are located opposite the maxillary first molars near the ear. As the largest salivary glands, parotid glands contribute up to 60% of the total saliva flow when stimulated by chewing or taste (Matsuo 2000; Silletti, Vingerhoeds et al. 2008), but only about 20% without stimulation (Humphrey and Williamson 2001). Submandibular glands are located in the front and both sides of oral floor, contributing 30-40% of total saliva production in response to mechanical or taste stimulation and as much as 70% of unstimulated saliva. Sublingual glands are found under the tongue, in the centre part of oral floor and secrete about 2% of

total saliva volume regardless of any stimulation (Aps and Martens 2005). Apart from their differing contributions to total saliva flow, the three pairs of major salivary glands also secret saliva with different compositions, which will be addressed later in this section. Besides the major salivary glands, there are also some minor glands which are located all over the mouth except for the gums and anterior portion of the hard palate, secreting about 10% of the total saliva and not significantly responsive to mechanical or taste stimulation (Aps and Martens 2005).

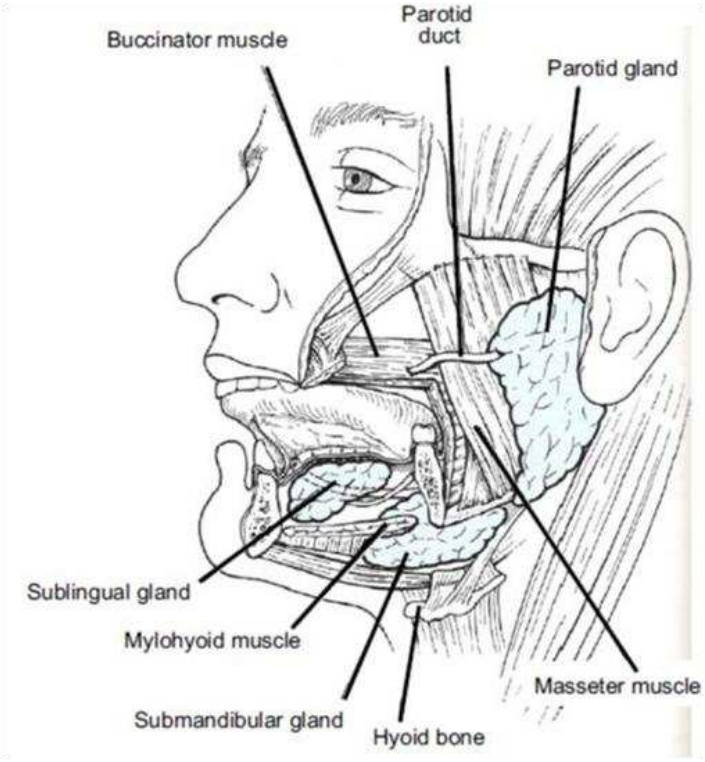

Figure 2.15： The location of major salivary glands (Ferguson, 1999)

As the saliva coats the entire surface within the oral cavity, it can be assumed to play a role in every step of oral processing. Saliva is a very dilute fluid that consists of

more than 99% of water and a large number of organic and inorganic constituents such as electrolytes, protein, enzymes and mucins which are glycoproteins. The detailed composition of saliva is introduced in section 2.2.3.2. The pH of natural saliva is slightly acidic for healthy individuals and a range of 6 to 7 has been reported (Chen, 2009). The production rate of saliva, also referred to as saliva flow rate, varies significantly from individual to individual. For unstimulated saliva, which is the result of low levels of autonomic stimulation by higher centres of the brain acting via the salivary centre on the salivary glands, a mean flow rate of 0.45 ± 0.25 $mL.min^{-1}$ has been reported with higher flow rates detected early morning and mid-day (Engelen et al., 2005). Unstimulated saliva is mainly secreted from sublingual and submandibular glands while the parotid gland contributes for about 60% of the total taste or mechanically stimulated saliva production (Matsuo, 2000, Silletti et al., 2008). The flow rate of stimulated saliva has been widely studied including following different types of taste and mechanical stimuli (Feller et al., 1965, Cowart and Beauchamp, 1986, Froehlich et al., 1987b, Fischer et al., 1994). It has been found that basic taste qualities are associated with a dose-response reflex parotid salivary secretion and the flow rate of the basic tastes from different researches follows a similar pattern for sour > salt > sweet (Feller et al., 1965, Speirs, 1971a, Froehlich et al., 1987b). However, for the other two tastes, umami and bitter, only a few studies have been published. Hodson and Linden (2006) found that the Monosodium glutamate (MSG) (umami) stimulated saliva flow rate was lower than

that of citric acid but higher than salt taste. These authors also found that bitter taste stimulated with magnesium sulphate produced the lowest saliva flow rate. Using quinine as the stimulus a saliva flow rate that was just below the flow rate following stimulation with salt was reported (Chauncey and Shannon, 1960). Factors contributing to the large variability of saliva flow rates reported include age, health status and drug intake by the donors. It is known that saliva flow rates are reduced appreciably for elderly people (Dodds et al., 2005).

2.2.3.2 Composition of saliva

As reported earlier in this chapter, saliva consists mainly (99%) of water. The composition of the other components in saliva can be divided into inorganic and organic constituents. The major inorganic constituents include hydrogen ions, calcium ions, inorganic phosphate and fluoride. These inorganic constituents serve different functions. Bicarbonate allows buffering while calcium and phosphate allow for maintenance of tooth mineral integrity (Dodds et al., 2005). Proteins make up the bulk of the organic components of saliva. Saliva contains a wide variety of proteins which have different roles to play. The major proteins include proline-rich proteins (PRPs), amylase, statherin, histatins and mucins. There are also some other anti-microbial proteins and enzymatic proteins such as IgA (immunoglobulin), lactoferrin, lysozyme and peroxidases. Among the proteins that are present in saliva, the large molecular weight mucins can be expected to be of most impact in relation

to oral processing. Mucin is a negatively charged polymer with a broad molecular weight distribution. It consists of high molecular weight O-linked glycoproteins, composed of a polypeptide backbone and covalently linked oligosaccharide side chains (Nyström et al., 2010) as depicted in Figure 2.16. Two types of mucin are found in saliva designated mucin glycoprotein1 (MG1) and the smaller mucin glycoprotein2 (MG2) (Gibson and Beeley, 1994).

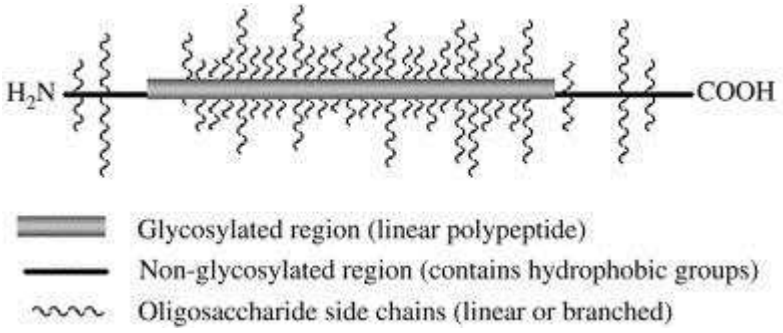

Figure 2.16: Structure of salivary mucin (Nyström et al., 2010).

As well as the different glands secreting saliva at different rates into the mouth, each gland has a different profile of proteins. For example, some proteins are universal to all glands, such as IgA. However, proteins like mucins are only found in saliva secreted from the submandibular gland, the sublingual gland and most minor glands but not in saliva from the parotid gland. The latter produces saliva rich in amylase. Also, basic PRPs are found exclusively in saliva from the parotid gland whereby acidic PRPs are found in saliva scretions from the submandibular and parotid glands (Carpenter, 2012).

2.2.3.3 Role of saliva in taste and flavour perceptions

The function of saliva has been organised into five categories: (1) taste and digestion, (2) buffering action and clearance, (3) antibacterial activity, (4) maintenance of tooth integrity and (5) lubrication and protection (Mandel, 1987, Humphrey and Williamson, 2001). In accordance with the overall objective of this research only (1) and (5) are reviewed in the following.

Saliva plays an important role in taste perception both before and during the transduction of the taste stimuli. Taste substances have to be dissolved in saliva before they can reach the taste receptors. Saliva is isotonic when initially formed inside the acini. However, as it flows through the striated ducts, the sodium and chloride ions are reabsorbed. Therefore, it becomes hypotonic when secreted into the oral cavity. This hypotonicity provides saliva with its capability to dissolve taste substances and deliver them through diffusion, in addition to convective transport through action of tongue and teeth, to the taste receptors (Matsuo, 2000). Saliva may also change the taste perception due to its buffering effect. Buffering action is due to the bicarbonate and carbonate ions and partly due to the phosphate ions and presence of the proteins (Bardow et al., 2000). It was reported that due to the buffering effect, sourness perception could be changed among individuals as their flow rate of saliva would change the pH of acidic solutions (Christensen et al., 1987). To elicit salty perception, the sodium chloride concentration has to be higher than the sodium ion concentration in the unstimulated saliva (Omahony, 1979, Omahony

and Heintz, 1981). Some organic substances in saliva, such as basic PRPs, can interact with taste substances. The main function of PRPs is to bind with tannic acid immediately when it is present to diminish its bitterness and astringency (Glendinning, 1992). In addition, another protein secreted through von Ebner's gland was found to be important in taste perceptions. This protein is a type of lipophilic ligand carrier protein which enables it to transport hydrophobic molecules such as bitter taste substances (Matsuo, 2000).

Studying the relationship between saliva flow rate and flavour release in chewing gum, Guinard et al. (1997) found a positive correlation between saliva flow and the time at which maximum intensity of both sweetness and cherry flavour was reached (typically referred to as Tmax). Another not insignificant impact of saliva is that it may change the release of flavour by decreasing the viscosity of foods through the action of its enzymic constituents. It was found that α-amylase could reduce the viscosity of starch thickened foods sufficiently to enhance flavour release (Ferry et al., 2004). On the other hand, for foods thickened with physically modified starch amylase action was such that viscosity increased due to releasing the molecular constituents from the swollen starch granules and saltiness perception (Ferry et al., 2006b). This demonstrates the complex impact saliva may have on taste and flavour perceptions.

2.2.3.4 Role of saliva in texture perception

The effect of saliva on the texture perception of food starts when the food enters the oral cavity. The main functions of oral food treatment include: (1) particle size reduction through mastication; (2) lubrication of the particles by mixing with saliva (Prinz and Lucas, 1995). The main function of oral food treatment is directly related to swallowing as particle size and lubrication are the two main factors that determine the optimum moment of swallowing.

Saliva can affect the texture perception of food by its enzymatic constituents and α-amylase is one example. α-amylase initiates the starch digestion in the mouth by cutting the long carbohydrate strands at the $\alpha(1\rightarrow4)$ linkages between the glucose residues. The starch therefore loses its ability to bind water and the viscosity of food is reduced. By adding saliva related fluid such as α-amylase to custard prior to ingestion, Engelen et al. (2003) found that the sensory ratings for melting, thickness and creaminess were significantly decreased. Janssen et al. (2009) found that saliva could induce the breakdown of mixed protein and starch gels and therefore affect mouthfeel perception. It has also been reported that saliva can induce coalescence in emulsions when stabilised by starch-based emulsifiers due to the α-amylase (Dresselhuis et al., 2008a). The researchers suggested that saliva induced coalescence had an impact on sensory perceptions related to fat such as more creamy, fatty. Saliva could also induce flocculation in emulsions stabilized by several other emulsifiers including sodium caseinate and whey protein isolate (Vingerhoeds et al.,

2005, Silletti et al., 2007). The effect of saliva induced flocculation or coalescence in relation to sensory perception however, has not been widely studied.

Another important function of saliva during oral processing is lubrication. Oral lubrication is considered primarily to be provided by oral surface adsorbed layers of salivary proteins such as mucin, statherin and PRPs. By using saliva as the lubricant, it was found that the friction coefficient in the boundary regime was two orders of magnitude lower than when water was used as lubricant (Bongaerts et al., 2007a). It has been hypothesised that oral tribology plays a major role in the magnitude of surface related mouthfeel attributes such as roughness and astringency, and for transient lubrication properties (Selway and Stokes, 2013).

Saliva's lubrication function is imparted by its unique ability to adsorb onto any kind of surfaces and form a multi-component and protein-rich layer (Cardenas et al., 2007, Macakova et al., 2010, 2011). According to Macakova et al (2010, 2011), saliva can adsorb onto hydrophobic PDMS substrates to form a viscoelastic and highly hydrated film. This film has a heterogeneous structure consisting of a thin dense inner layer consisting of non-glycosylated anchoring domains of mucins and low molecular weight salivary proteins, and a thicker and viscoelastic upper layer consisting of glycosylated mucin chains protruding into the bulk fluid. The drop in friction is due to the low interpenetration between surface layers providing a low viscosity region for shear and energy dissipation (Macakova et al., 2011). The loss of saliva induced lubrication can result in unpleasant sensory perception, such as dry

and puckering mouthfeel known as astringency. The well-known astringent polyphenols, have been shown to cause the complexation of PRPs and therefore lead to the loss of saliva lubrication (Baxter et al., 1997). The astringency of food components such as epigallocatechin gallate (EGCG) and β-lactoglobulin (Rossetti et al., 2008, Vardhanabhuti et al., 2011) has been demonstrated through measurement of the friction coefficient of human saliva in their presence.

In addition to the lubrication behaviour, the rheological properties of saliva were also thought to be very important for their roles in oral perception (Waterman et al., 1988, Stokes and Davies, 2007, Davies et al., 2009). By using a series of beverages and stimulation, Davies et al. (2009) found that the viscoelastic properties and secretion rate of saliva changed significantly in response to stimulation and this could in turn affect mouthfeel perception. Traditionally saliva was thought to be a shear thinning and elastic fluid with a detected yield stress (Davis, 1971, Schwarz, 1987a). However, Waterman et al. (1988) proved that the detected yield stress was possibly caused by the artificial effect originating from the absorption of a protein layer at the air-liquid interface at the edges of the measuring geometry. By using a capillary rheometer Van der Reijden et al (1993a, b) solved this problem and suggested that the viscoelastic properties of saliva were different when collected from different glands. They hypothesised that this was due to the difference in the mucin concentration, conformation and molecular weight (Van der Reijden et al., 1993a, b). By using a cone-and-plate geometry with SDS (sodium dodecyl sulphate) applied at the rim of

the plates to desorb proteins from the sample surface, Stokes and Davies (2007) measured rheological properties of saliva stimulated by acid and mechanical means and found a strong dependence on the type of stimulation. The acid stimulated saliva was extremely elastic with a normal stress to shear stress ratio of the order 100. The extensional flow properties of saliva were studied by two groups of authors (Zussman et al., 2007, Haward et al., 2011). By using a modified extensional flow oscillatory rheometer (EFOR), Haward et al (2011) found that unstimulated saliva could reach Trouton ratios of up to 120 which indicating the highly elastic nature of saliva. Zussman et al (2007) studied the viscoelasticity of both unstimulated and 2% citric acid stimulated saliva by using an elongational viscometer. They found that the relaxation time for unstimulated from whole, parotid and submandibular /sublingual saliva were 39.5 ms, 1.04 ms and 42.1 ms, respectively, and under citric acid stimulus, the relaxation time of saliva from whole, parotid and submandibular /sublingual become 47.6 ms, 1.4ms, and 399 ms, respectively. However, to-date there is no evidence of published literature on the extensional properties of five basic tastes stimulated (sourness, salty, bitterness, umami and sweetness) saliva.

2.3 The Link between Fluid Mechanical Properties with Sensory Perception

2.3.1 Rheology and mouth-feel

Texture is one of the major constituents of food palatability. Although the appreciation of food texture can be traced to thousands of years ago, the term itself has only been studied as of around the middle of the 20th century (Matz, 1962, Szczesniak, 2002, Chen, 2009). The textural properties of food can be assessed by either descriptive subjects or instrumental analysis. Traditionally these two techniques have been used separately, with sensory evaluation using human subjects to evaluate sensory and physical properties of the food, and instrumental analysis delineating the chemical and physical properties of food (Ross, 2009). However, neither of these two techniques on its own can provide a complete picture of the food properties. Therefore researchers tend to combine the results from both techniques to understand texture perception more comprehensively.

Texture itself has been defined as "all the rheological and structural (geometric and surface) attributes of the product perceptible by means of mechanical, tactile, and where appropriate, visual and auditory receptors" (Lawless and Heymann, 2010). In terms of liquid and semi-solid foods, texture studies tend to be more focused on how rheological properties relate to texture perceptions.

Food researchers have sought for a long time to measure texture instrumentally due to the combination of time and high cost associated with sensory analysis, despite the fact that 'texture' is a sensory property (Szczesniak, 2002). There are three main

approaches: (1) use of imitative techniques such as 'texture analysis'; (2) application of empirical methods that try to align some kind of measurement to sensory perceptions; and (3) measurement of fundamental mechanical properties of the food such as rheological properties in relation to their underlying microstructure (Stokes et al., 2013).

In terms of texture studies, the rheological properties of liquid and semi-solid foods have been extensively studied to relate with their mouthfeel perceptions. Szczesniak and Farkas (1962) published one of the earliest studies on the correlation of the mouthfeel of liquid and semi-liquid foods with their shear rheological properties. Using a wide range of gum solutions of about the same low shear viscosity (around 1.2 Pa.s) these researchers suggested that within the shear rate range of 0 to 100 s^{-1}, perceived sliminess is negatively related to shear thinning rate. However, this work does not provide sufficient insight to know whether it is the rate of shear thinning, the shear rate of onset of shear thinning or the viscosity at shear rates relevant to in-mouth perception that determines sliminess. It was then Wood (1968) who for the first time studied the flow conditions in the oral evaluation of liquids. In his research, the shear rate chosen for the measurement of viscosity to relate to the perception of thickness was determined by asking the subjects to compare the thickness of cream soups to glucose syrups which were of shear thinning and Newtonian flow behaviour, respectively. He then postulated that the shear rate at which the viscosity curve of a soup and a syrup with similar perceived thickness crossed is pertinent to

thickness perception and this shear rate is 50 s^{-1} (Wood, 1968). However, in this work only a limited number of relatively similar non-Newtonian fluids were used. Later on, a similar approach was applied to a wider range of food products (Shama et al., 1973, Shama and Sherman, 1973) to investigate whether it is in fact a range of shear rates and shear stresses that is relevant to perception of thickness. It was found that the stimulus associated with oral viscosity perception of liquid and semi-liquid foods embraces a wider range of shear rates from 10 to 1000 s^{-1} strongly depending on the viscosity of the products. These authors suggested that for a less viscous liquid, the stimulus related to viscosity perception involves the shear rate developed at a constant shear stress of approximately 10 Pa. For viscous samples it involves the shear stress developed at a low shear rate of approximately 10 s^{-1}. Their results reveal the fact that during oral processing of less viscous foods, humans tend to apply a minimum stress with increased rate of deformation. However, when processing more viscous foods, the deformation rate is reduced to a minimum while the applied stress is increased proportionally with increased viscosity (Chen, 2009).

The shear stress and shear rate conditions for thickness perception from the Shama and Sherman's (1973 a,b) experimental work agree well with the results of a modelling approach developed by Kokini and co-workers (Dickie and Kokini, 1983, Kokini and Cussler, 1983, Kokini, 1985), see Figure 2.17 for explanation. In this so-called Kokine model the liquid food is considered as being sheared between the

tongue and the roof of the mouth and an oral shear stress can be calculated through Equation 2.33.

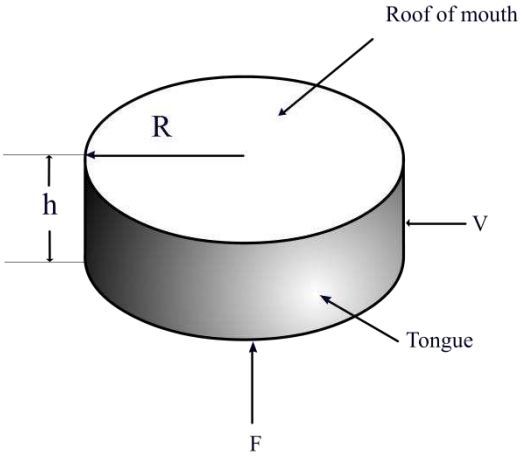

V =velocity of tongue (2cm/s)
F=Normal force (1N)
r=radius of plug (2.5cm)
t=time(s)
H_0=initial plug height (0.2cm)
m=consistency index
n=power law index

Figure 2.17: A model geometry of the mouth as developed by Kokini (Dickie and Kokini 1983). Typical values present in the mouth are included in the figure.

$$\tau = mV^n \left\{ \frac{1}{{h_0}^{(n+1)/n}} + \left(\frac{F}{R^{n+3}} \cdot \frac{n+3}{2\pi m} \right)^{1/n} + \frac{n+1}{2n+1} \cdot t \right\}^{n^2/n+1} \quad (2.33)$$

Several groups of researchers (Morris and Taylor, 1982; Cutler et al., 1983) studied an extensive range of fluid foods that included weak gels, and they found that the Sharma and Sherman method was suitable for many of the fluid samples studied, but increasingly failed as the shear thinning nature of the fluid was increased. For highly shear thinning fluids that were classed as weak gels, the perceived thickness was underestimated by an order of magnitude when compared to Wood's shear rate of 50 s^{-1}, although the correlation was improved when comparison was made at 10 s^{-1} (Morris and Taylor, 1982, Cutler et al., 1983).

Christensen (1979) suggested that the perceived viscosity is represented by an average viscosity over a range of shear rates rather than by viscosity measured at a single shear rate. This finding is based on a study using low, medium and high molecular weight carboxymethyl cellulose (CMC) solutions prepared to the same low shear viscosity value. The high molecular weight solution would be more shear thinning and an over shear rate averaged viscosity reflects the sensory findings (Christensen, 1979).

Compared with large deformation viscosity measurement, researchers also found small deformation viscosity measurement was useful. Richardson et al (1989) found that the underestimation of assessed thickness of extremely shear thinning samples (such as weak gels) was eliminated with small deformation viscosity measurements. Using Newtonian fluids, true solutions and weak gels, small deformation measurements of dynamic viscosity over a range of frequencies showed increasing correlation with panel scores for assessed thickness. They suggested that for Newtonian true solutions and shear thinning weak gels, the dynamic viscosity measurement at a single frequency of 50 $rad.s^{-1}$ directly correlated with panel scores of thickness perceptions (Richardson et al., 1989b). Some other researcher reported that the dynamic viscosity measurements at a frequency of 50 $rad.s^{-1}$ correlate closely with the activity of muscles that control tongue movement measured using electromyography (EMG) for Newtonian liquids, weak gel model systems and homogenised full cream milk (Dea et al., 1989). However, it is not clear why this

should be the case. Richardson et al (1989a) suggested the reason could be that the mouth is capable of far more subtle sensory evaluation of texture and could indeed subject fluids to 'small deformation' (Richardson et al., 1989a).

It is almost clear that from previous studies, that a universal single shear rate that can be used to predict sensory perception does not exist. However, it seems reasonable to use the viscosity measured at shear rate around 50 s^{-1} or 50 $rad.s^{-1}$ to predict certain sensory perceptions of liquid foods. The term 'liquid foods' denotes any systems with a viscosity of less than 100 mPa.s and are not weak gels or highly shear thinning (Stokes et al., 2013). For other liquids which are designed using hydrocolloids to have the similar viscosity around 50 s^{-1}, the viscosity may still vary above and below this shear rate and also their elasticity. In addition, the apparent yield stress and storage modulus have been found highly related to some initial perceptions such as firmness of yogurts and mayonnaise (Harte et al., 2007).

Over a decade ago, Nicosia and Robbins (2001) found that the transient shear rate could reach up to 10^5 s^{-1} during oral processing of food, and following this insight researchers have started to consider high shear viscosity in relation to the in-mouth behaviour of foods (de Vicente et al., 2006, Davies and Stokes, 2008, Koliandris et al., 2010). This further brings the study of transition from rheology to tribology which might be even more related to mouth-feel perception during later stages of oral processing. The details are discussed in section 2.3.3.

In addition to behaviour in shear flow, most often assumed to be the prevailing flow pattern during the oral processing of liquid and semi-liquid foods, some researchers have provided evidence that extensional flow properties could be similarly important (Debruijne et al., 1993, van Vliet, 2002, Koliandris et al., 2011). The concept is that foods are initially compressed between the tongue and the palate similar to squeezing flow between two parallel plates. Then, on separation, biaxial extensional flow develops as if the plates were lubricated (Chatraei et al., 1981). However, the relationship between extensional flow behaviour and sensory perception has barely been investigated. One exception is the use of Boger fluids to study the relationship between the perception of saltiness and extensional viscosity(Koliandris et al., 2011). However, mouthfeel perceptions were not considered in this work.

2.3.2 Rheology and flavour perception

The study of how changing the viscosity of solutions affects perceived flavour and taste has been developed over many years(Stone et al., 1974). The influence of the rheology of a particular food material on the perception of its intensity of flavour and taste can be divided into two categories: (1) a physiological effect due to the proximity of the taste and olfactory receptors to the kinaesthetic and thermal receptors in the mouth, since an alteration of the physical state of the material may have an influence on its sensory perceptions; and (2) an effect related to the bulk properties of the material such as viscosity, since the physical properties of the

material may affect the rate and the extent with which the sensory stimulus reaches the gustatory receptors (Rao, 2007).

It is generally understood that increasing viscosity through the addition of thickeners such as hydrocolloids results in a decrease in perceived intensity of volatile and non-volatile components (Vaisey et al., 1969, Moskowitz and Arabie, 1970, Baines and Morris, 1987). However, the mechanism behind this has always been a debate. Some researchers hypothesised that an increase in aqueous solution viscosity resulted in increased threshold values for perceptions of saltiness and sweetness (Stone and Oliver, 1966, Paulus and Haas, 1980). In addition, it was found that different hydrocolloid systems affect taste perceptions to different extent. Vaisey et al (1969) found that systems thickened with more shear thinning hydrocolloids tended to decrease the perception of sweetness to a lesser extent than those that are less shear thinning. Some researchers found that for different tastants, the perceived intensities were affected differently: for saltiness, bitterness and sourness, the perceived intensity seemed to depend more on the nature of the hydrocolloid than on the viscosity level. However, for sweetness imparted by sucrose, the perception was found to be highly dependent on viscosity of the hydrocolloid (Pangborn et al., 1973, Pangborn and Szczesniak, 1974, Pangborn et al., 1978).

Baines and Morris (1987) found that perceived taste and flavour was greatly affected by the addition of guar gum at concentrations above the point of random coil overlap (c^*). They proposed that the perceived change in flavour might be linked to

inefficient mixing with saliva for solution concentration above c*, inhibiting the transport of small taste and aroma molecules to their respective receptors (Baines and Morris, 1987, Baines and Morris, 1988). However, by using an atmospheric pressure ionization mass spectrometry (APCI-MS) Taylor et al. (Taylor et al., 2000) and Hollowood et al. (Hollowood et al., 2002) found that the detected concentration of aroma released in the nose was not significantly changed in hydroxy propylmethyl cellulose (HPMC) at concentrations of up to 2.1 × c*. Therefore, the hypothesis that the change of flavour perception was due to inhibition of volatile release can be rejected and two further hypotheses should be considered: (1) increased viscosity may result in a reduced rate at which the tastants reach their receptors on the tongue and palate; (2) the somatosensory tactile stimuli such as oral shear stress can interact with taste and aroma signals and further modify the flavour perception (Mitchell and Wolf, 2011).

It should be noticed that for hypothesis (1), there are some differences in the thickeners used. It was found that in starch thickened system the viscosity induced flavour and taste suppression was much smaller than that in a system thickened with linear hydrocolloids such as HPMC. It is then further hypothesised that both flavour perception and mouthfeel can be related to the efficiency of mixing of the thickened solutions with water (Hill et al., 1995, Ferry et al., 2006a, Ferry et al., 2006b) which was clearly reduced for HPMC solutions compared to equiviscous suspensions of modified starch. Very recently, a break-down of this relationship has

been demonstrated for xanthan gum comparing a physically modified granular form of xanthan gum with its molecularly dissolved counterpart (Abson et al., 2014). It appears that xanthan gum may play a unique role in flavour perception and an impact of interaction with saliva has been suggested that cannot be predicted by rheological analysis of the aqueous polysaccharide solution alone.

For hypothesis (2), a series of work done by Cook et al (2003) suggests that the aroma and flavour perception in hydrocolloid thickened solutions is directly related to the Kokini oral shear stress (Figure 2.17). He developed the hypothesis that the sensory signal for viscosity corresponding to the shear stress generated in-mouth can modulate the perception of taste and aroma.

As it has been suggested that elongational flows are more effective than simple shear flows for mixing fluids (Connelly and Kokini, 2004), Ferry et al. (2006) proposed that extensional behaviour is more likely to correlate with mouthfeel and taste perception than rheological behaviour evaluated in shear. This proposal is especially linked to the idea of enhanced flavour perception from granular starch systems at equiviscous to molecularly dissolved solutions of HPMC. However, there are not many studies in this area except one work by Koliandris et al. (2011) on food grade Boger fluids that investigated how extensional flow affects saltiness and mouthfeel perception. Surprisingly, no significant differences in mouthfeel and flavour perceptions between Newtonian and Boger fluids were detected which was suggested to be due to the unusual nature of the samples demanding more training of the sensory panel.

Up to date, there are no studies that link extensional rheology with sweetness and aroma perception.

2.3.3 Tribology and mouthfeel perceptions

The tribological behaviour of a material is critical in many engineering and machinery design applications and it is also plays an important role during oral processing and thus in sensory perceptions. However, there has been few investigations in oral tribology and oral lubrication that relates to food texture and oral sensation, although the importance of lubrication in this context has already been recognised about four decades ago (Kokini et al., 1977, Kokini and Cussler, 1983, Kokini, 1987, Hutchings and Lillford, 1988). These authors applied a tribology approach to explore the dominating physical properties of sensory perceptions such as smoothness, slipperiness, and creaminess. They found that the sensory perception of smoothness is inversely correlated with friction force between tongue and palate. Slipperiness was reported to correlate with the inverse of the sum of viscous force and friction force. However, the perception of creaminess was found to be a combined effect of thickness, smoothness and slipperiness which can be expressed as Equation 2.34 :

$$Creaminess = thickness^{0.54} \times smoothness^{1.56} \times slipperiness^{0.32} \quad (2.34)$$

However, Kokini's findings were not fully appreciated and until the last decade, the potential importance of tribology and friction measurements was recognised again by food researchers. Due to the complexity of food system and oral processes, most of the tribological studies found in literature are focused on two types of model food systems: hydrocolloid solutions and food emulsions.

Malone et al. (2003) studied the oral behaviour of food hydrocolloids and emulsions and found that thin film rheological properties and surface deposition played important roles in sensory perceptions such as fattiness, smoothness and astringency. By using a series of different tests including rheology and tribology, De Wijk et al. (2006) found that the mouthfeel perceptions could be divided into three dimensions and each dimension was related to different properties, see Figure 2.18.

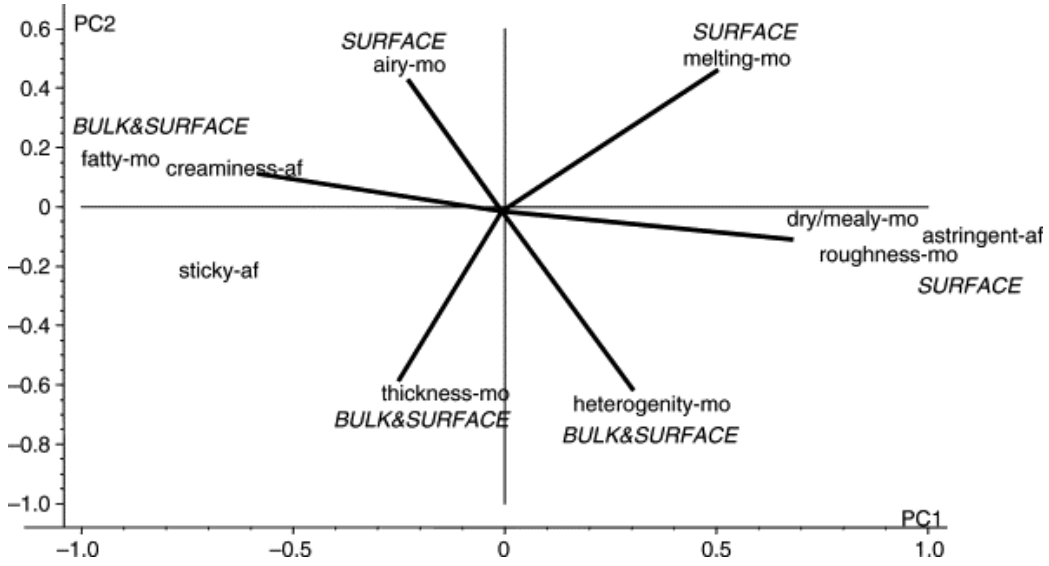

Figure 2.18: PCA analysis of selected sensory mouthfeel (-mo) and afterfeel (-af) attributes summarised by three sensory dimensions. Extremes of each dimension reflect either surface properties of the oral food bolus or surface plus bulk properties. Reproduced from (Adapted from De Wijk et al.2006).

There are also some researchers who used real foods to investigate the relationship between mouthfeel and tribology. Giasson et al. (1997) and Luengo et al. (1997) studied the thin film tribological properties and texture perception of mayonnaise and chocolate respectively, and found that thin film tribological properties rather than bulk rheological properties correlated with composition and the texture of samples. However, they did not use any sensory tests to find out how tribological properties are related to sensory perceptions.

As already mentioned in section 2.3.1, Nicosia and Robbins (2001) found that the transient shear rate in the mouth can reach up to 10^5 s^{-1} during oral processing of food. Following this insight researchers have started to consider high shear viscosity in relation to the in-mouth behaviour of foods (de Vicente et al., 2006, Davies and Stokes, 2008, Koliandris et al., 2010) and tribological analysis is one way of imparting these high shear rates. However, it is worth mentioning that the actual shear rate in a tribometer is not known or can be controlled as the gap height is not known.

In a study which attempted to correlate friction measurement with perceived slipperiness of guar gum solutions, it was found that the correlation coefficient between sensory perception of 'slipperiness' and fluid lubricant properties at entrainment speeds between 10-100 mm/s was highest across all speed (Malone, et al, 2003). The researchers suggested that this regime is the most relevant in describing oral processing associated with the mouthfeel perception of slippery.

2.3.4 Tribology and flavour perception

The relationship between rheological properties and flavour perception has been reviewed in section 2.3.2. With regard to relating tribological properties with flavour perception there is a complete gap in the published literature.

2.4 Physicochemical properties of polysaccharides used in this thesis

The physicochemical properties of the main hydrocolloids used in this PhD research are introduced in this section. These include xanthan gum, dextran, guar gum and methylcellulose.

2.4.1 Xanthan gum

Xanthan gum is a widely used polysaccharide in the food industry that is produced through microbial fermentation of glucose or sucrose by *Xanthomonas campestris* (Morris, 2006). The primary structure of xanthan gum, see Figure 2.19, consists of a cellulose backbone of β-1→4-linked D-glucose units with a trisaccharide side chain attached to every other glucose. The side chains are linked through the 3 position and consist of β-D-mannose, β-1→4-linked D-glucuronic acid, and α-1→2-linked D-mannose (Sworn, 2009). The molecular weight of xanthan gum ranges from 2×10^6 to 20×10^6 Da depending on the association between chains, formation of aggregates of

several individual chains, and also the fermentation conditions during the xanthan gum production (Garcia-Ochoa et al., 2000).

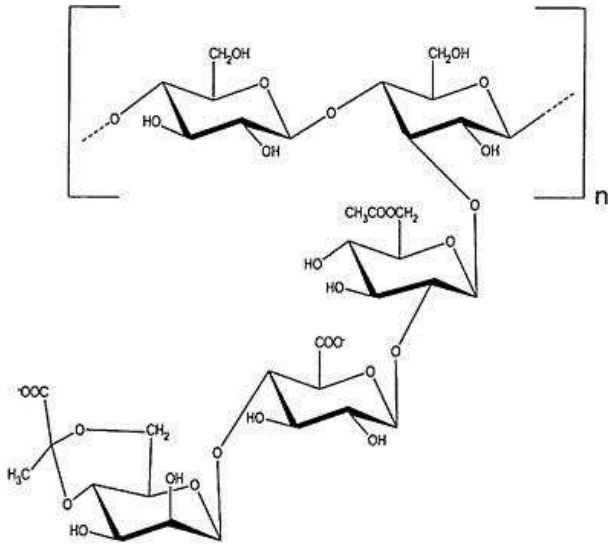

Figure 2.19: Primary structure of xanthan gum (Adapted from Kool et al., 2013).

Xanthan gum has been widely used due to its unique rheology property as it develops a high viscosity at relatively low concentration and shows strong shear thinning behaviour compared with other thickeners (Sworn, 2009). The flow behaviour of xanthan gum is a result of intermolecular association among the polymer chains which results in the formation of a complex network of entangled rod-like molecules. Also xanthan gum has the ability to form thermoreversible gels in the presence of certain galactomannans such as locust bean gum, guar gum, tara gum as well as glucomannan konjac (Fitzpatrick et al., 2013).

2.4.2 Dextran

Dextran is a polysaccharide that is produced through the fermentation of sucrose by *Leuconostoc mesenteroides* (Monsan et al., 2001). The structure of dextran, see Figure 2.20, is composed of D-glucose units and features substantial numbers (at least 50%) of consecutive α-1→6 glycosidic linkages in the main chain and α-1→2, α-1→3 and α-1→4 branch glycosidic linkages (Ahmed et al., 2012). The most widely used dextran is produced by *Leuconostoc mesenteroides* B512F which is a linear dextran with around 5% α-1→3 linked branches (Maina et al., 2011).

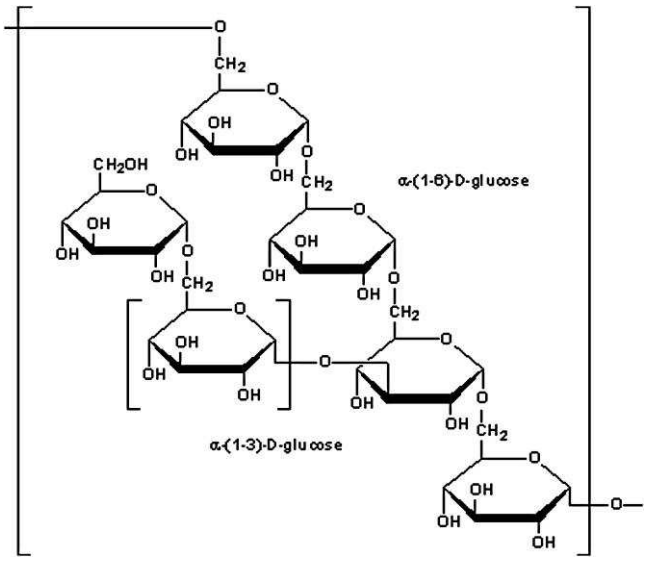

Figure 2.20: Primary structure of dextran (Adapted from Ertmer et al., 2009).

The molecular weight of dextran ranges from 10 to 2000 KDa depending on the fermentation conditions. The high percentage of 1,6-glycosidic linkages promotes the high solubility and low solution viscosities that are characteristic for dextran

(McCurdy et al., 1994). Also solutions of dextran show Newtonian behaviour even at shear rate as high as 10^5 s^{-1} (Koliandris et al., 2010).

2.4.3 Guar gum

Guar gum is a naturally occurring polysaccharide that is obtained by grinding the endosperm portion of *Cyamoposis tetragonolobus. L*. The structure of guar gum, see Figure 2.21, is composed of long, straight chains of α-D-mannopyranosyl units linked together by β-D(1→4)-glycosidic linkages (Yoon et al., 2008). The molecular weight of guar gum ranges from 50k to 8000 kDa (Roberts, 2011). Since it is not affected by ionic strength or pH at moderate temperature due to its non-ionic nature, guar gum is widely applied in pharmaceuticals for the delivery of drugs (Rubinstein, 2000). The structure of guar gum gives it a large number of hydroxyl groups that can form many hydrogen bonds with water and thereby increase the solution viscosity (Mannarswamy et al., 2010). Therefore guar gum is widely used in the food industry as a thickener or emulsion stabiliser.

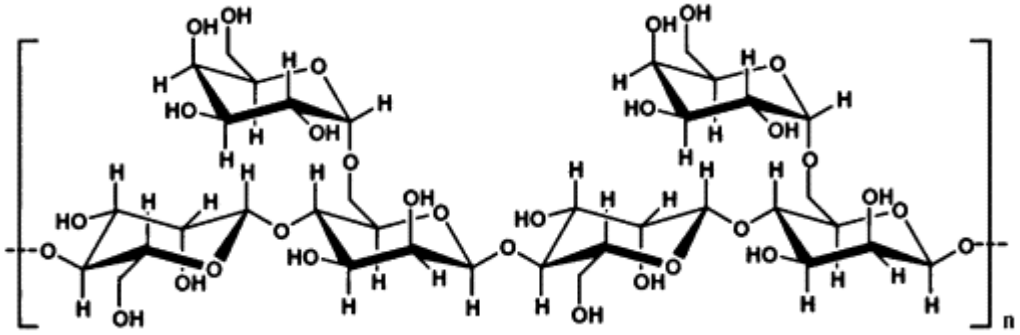

Figure 2.21: Chemical structure of guar gum (Adapted from Abdel-Halim and Al-Deyab, 2011).

2.4.4 Methylcellulose

Methylcellulose is a synthesised polysaccharide produced by replacing hydroxyl groups with methoxyl groups in cellulose, see Figure 2.22). This procedure can be achieved through etherification of alkali cellulose with methyl chloride and the degree of substitution ranges from 1.6-1.9. The properties of methylcellulose depend on both the degree of substitution and the distribution of the substituents along the cellulose backbone (Park et al. 2001).

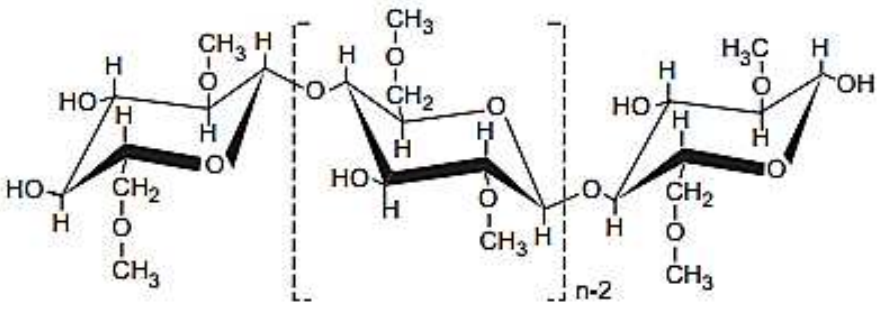

Figure 2.22: Chemical structure of methylcellulose (Adapted from Park et al. 2001).

Methycellulose shows reversible thermogelation and this is attributed to hydrophobic interactions between chains upon heating (Desbrieres et al., 2000, Park and Ruckenstein, 2001). This thermogelation property makes it a widely applied hydrocolloid in the food industry such as in batter and edible coatings (Sanz et al., 2005).

3 MATERIAL AND METHODS

3.1 Samples

3.1.1 Polysaccharides and polysaccharide solutions

In this research a selection of aqueous polysaccharide solutions were used for sensory evaluation and instrumental analysis of rheology and friction properties. All samples destined for sensory evaluation were prepared with bottled water (Evian, Danone, France, conductivity=112.4 S/m). For instrument measurement, samples were prepared using bottled water with addition of 0.05% (w/v) Sodium azide (NaN_3) as an antimicrobial. Solutions for sensory analysis were stored at 4˚C and used within one week of preparation. Independent of polysaccharide concentration, the samples contained 3% w/w sucrose (purchased in a local supermarket) and 100 ppm banana flavour (isoamyl acetate, Firmenich, Geneva, Swizerland). Banana flavour was not added to samples prepared for instrumental analysis.

Table 3.1 provides an overview of the polysaccharides used in this research. Initially, stock solutions of polysaccharides were prepared as follows.

Table 3.1: Hydrocolloids used in this research including their molecular weight and type.

Hydrocolloids	Molecular weight	Type and source
Xanthan	200 kDa	Keltro RD(CP, Kelco, San Diago, USA)
Dextran 10	10 kDa	Dextran 10(Meito Sanyo, Tokoyo,Japan)
Dextran 500	500 kDa	Dextran 500(Pharmocosmo, Denmark)
Guar	1640 kDa	Meyprodor 100(Danisco, Denmark)
Methycellulose	86 kDa	Methocel A40M(Dow,Michigan,USA)

Xanthan gum solution was prepared at a concentration of 2 %(w/w) by dispersing 20 g of powder into 980 g of water pre-heated to 95 ˚C , while mixing with an overhead mixer (RW20 fitted with a Propeller 4-bladed stirrer, IKA, Staufen, Germany) at moderate speed (1500 rpm). The temperature (95 ˚C) was maintained for one hour by placing the sample into a water bath and the sample was continuously mixed during this time to minimise clumping. The container with the stock solution was placed on a rolling bed for a further overnight mixing at 4 ˚C to allow the polysaccharide to fully hydrate.

Guar gum solution was prepared at a concentration of 1% (w/w) following the same protocol as for xanthan gum based on 10 g of guar gum powder and 990 g of water.

1000 g of Dextran 10 and Dextran 500 solution was prepared at a concentration of 38% (w/w) and 20 %(w/w), respectively, by dispersing the appropriate amount of powder into water while mixing a magnetic stirrer at room temperature for 3 hours. Then these solutions were also put on the rolling bed for further overnight mixing at 4˚C.

Methylcellulose solution was prepared at a concentration of 1%(w/w). Initially 10g of powder was dispersed into 1/3 of the required amount of water (330 g) which was preheated to 95 ˚C while mixing using the same overhead mixer previously introduced for 30 min at 1000 rpm until it was evenly dispersed. The rest of the water (660 g) pre-cooled to 4˚C, was added and mixing continued for a further 30

min after the container had been placed in a 4˚C water bath. This solution then was also placed on the rolling bed for a further overnight mixing at 4 ˚C.

3.1.2 Collection of whole human saliva (WHS)

Whole Human Saliva (WHS) was collected from 3 healthy volunteers (1 female and 2 male) following published protocol (Stokes and Davies, 2007). The subjects were asked to refrain from eating and drinking anything except for water for at least 2 hours before donating saliva.

There are several ways of collecting saliva samples according to Navazesh (1993): draining, spitting, sucking and swabbing. Spitting was used here due to its simplicity and the protocol outlining steps for collecting non-stimulated as well as saliva following taste stimulation is shown below.

(1) The subjects were asked to rinse their mouth using the bottled water (Evian) for at least 30 seconds to make sure the mouth reaches a neutral status.

(2) To collect non-stimulated saliva, the subjects were initially asked to expectorate saliva for 30 seconds into an empty waste container as this part of the procedure was aimed at removing potentially present food residues from the oral cavity. Then, saliva was expectorated and collected into the pre-weighed container at a frequency of 30 seconds for 2 minutes. The ideal technique for collecting saliva is to make sure

that the subject is not under any stress and the head is slightly tilted so that the saliva will pool in the subject's mouth.

(3) To collect stimulated saliva, initially, 5 ml of one stimulation solution were sipped and swilled in the subjects' mouth for 30 seconds and expectorated. This process was repeated once. The types of stimuli and concentrations are displayed in Table 3.2 . Expectoration protocol was as for non-stimulated saliva, see (2).

Table 3.2: Stimuli used for the collection of HWS.

Attributes	Stimulus solution	Sample size	Stimulus Concentration
Sweetness	Sucrose	10mL	0.1, 0.5, 1, 2 M
Umami	MSG	10mL	0.05, 0.1, 0.25, 0.5 M
Bitterness	caffeine	10mL	0.54, 1.08, 2.7, 5.4 $g.L^{-1}$
Salty	NaCl	10mL	0.1, 0.25, 0.5, 1 M
Sourness	Citric acid	10mL	0.01,0.05, 0.125, 0.25 M

3.2 Rheological methods

All rheological measurements were conducted on a rotational rheometer (MCR301, Anton Paar, Austria) either at 20 °C or 35 °C.

3.2.1 Shear Rheology and Thin Film Rheology

Steady state shear viscosity of the polysaccharide samples was measured at shear rates up to 10^6 s^{-1} using a smooth parallel plate geometry of 50 mm diameter at 20°C. A published protocol for thin film rheology (Davies and Stokes, 2008) was followed.

Viscosity at low shear rate was acquired at a "classic" gap height of 0.5 mm whereas viscosity at high shear rate required a smaller gap height in order to prevent inertia based measurement artefacts. These are recognisable through an upturn in viscosity at high shear rates for samples that are not shear thickening. For each sample, viscosity at different shear rates was acquired at different gap height: 0.5 mm, 0.05 mm and 0.03 mm for shear rates of $0.1\sim10^3\ s^{-1}$, $10^3\sim10^5\ s^{-1}$,$10^5\sim10^6\ s^{-1}$, respectively. The data was then corrected for gap error and non-Newtonian behaviour using Excel (Microsoft Inc.,USA) as described below.

3.2.1.1 Correction for gap error

In order to achieve high shear rates (up to $10^5\ s^{-1}$), it is important to reduce the gap height to as small as possible for three reasons: Firstly to achieve an as high shear rate as possible. Secondly to minimize secondary flow effects. Thirdly to minimize the errors arising from viscous heating. However, for narrow gap measurements, the gap heights are never the desired values. When the rheometer performs the zero gap setting, the gap never reaches 'real zero' either because of the imperfect alignment of the plates or imperfections on the plates surfaces. Therefore, when performing small gap measurements, it is important to take the gap error into account. Here, a method described by Kramer et al (Kramer et al., 1987) was applied.

For a Newtonian fluid, the viscosity can be determined in a rotational shear rheometer fitted with a parallel plate geometry with R = plate radius by measuring the torque (M) which is related to shear stress (τ) by Equation 3.1:

$$M = \frac{\pi R^3}{2}\tau \tag{3.1}$$

where R is radius of the plate and τ is the shear stress.

Equation 3.2 defines the shear stress and links the torque to the applied shear rate ($\dot{\gamma}$) through viscosity (η). Shear rate in a parallel plate gap is zero in the centre and maximal at the outer radius R, see Equation 3.3, which is considered for data analysis at this point.

$$\tau = \dot{\gamma}_R \eta \tag{3.2}$$

$$\dot{\gamma}_R = \frac{\omega R}{h} \tag{3.3}$$

Shear rate depends on gap height and at narrow gaps and variation in h has a large impact on the shear rate value and thus the final viscosity value reported. The actual gap height may be defined as h + ε with ε = gap error. Thus, the actual shear rate, still at the outer plate radius, is as shown in Equation 3.4:

$$\dot{\gamma}_{R,act} = \frac{\omega R}{h + \varepsilon} \tag{3.4}$$

Therefore, the actual shear stress is:

$$\tau_{act} = \frac{\omega R \eta}{h + \varepsilon} \tag{3.5}$$

By substituting angular velocity based on Equation 3.3, this relationship transforms into Equation 3.6 which then is re-arranged according to Equation 3.7 based on which the gap error ε can be assessed.

$$\tau_{act} = \frac{\dot{\gamma}_R h\,\eta}{h+\varepsilon} \tag{3.6}$$

$$\frac{\dot{\gamma}_R h}{\tau_{act}} = \left(\frac{1}{\eta}\right) h + \left(\frac{\varepsilon}{\eta}\right) \tag{3.7}$$

Equation 3.7 shows the gap error as a function of measurement parameters (shear rate and gap height) and measurement results (shear stress and viscosity). By plotting $\frac{\dot{\gamma}_R h}{\tau_{act}}$ against h, a slope of $1/\eta$ and an intercept of ε/η are obtained, and the gap error ε is determined.

In this research, a reference liquid (100 cS silicon oil, Dow Corning, USA) was used to determine the gap error every time before performing narrow gap measurements. Viscosity data of the reference liquid was collected at 4 different gap heights (0.5 mm, 0.25 mm, 0.125 mm, and 0.05 mm), and then the gap error was determined by using Equation 3.7.

3.2.1.2 Correction for non-Newtonian behaviour

The shear rate across a parallel plate is not uniform and varies from zero in the centre to maximum at the rim. Normally, shear rate refers to the shear rate at the rim rather than an average shear rate. To correct the error caused by the radial shear rate distribution, several methods have been proposed in literature. A single-point correction was brought up by Cross and Kaye (Cross and Kaye, 1987). In this method it is assumed the sample is Newtonian but the shear rate assigned to the observed 'Newtonian' viscosity is ¾ of the rim shear rate. Later on (Shaw and Liu,

2006) further proved that this shift factor should be 4/5 and this factor was applied here. The corrected shear rate as used in Equation 2.1, for calculation of viscosity and in the results section, where it is simply referred to as shear rate, was calculated with Equation 3.8:

$$\dot{\gamma}_{corrected} = \frac{4}{5}\dot{\gamma}_R \tag{3.8}$$

Figure 3.1 illustrates one example of results before and after correction for both gap error and 'non-Newtonian' behaviour. As can be seen from the figure after the corrections have been applied, the viscosity values from different gap height were merged together.

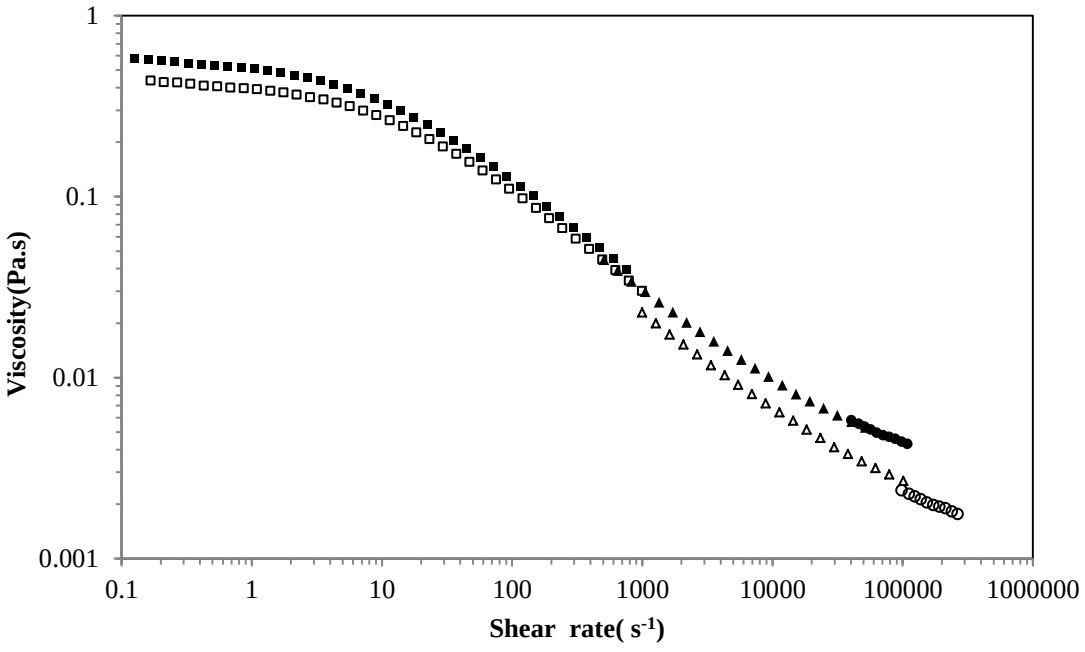

Figure 3.1: Viscosity results for guar gum solution (0.5 % w/w) before (void symbols) and after correction (full symbols) for gap error and 'non-Newtonian behaviour' at different gap height: 500μm (■), 50 μm (▲), 30 μm (●).

3.2.1.3 Model fitting

A four parameter logarithmic model has been used to fit on the viscosity data, see Equation 3.9 and Figure 3.2 illustrating the "role" of the four fit parameters α, β, γ and δ. Model fitting was conducted using the Solver function in Microsoft Excel® (Microsoft 2010, USA). After fitting, the models were used to calculated viscosity at low (50 s^{-1}) and high shear rate (10^5 s^{-1})

$$\log(\eta) = \delta + \frac{\alpha}{(1 + e^{(\beta - \gamma \times \log(\dot{\gamma}))})} \tag{3.9}$$

where, $\delta = Lower\ Asymptote$

$$\alpha + \delta = Upper\ Asymptote$$

$$\beta/\gamma = Point\ of\ inflection$$

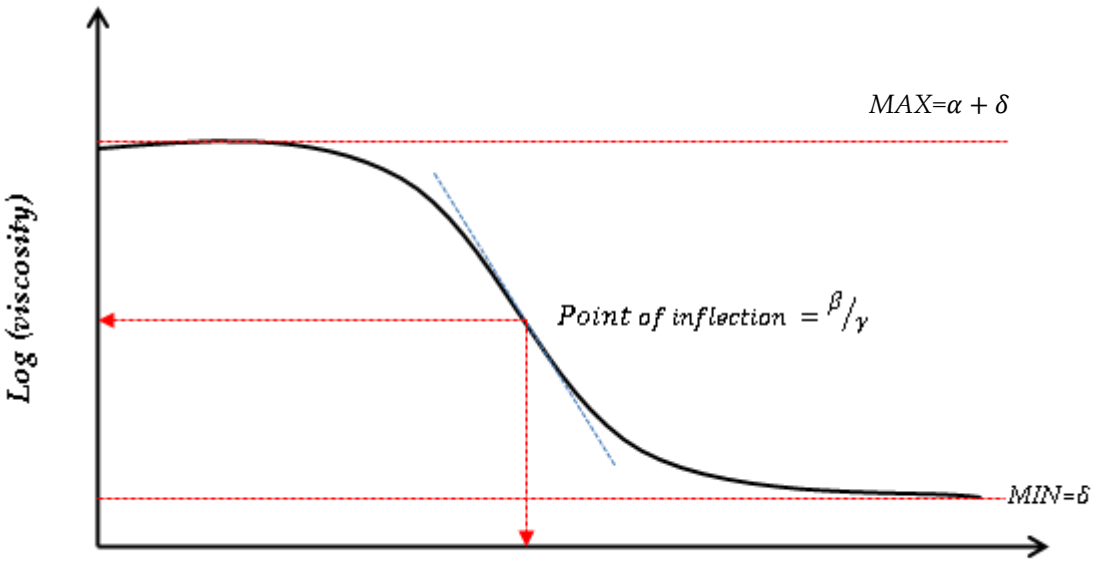

Figure 3.2: model used to fit the viscosity curves

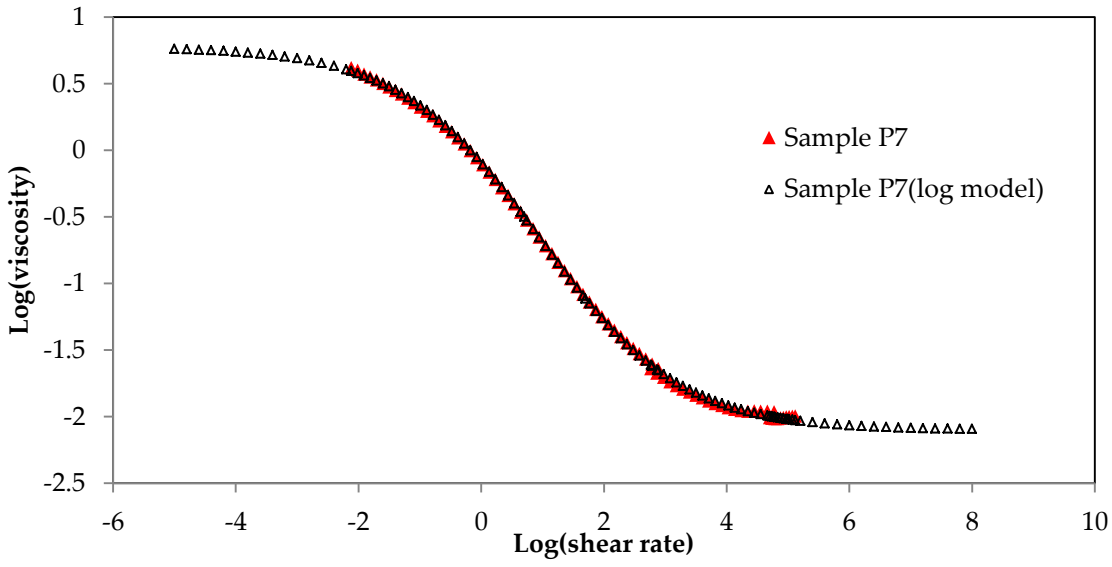

Figure 3.3: An example showing the measured (corrected) data of a sample P7(▲) and the log-log model fitted data (Δ)

3.2.1.4 Small Amplitude Oscillatory Shear (SAOS)

Small amplitude oscillatory shear tests using a cone and plate geometry (50 mm diameter and 2° angle) to obtain the dynamic moduli G′ and G′′ (storage modulus and loss modulus respectively) were carried out within the angular frequency range of 0.1 to 100 rad.s^{-1} within the linear viscoelastic region (LVE). The LVE was initially probed by stepwise increasing the strain from 0.001 to 10 at an angular frequency of 10 rad.s^{-1}. All SAOS measurements were conducted at 20°C.

3.2.1.5 Filament breakup

Viscosity behaviour in predominantly extensional flow or stretching flow was evaluated by means of the technique of filament breakup using the commercial equipment Haake CaBER1 (Thermo Haake GmbH, Karlsruhe, Germany). The instrument was fitted with 6 mm parallel plates and the initial gap height was 3 mm. Samples were loaded using a syringe followed by increasing the gap height to 10 mm in a strike time of 50 ms (linear mode) and acquisition of filament diameter data (D_{mid}) at the midpoint between the two plates over time *t*. Apparent extensional viscosity η_e was calculated using Equation 3.10 assuming that the surface tension σ of the samples can be approximated with the surface tension of water (72 mN.m^{-1} at 20°C):

$$\eta_e = -\frac{\sigma}{\frac{dD_{mid}}{dt}} \tag{3.10}$$

dD_{mid}/dt is the rate at which the mid-point filament diameter decreases with time. For each sample, at least 10 replicate measurements were conducted and the average of 3 representative sets of data is shown as result.

The Trouton ratio T_R, defined in Equation 3.11, was then used to quantify the relative importance of the viscoelastic sample behaviour; for inelastic fluids T_R= 3.

$$T_R = \frac{\eta_e(\dot{\varepsilon})}{\eta(\dot{\gamma})} \tag{3.11}$$

where $\dot{\varepsilon}$ = strain rate.

3.2.2 Shear Rheology of Saliva Samples

The rheological properties of the saliva samples were measured using the rheometer fitted with a cone and plate geometry (50mm diameter and cone angle: 0.02°). Temperature of analysis was 35 °C. After loading the fresh saliva sample two or three drops of 0.1% aqueous solution of Sodium Dodecyl Sulfate were applied at the rim of the geometry to avoid interfacial effects to impact on the results. It has previously been reported that proteins adsorbed at the sample/air interface impart elastic effects and that addition of the highly surface active SDS limits measurement artefact through competing with the protein for the interface leading to protein

desorption (Proctor et al., 2005). A steady shear viscosity measurement was performed in the shear rate range from 1 to 1000 s^{-1}.

3.3 Friction measurements

All friction measurements were conducted on the same rotational rheometer used for shear viscosity analysis either at 20 °C or at 35 °C. For this purpose the rheometer was fitted with a commercial attachment designed for tribology measurement.

3.3.1 Friction device

3.3.1.1 Overview of the tribology cell

Friction properties are assessed in tribometers and food materials have been analysed in the Mini Traction Machine (Malone et al, 2003). Instead of such a device, tribology cell that fitted to a rheometer can be used to measure friction behaviour (Heyer and Lauger, 2008, Lauger and Heyer, 2009). A detailed schematic view of the tribology cell is shown in Figure 3.4.

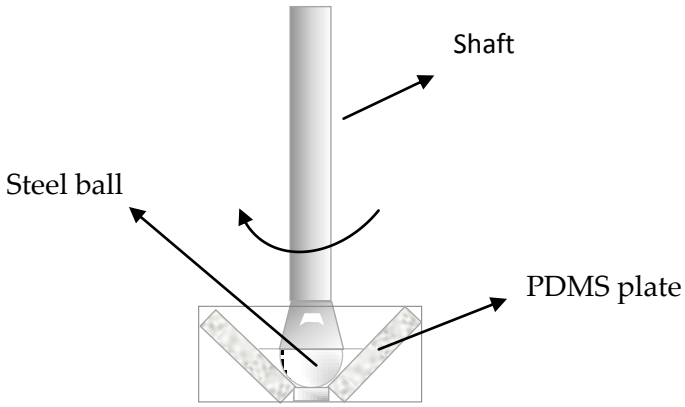

Figure 3.4: Schematic of the tribology cell from the side view

As can be seen from Figure 3.4, the cell is based on a ball-on-three-plates principle. The steel ball (diameter: 1.27 cm) is held at the end of the shaft. The three plates are evenly placed in an inset. As the geometry is lowered to the measuring position, there will be three contacting points between the sphere and the plates. The steel ball as well as the plates are exchangeable to desired materials, e.g. elastomers. In this research all the plates are made from PDMS(Polydimethylsiloxane).

3.3.1.2 Measurement principle of the cell

As mentioned previously, tribology is the study of friction between two materials and the effect of a lubricant on friction. As a result of tribological analysis, the friction coefficient (μ) is plotted against sliding speed (v_s) (Stribeck Curve , see

Figure 2.10) or the sliding distance S_s. The friction coefficient was introduced in section 2.1.5.1 and in the following it is described how the parameter of the friction coefficient are obtained with the tribology cell used here.

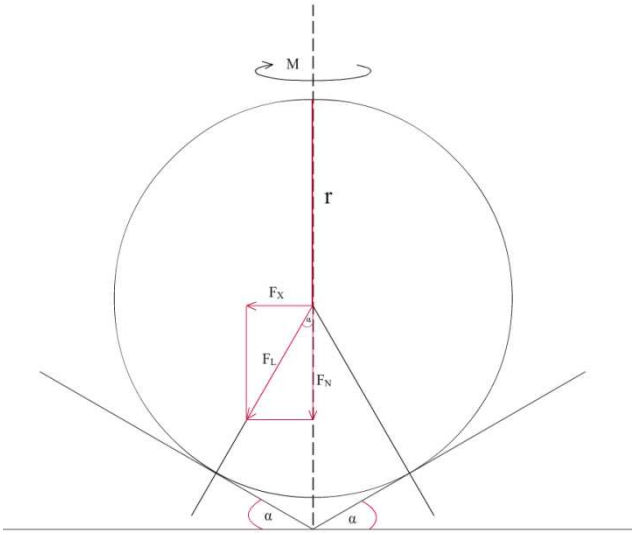

Figure 3.5: Schematic details of the tribology cell, where M is the Torque, F_N is the normal force, F_L is the normal load, r is the ball radius and α is angle of the plates.

As the measuring starts, the measuring ball is pressed against the three plates at a given normal force F_N, see Figure 3.5, and then the normal load F_L which is the force vertical to the friction surface can be calculated by Equation 3.12 :

$$F_L = \frac{F_N}{\cos \alpha} \tag{3.12}$$

As the measuring ball is rotating with a speed n, the sliding speed v_S can be calculated through:

$$v_S = \frac{2\pi}{60} \cdot n \cdot r \cdot \sin \alpha \tag{3.13}$$

Sliding distance is calculated from the measuring ball radius r and angular displacement φ measured by the rheometer (Equation 3.14):

$$s_S = \varphi \cdot r \cdot \sin \alpha \tag{3.14}$$

In order to maintain the defined speed, a certain torque is required which is measured by the rheometer. The friction force is calculated from the torque with Equation 3.15:

$$F_R = \frac{M}{r \cdot \sin \alpha} \tag{3.15}$$

Finally, the friction coefficient can be calculated as given by Equation 3.16:

$$\mu = \frac{F_R}{F_L} = \frac{M}{r \cdot \sin \alpha} \cdot \frac{\cos \alpha}{F_N} = \frac{M \cot \alpha}{r \cdot F_N} \tag{3.16}$$

3.3.2 Manufacture of friction surface

In order for tribological measurements best represent the conditions in the oral cavity, soft plates were manufactured using PDMS (Polydimethylsiloxane). The detailed procedure of manufacturing the plates is described in the following.

The elastomer surfaces were made of polydimethylsiloxane, fabricated from a two component silicone elastomer kit which including a base and a curing agent (Sylgard 184, Dow Corning). The base and curing agent were mixed at the weight ratio of 10:1. There are four steps in manufacturing the desired plates: Mixing, curing, cutting and cleaning.

3.3.2.1 Mixing

The 2 components of the PDMS kit were mixed in a glass bottle. Before use, the bottle was washed in ethanol and rinsed several times with copious amounts of deionised water followed by air drying to make sure that the inside of the bottle was completely clean. The required amounts of the base component followed by the curing agent were weighed into the bottle. It was advantageous to add the curing agent into the base rather than the opposite as the base is more viscous and the amount of curing agent was adjusted to the actual weight of the base.

The mixture was then homogenised using a vortex mixer (Reax Top, Heidolph, Schwabach, Germany) for 10 minutes. After mixing, there were numerous air bubbles in the mixture and to remove these, the bottle was placed in an ultrasonic water bath (USC1700D, VWR, Pennsylvania, USA) using the 'Degas' function at 20°C for 30 minutes. When there were no air bubbles visibly left in the mixture, it was judged ready for the curing process.

3.3.2.2 Curing

A pre-set amount of the air bubble free mixture was then carefully transferred into a standard 84 mm diameter plastic Petri dish to cure. The reason for controlling weight in the Petri dish was to ensure that the cured plates were of identical height. . After gently pouring the exact amount of mixture into the petri dish, for curing, the dishes were placed for 4 hours into a 65 °C oven followed by overnight cooling at 25 °C.

3.3.2.3 Cutting

In order to fit the cured plates into the tribology cell, they had to be cut into specific dimensions: 15.5 mm (L) × 6.0 mm (W) × 3.0 mm (H). After marking the plates with a fine marker pen, a sharp scalpel was used to cut the material into shape. A digital calliper was used to measure the cut plates to ensure that they have the same dimensions.

3.3.2.4 Cleaning

All of the contacting surfaces should be as clean as possible prior to use. The plates and the steel ball were firstly washed in ethanol and then rinsed several times with deionised water followed by air drying to remove any possible contamination caused by handling of the surfaces.

3.3.3 Method development

3.3.3.1 Data reproducibility

For the tribology study, data reproducibility tends to be not as good as for rheological measurements. Here it was found that the method for surface preparation had to be refined to the protocol that is described in 3.3.2 following initial very poor data reproducibility. It is worth outlining the steps of protocol development to help future work in this field. Also tests were carried to explore whether it was possible to use the same set of plates more than once. Figure 3.6 shows the results of replicate measurements acquired on one sample using the same

set of surfaces. Measurement was carried out at the normal load of 1.5N with speed range from 0.05-700mm/s.

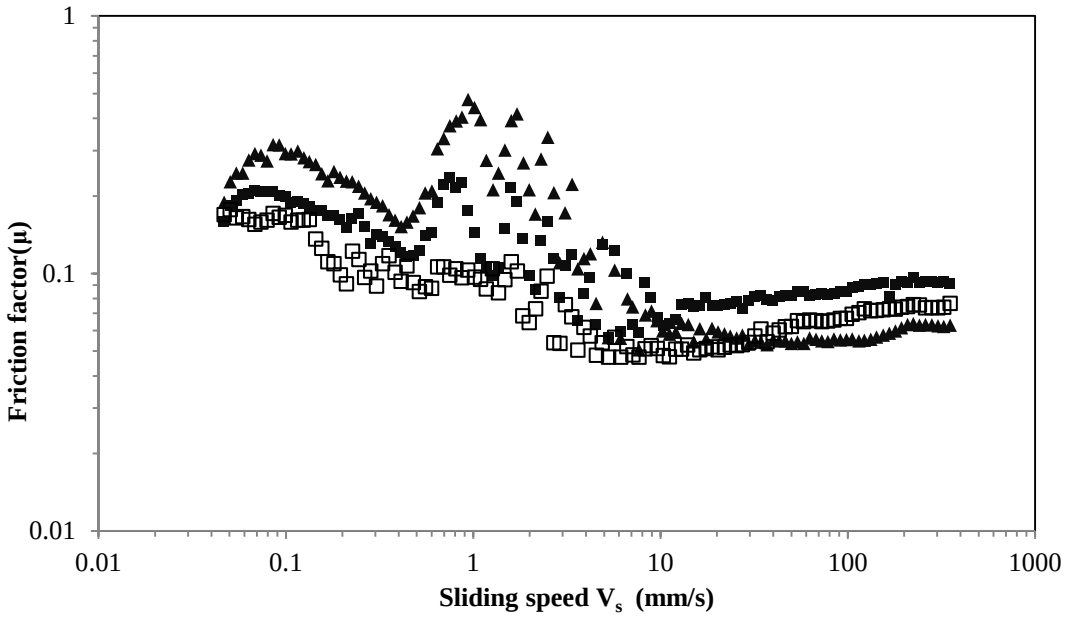

Figure 3.6: Tribological results of sample 2-3 (containing 0.09% xanthan and 17.11% dextran) with a normal force of 1N: replicate 1(▲),replicate 2(■),replicate 3(□).

Figure 3.6 shows clearly that the tribological results for sample 2-3 using the same set of plates showed large inconsistencies, especially in the low to mid speed range. There were two reasons for this: Firstly, the thickness of the plates was not identical. If the plates are not evenly thick, the normal force cannot evenly spread cross the contact surfaces. Therefore when the geometry is rotating, the contacting points are unstable and thus cause an unstable feedback to the motor which caused the

unstable Torque (M). In this particular case, the thickness of three plates used for the measurements was 2.74 mm, 2.86 mm and 2.84 mm, respectively.

Secondly, to produce more reproducible data, it was found that three things have to be checked: Firstly, all the plates should be the same thickness. As it is impossible for self-made plates to have the exactly same thickness, they should be the same at least to ± 0.1mm. This can be measured by a digital calliper. While measuring the thickness of the plates, at least three different points were measured and the average was taken. Secondly, each set of plates was cleaned both before and after each measurement. It has been seen in this research that if the plates were not cleaned properly, the results varied significantly. As explained previously, there are three regimes in the Stribeck Curve. In the low and medium speed boundary regime, the property of contacting surface plays an important role in determining the friction results (Bhushan, 2001). Therefore, the contacting surfaces were cleaned properly before and after use.

Thirdly, it has been found that the positioning of the plates, i.e., how the plates were placed in the cell, was very important. If using the same set of plates, the same surfaces should always be used for the measurements. It has been found if one or two of the plates were using the other side of the surfaces, the results changed significantly.

Finally, before a set of surfaces was used for actual measurements, it was "calibrated" with a 1% guar gum solution as a reference sample. Experimental samples were only measured if the results of the reference sample were with standard deviation less than 5%. Figure 3.7 shows an example of improved data following all pre-cautions and measures described.

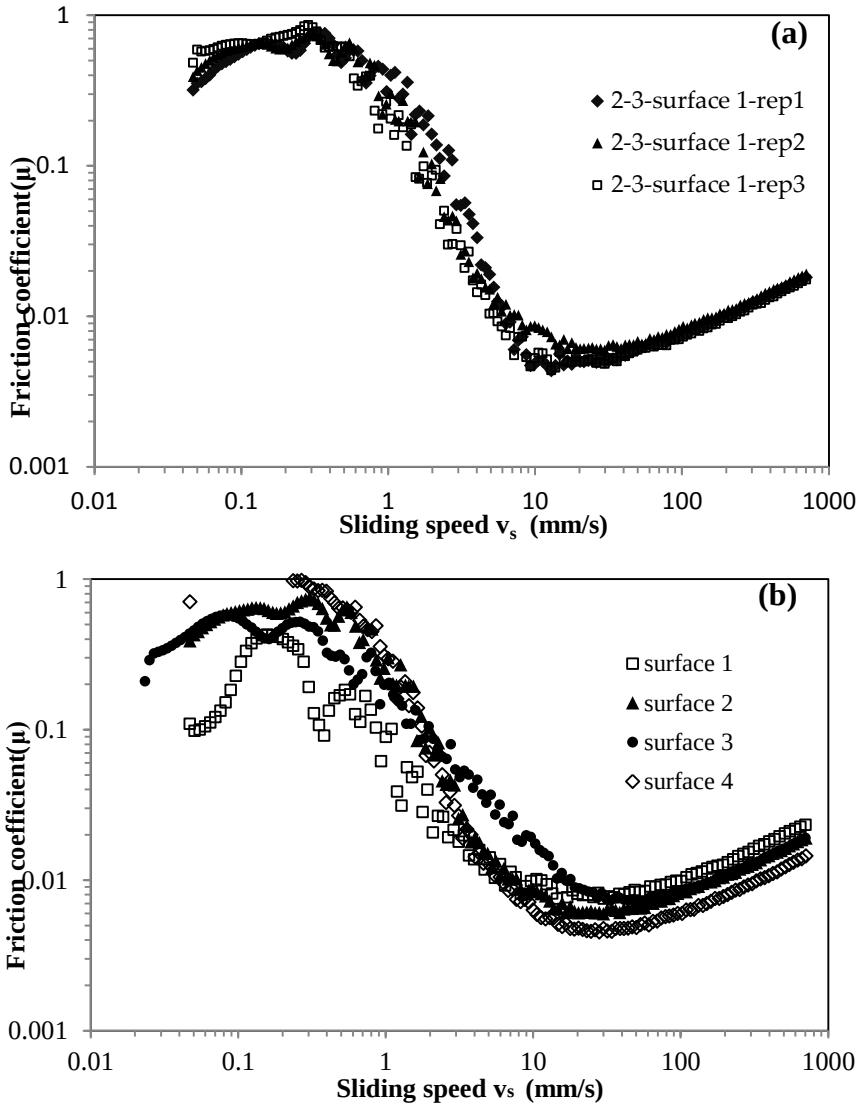

Figure 3.7: Replicate results for sample 2-3 (containing 0.09% xanthan and 17.11% dextran) based on (a) using same set of plates(3 replicate measurements) and (b) using 4 different sets of surfaces. .

As can be seen from Figure 3.7, results from (a) the same set of plates are very consistent, and (b) four sets of plates were within the standard deviation of 5%.

3.3.3.2 Data Analysis

As mentioned previously, the reproducibility of the friction measurements is not as good as found for rheology. Therefore, a considerable number of replicate measurements based on both the same and different sets of plates were acquired for each sample. Thus, to obtain the friction results for one sample, for each set of plates, at least 5 replicate measurements were conducted from which three representative results were selected and averaged and at least 5 sets of plates were used**.** Therefore, the final result was the average of results from 15 measurements, see Figure 3.8 for an example of a typical result.

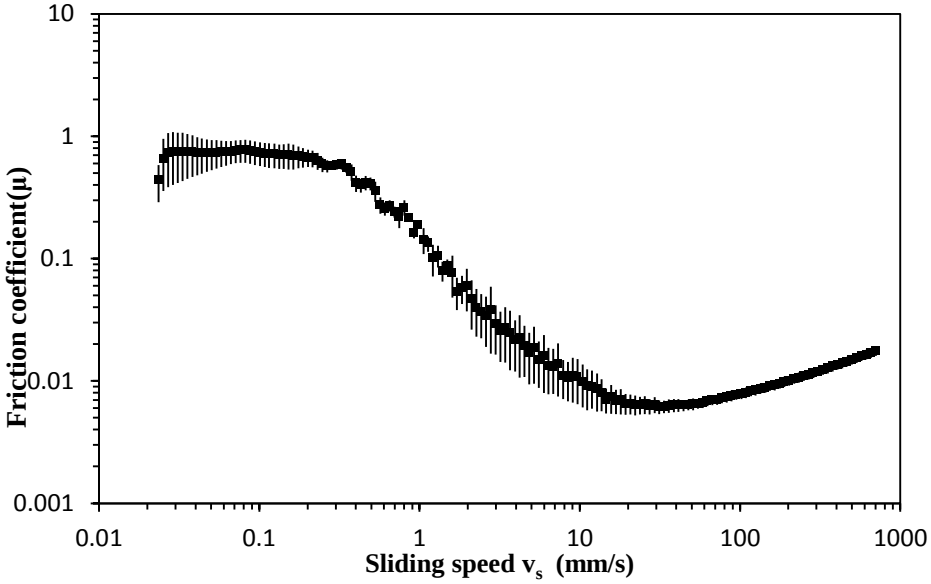

Figure 3.8: Final result for sample 2-3 (containing 0.09% xanthan and 17.11% dextran) showing average friction coefficient for each sliding speed and error bar corresponding to ± one standard deviation.

3.4 Sensory methods

The sensory experiments carried out in this study were given ethical approval by the Medical School Research Ethics Committee of the University of Nottingham. Before attending any sensory tests sessions, panellists were informed about the nature of the samples and sessions they were to attend. All panellists signed to indicate their informed written consent to participate. All the sensory experiments were carried out in the Sensory Science Centre in the University of Nottingham.

3.4.1 Descriptive Analysis (DA)

Descriptive analysis was one of the selected sensory methods in this study to describe and appraise the intensities of the sensory attributes of samples (Stone et al., 1974). The sensory attributes used in this study were mainly from a previous study conducted in the University of Nottingham on similar samples (Zhang, 2009). However, in the training sessions, there was a session used for panellists to generate and define any attributes that were relevant to the current samples but were not covered by the existing lexicon.

3.4.1.1 Subjects

A total of 10 assessors (9 female and 1 male) from the University of Nottingham (UoN) external sensory panel were invited to take part in the study. All panellists had been members of the UoN for between 10 and 14 years and had previous experience in a range of different sensory tests and product categories.

3.4.1.2 Sample preparation

All samples were prepared no more than one week before the tests and stored at refrigerator at 4 °C. All samples (25 ml) were presented in identical plastic pots with a lid and were labelled with randomly generated 3 digital codes. The samples were removed from refrigeration (4°C) at least two hours before the tests to make sure

they were at room temperature. A teaspoon (5ml) was used to transfer the samples to the mouth.

3.4.1.3 Sensory Panel Training

A total of 11 training sessions were carried out and each session lasted approximately 2 hours. There were several tasks carried out in the training sessions including: (i) attribute generalization and familiarization: as mentioned above, most of the attributes used were from previous study, however, there were no protocols in terms of how to evaluate these attributes. Also, some new attributes were developed by the panel during the study. Therefore, in these sessions, the previous attributes were introduced and the protocols used to evaluate these attributes were discussed and agreed upon by the panel. The new attributes were also discussed and the definition and protocols were agreed by the panel (see Table 3.3) for the definition and protocols of the attributes.

Table 3.3: Attributes including their definitions and protocol as defined by the panel.

	Attributes	Definition	Protocols	Scale
Mouthfeel	Initial Thickness	The pressure needed to press the sample between the tongue and the palate.	Put a spoonful of sample onto the tongue, gently press the tongue against the palate 3 times.	10 points line scale
	Thickness in mouth	The pressure taken to move the sample between the tongue and the palate	Put a spoonful of sample onto the tongue, move the sample in the mouth, rub the tongue for 5 times.	10 points line scale
	Stickiness on lips	The pressure to separate the sample from the lips.	Use lips to take a tip of sample (avoid touching from lips), and hold there for 5 seconds, then separate the lips for 3 times.	10 points line scale
	Stickiness in mouth	The elasticity between the tongue and the palate	Put a spoonful of sample onto the tongue, gently press the tongue against palate and hold there for 3 seconds and then separate for 5 times.	10 points line scale
	Mouthcoating	The amount of residues left in the oral cavity after swallowing	Put a spoonful of sample into the mouth, move around the tongue and chew the sample for 5 times and swallow.	10 points line scale
Flavour and taste	Overall Flavour	The overall intensity of flavour perceived	Put a spoonful of sample into the mouth, move around the tongue and chew the sample for 5 times and swallow.	10 points line scale
	Overall Sweetness	Overall intensity of sweetness of the samples`	Put a spoonful of sample into the mouth, move around the tongue and chew the sample for 5 times and swallow.	10 points line scale
	Musty/Fusty	The perceived intensity of musty/fusty of samples.	Put a spoonful of sample into the mouth, move around the tongue and chew the sample for 5 times and swallow.	10 points line scale

(ii) Rank and rating practice: four samples from two groups of designed samples were selected which were evenly spread across the range in the sample set for each attribute. Before each training session, four selected samples labelled with random 3-digits code and a rank and rating card (as shown in Figure 3.9) were prepared. During the session, panellists were asked to taste the four samples in the order presented and write down the sample number in rank order for each attributes. They were asked to assign scores for each sample for perceived intensity of each attributes. Initially, each panellist was asked to do the rank and rating on their own. When finished, all their results were collected and presented on the board for discussion. Any disagreement in terms of the rank and rating among the panellists was discussed and also the panel were asked to re-taste their samples and report the results.

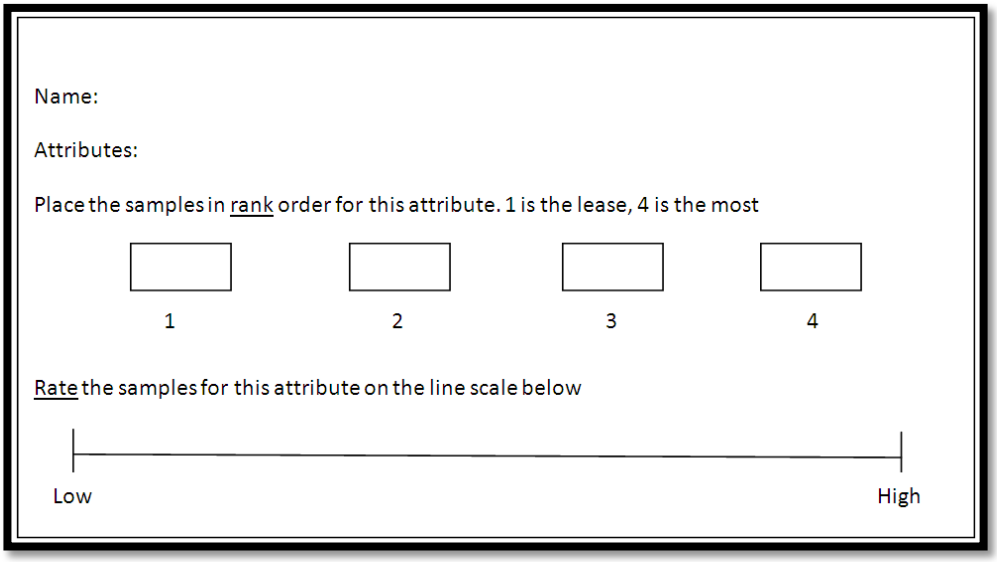

Figure 3.9: Rank and rating card used in the training.

(iii)Practice rating: practice rating sessions were carried out to familiarise panellists with the scale and to check panellist performance. Two practice rating sessions were carried out and replicate scores were examined for each panellist to find out if he/she was consistent in terms of individual scores. Individual mean scores were also compared to panel mean scores to find out whether the panellist was too high/low in terms of scale usage and each individual's mean value were within 10% of difference compared with the overall panel mean. If the panels' scores were not consistent, more rank and rating practices were carried out until their results became consistent.

During the training, panel performance was monitored using Fizz sensory software. One-way ANOVA was calculated for each panellist and individual coefficient of variance (CV) and discrimination probability values (FPROD) were calculated to

monitor panels' precision, accuracy and ability to discriminate between sample(*p* value).

3.4.1.4 Data collection

Once training sessions were finished, the final rating sessions were carried out to characterise the designed hydrocolloid solutions for each attribute, see Table 3.3. All the data were collected using the computerised data acquisition system Fizz (Biosystèmes, France) Tests were conducted in individual booths lit with northern hemisphere lighting in a quiet and air-conditioned room (20 °C).

To avoid the carry over effect, plain crackers (99% fat free, Rakusen's UK) and water (Evian, Danone, France) were provided as palate cleansers. Also, as some of the samples were very thick and it was likely that residues would be left on the lips, a cotton ball soaked with water was provided to wipe off any residues on the lips. After wiping with the cotton ball, the panellists were asked to dry the lips with tissues provided. This was important in case there was any water left on the lips to dilute the samples. A two minute break was given between two samples, and a long ten minute break was given between every five samples to avoid any fatigue effects. A partial Latin Square Design was used when presenting the samples. The partial Latin Square design ensured that each sample occurred in every presentation order and also before/after every other sample in the design and equal number of times At

the beginning of each session, two reference samples which represented the low and high end of the scale of mouthfeel attributes were given to the panel to help calibrate against the scale, the two reference samples were available throughout the tests if required.

3.4.1.5 Data analysis

3.4.1.5.1 Correlation analysis

Correlation analysis was performed to investigate the relationship between physical parameters (viscosity at low and high shear rate, dynamic viscosity, extensional viscosity, etc.) and sensory perceptions using Pearson's r with a minimum significance level defined as $p<0.05$. All the analyses were performed using software Excel (Microsoft 2010, USA).

3.4.1.5.2 ANOVA and Post-Hoc tests

Analysis of variance (ANOVA) is a useful method which can be used to investigate product differences in sensory and other studies. The main purpose of the ANOVA test is to identify and quantify the factors which are responsible for the variability of the response and then followed by investigating which ones are the most important factors by using the so called post-hoct tests (Næs et al., 2010).

Two-way ANOVA (analysis by attribute with sample and judge factors) were performed using SPSS (Version 19, IBM, USA) to identify any significant differences

between samples. In addition, where appropriate, Tukey's HSD multiple comparison tests (significant level α=0.05) were performed to determine which samples were significantly different for rated intensity of each of the attributes.

3.4.1.5.3 Principal Component Analysis (PCA)

PCA is an exploratory tool used to simplify a large and complex data set into a smaller and more easily understood data set by summarizing complex data sets by creating new variables which are linear combinations of original data (Lawless and Heymann, 2010). In this study, PCA was performed on the mean panel data in order to identify the main attributes contributing the variation between samples within the design space. Also in order to facilitate the interpretation, orthogonal rotation was used (Abdi and Williams, 2010) by using software XLSTAT (version 2011.2.02, Addinsoft, USA). The orthogonal rotation was used to simplify the interpretation; after a varimax rotation each original variable tends to be associated with one (or a small number) of components and each component represents only a small number of variables.

3.4.2 Napping®

The Napping® method (Pagès, 2003,2005) was also employed in this study to further understand issues concerning the differences in the nature of the taste and aroma, which were observed during the DA sessions. Napping allows the direct collection

of a Euclidian configuration for the samples for each subject in a unique session (Perrin et al., 2008). It involves collecting perceived sensory distances between samples by positioning the samples on a sheet of blank paper. Panellists lay out the samples, which are simultaneously presented, on the paper in such a way that two samples that are perceived as similar are very close to each other and if different are placed further apart. This enables each panellist to select their own difference criteria and the relative importance assigned to each criteria (Perrin et al., 2008).

3.4.2.1 Subjects

A total of 9 assessors (8 female and 1 male) from the University of Nottingham (UoN) external sensory panel were invited to take part in the study. All panellists have been members of the UoN for between 10 and 14 years and had previous experience in a range of different sensory tests.

3.4.2.2 Sensory panel training

Unlike Qualitative Descriptive Analysis, the method of Napping® does not require a large amount of training. Therefore only two training sessions of 2.5 hours each were used. In the training sessions, the panels were explained how the method worked and five samples randomly selected from the designed samples were used to help them to practice.

3.4.2.3 Data collection

16 samples of 20ml in small plastic pots were simultaneously presented to each panellist who was then asked to position them on a large blank paper (40cm×60cm) and given instructions according to Pagès (2005):

(1) You are asked to taste and position the samples according to their similarities or dissimilarities. You have to do this according to your own criteria which are significant to you. You do not have to state the criteria you used and there are no good or bad answers.

(2) You have to start from left to right with the samples provided and position them on the paper in such a way that two samples are close to each other if they are similar and distant if they are different. You are always allowed to re-taste the samples. Do not hesitate to use the extreme part of the paper to express the strongly difference between samples. Once finished, write down the codes that represent the samples and any descriptive words that can be used to describe the samples. Remember to use cracker and water to clean the palate.

Once finished, the papers were collected and for each sample, the X-co-ordinate and Y-co-ordinate were measured using a ruler and then input in a table in Excel. The origin can be placed anywhere and here the left bottom corner was used (Pagès, 2005). Also, the corresponding descriptive words to each sample were

collected as well. The data were organised into two parts according to Figure 3.10, the first part is a table which has 10 rows and 18 columns. The 10 rows are the samples and first 18 columns are the X and Y co-ordinates of the samples. The second part is a table that summarize the descriptors for each samples and the number of times that each descriptors have been used by the panellists.

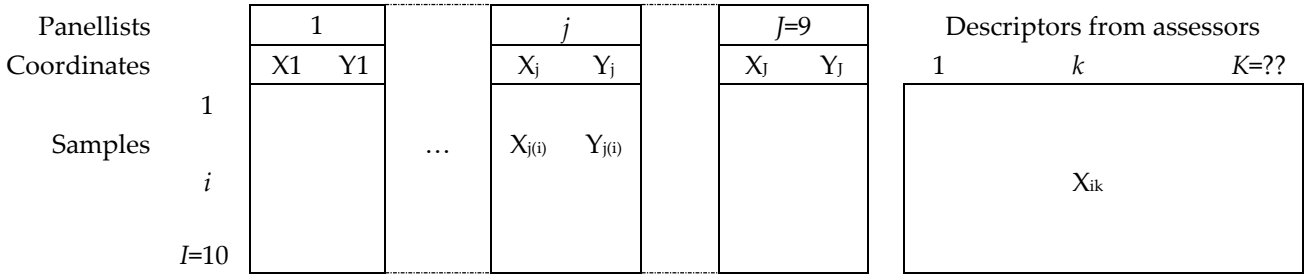

Figure 3.10: Organization of Napping® data. Two columns represent each panellists *j*: the X-coordinate(X*j*) and the Y-coordinate(Y*j*). X*ik* corresponds to the number of descriptor *k* used in the whole panel for the sample *i*.

3.4.2.4 Data analysis

3.4.2.4.1 Multiple factor analysis (MFA)

Multiple factor analysis (MFA) can be seen as an extension of principle component analysis (PCA) tailored to handle multiple data tables that measure sets of variables collected on the same observations or, alternatively, multiple data tables where the same variables are measured on different sets of observations. The goals of MFA are (1) to analyse several data sets measured on the same observations; (2) to provide a

set of common factor scores and (3) to project each of the original data sets onto the compromise to analyse communalities and discrepancies. MFA proceeds in two steps: first it computes a PCA of each data table and normalises each data table by dividing all its elements by the first singular value obtained from its PCA. Second, all the normalized data tables are aggregated into a grand data table that is analysed via a PCA that gives a set of factor scores for the observations and ladings for the variables (Escofier and Pagès, 1994, Abdi et al., 2013).

MFA provides five main representations from the same components in this study:

(1) A representation of the 16 samples (see Table 4.6) in such a way that two samples are close to each other if they are globally perceived as similar by the panel.

(2) A representation of the two dimensions of each paper. These variables are represented by their correlation coefficients with components of MFA, although these dimensions are not standardised in constructions of the axes.

(3) A representation of the samples described by each panellist.

(4) A representation of the panels such as a proximity between two panellists indicates a resemblance between two paper they provided.

(5) A representation of the descriptor used by the panel through their correlation with the components of MFA.

Multiple factor analysis has been performed using the software XLSTAT(version 2011.2.02, Addinsoft, USA).

3.4.2.4.2 **Agglomerative Hierarchical Clustering (AHC)**

Clustering analysis is a method that used to identify homogeneous subgroups of samples in a population and groups which minimize within group variation and maximize between group variation (Meullenet et al., 2007). There are two main approaches to clustering, hierarchical and criterion based methods (Bezdek et al., 1981, Dahl and Naes, 2004). The former method is used in this study.

Hierarchical clustering methods can be divided into two categories: agglomerative and divisive (Wajrock et al., 2008). The agglomerative method is used in this study. In agglomerative hierarchical clustering, every sample is initially considered to be in a separate cluster. The two samples with the smallest distance between them are grouped into a cluster. The sample with the smallest distance from either of the first two samples is the considered next. If the data for that individual are closer to that for a fourth sample than they are to either of the first two, the third and fourth samples are grouped into a second cluster. If not, the third sample is grouped in the first cluster. The process is then repeated, adding samples to existing clusters or creating new clusters until every sample has been considered (Meullenet et al., 2007). In terms of the measure of similarity or dissimilarity, the most commonly used and straightforward method was used which is call *Euclidean distance* (or straight-line

distance) (Mooi and Sarstedt, 2011). The distance of between two samples (A and B) can be easily calculated with the following formula:

$$d_{Euclidean}(A,B) = \sqrt{(x_A - x_B)^2 + (y_A - y_B)^2} \tag{3.17}$$

In addition, to decide whether two clusters can be regrouped together or not, there are several agglomerative procedures to choose from: single linkage, complete linkage, average linkage and centroid (see Figure 3.11).

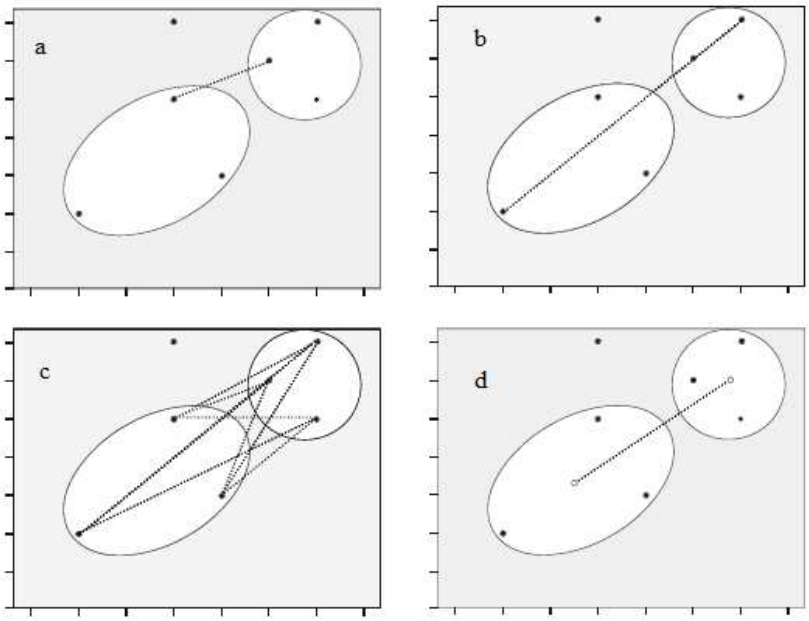

Figure 3.11: Four types of clustering algorithm: (a) single linkage,(b)complete linkage,(c) average linkage and (d) centroid (Mooi and Sarstedt, 2011)

In addition there is another method called Ward's method (Ward, 1963). This method suggests that the distance between two clusters, A and B, is how much the sum of squares will increase when they are merged (Hand et al., 2001):

$$\Delta(A,B) = \frac{n_A n_B}{n_A + n_B} \|\overrightarrow{m_A} - \overrightarrow{m_B}\|^2 \tag{3.18}$$

where Δ is the merging cost of combining cluster A and B, n is the number of points in this cluster, $\vec{m}$ is the centre of the cluster.

Agglomerative hierarchical clustering was applied in this study to the results from Napping® in order to identify clusters of samples which were perceived as similar in terms of aroma and taste by the panel. Euclidean distance was used to identify the similarities of two samples and Ward's method was selected clustering algorithm. Results of applying an AHC method are visualized with a tree diagram called a dendrogram (Härdle and Simar, 2012). The AHC was achieved using the software XLSTAT (version 2011.2.02, Addinsoft, USA).

3.5 *In vivo* Release measurements

Real time in-nose release of isoamyl acetate during consumption of the samples was measured via Atmospheric Pressure Chemical Ionisation-Mass Spectrometry (APCI-MS) (Micromass, Manchester, UK) using three of the ten panellists. All samples were included in duplicate. The panellists were asked to put 10 ml of sample into the mouth using a spoon, then close their mouth and chew and breathe normally while air from the nose was sampled into the APCI-MS nasal sampling tube. Air sampling rate was 30 $mL.min^{-1}$ and the release of isoamyl acetate was followed by monitoring m/z 131 (the mass to charge ratio for the molecular ion) (Taylor et al., 1999). The

breath by breath data were recorded as peak heights and analysed to generate two parameters: the maximum aroma intensity (Imax) and the cumulative area under the 1.5 min release profile (Auc) (Taylor et al., 2001). Crackers (99% Fat Free, Rakusen's, Leeds, UK) and water (Evian Danone, Evian, France) were provided as palate cleansers and a two minutes break observed between each sample.

Two-way ANOVA was performed to identify significant differences between samples in terms of the in-vivo flavour release for both Maximum Intensity (Imax) and Areas Under the Curve (AUC), where appropriate, Tukey's HSD multiple comparison tests (significant level α=0.05) were performed to determine which samples were significantly different for both Imax and AUC.

3.6 Microscopy methods

The freshly collected saliva was imaged using a confocal laser scanning microscope (Eclipse Ti, Nikon, Japan) equipped with argon(Ar) laser (wavelength λ=488nm) and HeNe laser (wavelength λ=543 nm). In order to locate the protein in the saliva, Rhodamine B (Sigma-Aldrich, UK) was selected as the stain. The stain was prepared at the concentration of 0.1 $g.L^{-1}$. The fluorescence emission of the Rhodamine B was detected through green filter (emission wavelength λ= 515-530nm) and red filter(emission wavelength λ= 605-675nm).

4 RESULTS AND DISCUSSION

4.1 Model sample development and physical properties

4.1.1 Introduction

In this chapter, the process of designing two groups of aqueous solution samples based on xanthan gum and dextran and their physical properties are reported. Due to the specific rheological properties of the two groups of samples, it is important to understand the contributions of the individual polysaccharides in terms of their solution concentration. As a first step this relationship was explored experimentally for rheological behaviour in steady shear. In the second study, a series of samples were used to build a model that can be used to predict the relationship between the solution concentration of these two polysaccharides and steady shear rheological properties. In the third study, based on the model developed, two groups of samples were designed and these corresponded to the final study samples employed in this research. In addition to viscosity in steady shear, behaviour in oscillatory shear, uniaxial extensional flow and as lubricant entrained between two friction surfaces was explored. The results of this comprehensive analysis of flow and friction properties are reported in this chapter.

4.1.2 Steady shear flow behaviour

This study was designed to investigate the flow behaviour of the two polysaccharides xanthan gum and dextran at different concentration in aqueous solution. All solutions contained 3% (w/w) sucrose and 0.05% (w/w) sodium azide.

The concentration of xanthan gum was varied between 0.05 and 1.02 % (w/w) and the concentration of dextran ranged from 5 to 45 % (w/w). The viscosity curves obtained for the xanthan gum solutions are shown in Figure 4.1. As expected, the xanthan gum solutions were highly shear thinning and viscosity over the whole range of shear rates investigated decreased with decreasing concentration. The shear rates were high enough to reach or at least indicate presence of a high shear viscosity plateau. Without the method of thin film rheology, this would not have been identified. It is also worth mentioning that in the case of the highest concentration of xanthan gum the shear rates were not low enough to show a zero shear plateau viscosity. The shear thinning behaviour is normally due to the chain orientation or alignment of microstructures with the flow direction which result in reduction in drag. The highly shear thinning behaviour of xanthan gum is a result of intermolecular association among xanthan polymer chains which results in the formation of a complex network of rigid-rod like molecules (Song et al., 2006, Sworn, 2011). The high viscosity of xanthan at low shear rate is due to the aggregation through hydrogen bonding and polymer entanglement. However, under the application of shear flow, the polymer network of xanthan will be disentangled and the molecules will be partially aligned to the direction flow and hence cause the reduction in viscosity (Choppe et al., 2010).

The experimental data were fitted with the Carreau model (see Equation 2.8 and the fitted curves are included in Figure 4.1. The values of the model parameters are reported in Table 4.1

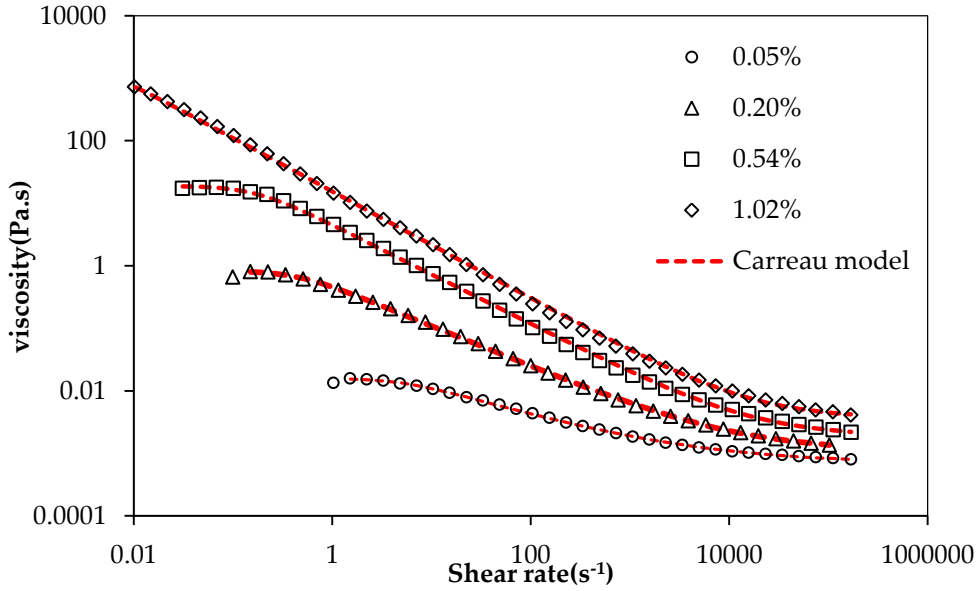

Figure 4.1: Steady shear Viscosity curves for different concentrations of xanthan gum (Measured using geometry PP-50 at 20 °C, the standard deviation is within ±0.1% in all cases). Shown are experimental data and Carreau model fit for each xanthan gum concentration.

Table 4.1: Carreau model parameter values for the results shown in Figure 4.1: η_0 denotes the zero shear viscosity, η_∞ is the infinite shear viscosity, C is the relaxation time and p is the power law index as indication of the degree of shear thinning. The fitting quality is shown in correlation coefficient (R^2).

Concentration %(w/w)	η_0 Pa.s	η_{50} Pa.s	η_∞ Pa.s	C	p	Correlation coefficient (R^2)
0.05	0.0157	0.0057	0.0007	0.2	0.24	0.99
0.2	0.831	0.0386	0.0011	2.29	0.33	0.99
0.54	18.83	0.194	0.002	5.99	0.4	0.99
1.02	1618.9	0.561	0.004	231	0.43	0.99

As can be seen from Table 4.1, the Carreau model fits the measured flow curves of all the concentrations of xanthan with correlation coefficient all above 0.99. The viscosity values at zero, 50 s^{-1} and infinite shear rate increased with concentration. As expected, the polymer relaxation time (C) increased with increasing concentration, which indicated that as the concentration increased the polymer structure needed more time to return to its equilibrium status. The power law index (p) was also increased with concentration which indicated that as concentration increased, the polymer solution became more shear thinning.

The dependency of the Carreau model parameters on solution concentration was then analysed using Design Expert. It was found that both η_0 and η_{50} can be described with a quadratic relationship, see Equations 4.1 and 4.2. The infinite viscosity followed a linear relationship with the concentration of xanthan gum, see Equation 4.3. All the models are significant ($p<0.05$) with correlation coefficient $R^2>0.99$.

$$\eta_0 = 26.96 + 729.97 \times [Xan] + 850 \times [Xan]^2 \quad (4.1)$$

$$\eta_{50} = 0.18 + 0.28 \times [Xan] + 0.1 \times [Xan]^2 \quad (4.2)$$

$$\eta_\infty = 0.0021 + 0.0017 \times [Xan] \quad (4.3)$$

The viscosity curves of different concentrations of dextran are shown in Figure 4.2.

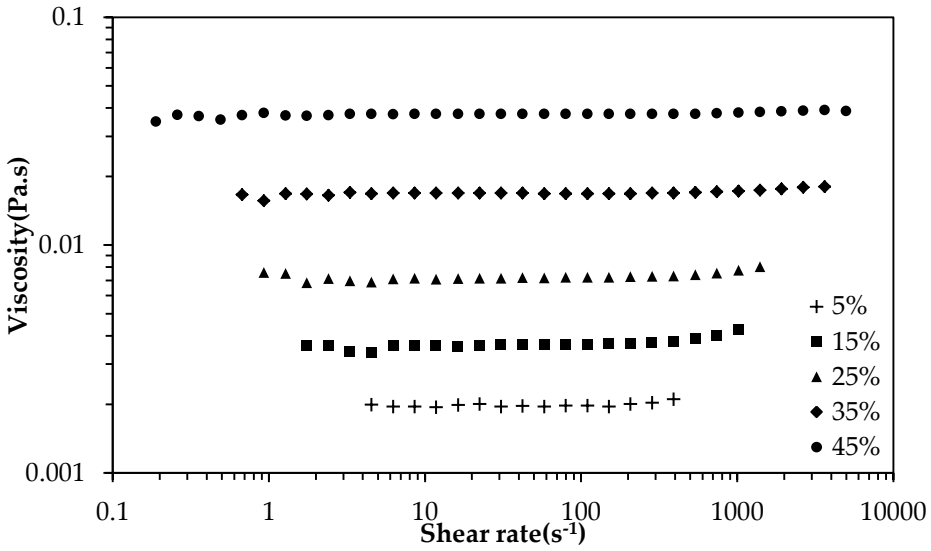

Figure 4.2: Viscosity curves for different concentrations of dextran. The viscosity values are shown for different range of shear rate for different concentration due to lack of torque sensitivity in the case of low shear rate end and measurement artefacts due to secondary flow at high shear rate. (Measured using PP-50 at the 20 °C, the standard deviation is within ±0.01% in all cases)

Table 4.2: Viscosity values of different concentrations at shear rate of 50 s^{-1}. The viscosity values are averaged from 3 replications.

Concentration %(w/w)	Viscosity at 50 s^{-1} Pa.s
5	0.002 ± 0.01%
15	0.0036 ± 0.01%
25	0.0072 ± 0.01%
35	0.0169 ± 0.01%
45	0.0376 ± 0.01%

Figure 4.2 shows the steady shear viscosity curves of dextran at different concentrations. The viscosity behaviour is Newtonian over the range of concentrations measured and this is in agreement with previously reported results (Nomura et al., 1990)

The relationship between dextran concentration and Newtonian viscosity values from Table 4.2 was investigated using Design Expert and it was found that they follow a Cubic model Equation 4.4 with correlation coefficient of R^2=0.99.

$$\eta = 0.007 + 0.012 \times [Dex] + 0.013 \times [Dex]^2 + 0.006 \times [Dex]^3 \quad (4.4)$$

4.1.3 Model samples development

In order to build a model which can be used to predict the solution concentration of xanthan gum and dextran required to impart the desired shear rheological behaviour, Design Expert was used. A D-optimal Response Surface design was used and based on the pre-set concentration ranges of xanthan gum (0.2 - 1.0 % (w/w)) and dextran (0 – 30 % (w/w)), an initial set of 16 samples was generated. The composition of these 16 samples is detailed in Table 4.3 and their location in the 3D response surface is depicted in Figure 4.3.

Table 4.3: Polysaccharide concentration of the16 samples comprising the initial set of samples generated through Design Expert D-optimal Response Surface design.

Sample number	Concentration of xanthan %(w/w)	Concentration of dextran %(w/w)
1	0.2	30
2	1	30
3	1	0
4	0.2	30
5	0.2	15
6	0.6	30
7	0.2	0
8	0.6	0
9	0.6	15
10	1	15
11	1	30
12	0.2	0
13	0.6	15
14	0.8	30
15	0.8	15
16	0.4	15

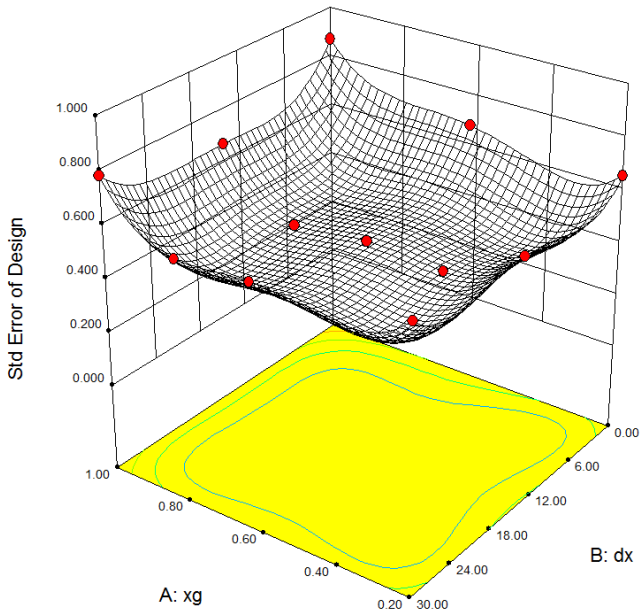

Figure 4.3: 3D response surface of the design: the red dots represent the designed samples; the green curves represent different levels of standard error.

The viscosity curves of the 16 samples were measured in steady shear and the results are shown in Figure 4.4. As can be seen that by varying the concentration of xanthan and dextran, the shear viscosity of the 16 samples could cover a wide range in both low and high shear rate. Samples containing the highest xanthan and dextran concentrations were highest for both low and high shear viscosities (sample 2 and 11). For samples containing the same level of xanthan, the ones that were higher in dextran concentration were found to have higher viscosities at high shear rate. However, samples which contained the same level of dextran, but with the highest xanthan concentrations had higher viscosities at low shear rate. The results indicated that the concentration of xanthan has a major effect on the low shear viscosity while concentration of dextran has a major effect on high shear viscosity. The dextran concentration seemed have a 'push' effect on the high shear viscosity of the xanthan solutions.

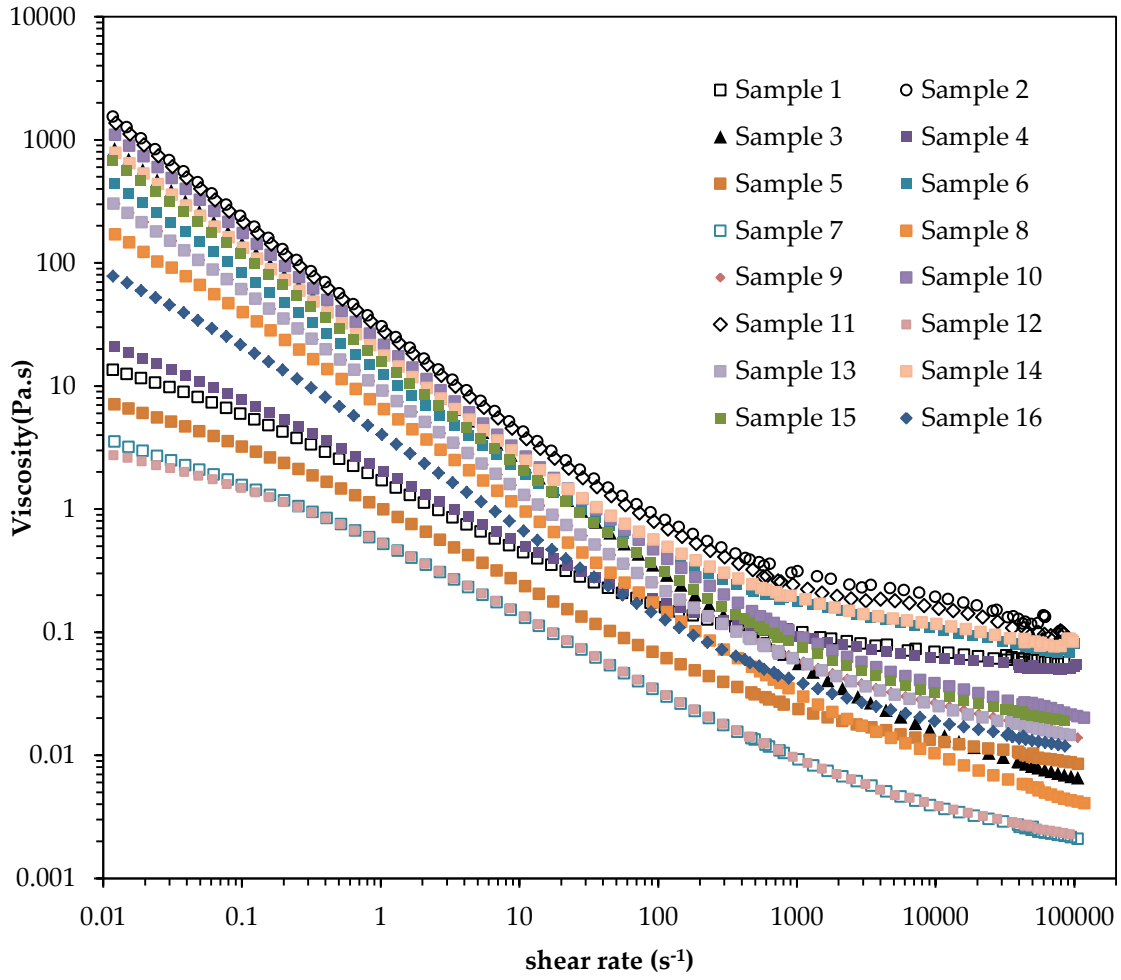

Figure 4.4: Viscosity curves for 16 model building samples. Samples were measured using PP-50 at three different gap heights (*h*) for varied shear rate ranges (*h*=500μm for shear rate 0.01-1000 s^{-1}; *h*=50μm for shear rate 1000-10000 s^{-1}; *h*=30μm for shear rate 10000-100000 s^{-1}. All shear rates were corrected for gap error and non-Newtonian behaviour, see 3.2.1). All results are highly reproducible with standard deviation less than 0.1%. Measurements were conducted at 20 °C.

The experimental data were then fitted using the 'log-log' model (see Equation 3.9), and as an illustration of the fitting quality, several selective samples with fitting curves are displayed in Figure 4.5. In addition, all fitting parameters of the 'log-log'

model including correlation coefficients between experimental and model fitting results are presented in Table 4.4. As can be seen, the 'log-log' models fit the experiment accurately with all correlation coefficients over 0.99. Based on the fitted 'log-log' models, the viscosity values at 50 s^{-1} and 10^5 s^{-1} , which were denoted as the low and high shear viscosities, respectively, were calculated and the results are reported in Table 4.5.

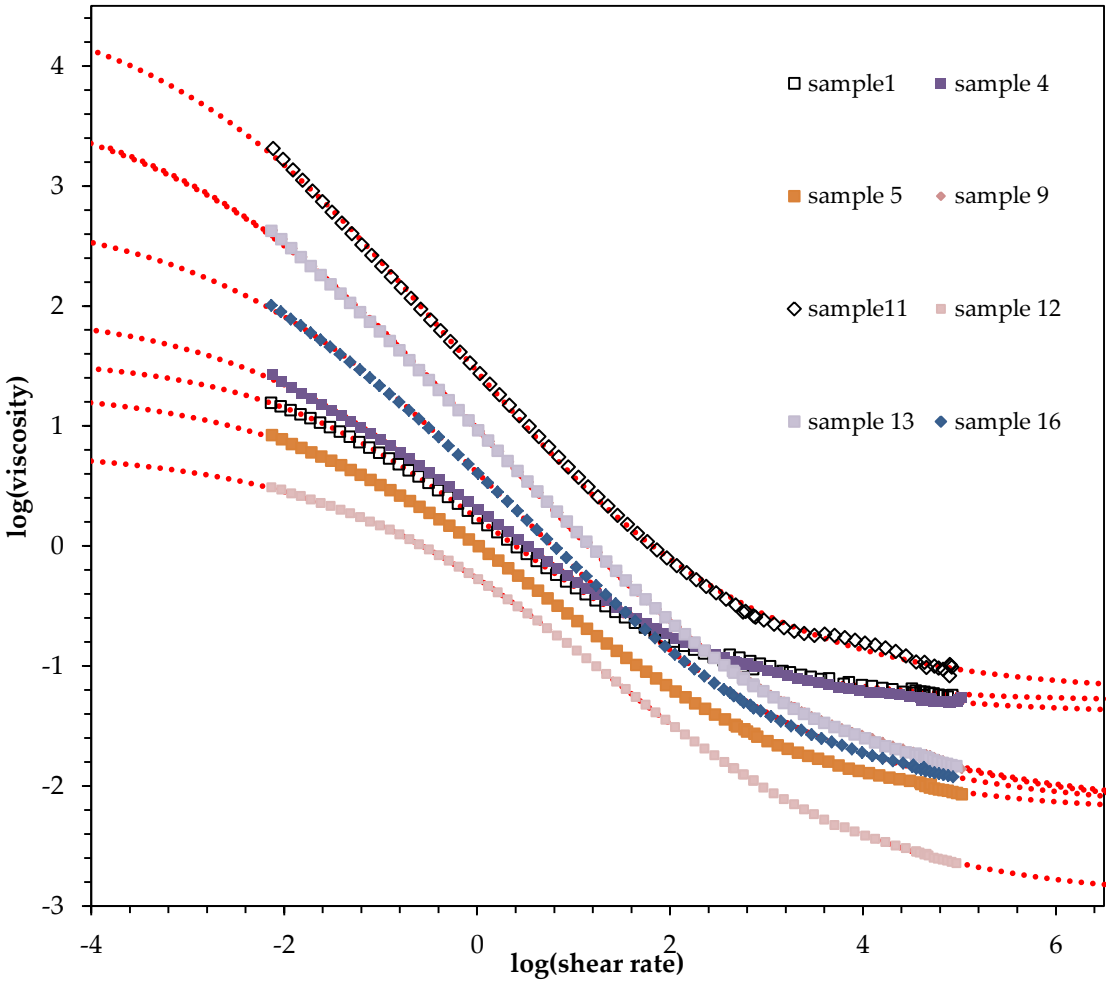

Figure 4.5: Experiment results fitted using the Log-Log model for selected samples.

Table 4.4: The log-log model parameter values for the results shown in Figure 4.5: α+ β denotes the upper asymptote, β/γ is the point of inflection and δ is the lower asymptote. The fitting quality is shown in correlation coefficient (R^2).

No.	Concentration of xanthan %(w/w)	Concentration of dextran %(w/w)	α	β	δ	γ	Correlation coefficient (R^2)
1	0.2	30	2.861	-0.126	-1.288	-0.816	0.99
2	1	30	-5.862	-0.233	4.752	0.634	0.99
3	1	0	-7.965	0.164	4.950	0.468	0.99
4	0.2	30	-3.366	0.023	1.974	0.724	0.99
5	0.2	15	-3.533	0.525	1.316	0.701	0.99
6	0.6	30	-5.365	-0.196	4.404	0.639	0.99
7	0.2	0	-4.104	0.721	1.069	0.611	0.99
8	0.6	0	-6.584	0.349	3.570	0.514	0.99
9	0.6	15	-6.077	0.085	3.887	0.573	0.99
10	1	15	-6.844	0.019	4.748	0.553	0.99
11	1	30	-5.856	-0.169	4.629	0.637	0.99
12	0.2	0	-3.731	0.906	0.803	0.681	0.99
13	0.6	15	-3.731	0.906	0.803	0.681	0.99
14	0.8	30	-5.516	-0.165	4.244	0.663	0.99
15	0.8	15	-6.540	0.051	4.393	0.562	0.99
16	0.4	15	-5.011	0.235	2.826	0.633	0.99

Table 4.5: Calculated shear viscosity values at shear rate of 50 (η_L) and 10^5 s^{-1} (η_H) from the log-log model.

No.	Concentration of xanthan %(w/w)	Concentration of dextran %(w/w)	η_L Pa.s	η_H Pa.s
1	0.2	30	0.221	0.058
2	1	30	1.363	0.120
3	1	0	0.562	0.006
4	0.2	30	0.241	0.050
5	0.2	15	0.096	0.009
6	0.6	30	0.693	0.071
7	0.2	0	0.050	0.002
8	0.6	0	0.271	0.004
9	0.6	15	0.382	0.015
10	1	15	0.713	0.021
11	1	30	1.189	0.093
12	0.2	0	0.051	0.002
13	0.6	15	0.378	0.014
14	0.8	30	0.825	0.078
15	0.8	15	0.550	0.018
16	0.4	15	0.212	0.012

The calculated low and high shear viscosities values from 'log-log' model, as shown in Table 4.5 were then used to explore the relationship between viscosities and concentrations of both xanthan and dextran. Based on the viscosity data the Design Expert software was used to generate models for the low shear and high shear viscosity as a function of polymer concentrations (see Equation 4.5 and 4.6). Also the contour plots are used to show how the concentration of xanthan and dextran affect both low and high shear viscosities (Figure 4.6).

$$\sqrt{\eta_{50}} = 0.11 + 0.65[Xan] + 0.00093[Dex] + 0.00022[Xan]^2 \quad (4.5)$$

$$+ 0.0045[Xan][Dex]$$

$$\log[\eta_{10^5}] = -1.85 + 0.18[Xan] + 0.63[Dex] + 0.066[Dex]^2 \quad (4.6)$$

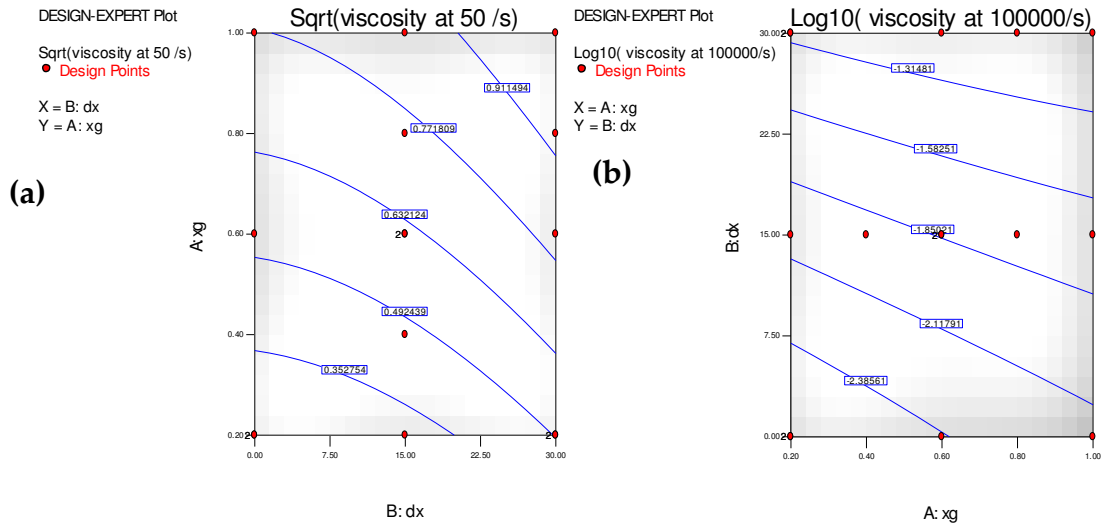

Figure 4.6: Two dimensional contour plot-derived from the model for viscosity at (a) low and (b) high shear rate. Each contour represents a viscosity value, whilst its shape illustrates how viscosity is affected by relative concentration of xanthan and dextran.

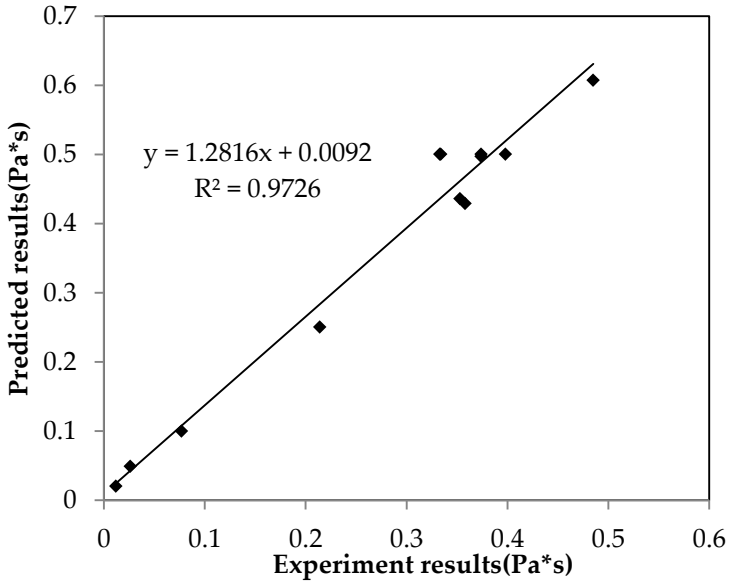

Figure 4.7: A comparison of the predicted values and experimental results for low shear viscosity.

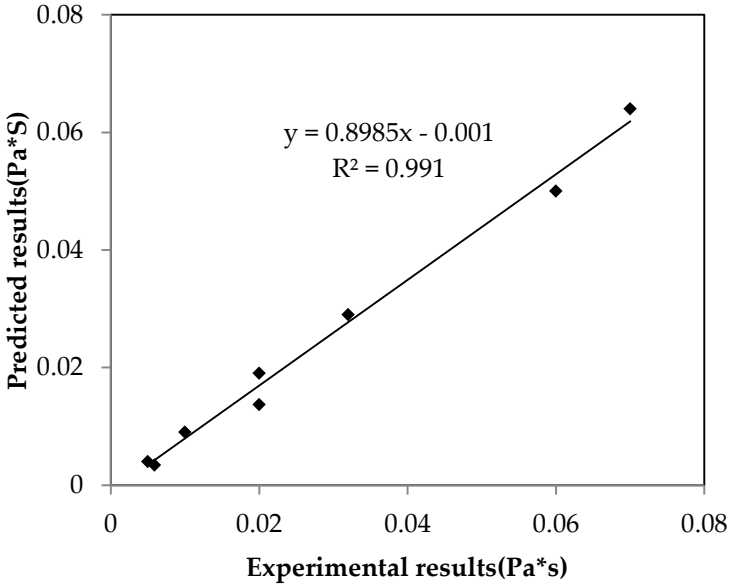

Figure 4.8: A comparison of predicted values and experiment values for high shear viscosity

The model for viscosity at 50 s^{-1} includes a linear and quadratic term for xanthan gum concentration and an interaction term for the two thickener concentrations. The

model was highly significant (p<0.001) with adjusted R^2 and predicted R^2 values of 0.99 and 0.97, respectively, and an 'adequate precision' (signal-to-noise ratio) of 48.28. These statistics indicate a robust model that describes variation across the design space well. The model was examined by plotting the experimental results against the predicted results (R^2=0.97)(see Figure 4.7).The model for viscosity at high shear rate includes a linear term for xanthan gum concentration, a linear and quadratic term for dextran concentration, and an interaction term for the two thickeners concentrations. The model was highly significant (p<0.001) with adjusted R^2 and predicted R^2 values of 0.99 and 0.99, respectively, and an 'adequate precision' of 109.06. The model for predicting the viscosity at high shear rate was robust and an examination of the model was carried out by plotting the experimental results against the predicted value (R^2=0.99)(see Figure 4.8).

The models reveal that the concentration of xanthan gum has a larger effect on the low shear viscosity of the samples while the concentration of dextran has little effect. On the other hand, the concentration of dextran impacts to a larger extent on the high shear viscosity. Based on the two functions describing the relationship between low and high shear viscosities and concentrations of polymers, two groups of samples with the desired rheological properties, i.e. either identical low or high shear rate, have indeed been designed and as shown in Figure 4.9 and Figure 4.10.

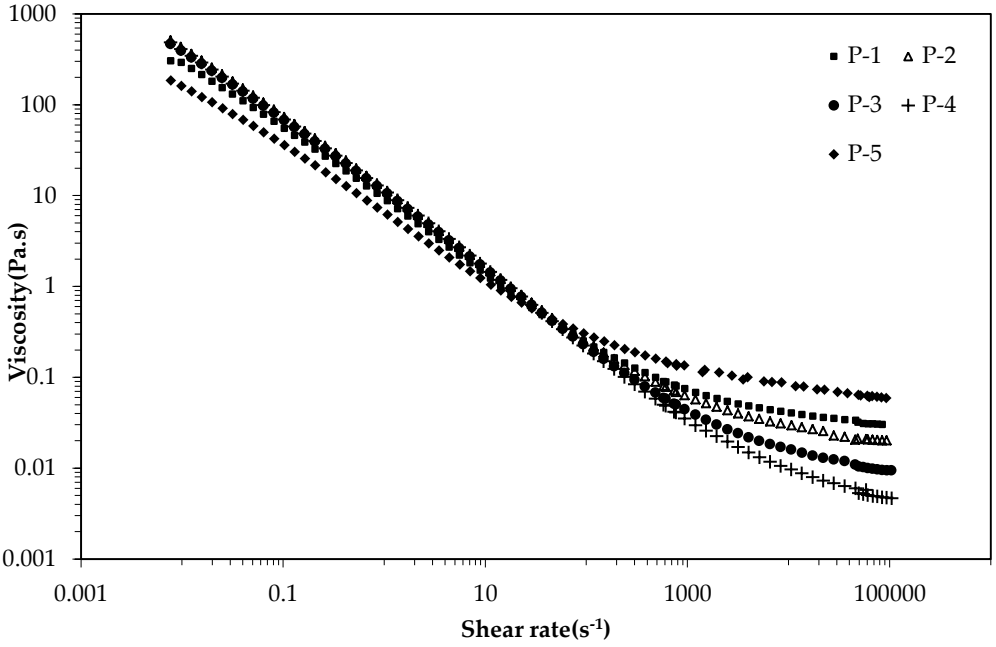

Figure 4.9: Sample of Group 1: iso-viscos at low shear rate but different viscosity at high shear rate.

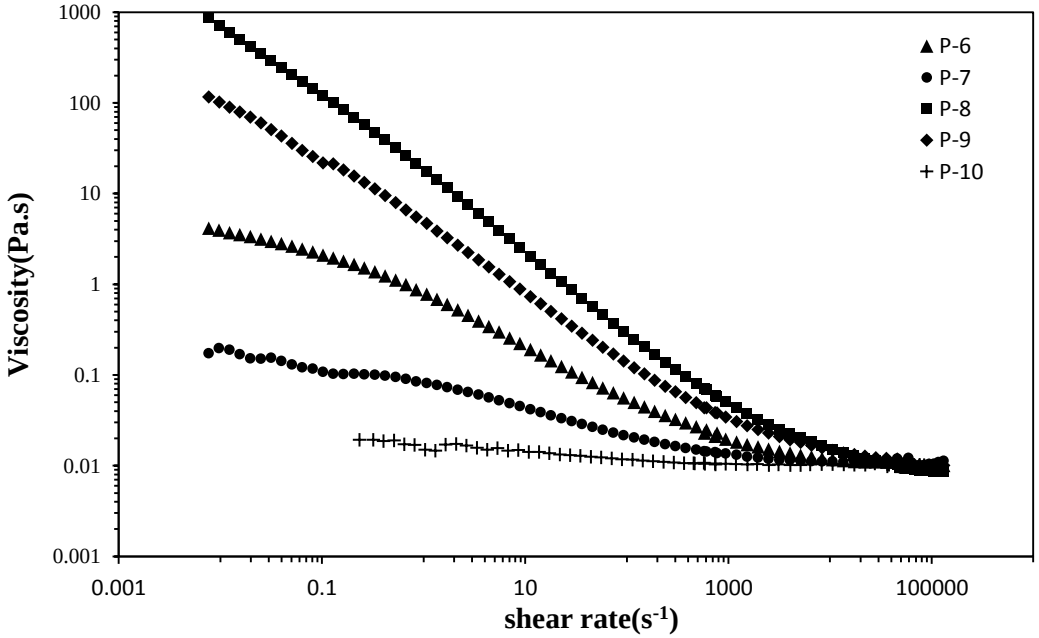

Figure 4.10: Samples of Group 2: iso-viscos at high shear rate but different viscosity at low shear rate.

The 10 designed samples were also fitted with log-log model and the fitting parameters including the viscosity results are shown in Table 4.6.

Table 4.6: Polymer concentration, log-log model fitting parameters, and viscosity values for the designed samples.

	Xanthan %(w/w)	Dextran %(w/w)	η_L Pa.s	η_H Pa.s	α	β	γ	δ
P 1	0.61	22.59	0.374	0.029	-4.907	0.164	0.722	3.22
P 2	0.71	17.33	0.398	0.019	-0.544	0.210	0.674	3.51
P3	0.74	9.4	0.358	0.009	-6.037	0.311	0.604	3.61
P 4	0.83	0	0.353	0.004	-6.847	0.380	0.532	3.85
P 5	0.4	32	0.42	0.063	-4.348	-0.06	0.731	3.05
P 6	0.21	15.7	0.077	0.01	-2.875	0.841	0.878	0.78
P 7	0.09	17.11	0.026	0.01	-1.284	0.950	0.974	-0.73
P 8	1	6.18	0.485	0.008	-6.446	0.373	0.595	3.90
P 9	0.47	12.59	0.214	0.01	-4.965	0.392	0.669	2.70
P 10	0.02	17	0.012	0.01	-	-	-	-

In Group 1 samples have relatively higher low shear viscosities compared with sample in Group 2, therefore the xanthan concentrations are higher in Group 1. Also it was found that high shear viscosities were increased with dextran concentration which indicates again that dextran plays an important role in the high shear viscosity characteristics due to its Newtonian behaviour. In Group 2 samples are less viscous compared with sample in Group 1 except for sample 8 which was most shear thinning across all the samples. Also it should be noticed that for sample 10, it was almost a Newtonian fluid and therefore log-log model was not applicable here.

4.1.4 First normal stress difference of the ten study samples

The rotational shear rheometer used in this research allows acquisition of normal forces. The normal forces recorded during the steady shear experiments are reported here as the first normal stress difference (N_1). A value different from zero denotes elastic sample behaviour in large shear deformation. As normal force is very sensitive to inertial effects, it is necessary to correct the inertial contribution to the normal force using Equation 4.7 for the case of a parallel plate geometry (Davies and Stokes, 2008).

$$F_{inertia} = -\frac{3\pi\rho\omega^4 R^4}{40} \tag{4.7}$$

Where ρ is the density ($kg.m^{-3}$), ω is the angular velocity (s^{-1}) and R is the radius of the parallel plate measurement geometry (m).

The first normal stress difference corrected for inertia and gap error for all of the ten designed samples are shown in Figure 4.11 and Figure 4.12 separately for samples of Group 1 and samples of Group 2. The results for Group 1 are discussed first. All samples of Group 1 showed positive first normal stress differences which is indicative of the viscoelastic characteristics of these samples. The slope of N_1 in the power law region was around 0.65 for most samples which is very close to value of 2/3 that has been suggested for dilute solutions of rigid rod-like molecules (Zirnsak et al., 1999). For single polysaccharide xanthan gum solutions, N_1 increased with concentration (Song et al., 2006). However, the presence of dextran gum enhanced

the normal stress response disproportionately. For example, the N_1 versus shear rate curve for sample P4 with 0.83 % (w/w) xanthan gum and no added dextran lies about one decade below the curve acquired for sample P5 with 0.4 % (w/w) xanthan gum and 32 % (w/w) dextran. This same system, aqueous mixtures of xanthan gum and dextran gum, have previously been used for the formulation of food grade Boger fluids (Koliandris et al., 2011). In that case, the xanthan gum concentration was kept very low to minimise shear thinning behaviour while imparting large elastic effects.

The magnitude of N_1 for samples was found to follow the same order as their results for relaxation time and breakup time in the CaBER experiments. It was reported by some researchers that normal stress differences from shear rheology were directly related to relaxation time deduced from filament thinning behaviour following a quadratic relationship (Zell et al., 2010). In addition, samples with higher η_H were also found to have a higher N_1.

For samples of Group 2 only P6, P8 and P9 showed a normal stress response. Thus these three samples of Group 2 can be regarded as viscoelastic whereas samples P7 and P10 were inelastic. For these same two samples, both the relaxation time and breakup time were shortest in the filament breakup measurements. The three samples which were observed for N_1 were found to have much higher concentrations of xanthan than those ones without any normal stress responses. While for the two inelastic samples, they contained higher concentration of dextran

than the three elastic samples in the group. The viscosity curves showed that these two samples are either slightly shear thinning or almost Newtonian. Therefore the normal stress difference response was either too low to detect or can be neglected.

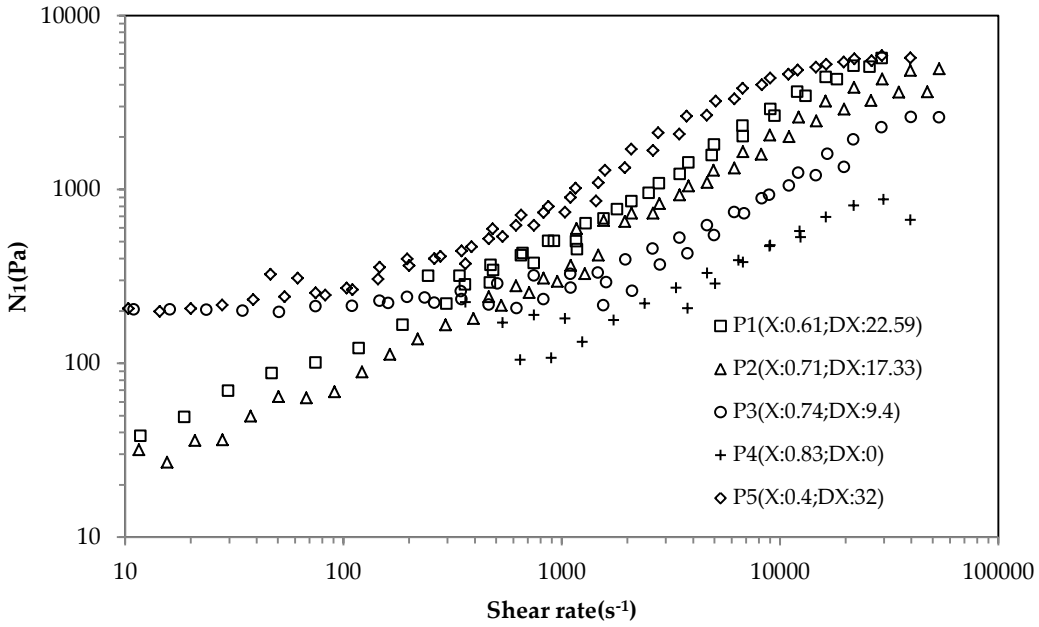

Figure 4.11: The first normal stress difference (N_1) against shear rate for samples in Group 1. The results are corrected for inertia, gap error and non-Newtonian behaviour. In the legend, the composition of each sample is included where X is the concentration of xanthan (%(w/w)) and DX is the concentration of dextran (%(w/w)). All measurements are conducted at 20 °C

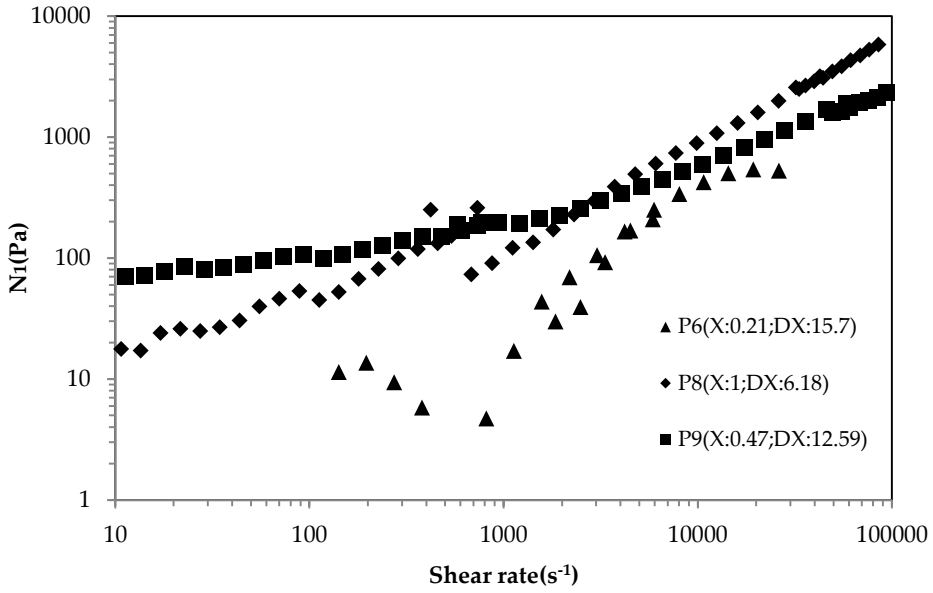

Figure 4.12: The first normal stress difference (N_1) against shear rate for sample P6, P8, and P9 and in Group2. The results are corrected for inertia, gap error and non-Newtonian behaviour. In the legend, the composition of each sample is included where X is the concentration of xanthan (% (w/w)) and DX is the concentration of dextran (%(w/w)). All measurements are conducted at 20 °C

4.1.5 Small deformation oscillatory shear properties of the study samples

The elastic modulus G′ and the loss modulus G″ as a function of strain for the two groups of samples are shown in Figure 4.13 and Figure 4.14.

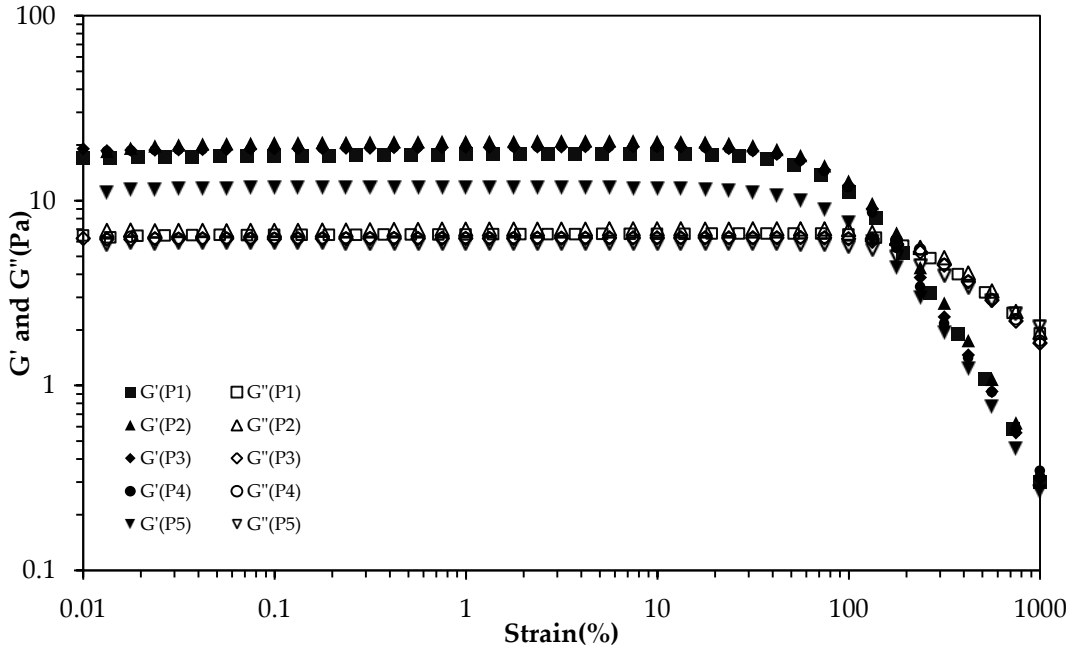

Figure 4.13: Storage modulus G′ (filled symbols) and loss modulus G″ (open symbols) as a function of strain at a constant angular frequency of 10 rad.s^{-1} for samples of Group 1. The standard deviation is within 0.1% in all cases. All measurements are conducted using PP-50 at 20 °C.

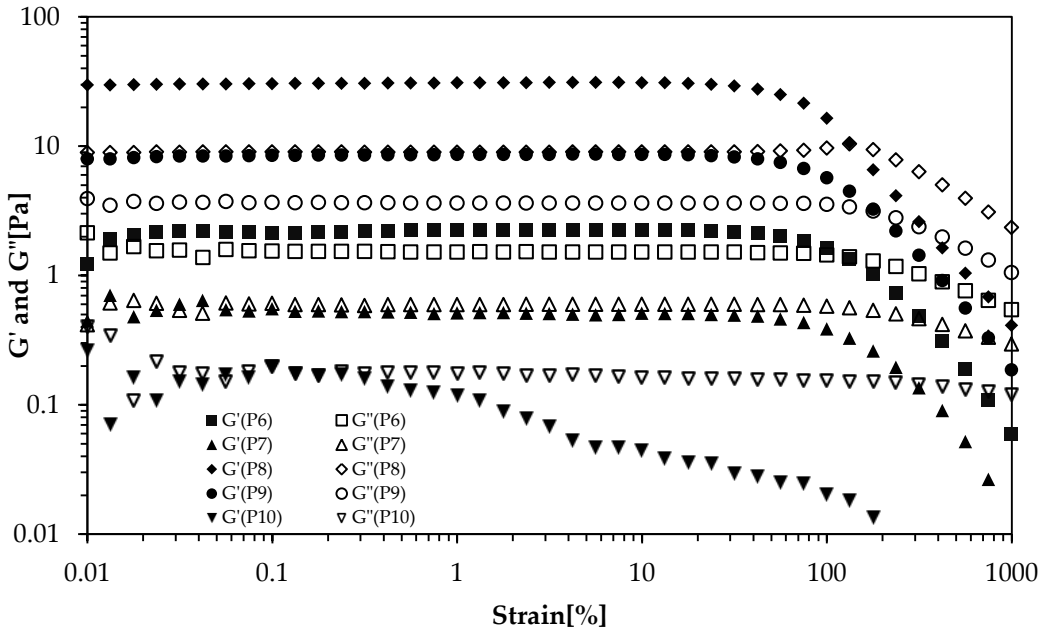

Figure 4.14: Storage modulus G′ (filled symbols) and loss modulus G″ (open symbols) as a function of strain at a constant angular frequency of 10 rad.s^{-1} for samples of Group 2. The standard deviation is within 0.1% in all cases. All measurements are conducted using PP-50 at 20 °C.

As shown in Figure 4.13 and 4.14, all samples of Group 1 had higher G′ than G′′ whereby the values for G′ as well as G′′ were very much the same when measured at an angular frequency of 10 rad.s^{-1}. As an exception P5 showed slightly lower storage modulus values. The upper limit of the linear viscoelastic domain was about 30 % strain for all samples. Similar values have been reported previously in literature for polysaccharide solutions (Song et al., 2006). The linear viscoelastic domain that occurred at lower stain is due to that the entanglement density remains unchanged, caused by a balanced status between structure breakdown and rebuilding (Isono and Ferry, 1985). The G′ and G′′ curves cross over at around 170 % strain. It seems that the concentration of xanthan has a major effect on the magnitude of storage modulus

and this explains lower values of G′ for sample P5. The samples in Group 1 seemed to be no big difference in small deformation oscillatory shear as for the elasticity that measured in large deformation shear.

The Group 2 samples, the viscosity of which were matched at high shear rate, differed appreciably in terms of G′ and G′′. For sample P6, P8 and P9, the G′ is higher than G″ within the linear viscoelastic domain which indicated the solid-like behaviour in this domain. Also, it should be noted that sample P8 has the highest value of G′ and G″ among all the 10 designed samples. When checking the composition of P8, it was found that the sample has the highest concentration of xanthan at 1%. For sample P7, the G′ is almost identical to G″ and for P10, G″ was higher than G′ for most of the strain ranges which indicated the liquid-like characteristics. Also for P7 and P10, the concentrations of xanthan were lowest among all designed samples. The linear viscoelastic domain for sample P6, P7, P8 and P9 were found to be similar as samples in Group 1 which is around 30%. However for sample P10, there was only a short linear viscoelastic domain.

From the results of the strain sweeps, see Figure 4.13 and Figure 4.14, the strain amplitude of 0.1 % was chosen to conduct frequency sweeps within the LVE region on all ten samples. Frequency was increased from 0.1 to 100 rad.s^{-1} and the results are shown in Figure 4.15.

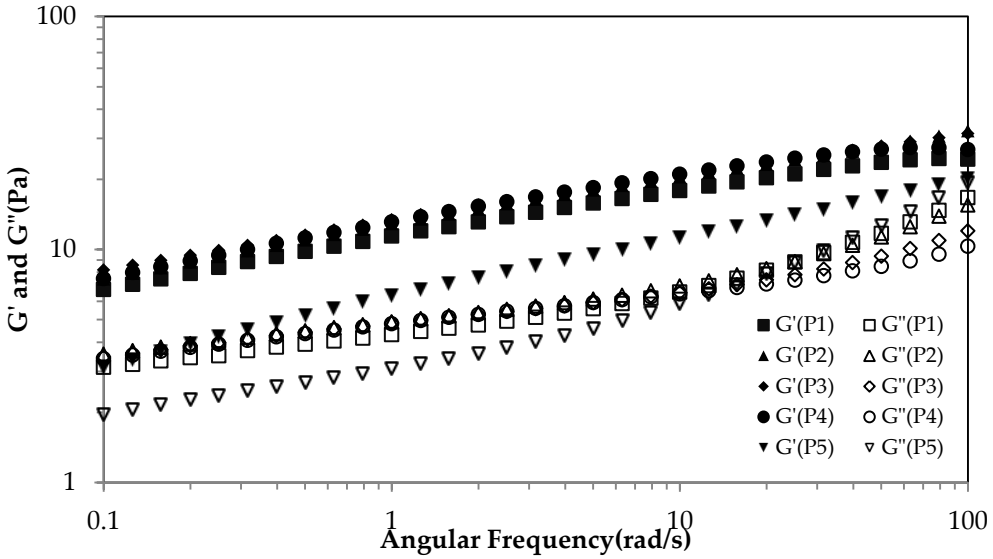

Figure 4.15: Storage modulus G′ (filled symbols) and loss modulus G″ (open symbols) as a function of frequency for samples of Group 1 , acquired at the strain of 0.1% and at 20°C.

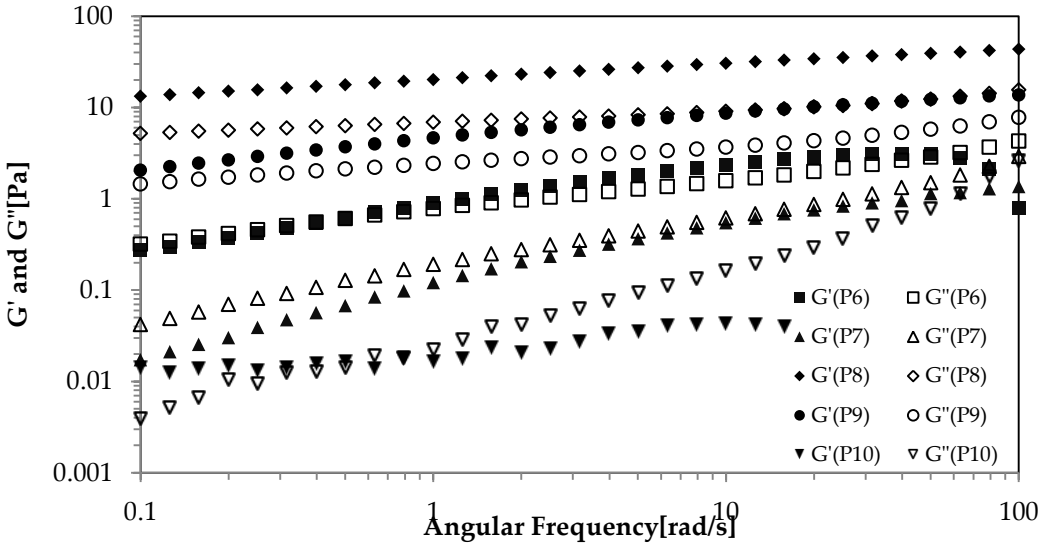

Figure 4.16: Storage modulus G′ (filled symbols) and loss modulus G″ (open symbols) as a function of frequency for (a) samples of Group 2, acquired at the strain of 0.1% and at 20°C.

As can be seen that samples in Group 1 all have G′ larger than G′′ over the whole range of frequency analysed and this is in accordance with the strain sweep that was at 10 rad.s^{-1}. Applying the criterion of the value of the storage modules (G′) being larger than the value of the loss modulus (G′′) over the whole frequency range analysed, all samples of Group 1 clearly were dominated by elastic nature within LVE. The behaviour for P5 is different from other samples in this group with a lower G′ level, as already found in the strain sweep, and a larger frequency dependency of G″. There is a clear change in slope at around 10 rad.s^{-1} and the slope at lower frequencies as well as higher frequency is higher for P5 compared to the other four samples of this group. This higher dependency of frequency for P5 is probably related to the lower concentration of xanthan. It has been reported that as with increasing of xanthan concentration, both G′ and G″ become less dependent on the frequency (Choppe et al., 2010). It is also the case for other samples in this group: clearly the trend showed that the value of G″ was higher for samples with the lowest concentrations of xanthan. The possible reason could be that for lower concentrations of xanthan, the disentanglement of polymer molecules is more likely to happen as the angular frequency increased. The data acquired for sample P5 also indicate that G′ and G′′ may cross over at a frequency just above 100 rad.s^{-1} that is the highest frequency applied in this measurement. There is no such indication for P1 to P4. Again, this can be explained by the entanglement of polymers: for less

concentration of xanthan samples, the entanglement structure can be broken at smaller frequency compared with higher concentration samples.

As can be seen in Figure 4.16, the storage and loss moduli among the samples of Group 2 showed large differences in frequency sweep. The values of G′ and G″ were largely different and dependent on the concentration of xanthan. For sample P8 and P9, the near parallel G′ and G″ moduli is indicative of the behaviour of a weakly associated network. This indicated that elastic behaviour was the dominating characteristic for these two samples within the frequency range studied. For sample P6, G′ was found slightly higher than G″ and crossover point was observed at frequency of 50 rad.s^{-1}. This indicated that for P6, there was a weak-elastic nature in low frequency range. For sample P7 and P8, the higher values of G″ indicated the viscous nature of these samples in the frequency studied.

The shear viscosity and complex viscosity have been plotted against shear rate and angular frequency, respectively, as an examination of the Cox-Merz rule and the results are shown in Figure 4.17 and Figure 4.18. The Cox-Merz rule has been widely used in polymer research and it states that complex viscosity measured with an oscillatory rheometer equates to shear viscosity measured in steady shear flow where frequency is taken as shear rate in the oscillatory tests (Cox and Merz, 1958). Therefore the Cox-Merz rule can be used as a prediction of steady shear properties of materials from dynamic properties obtained without extensive alteration of

structures. However, this rule may not be obeyed if there are hyper-entanglements or aggregated in biopolymer dispersions (Da Silva et al., 1998).

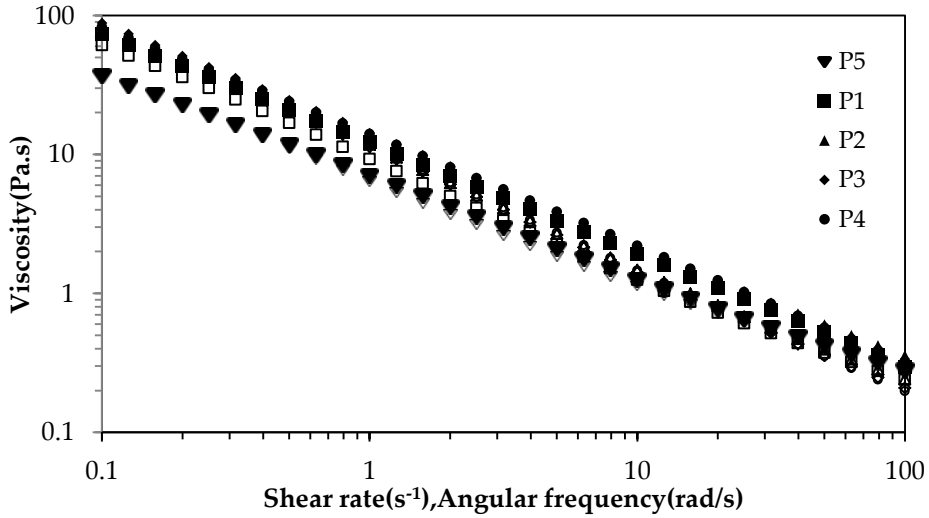

Figure 4.17: Complex viscosity (filled symbols) and shear viscosity (open symbols) plotted against shear rate and angular frequency for samples of Group 1. The standard deviation is within 0.1% in all cases.

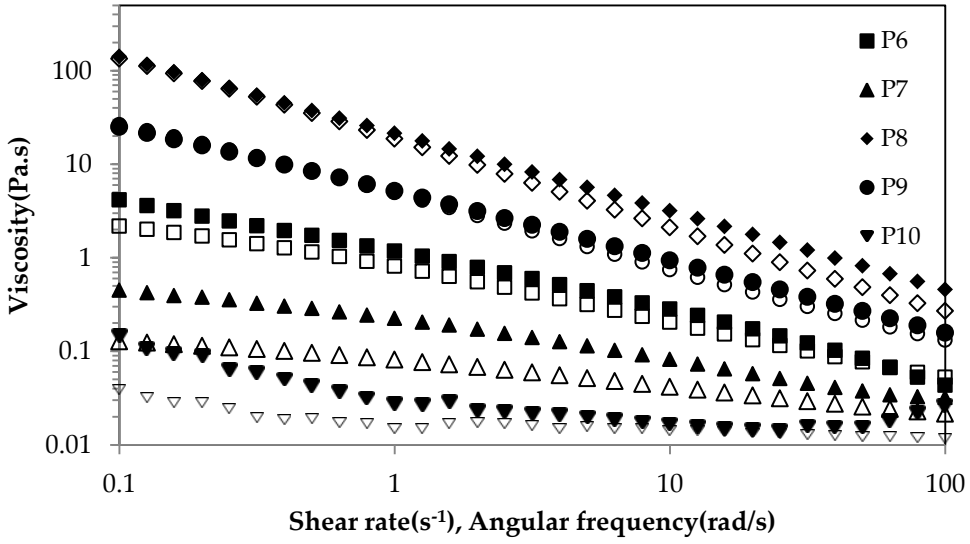

Figure 4.18: Complex viscosity (filled symbols) and shear viscosity (open symbols) plotted against shear rate and angular frequency for samples of Group 2. The standard deviation is within 0.1% in all cases.

It was found that the Cox-Merz rule was fairly obeyed for the samples of Group1. For most samples the complex viscosities were only slightly higher than the shear viscosities especially at higher shear rates or frequencies. For the samples of Group 2, the complex viscosities were also slightly higher than the shear viscosities for most of the samples. It is worth noting that sample P7 showed a larger deviation from the Cox-Merz rule than the other samples. It is interesting as large deviation has often been observed at high polymer concentration where there is the possibility that entanglements are present (Rao, 2007). However, sample P7 is a relative dilute solution with 0.09% of xanthan gum and 17% of dextran. It has been reported that for xanthan gum the shear viscosity crosses to below the complex viscosity as shear rate and frequency were increased for concentrations lower than 4.3% (Lee and Brant, 2002). For most samples, the complex viscosity is higher than shear viscosity at equivalent shear rate or frequency. This is due to the fact that polymer molecules, especially the ones that are more entangled , are less disturbed during oscillatory than in a shear flow (Chamberlain and Rao, 1999). Therefore for most of designed samples, there are some weak entanglements which can be reflected as the weak viscoelastic characteristics.

4.1.6 Extensional flow behaviour of designed samples

The extensional flow behaviour of the final sample set (see Table 4.6) for this research was evaluated through acquisition of filament thinning data, see 3.2.1.5 for

the method used. The evolution of the normalised filament diameter is shown in Figure 4.19 and Figure 4.20. With reference to Figure 4.19 and Figure 4.20, it is worth noting that the time scale of breakup for both sets of samples varies by one decade and therefore the results have been plotted on different x-axis scales.

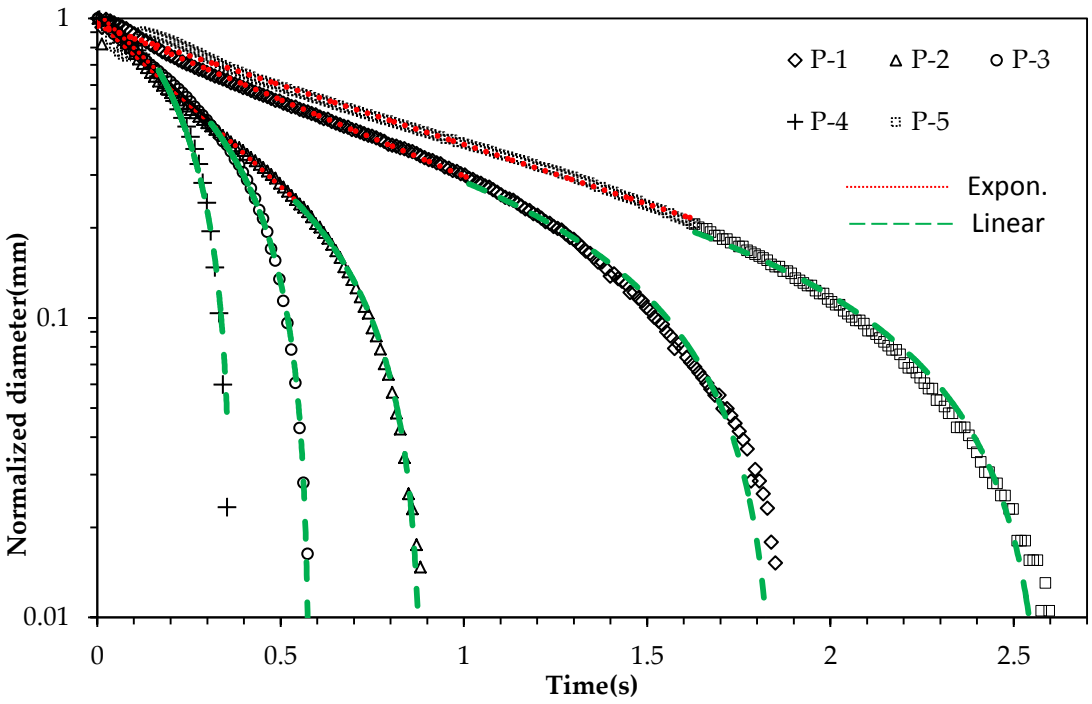

Figure 4.19: Evolution of the normalised filament mid-point diameter for Group 1 Samples: (·····) is the elastic domain fitted with exponential model and (– – – –) is inelastic domain fitted with linear model. The standard deviation of the samples are within 5% in all cases. The stretch time is 50ms and all the measurements were conducted at 37 °C.

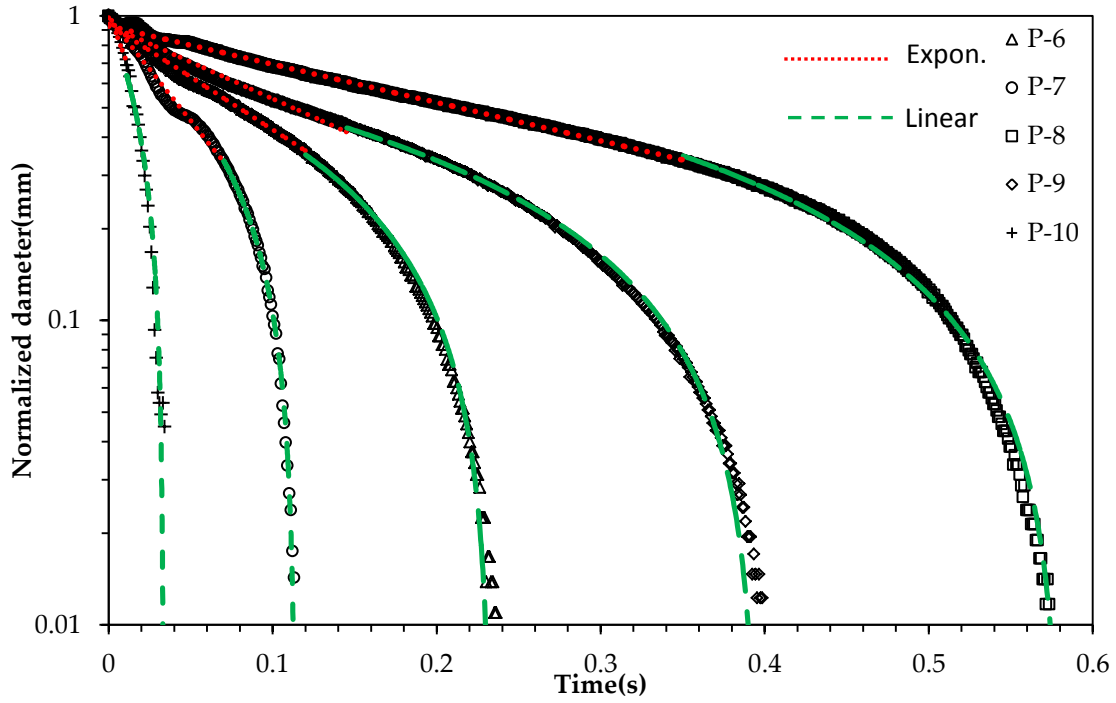

Figure 4.20: Evolution of the normalised filament mid-point diameter for Group 2 Samples: (·····)is the elastic domain fitted with exponential model and (- - - -) is inelastic domain fitted with linear model. The standard deviation of the samples are within 5% in all cases. The stretch time is 50ms and all the measurements were conducted at 37 °C.

As can be seen from the results, these two groups of samples vary significantly in terms of breakup time. For Group 1 samples, the breakup time ranged from 0.354 to 2.642 s while for Group 2 samples the breakup time ranged from 0.036 to 0.58 s. It was also found that in Group 1, sample with higher η_H took longer time to break up whereas in Group 2, samples with higher η_L took longer time to break up. Moreover, it seemed that in Group 1 the concentration of dextran strongly influenced the length of breakup time: the filament of samples with higher concentration of dextran took longer to breakup. However, in Group 2, it was the concentration of xanthan that

affected the breakup time: samples with higher concentration of xanthan took a longer time to break up.

The filament diameter curves are fitted with an exponential (see Equation 2.29) and a linear model (Equation 2.30) in elastic and inelastic domain, respectively. The fitting parameters exponential and linear index and also the calculated relaxation time and steady state apparent viscosity η_E from the models are reported in Table 4.7. The breakup time from experimental results are also reported.

Table 4.7: The relaxation time λ, extensional viscosity η_E obtained from elastic and inelastic model fitted the filament breakup experiments, and model fitting parameters exponential and linear index. The fitting quality in all cases is high with correlation coefficients over 0.99. Breakup time t_B from the experimental results are also reported.

	Xanthan	Dextran	Expon. index	Lin. index	t_B	λ	η_E
	%(w/w)	%(w/w)			s	s	Pa.s
P-1	0.61	22.59	-1.17	-1.07	1.872	0.284	65.165
P-2	0.71	17.33	-2.54	-2.17	0.893	0.131	32.225
P-3	0.74	9.40	-2.57	-4.80	0.574	0.130	14.595
P-4	0.83	0.00	-2.74	-7.84	0.354	0.122	8.925
P-5	0.40	32.00	-0.91	-0.69	2.642	0.365	88.143
P-6	0.21	15.70	-7.97	-3.10	0.239	0.042	7.617
P-7	0.09	17.11	-15.55	-7.67	0.113	0.021	9.122
P-8	1.00	6.18	-2.89	-5.30	0.580	0.115	13.199
P-9	0.47	12.59	-5.56	-1.71	0.407	0.060	11.482
P-10	0.02	17.00	-32.70	-55.82	0.036	0.010	1.254

It was also found that samples with shorter breakup time, the filament thinning behaviour is characterised by fast exponential decay, e.g. P10. Also the polymer concentrations seemed to have a large effect on the breakup time. It has been

suggested that the filament thinning in the exponential decay domain was mainly due to the disentanglement and orientation of polymers (Bousfield, et al, 1986). Therefore, in higher concentration of polymers, this domain is longer. The longer exponential domain also resulted in a longer relaxation time.

Values calculated for the Trouton ratio have been plotted as a function of Hencky strain in Figure 4.21 and Figure 4.22.

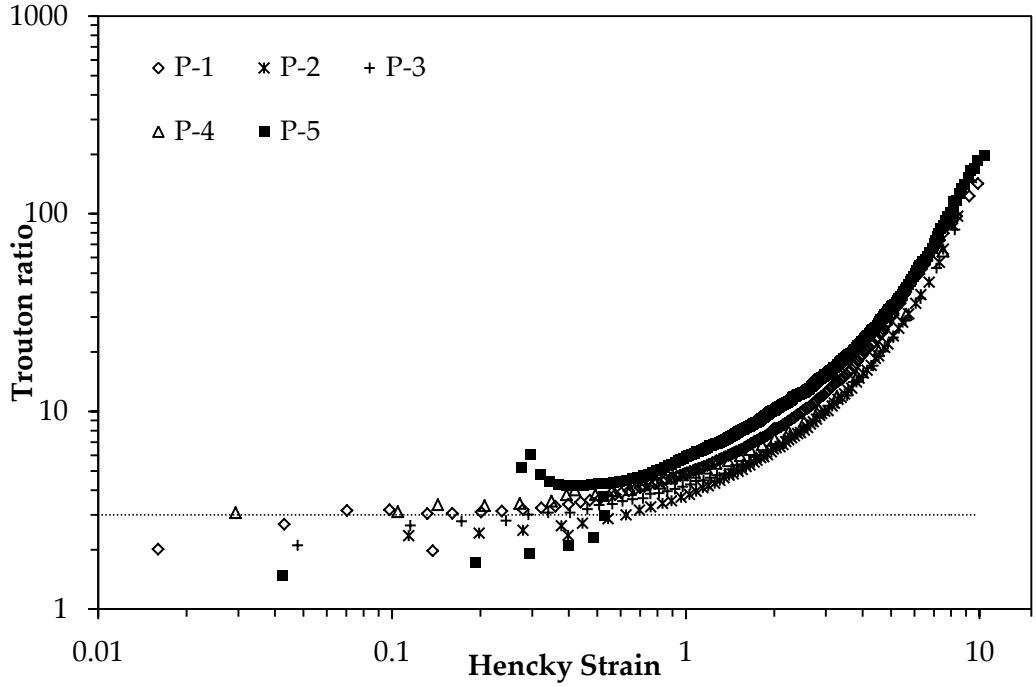

Figure 4.21: Trouton ratio plotted against Hencky strain for Group 1

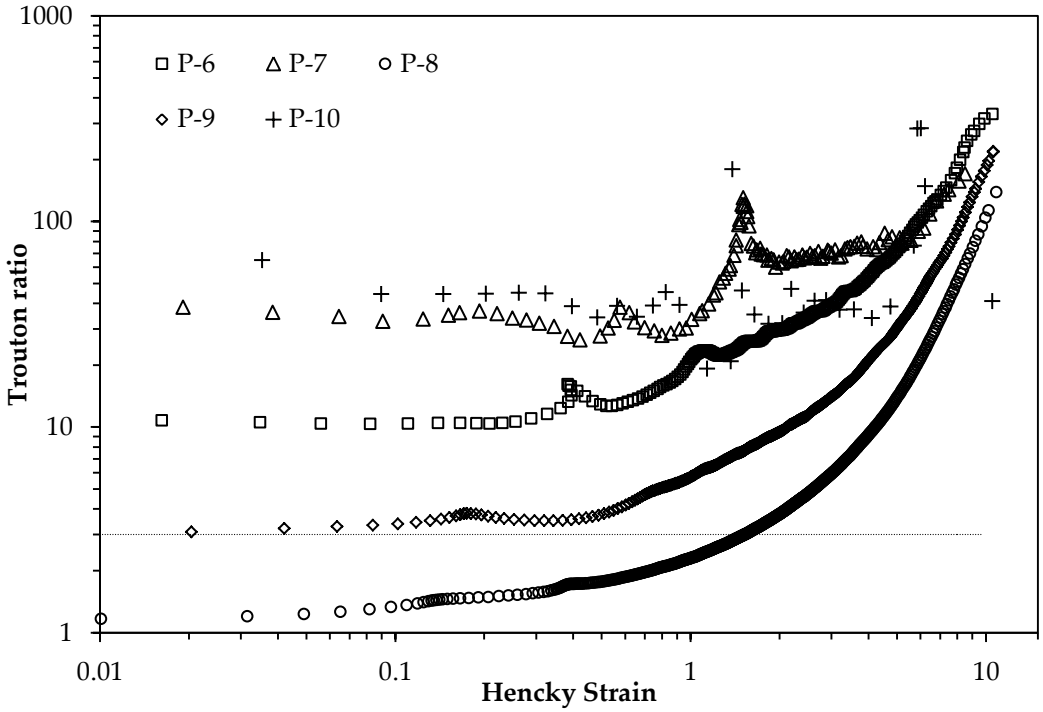

Figure 4.22: Trouton ratio plotted against Hencky strain for Group 2

The Tronton ratio of samples of Group 1 and Group 2 are shown in Figure 4.21 and Figure 4.22. For the samples in Group 1, there were plateau found for Trouton ratio at low Hencky strain below 0.2 which was around 3. As with increased strain, the Trouton ratio increased dramatically to 200 at the highest strain of 10. Also it was found that the Trounton ratio was overlapped for the samples in Group 1 at higher Hencky strain. For samples in Group 2, the Trouton ratios were significantly different across the samples. Plateaus were found for all samples below the Hencky strain of approximately 0.2 and only sample P8 was found below 3. Sample P10 had the highest value of Trounton ratio of approximately 44. The results indicated that it

was mainly the shear rate at low to moderate range (up to 500 s-1) that affected the Troution ratio at low Hencky strain range.

Also the results indicated for elastic samples, as with increased strain, the extensional flow becomes increasingly dominating the flow properties of polymer solutions. The results clearly show that the samples vary considerably in their extensional flow characteristic and consideration of shear viscosity data alone may not suffice to model sensory perception due to the complex nature of 'oral flow fields' during the consumption of food.

4.2 Sensory properties of designed samples

In this chapter, the results from two sensory tests: Descriptive Analysis (DA) and Napping® will be reported. In addition the results from in-*vivo* flavour release using APCI-MS will also be reported in this chapter.

4.2.1 Results from Descriptive Analysis (DA)

4.2.1.1 Assessment of panel performance

As mentioned previously, most of the attributes that are used in this research were pre-set. However, during training it was found that the pre-set attributes could not reflect the entire mouthfeel and flavour perceptions of the samples. After discussion and retesting of samples, the panel agreed to add two more attributes: mouth-coating and musty/fusty.

It is important to make sure that the panel are able to discriminate samples for the attributes and consistent in giving scores for the same samples. Therefore measures of repeatability and discriminative ability of panellists were used to assess the performance of panel. The panels' ability to score consistently was assessed by calculating the coefficient of variance (CV) and their ability to discriminate samples were calculated as probability value (FPROD) though FIZZ software (Biosystems, France). As shown in Figure 4.23, each colour dot represents one of the panellists' ability of repeatability and discrimination for one attribute and it should be noted there were 10 panellists in total.

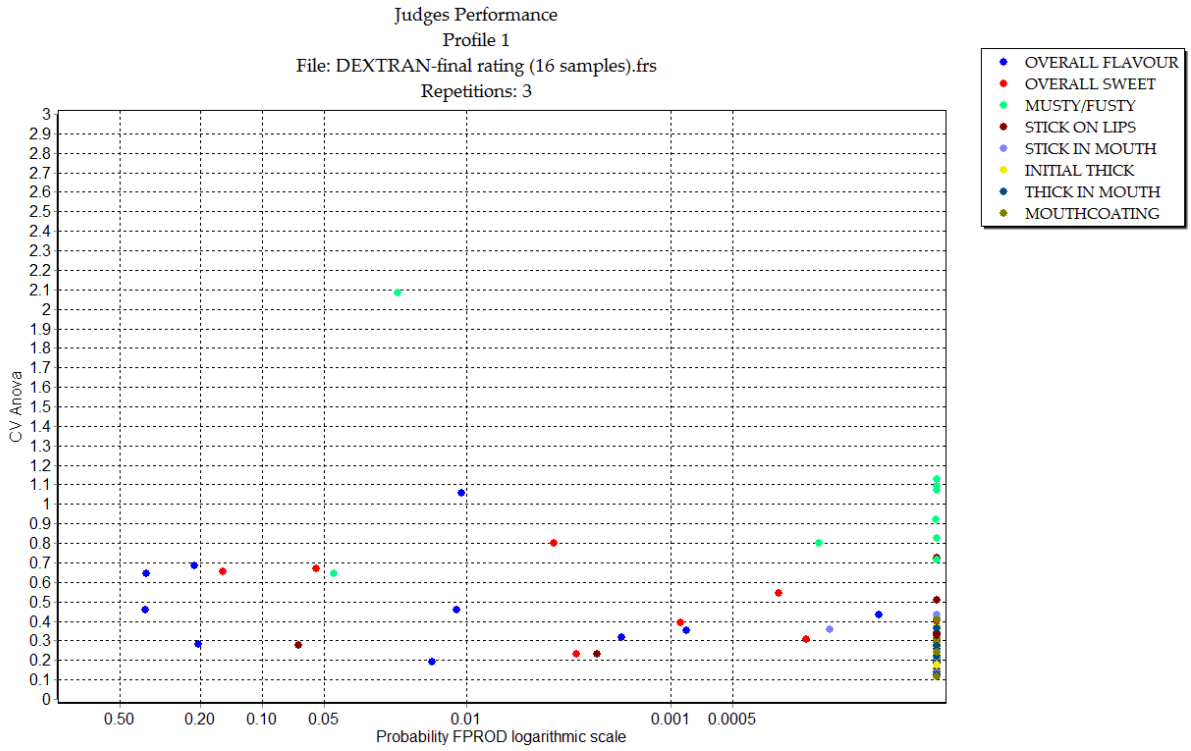

Figure 4.23: Repeatability and discrimination performance of the panel (10 panellists in total).

As can be seen from Figure 4.23 , most of the panellists were able to give consistent scores which were indicated by the low CV values of around 10%. However, it should be noted that one panellist gave relatively higher CV values (21%) for Musty/Fusty attribute. It should also be noted that for most of the mouthfeel attributes, the panel were able to give scores in a highly consistent manner (CV<5%). In terms of the discrimination performance, it was found that most panels could discriminate between samples for most of the attributes (p<0.05). However, for the attribute of Overall Fruity Flavour, it was found that 4 of the panellists could not

discriminate between samples ($p>0.05$). A further two of the panellists could not discriminate the Overall Sweetness of samples, although one of them was close to the significant level of 0.05. Also there was one panellist could not discriminate the Musty/Fusty between samples. Again for the mouthfeel attributes, most of the panellists could discriminate them very well.

4.2.1.2 ANOVA and post-Hoc tests

Two-way ANOVA (panellist and sample factors) was performed on the mean data that was acquired through the 3 replicates. A Tukey's HSD post-hoc test was used to determine the significant differences between samples for each attribute. The results for mouthfeel and flavour perception will be reported separately in section 4.2.1.2.1 and 4.2.1.2.2.

4.2.1.2.1 Mouthfeel attributes

The ANOVA and post-hoc results for Initial Thickness and Thickness in Mouth are shown in Table 4.8. Results showed a significant differences between panellists and products ($p<0.001$), and also there were significant interactions between product and panellists for both of the attributes ($p<0.001$). The differences in panellists indicated that they were using the scale differently. Normally the interaction between panellists and products indicates the poor understanding of the attributes which could cause 'cross-over' effects. However, when checking the graph of scores, as can be seen in Figure 4.24, there were no real 'cross-over' effect.

Table 4.8: ANOVA *p*-value and mean sample scores for two thickness attributes. Samples coded with the same letter in any one column are not significant different (*p*>0.05)

		Initial thickness		Thickness in mouth	
p-values	Product	<0.001		<0.001	
	Panellists	<0.001		<0.001	
	Products*Panellists	<0.001		<0.001	
Mean Sample score	P- 1	8.67	*b*	8.32	*b*
	P- 2	7.68	*c*	7.41	*c*
	P- 3	6.49	*d*	5.99	*d*
	P- 4	5.29	*e*	4.6	*e*
	P- 5	9.26	*a*	9.05	*a*
	P- 6	1.83	*g*	1.44	*f*
	P- 7	0.92	*h*	0.84	*g*
	P- 8	8.09	*c*	7.85	*b,c*
	P- 9	4.37	*f*	4.09	*e*
	P- 10	0.54	*h*	0.42	*g*

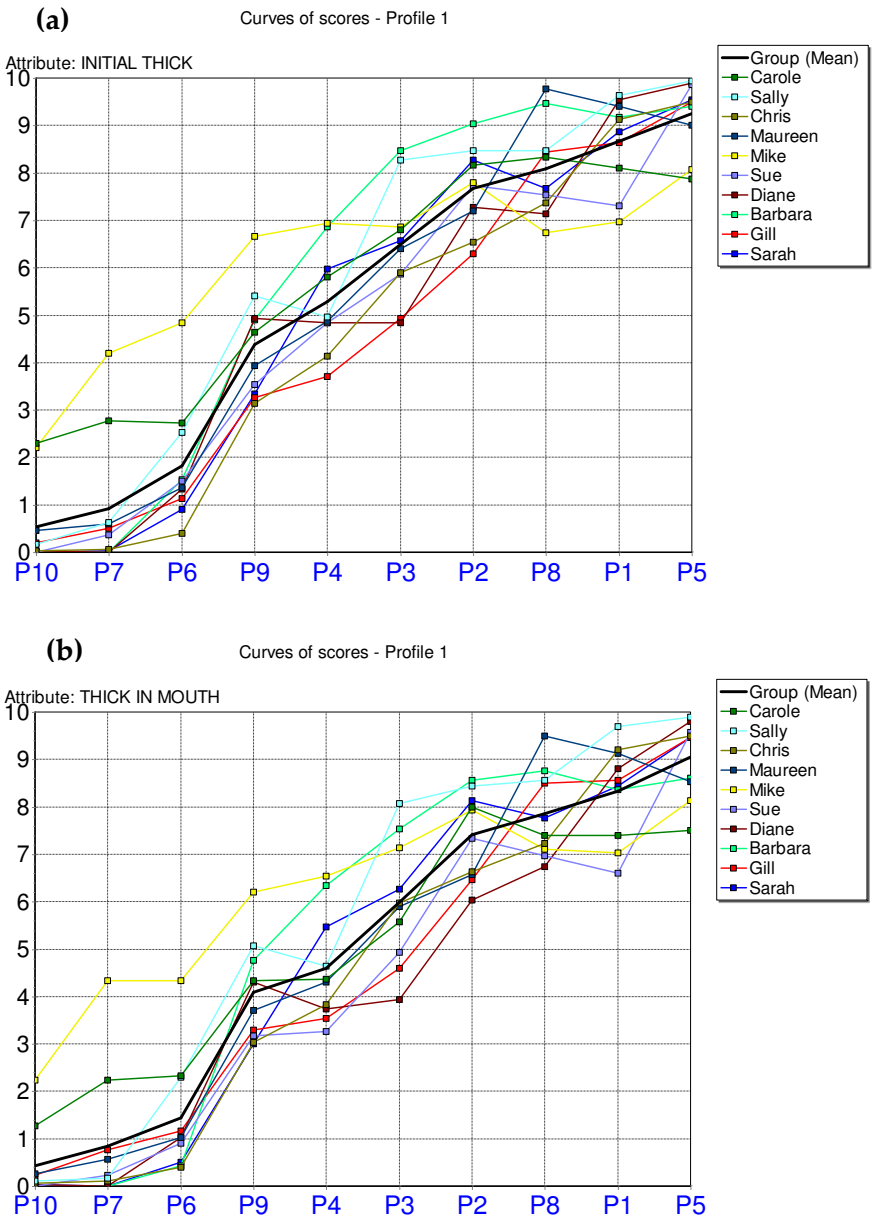

Figure 4.24: Graph of scores for attributes of (a) Initial Thickness and (b) Thickness in Mouth. Each coloured curve represents the mean score of one panellist from three replicates.

The results from ANOVA and post-hoc tests indicated that for sample P-1 to P-5, although they have similar low shear viscosities, the perceptions of both Initial Thickness and Thickness in mouth were significantly different. For sample P-6 to P-10, there were significant differences between most of the samples even though they

were found to have similar high shear viscosities. It should be noticed that for sample P-7 and P-10, there were no significant difference for both Initial Thickness and Thickness in mouth. Also it was found that these two attributes were highly correlated(r=0.99).

ANOVA and post-hoc results for stickiness and mouthcoating are reported in Table 4.9. There were significant differences for panellist, product and interaction between the two factors. As discussed previously, the interaction between panellists and products did not cause any real 'cross-over' effects when checking the graph of scores.

Table 4.9: ANOVA *p*-value and mean sample scores for Stickiness and Mouthcoating. Samples coded with the same letter in any one column are not significantly different (*p*>0.05)

		Stickiness on lips		Stickiness in mouth		Mouth coating	
p-values	Product	<0.001		<0.001		<0.001	
	Panellists	<0.001		<0.001		<0.001	
	Products*Panellists	<0.001		0.0052		0.0012	
Mean Sample score	P- 1	8.06	*a*	7.77	*b*	7.63	*b*
	P- 2	6.56	*b,c*	6.41	*c*	6.56	*c*
	P- 3	5.91	*c*	5.06	*d*	4.86	*d*
	P- 4	3.91	*d*	3.14	*e*	3.66	*e*
	P- 5	8.85	*a*	8.79	*a*	8.52	*a*
	P- 6	2.66	*e*	1.7	*f*	1.56	*f*
	P- 7	2.08	*e,f*	1.41	*f*	0.99	*f,g*
	P- 8	6.88	*b*	6.65	*c*	6.52	*c*
	P- 9	3.97	*d*	3.6	*e*	3.3	*e*
	P- 10	1.52	*f*	0.65	*g*	0.64	*g*

The results indicated that for sample P-1 to P-5, the perceived Stickiness and Mouthcoating were significantly different. Only P-2 and P-3 were not different for

Stickiness on lips. The results indicated that low shear viscosity could not interpret the entire information for stickiness and mouthcoating perceptions. Likewise for sample P-6 to P-10, although identical in high shear viscosities, the perceived Stickiness and Mouthcoating were significantly different for most of the samples. It should be noticed that for sample P-6 and P-7, there were no significant difference for both Stickiness and Mouthcoating, sample P-7 and P-10 were not significantly different for Stickiness on lips and Mouthcoating. It was also found the three attributes were highly correlated with each other.

4.2.1.2.2 Taste and flavour attributes

The ANOVA and post-hoc tests results for taste and flavour attributes are shown in Table 4.10. There were significant differences for product and panellists for the three attributes. Also there were significant product and panellists interactions found for Overall Fruity Flavour and Musty/Fusty. When checking the graph of scores, it was found that there were some 'cross-over' effects for these two attributes. These differences may be due to poor understandings of the attributes used or confusion caused when experiencing different viscosities in mouth.

Table 4.10: ANOVA *p*-value and mean sample scores for flavour and tastes. Samples coded with the same letter in any one column are not significant different (p>0.05)

		Overall fruity flavour		Overall sweetness		Musty/ Fusty	
p-values	Product	0.002		<0.001		<0.001	
	Panellists	<0.001		<0.001		<0.001	
	Products*Panellists	0.0197		0.275		<0.001	
Mean sample score	P-1	5.45	*a,b*	6.5	*b,c*	1.67	*a*
	P-2	5.84	*a,b*	6.34	*b,c,d*	0.87	*b*
	P-3	4.86	*b,c*	5.02	*d,e*	0.59	*b,c*
	P-4	3.23	*d*	2.94	*f*	1.54	*a*
	P-5	6.34	*a,b*	7.6	*a,b*	0.75	*b,c*
	P-6	6.13	*a,b*	6.99	*a,b,c*	0.44	*b,c*
	P-7	6.62	*a*	7.34	*a,b,*	0.16	*c*
	P-8	3.8	*c,d*	3.78	*e,f*	0.84	*b*
	P-9	5.4	*a,b*	5.78	*c,d*	0.33	*b,c*
	P-10	6.87	*a*	8.01	*a*	0.17	*c*

The results for 'Overall fruity flavour' indicated that although these samples were identical in terms of the flavour levels, the panel still gave scores ranged from 3.23 to 6.87. For Group 1 samples, it was found that most of the samples were not significantly different from others except for sample P-4 which had the highest concentration of xanthan in this group. It was the same case for Group 2 that most of the samples were not significantly different from each other except for sample 8 which had the lowest score in this group. From the aspect of the whole samples set, it was found sample P-3, P-4 and P-8 were different from other samples. Also it was found that these three samples had the highest amount of xanthan and lowest amount of dextran. It was also worth noting that although most of the samples were

not significantly different, however, the panel suggested there were some different in terms of the nature of the flavour. Therefore the Napping® method was used in order to find the further difference of the flavour perception. The results will be discussed in Section 4.2.3

The Overall sweetness attributes for samples were scored from 2.94 to 8.01 despite having the same level of 3% sucrose. For samples in Group1, sample P-1, P-2 and P-5 were not significantly different from each other, sample P-3 and P-4 were found to be significantly different from others. In Group 2, sample P-8 and P-9 were significantly different from others. The scores for Overall sweetness and Fruity flavour were found to be highly correlated (r=0.99).

The scores for the attribute of Musty/Fusty were relatively low for most of the samples. As this attribute was introduced when the model testing samples were added to the sample sets, therefore, this attributes could be mainly caused by the model testing samples. The results from model testing samples will be discussed in Section 4.3.3.4.

4.2.1.3 Principal Component Analysis (PCA)

The Principal Component Analysis (PCA) was performed on the sensory data using software XLSTAT (version 7.5,Addinsoft,USA). Table 4.11 detailed the correlations between attributes and contribution of each attribute to each PC as well as the percentage of variance explained by each PC.

Table 4.11: PCA attribute correlations, contribution of each attribute to each PC, and percentage of variance explained by each PC.

	PC1 (68.59%)		PC2 (22.64%)	
	Correl.	**Contri(%)**	**Correl.**	**Contri(%)**
Overall flavour	-0.278	1.409	**0.805**	35.782
Overall sweetness	-0.260	1.236	**0.864**	41.234
Musty/Fusty	**0.736**	9.863	-0.502	13.917
Stickiness on lips	**0.969**	17.127	0.236	3.069
Stickiness in mouth	**0.966**	17.021	0.244	3.296
Initial thickness	**0.992**	17.929	0.073	0.290
Thickness in mouth	**0.989**	17.839	0.106	0.615
Mouthcoating	**0.982**	17.576	0.180	1.798

The PCA results indicated that the first two PCs account for about 91.23% of variance in the data. For PC 1, which described around 68.59% of the variance, the examination of correlation and contribution of attributes suggested that it mainly described the mouthfeel attributes. For PC 2, which described about 22.64% of variance, it mainly reflected the overall flavour and sweetness. These relationships can be clearly seen through a bi-plot of both attributes and samples as shown in Figure 4.25.

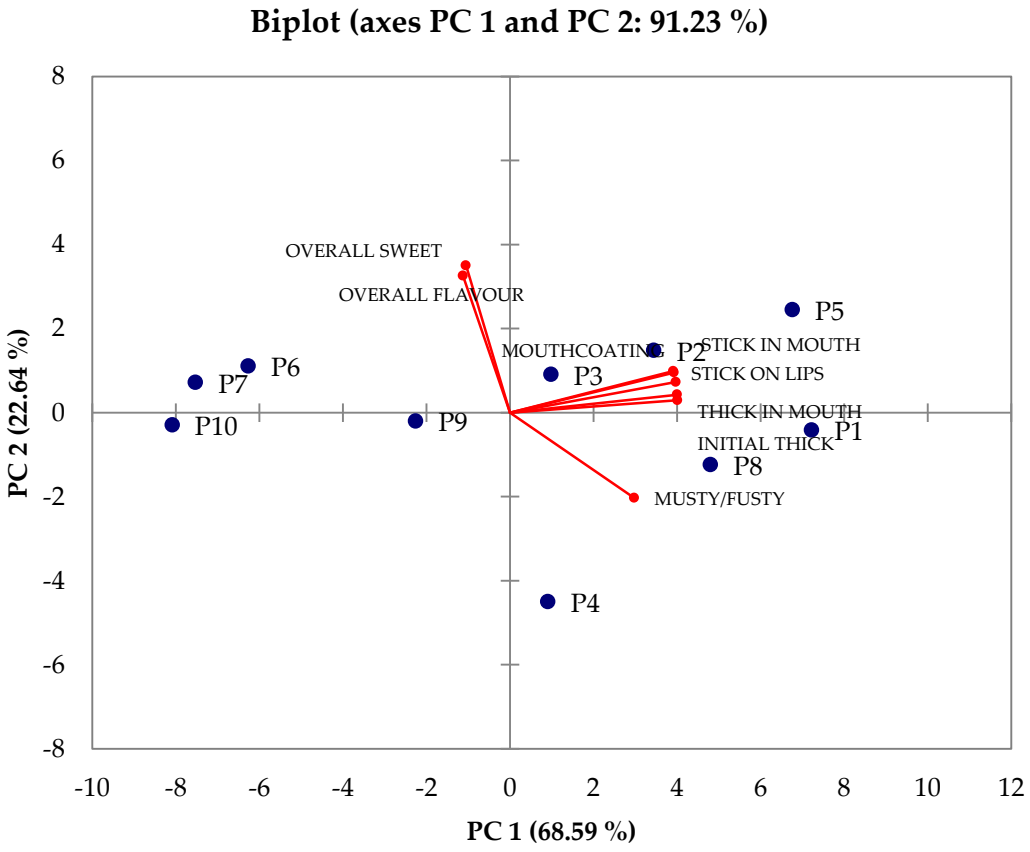

Figure 4.25: Biplot showing loading of attributes along PC1 and PC2 together with the samples distribution along the two axes.

As it showed in the PCA biplot, PC1 mainly described the mouthfeel attributes with least to most from left to right. It seemed that all samples in Group 1 were at the higher end of the axes whereas most of the Group 2 samples were at the lower end along the PC1 axis except for sample P8. The results clearly indicated that shear rheology of the sample did have a large effect on the mouthfeel attributes, but it could not reflect the whole picture, there will be detailed discussion in Section 4.3. Overall flavour and sweetness contributed most of the PC 2. The overall flavour and

sweetness of samples were located along PC 2 with less intense samples at the bottom and most intense samples at top. It was found that most of samples were located relatively close to each other although there are some exceptions such as P5 and P4 which represent the extremes of the sample sets.

4.2.2 *In vivo* flavour release measurements

The average maximum intensity (Imax) and cumulative area (AUC) for the ion monitoring IAA (ion 131) for the 10 samples are shown in Figure 4.26. It should be noted that the results are average of 3 replicates from 10 panellists. Also ANOVA and post-hoc test using Tukey's HSD were performed to the data and the results are shown in Table 4.12. It was found that for both Imax and AUC, there were no significant differences across the samples ($p>0.05$). The results indicated that during consumption of the samples, both the maximum intensity and total amount of aroma compounds were not significantly different for all the samples.

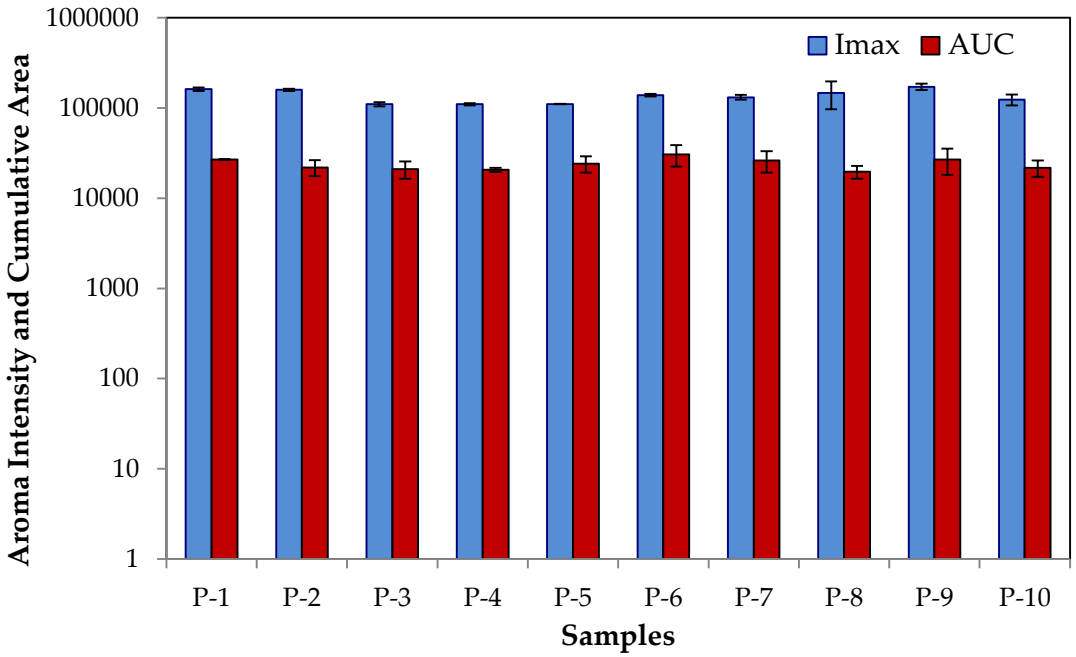

Figure 4.26: Maximum aroma intensity (Imax) and Cumulative area(AUC) of the in-vivo flavour release

Table 4.12: Average results for maximum intensity (Imax) and cumulative area (AUC) for *in vivo* flavour release during sample consumption. ANOVA and Tukey's HSD were performed and samples with same letter within a column are not significantly different (p>0.05).

Samples	Imax			AUC		
	Mean	SD		Mean	SD	
P-1	1.6E+05	7.3E+03	*a*	2.7E+04	2.0E+02	*a*
P-2	1.6E+05	4.4E+03	*a*	2.2E+04	4.5E+03	*a*
P-3	1.1E+05	6.1E+03	*a*	2.1E+04	4.5E+03	*a*
P-4	1.1E+05	3.3E+03	*a*	2.1E+04	1.0E+03	*a*
P-5	1.1E+05	4.8E+02	*a*	2.4E+04	5.0E+03	*a*
P-6	1.4E+05	4.9E+03	*a*	3.1E+04	8.2E+03	*a*
P-7	1.3E+05	8.2E+03	*a*	2.6E+04	7.0E+03	*a*
P-8	1.5E+05	5.0E+04	*a*	2.0E+04	3.2E+03	*a*
P-9	1.7E+05	1.4E+04	*a*	2.7E+04	8.7E+03	*a*
P-10	1.2E+05	1.7E+04	*a*	2.2E+04	4.5E+03	*a*

4.2.3 Results from Napping®

The Napping® was used in this research to explore the flavour difference of the samples. In the Napping tests, 16 samples were tested including 10 designed samples (see Table 4.6) and 6 model testing samples (see Table 4.19). Multiple Factor Analysis (MFA) and Agglomerative hierarchical Clustering (AHC) were performed for the data and the results will be reported in the following sections.

4.2.3.1 Preliminary examination of tablecloths

During the training sessions, the panels were trained to use the whole area of the tablecloths. Therefore some of the tablecloths are reproduced here as an examination of the panel's utilisation of the tablecloths. Four tablecloths results from nine panellists were selected and reproduced as an examination of their utilisation of the tablecloths, the results are shown in Figure 4.27. The panel's utilisation of tablecloths indicated that both vertical spaces (Y-axis) and horizontal spaces (X-axis) were not fully used. The panel tend to use the up-left 80% areas of the entire tablecloths.

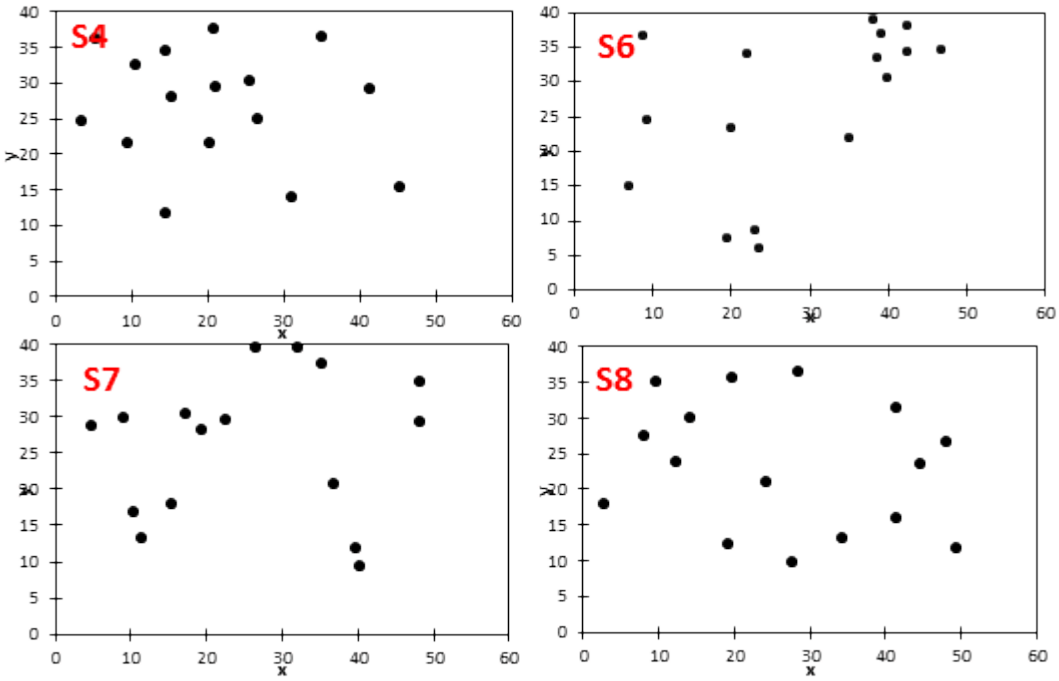

Figure 4.27: Randomly selected representative tablecloths from 4 panellists. Each black dot represents a sample and the panellists also wrote down any words that can be used to describe the attributes (results not shown here)

4.2.3.2 Results of Multiple Factor Analysis (MFA)

The results of MFA including the scores and contributions of each sample to the factors are shown in Table 4.13. Figure 4.28 shows the results from MFA for samples in two PCA plots with the first three factors. In the first PCA plot where F1 and F2 accounted for 40.855, there were three clusters of samples and the rest of samples were widely spread along the two axes. In order to find out what attributes are explained by these factors, the descriptors that were used to describe the samples were examined. The attributes and the number of times that the attributes have been used to describe the samples are reported in Table 4.14.

Table 4.13: MFA scores and contribution of each sample to each factor and variability of each factor.

Observation	F1(23%)		F2(17.79%)		F3(14.22%)	
	Scores	Contri(%)	Scores	Contri(%)	Scores	Contri(%)
P1	-0.858	1.390	-1.565	5.999	-0.402	0.495
P2	0.827	1.291	-1.007	2.480	0.915	2.561
P3	-1.531	4.423	0.956	2.238	1.111	3.777
P4	1.172	2.593	0.202	0.100	1.988	12.109
P5	-1.175	2.606	-0.897	1.971	-1.322	5.355
P6	-2.991	16.887	0.900	1.981	-0.674	1.392
P7	-2.513	11.923	-0.875	1.872	-1.337	5.474
P8	-1.432	3.871	-1.766	7.634	-1.030	3.248
P9	-1.111	2.330	0.646	1.023	1.100	3.708
P10	-1.185	2.651	0.602	0.887	1.150	4.051
DX Low	-0.238	0.107	1.946	9.266	2.417	17.885
DX High	1.032	2.012	0.362	0.321	-0.859	2.260
MC Low	2.167	8.870	0.224	0.123	-2.860	25.047
MC High	2.248	9.542	4.157	42.289	-1.485	6.749
Guar Low	2.692	13.681	-2.770	18.774	1.383	5.860
Guar High	2.895	15.823	-1.115	3.042	-0.095	0.028

As can be seen from the PCA plot, it is clear that most of the designed samples were located on the left half along F1 except for P2 and P4 and most of the models testing samples were located on the right half of F1 except for sample DX Low. Examination of both type and times of descriptor used for these samples indicated that F1 was more related to the 'type of flavour' from negative 'banana, sweet and peardrop' to positive 'chemical, plastic, bitter' attributes. For F2 which accounted for about 17.79% of the variability, it seemed mainly described the 'Musty/Fusty' nature of the samples as sample MC High was at almost the extreme of the axis. For F3, however, it was difficult to draw solid conclusions what it described due to the low variability (14.22%).

There are two groups of samples that were relatively close in the PCA plot which indicated that they were perceived as similar by the panels. However, it was very difficult to find solid reason why these samples are close to each other. It seemed that for sample P3, P9 and P10, the descriptor 'peardrop , banana and fruity' has been used approximately the same times by the panellists, and also the negative descriptors such as 'musty/fusty, plastic' were used the similar times. For sample P4 and DX Low however, on obvious reasons were found to explain why they are close to each other.

Overall, the Napping® was useful to find the differences between samples in this research especially for some obvious attributes such as 'musty/fusty, and sweetness'. However, for some samples it was very difficult to find the reason why samples are close to or far from each other based on the limited descriptors used by the panellists. In order to further explore the differences between these samples, AHC were performed for both whole sample set and designed samples only.

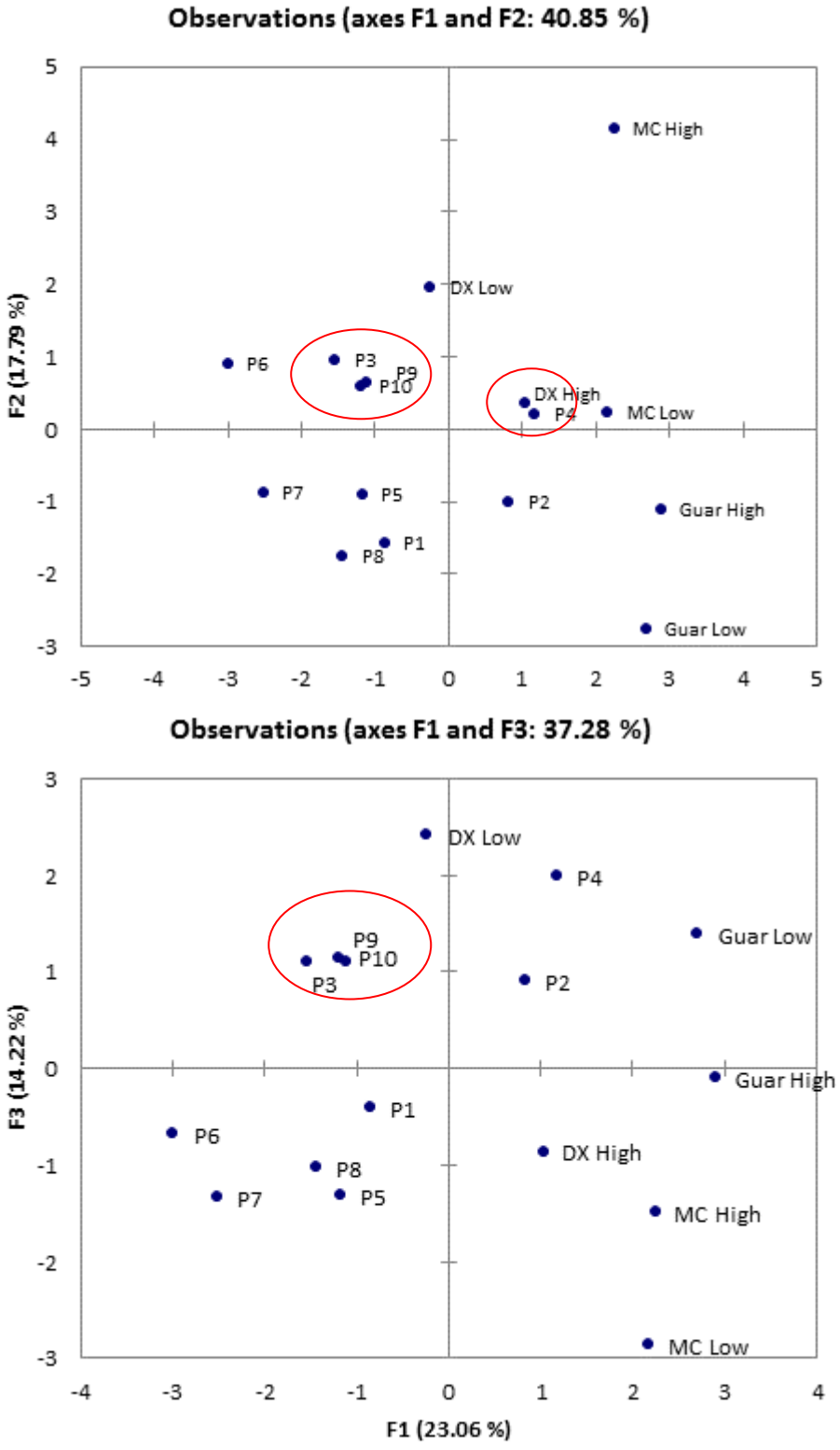

Figure 4.28: PCA plot showing the MFA output from the Napping® with 16 samples.

Table 4.14: Attributes and number of times the attributes have been used by the panel to describe the samples in the Napping®.

Samples	Attributes
P1	sweet(6), vanilla(2), bubble gum, banana(4), fruity, custard, peardrop(3), icing sugar, antiseptic, musty/fusty.
P2	marzipan, fruity, sweet(3),peardrop(4),icing sugar, fruity(2), banana(3),bubble gum, buttery, gluey, antiseptic
P3	banana(6),fruity(4),peardrop(6),chemical(2),bitter
P4	peardrop(4),fruity(2),banana(2),plastic(4),bitter(5), Chemical(3),artificial(2),
P5	sweet(7)banana(5), custard, vanilla, fruity, peardrop((4), bitter(2),icing sugar, glue, musty, floral(2)bubble gum
P6	sweet(5),banana(6),musty, plastic, icing sugar, vanilla,fruity, custard, peardrop(4),bubble gum,
P7	peardrop(6),fruity(3),sweet(3),bland(2),icing suger, vanilla(2), custard, banana(3),artificial, plastic
P8	sweet(2),bland, bubble gum(3),bitter aftertaste(2),peardrop(3),fruity,banana(4),musty/fusty(2)antiseptic
P9	banana(4),fruity(2),peardrop(7),sweet(4),custard, bubble gum(3),plastic, musty/fusty,antiseptic
P10	fruity(3),banana(5),sweet(5),chemical, icing sugar, custard, vanilla, peardrop(5),musty/fusty,
DX Low	fruity(2),banana(3),sweet(2),peardrop(4),musty/fusty(2), plastic(2),bubble gum, custard(2),powdery, antiseptic
DX High	banana(4),fruity(2),sweet(4),musty/fusty(2),powdery(2), custard(2),vanilla(2),glue(3), peardrop(4), plastic, chemical
Guar Low	Musty/Fusty, bitter(4),menthol, chemical(2),pasty, antibiotics, gelatine, banana, sweet, floral, lime, bland, custard, vanilla, milky, peardrop, plastic.
Guar High	peardrop(3),fruity(2),chemical, bitter(2),antibiotics, plastic(2), banana(3),custard(2),glue(2),musty/fusty(2),powdery
MC Low	Musty/fusty(6), chemical after(3), plastic(2), peardrop(2), banana, fruity, icing sugar, custard, vanilla, sour,
MC High	fruity(2),musty/fusty(8),powdery, bitter(2),glue, peardrop, plastic(2),banana

4.2.3.3 Agglomerative hierarchical Clustering (AHC)

The clustering method AHC was also applied to the Napping results for both the entire samples sets and designed sample only, and the results are shown in the form of so-called dendograms in Figure 4.29.

Three clusters were found within the whole sample set: MC low and MC high were in one cluster which were mainly due to their high Musty/fusty flavour. Interestingly, two guar gum solutions and sample P4 were clustered as one group. When checking the ingredients of sample P4, it was found that the sample contained only xanthan gum but no dextran. Also it was found that the descriptor 'sweet' has been least used in these three samples. Results from the Descriptive Analysis also proved that these samples were scored least for the attribute 'overall sweetness'. Also it was found that the descriptor 'bitter' were mostly used for these samples. The rest of designed samples as well as two DX samples were clustered as one group. This was mainly due to that for most of these samples, the 'positive' flavour attributes such as 'fruity, sweet, banana, peardrop' were highly used and meanwhile the negative flavour attributes such as 'musty/fusty, chemical and plastic' were less frequently used. The clustering of the whole sample set indicated that the panels tend to put similar samples close to each other according to three main categories of attributes: musty/fusty, 'positive' flavour attributes and 'negative' flavour attributes.

In order to further explore the differences between the samples, AHC was performed on the designed samples only and the results are shown in Figure 4.29(b).

The results from AHC showed that four clusters have been identified. Sample P4 and P5 were identified as two individual clusters. It was found that these two samples were almost at two extremes of the attribute 'sweet': descriptor 'sweet' has been used least and most for P4 and P5, respectively. This result is also in accordance with the results from Descriptive Analysis: P4 and P5 had the least and most scores for the 'overall sweetness, respectively. However, for other two clusters, it was very difficult to draw the conclusion why these samples were in the same clusters as there are no such trend that which descriptors has been used more for samples within the same clusters. One possible reason could be that these samples are clustered by means of the rate at which the maximum intensity of sweet and flavour are perceived by the panels. Also the aftertaste could be another important factor to consider as some panellists did use 'strong aftertaste' when they describe the samples.

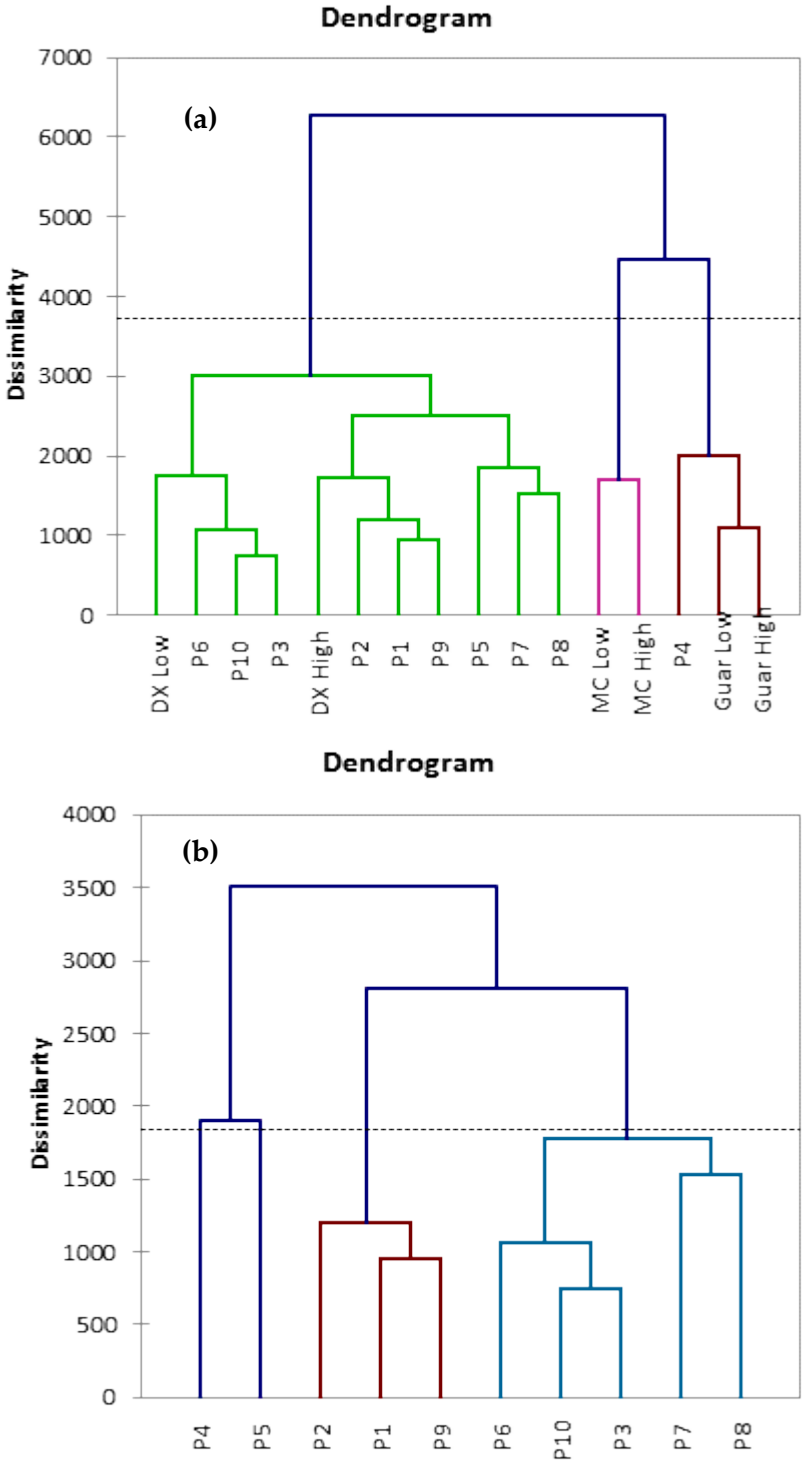

Figure 4.29: Dendrogram from the hierarchical agglomerative clustering for the napping results: (a) the whole sample sets and (b) designed samples only.

4.3 Relationship between sensory and rheological properties

In this chapter, the relationship between rheological properties of designed samples and their sensory properties will be explored. In addition models that including relevant rheological properties with the aim to predict sensory perceptions will be built and further examined with samples that made of other polysaccharides.

4.3.1 Mouthfeel and rheological properties

4.3.1.1 Mouthfeel and viscosities from large deformation

The results from the sensory studies showed that for samples with either similar low shear or high shear viscosity, the perceived mouthfeel perceptions were different. The results proved the hypothesis that viscosities at low shear rate alone could not reflect what is happening during oral processing and viscosity at high shear rate is also important.

For the attributes of thickness, 'Initial Thickness' and 'Thickness in Mouth' were found to be highly correlated with each other (r=0.99). As discussed previously, although samples were identical in either low or high shear viscosities, the perceived thickness were different by the panels. When performing a correlation between the viscosity values with the sensory scores, it was found that perceived initial thickness was highly correlated with viscosity at low shear rate (r=0.961) but less well correlated with high shear viscosity (r=0.556). Similarly, 'Thickness in Mouth' had a correlation coefficient of r=0.952 and r=0.577 with low and high shear viscosity,

respectively. These results are in agreement with Wood who reported that viscosity at 50 s^{-1} related to thickness perception (Wood, 1968). However clear results from this research suggest that the viscosity at high shear rate did have a certain effect on perception of thickness. Models including or excluding high shear viscosities were compared as predictions for the sensory scores.

Table 4.15: The correlation coefficient(r) between shear and extensional rheological properties and sensory scores.

	Initial thickness	Thickness in mouth	Stickiness on lips	Stickiness in mouth	Mouthcoating
η at 50 s^{-1}	0.961	0.952	0.89	0.884	0.911
η at 10^5 s^{-1}	0.556	0.577	0.67	0.688	0.663
η_e	0.862	0.872	0.902	0.909	0.911

Table 4.16: Comparisons of prediction models for thickness perception with/out viscosity at high shear rate.

		R^2	Adj. R^2	Pred. R^2	Adeq. precision
Models without η_H	Initial Thick=0.44+17.95*η_L	0.92	0.913	0.889	19.686
	Thick in mouth=0.23+17.55*η_L	0.91	0.894	0.867	17.581
Models with η_H	Initial thick= -0.98+ 16.3*η_L +170*η_H-1839.4* η^2_H	0.996	0.993	0.936	50.32
	Thick in mouth=-1.3 +15.8*η_L +185*η_H-1993* η^2_H	0.995	0.992	0.971	47.7

As can be seen from Table 4.16, the models built for predicting thickness perceptions without η_H featured linear relationships with η_L with R^2 of 0.92 and 0.91 for Initial thickness and Thickness in mouth, respectively. The predicted R^2 ,which indicated

how precise the model is at predicting the results from the samples tested, for Initial thickness and Thickness in mouth were 0.889 and 0.867, respectively. The adjusted R^2, which indicated the how well the model would describe variation outside the sample range, were 0.913 and 0.894 for Initial thickness and Thickness in mouth respectively. The Adequate precision, which is a signal to noise ratio, were 19.686 and 17.581 for Initial thickness and Thickness in mouth, respectively. In order to further illustrate the model, the experimental results are plotted against values that have been predicted from the models and the results are shown in Figure 4.30 (a & c).

As can be seen from the figure, the predicted and experiment values were perfectly matched at samples with sensory scores approximately below 5. This indicated that for samples that were perceived as having less 'thickness', it is probably the low shear viscosity that mainly decided the 'thickness' perceptions. However it seems that as the score for perceived 'thickness' increased above 5, there were some deviations between the predicted and experiment values. This indicates that perhaps for samples that are perceived as more 'thickness', viscosity at low shear rate solely is not sufficient in predicting the sensory scores.

As a comparison, models that included both low and high shear viscosities were also examined. As can be seen from Table 4.16, models including both low and high shear viscosities featured linear relationships with both low and high shear viscosity and also a quadratic relationship with high shear viscosity. All the model description parameters were largely increased which indicated that the models were more

robust compared with models that only including low shear viscosities. A further illustration of the models can be found in Figure 4.30(b & d).

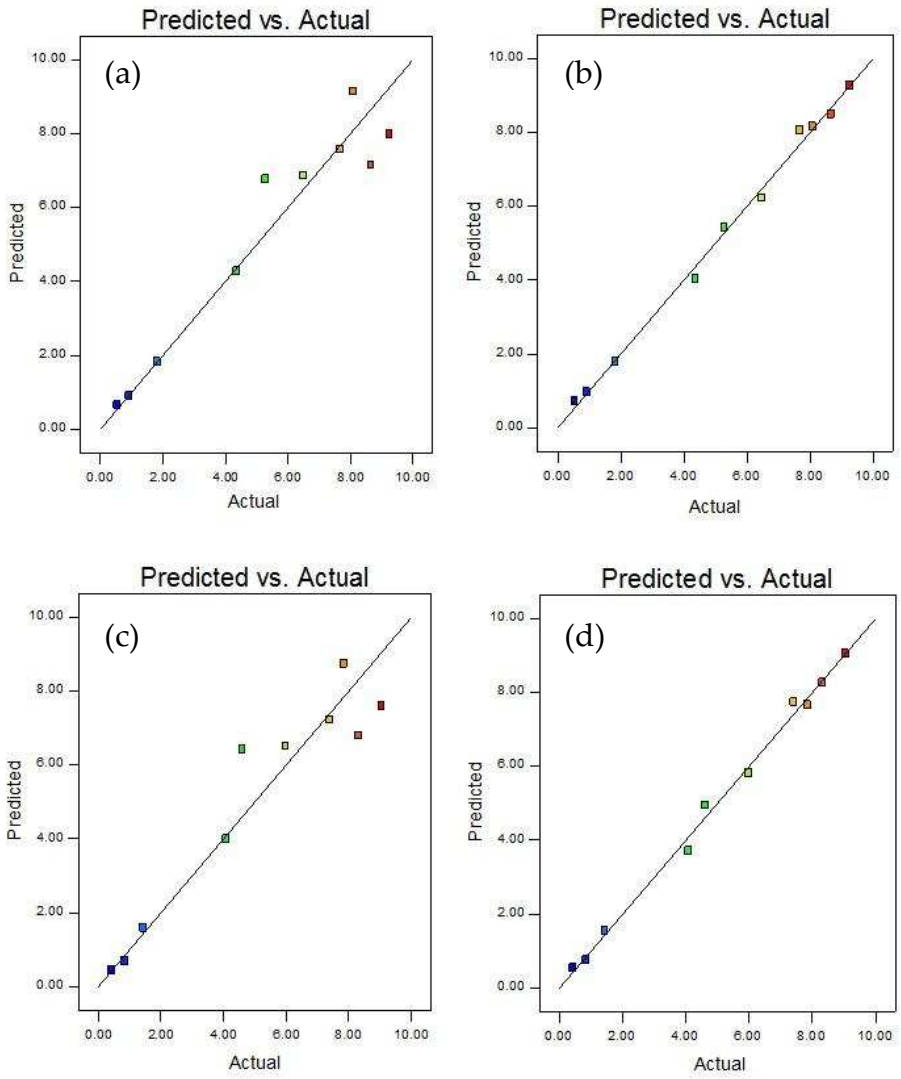

Figure 4.30: Comparisons of predicted values from models that with/without η_H and experiment values: (a) Initial thickness without η_H, (b) Initial thickness with η_H;(c) Thickness without η_H; (d) Thickness with η_H

As shown in Figure 4.30 , the comparison of predicted values from models with both low and high shear viscosities and experimental values revealed that by including the high shear viscosity in the models, the perceived 'thickness' can be better

predicted, especially for samples that are perceived as more 'thickness'. A further illustration of the models can be found in Figure 4.31. Each contour represents a 'thickness' score. The contour plot clearly illustrated that both low and high shear viscosities played role in deciding the final scores for thickness: as the for a given thickness score, the increased low shear viscosity will be increased to compensate for decreased high shear viscosity, and vice versa.

The results from this research clearly indicated that, for samples that are perceived as different 'thickness', the shear rates that are responsible for the perception were mainly within the low to moderate range. To illustrate this, the correlation coefficients between viscosity values and sensory scores for 'thickness' were plotted against all shear rates, as showed in Figure 4.32.

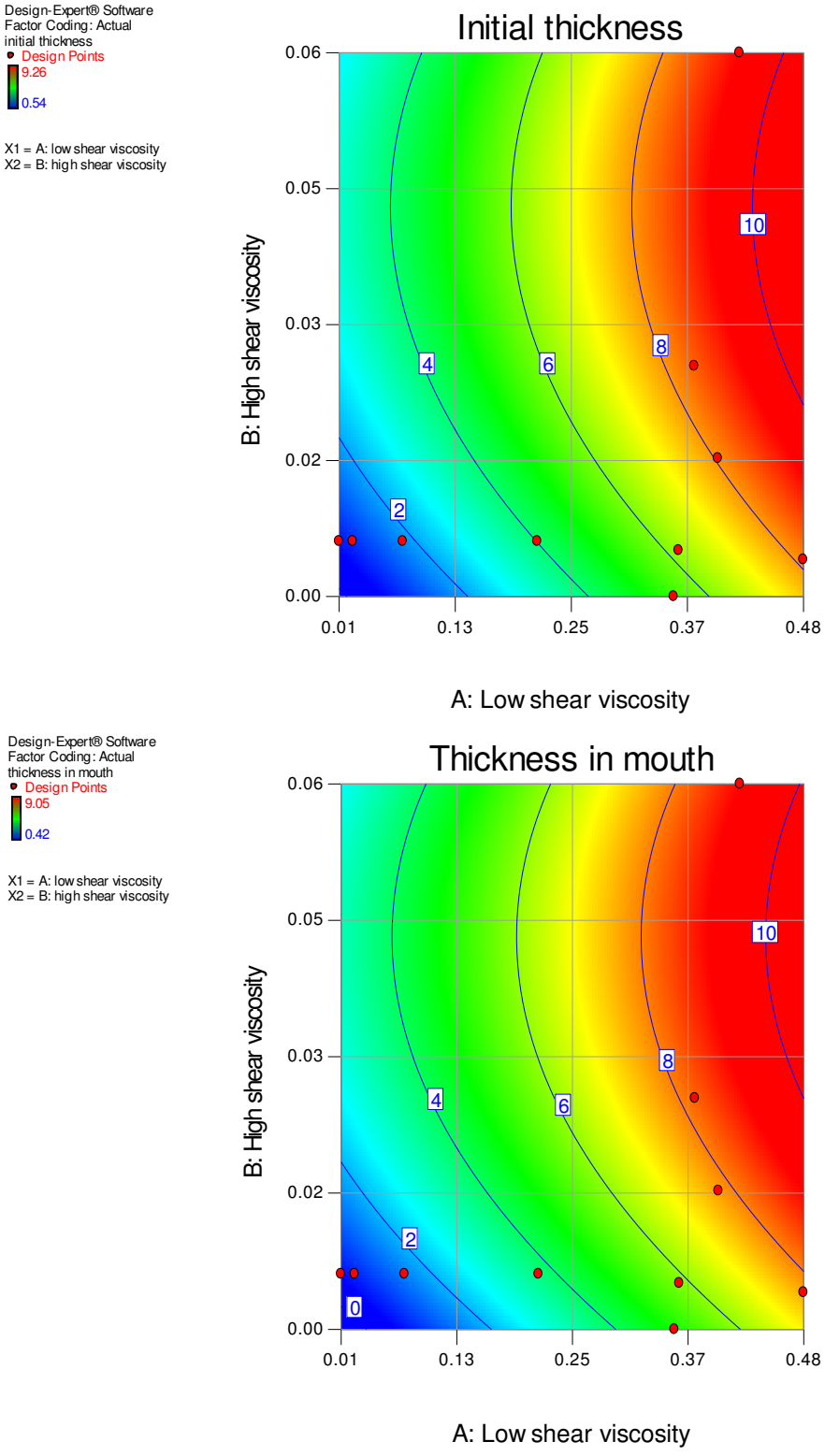

Figure 4.31: Contour plots derived from models for perceived 'Thickness'(see Table 4.16). Each contour represents a perceived thickness whilst its shape illustrates how thickness is affected by low and high shear viscosity.

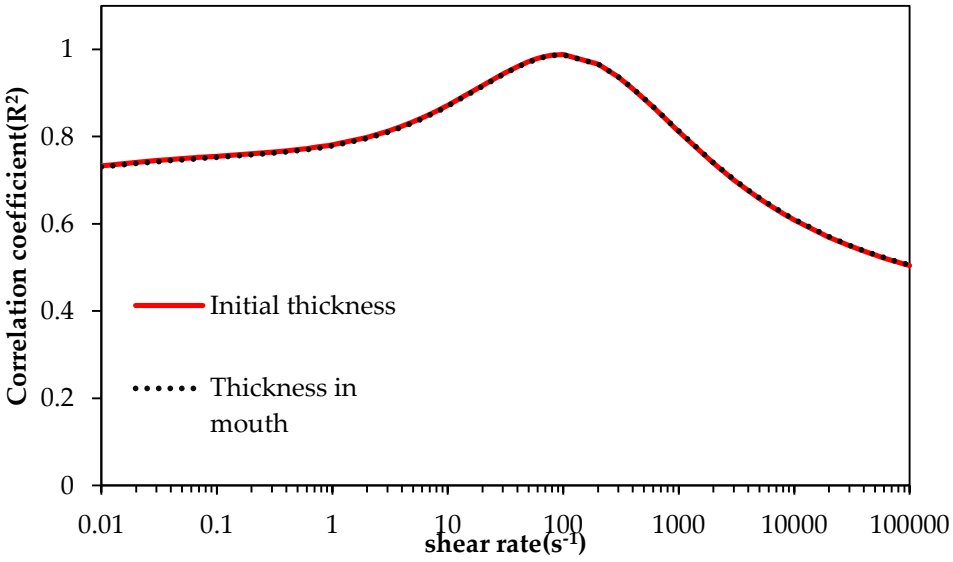

Figure 4.32: Correlation coefficients between viscosity values and sensory scores of 'Thickness' plotted against all shear rates.

As shown in Figure 4.32, the viscosity values that correlated better with sensory scores for thickness (r>0.9) happened within a shear rate ranged of 20 to 400 s^{-1}, with the highest correlation coefficient occurring at a shear rate of 100 s^{-1} (r=0.988). This shear rate is higher than the normally accepted shear rate of 10 to 50 s^{-1} which is related to thickness perception (Wood, 1968, Shama et al., 1973, Shama and Sherman, 1973). Similar results have been found by Koliandris et al. (2010) who suggested that thickness perception was best correlated with viscosities at shear rates ranging from 80-700 s^{-1}.

It is worth mentioning that for samples with the same viscosity values at shear rates below 50 s^{-1}, it seems that the highly shear thinning samples were perceived as less 'thick', or in other words, the samples with higher viscosities at high shear rate were

perceived as 'thicker'. Similar results have been reported by Christensen (1979) who found that at equivalent shear rate of 10 s^{-1}, solutions of more shear thinning carboxymethylcellulose (CMC) were perceived significantly thinner compared with less shear thinning solutions, and she suggested the perceived viscosity could be determined by averaging a range of shear rates. However due to the constraints of rheometer used, only a relatively low shear rate of up to 100 s^{-1} was used in their research.

The importance of viscosities at low shear rates from 10-50 s^{-1} should not be completely disregarded in the understanding of perception of thickness. As in Group 2, samples were mostly distinguished by their viscosities at low shear rate. This indicates that low shear viscosities are important especially when samples are largely different in terms of low shear viscosity. It has been argued that viscosities at low shear rate of approximately 50 s^{-1} are useful to predict the thickness perceptions for liquid foods that are not highly shear thinning with viscosities less than 0.1Pa.s (Stokes, 2012a). However, as with increased low shear viscosities and shear thinning, it becomes less correlated between low shear viscosities and thickness perception (Morris et al, 1982, 1984).

Stickiness and Mouthcoating

The attributes 'Stickiness on lips' and 'Stickiness in mouth' were highly correlated with each other (r=0.997). As shown previously from the sensory results (see section

4.2.1.2.1) that the samples of Group 1 as well as samples of Group 2 were perceived as different. Correlation of the sensory scores with the viscosities at low shear and high shear rate over all 10 samples revealed that the sensory scores were better correlated with low shear viscosity (r=0.89 and r=0.884 for Stickiness on the lips and Stickiness in mouth, respectively) but less well correlated with high shear viscosity(r=0.67 and r=0.688 for Stickiness on the lips and Stickiness in the mouth, respectively). It is worth pointing out that for the perception of two 'Stickiness' attributes, the correlation coefficient between high shear viscosity and sensory score is higher than for the perception of 'Thickness'. This implies the possibility that high shear rates may be more relevant in the process of evaluating the 'Stickiness' than 'Thickness' of viscous solutions. These higher shear rates would be a result of the attribute evaluation protocol which is to some extent surprising as it has been postulated that shear rates in the narrow gap between tongue and palate can reach very high values. Considering the assessment protocol for 'Stickiness', it seems obvious to inspect the relationship between the sensory scores and extensional viscosity as determined by filament breakup. Indeed the extensional viscosity was found to be even better correlated with 'Stickiness'(r=0.902 and r=0.909 for Stickiness on the lips and Stickiness in mouth, respectively) than low shear viscosity. When trying to build models to predict the sensory perceptions, it was found that for 'Stickiness' and 'Mouthcoating', models that included only low shear viscosity and

extensional viscosity predicted the sensory perceptions better than models that including all the three factors or only including low and high shear viscosities.

Table 4.17: Prediction models for Stickiness and Mouthcoating and model descriptors.

	R^2	Adj. R^2	Pred. R^2	Adeq. precision
Stickiness on lips=1.42+9.26*η_L+0.04*η_E	0.965	0.955	0.928	25.460
Stickiness in mouth=0.54+10.1*η_L+0.05*η_E	0.963	0.952	0.923	24.640
Mouthcoating=0.34+10.82*η_L+0.05*η_E	0.981	0.975	0.955	34.293

As shown in Table 4.17, the models for Stickiness and Mouthcoating are linear in terms of both low shear and extensional viscosities. For a given 'Stickiness' or 'Mouthcoating' score, the increased low shear viscosities have to be compensated decreased extensional viscosities, and vice versa. It also can be seen from the plot that the low shear viscosity was not as important as in thickness perceptions as the highest low shear viscosities did not necessarily resulted in highest 'Stickiness' or 'Mouthcoating'.

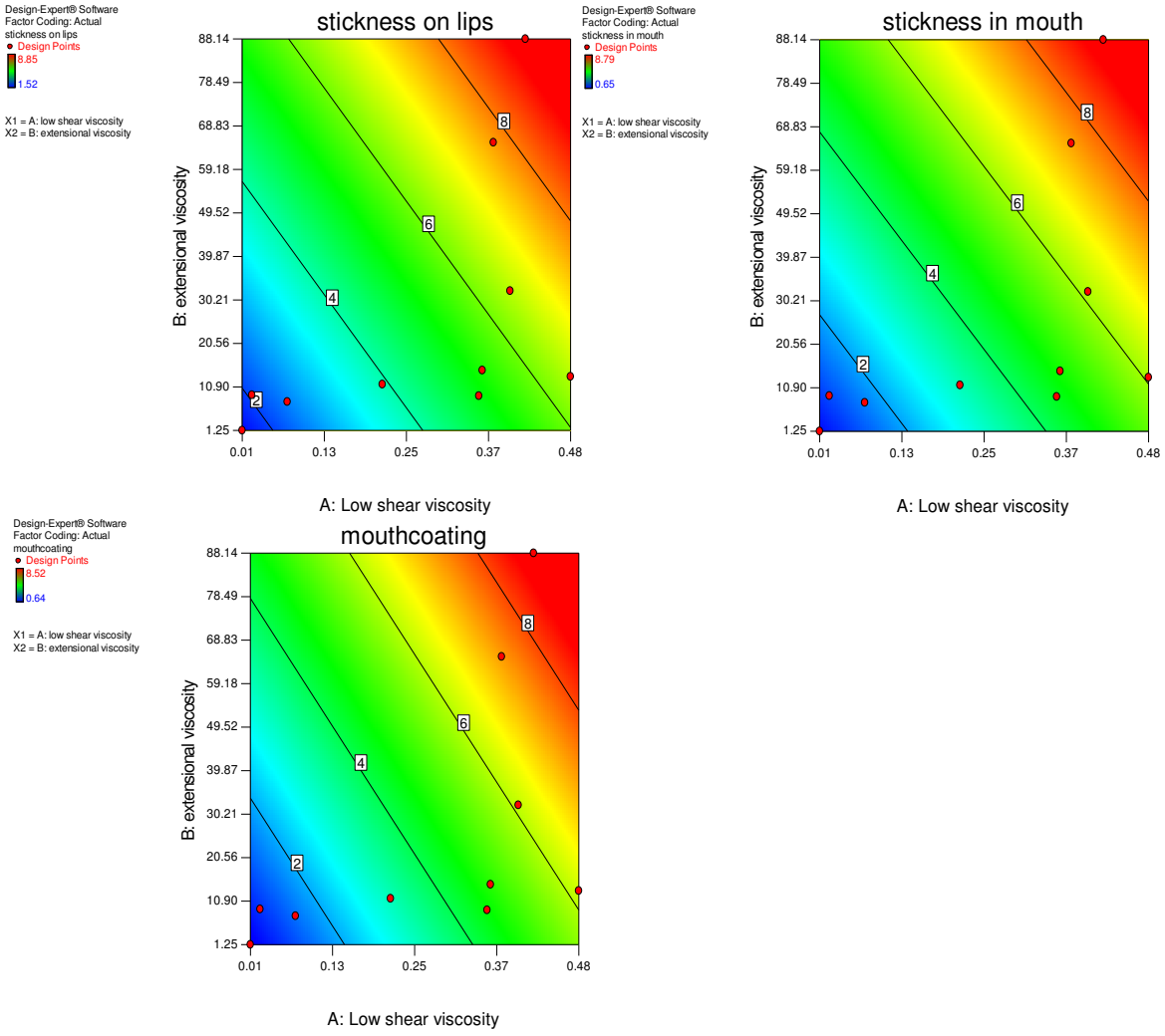

Figure 4.33: Contour plots derived from models for perceived 'Stickiness' and 'Mouthcoating' (See Table 4.17). Each contour represents a perceived sensory score whilst its shape illustrates how this attribute is affected by low and extensional viscosity.

Stickiness perceptions were found highly correlated with thickness perceptions, and similar results have been reported previously that these two attributes were found numerically not to be different from each other (Morris et al., 1984). However, it

should not be concluded that these two attributes were actually measuring the same perceptions. An example is sample P8. As can be seen from Table 4.8 and 4.9 that, sample P8 was scored 8.09 and 7.85 for Initial Thickness and Thickness in mouth, respectively. However, the same sample was scored 6.88, 6.65 and 6.52 for Stickiness on lips, Stickiness in mouth and Mouth coating, respectively.

There are few reported studies that have employed CaBER or extensional viscosity measurements to study the stickiness perception of foods. Similar results can be found in Chen et al. (2008) who studied the relationship between tensile force of foods and their sensory scores for stickiness which were evaluated by 'finger separation' experiment. The authors suggested that the maximum tensile force and the work till the maximum force were two useful parameters for predicting food stickiness. These findings are in accordance with present research as both of the results are actually trying to mimic what are sensed during the 'finger separation' experiment that happened in oral processing. However it is sensible to argue that the 'stickiness' that has been assessed from finger separation does not necessarily represents the actually perception of 'stickiness' during oral processing due to the different sensitivity between skin on the fingers and lips or oral mucosa . The results from this research indicated that for liquid and semi-solid foods, the perception of 'Stickiness' should not be treated as a single attribute, but rather a complex attribute that perhaps a combination of both perceptions of 'thickness' and 'elasticity'.

In terms of 'mouthcoating', it followed the same trend as 'stickiness': the model for predicting 'mouthcoating' also involved both low shear viscosities and extensional viscosities. Also it was found that for samples with similar low shear viscosities, such as samples in Group 1, higher 'mouthcoating' scores were given to the samples that are less shear thinning. This result further proved that a large range of shear rates occur during oral processing of foods. The inclusion of extensional viscosities in the model for prediction of 'mouthcoating' implies that oral processing of food is not simply and purely shear flow but also involves extensional flow.

4.3.1.2 Mouthfeel and dynamic viscosity

All designed samples were also characterised in small amplitude oscillatory shear and the results have been shown earlier in this thesis in Figure 4.15 and Figure 4.16. Correlation of complex viscosity values taken at different angular frequencies with mouthfeel attributes were evaluated in this research and are shown in Table 4.18.

Table 4.18: The correlation between complex viscosities at different angular frequency and sensory scores of mouthfeel attributes.

	Correlation Coefficient (r)				
	Initial thickness	Thickness in mouth	Stickiness on lips	Stickiness in mouth	Mouth-coating
η* at 0.1 rad/s	0.74	0.73	0.63	0.62	0.66
η* at 1 rad/s	0.78	0.76	0.66	0.65	0.69
η* at 10 rad/s	0.81	0.79	0.69	0.68	0.72
η* at 50 rad/s	0.86	0.85	0.76	0.75	0.78
η* at 100 rad/s	0.89	0.89	0.81	0.80	0.83

As can be seen from Table 4.18 , as with increased frequency, the correlation between complex viscosities and mouthfeel perception were increased and reached the highest value for all attributes at frequency of 100 rad/s. For 'Thickness' perceptions, the correlation between sensory scores and complex viscosities at 100 rad/s were highest (r=0.89) among all the attributes, followed by mouthcoating (r=0.83) and 'stickiness'(r=0.81 and r=0.8 for stickiness on lips and stickiness in mouth, respectively). The results were in accordance with Richardson et al (1989) who found that mouthfeel perceptions were best correlated with complex viscosity at 50 rad/s. They also suggested that for 'weak gels' such as xanthan solutions, the oral evaluation was based predominantly on the viscoelastic properties of the intact network structure rather than on those of the isolated species released after rupture of the network by shear.

Interestingly it was found that for samples in Group 2, the complex viscosities were highly correlated with mouthfeel perceptions at all frequencies (r>0.95) and with the highest correlation coefficient r=0.98 for all attributes occurring at frequency of 50 rad/s. However, the correlation between complex viscosities and mouthfeel attributes for samples in Group 1 were relatively poor and it seems that samples with higher complex viscosities were perceived as lower in terms of mouthfeel perceptions. These results may indicate that complex viscosity is a useful predictor for mouthfeel perceptions for samples that behave significantly different under small deformations. These samples covered the range from true solutions to samples that

showing 'weak gel' properties. However, the results from this research clearly indicated that for samples that behave similarly under small deformation, especially for samples showing 'weak gel' properties, complex viscosity cannot be used to predict the mouthfeel perceptions, and the properties under large deformation maybe more relevant to their mouthfeel perceptions.

4.3.2 Flavour and rheological properties

Overall sweetness

It has been discussed previously from sensory results that, despite all the samples containing the same level of sucrose at 3%, the overall scores for 'sweetness' still ranged from 2.68 to 8.18.

For samples in Group 1, it was found that higher scores of 'Overall sweetness' were given to samples that were higher in terms of mouthfeel perceptions. In other words, samples that were higher in terms of low and high shear viscosities were also perceived as sweeter. It is generally believed that the perceived taste is decreased with increased viscosities (Christensen, 1980, Baines and Morris, 1987, Mälkki et al., 1993, Cook et al., 2003) and also different hydrocolloids were found to affect sweetness to different extents (Vaisey et al., 1969, Pangborn and Szczesniak, 1974). The results from this research seem to somewhat disagree with the results from these previous studies. However, it is worth noting that for samples in Group 1, samples that were higher in sweetness perception contained lower concentrations of xanthan

gum but meanwhile contained higher concentration of dextran. This rule also seemed true across the whole samples set. For samples with the same levels of xanthan gum, such as P5 (0.4%) and P9 (0.47), the one with higher dextran was given higher scores of 'sweetness'. The results indicated that within the design space, the concentration of dextran and xanthan have opposite effects on the perception of sweetness. A model that includes both xanthan concentration and dextran can be used to better illustrate this relationship. The model is highly significant with correlation coefficient R^2=0.97.

$$Overall\ sweetness = 5.68 - 2.16 \times [Xan] + 0.11 \times [Dex] \quad (4.8)$$

As can be seen from Equation 4.8, the model for predicting 'overall sweetness' include a negative and positive relationship with xanthan and dextran, respectively. To further illustrate the relationship between concentrations of polymer and the perceived sweetness, a contour plot is shown in Figure 4.34. The contour plot clearly demonstrates that for a given sweetness score, the concentration of dextran and xanthan should be increased or decreased at the same time. Also it indicates that at a constant concentration of xanthan, the perceived sweetness will be enhanced with increased concentration of dextran.

The results from Group 1 samples also indicate that the perceived sweetness may be affected to a lesser extent in samples that are less shear thinning. The relationship between rheological behaviour of hydrocolloids and their sweetness perceptions

were also reported by Vaisey et al. (1969), and they found that hydrocolloids solutions that were more shear thinning tend to mask the sweetness perception to a smaller extent. However, this research only compared the time needed for different hydrocolloid solutions to be perceived as sweetness, but not the overall intensity of sweetness.

As discussed previously, the addition of dextran will increase the high shear viscosity, elasticity and extensional viscosity of samples. Therefore, at either similar xanthan concentration or similar low shear viscosity, increased elasticity or extensional viscosity will result in increased sweetness perception. The elasticity and saltiness perception has been studied using Boger fluids by Koliandris et al. (2011) but they found no significant difference in terms of saltiness and mouthfeel perception between Boger fluids and inelastic viscous reference samples. However, as Boger fluids are almost shear independent materials (James, 2009), it is very difficult to say how the elasticity affects the taste and mouthfeel perceptions for shear thinning materials.

The overall flavour perception was found to be highly correlated with sweetness perception (r=0.98). This indicated the possibility that these two perceptions were actually interacted with each other. Results from APCI-MS as seen in Figure 4.26 indicated that during consumption of the samples, both the maximum intensity of flavour released and the total amount of flavour released were not significantly different between samples(p>0.05). This revealed that it was the perception of

sweetness that affected the perception of flavour. Indeed, the interactions between volatile and non-volatile stimuli are well documented (Davidson et al., 1999, Hollowood et al., 2000, Hollowood et al., 2002, Taylor et al., 2002, Hort and Hollowood, 2004, Pfeiffer et al., 2006, Hewson et al., 2008). Davidson et al. (1999) found that the reduction of perceived mint flavour was correlated with decreased sugar release in chewing gum despite the fact that release of mint volatile remained constant. Hollowood et al. (2002) suggested that the perception of flavour was reduced not because of the reduced flavour release but due to the reduced sweetness perception , and they thought it was due to the increased concentration of hydrocolloid that reduced the amount of free water to carry tastants to the receptors.

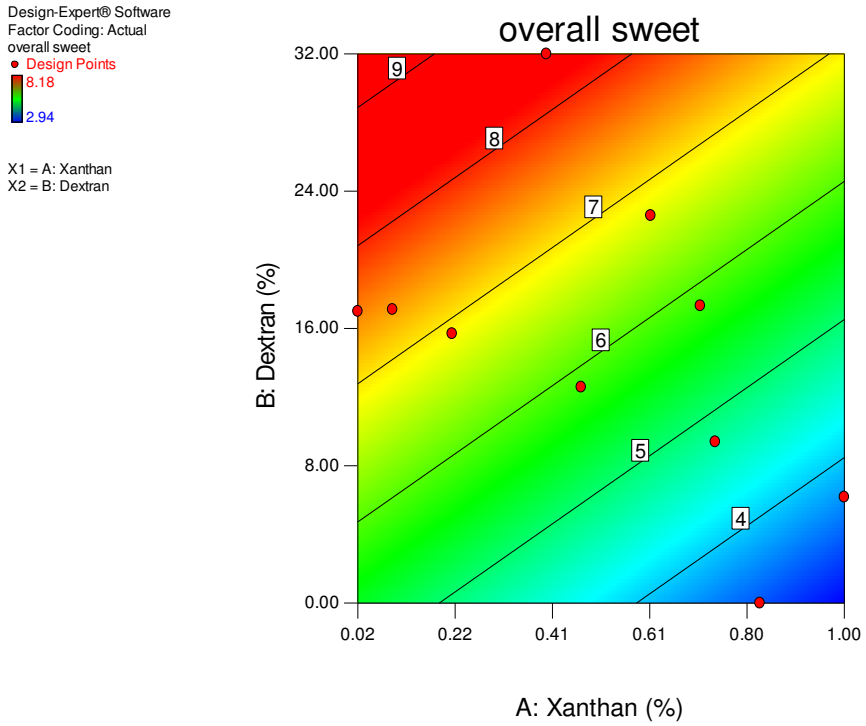

Figure 4.34: Contour plots derived from models for perceived 'Sweetness' (See Equation 4.8). Each contour represents a perceived sensory score whilst its shape illustrates how this attribute is affected by concentration of xanthan and dextran.

4.3.3 Validation of the predictive model with additional samples prepared from other polysaccharides

In order to validate the predictive models presented in section 4.3.1, six aqueous solutions samples were prepared from guar gum, dextran 500 and methylcellulose (MC). The concentrations were selected so that their viscosity at 50 s^{-1} can be matched at different level and this was achieved through studying their viscosity behaviour at different concentrations. While the attempt to match the shear viscosity of these samples at 50 s^{-1} was successful, it was not possible to identify

concentrations to viscosity match at 10 s^{-1}. This was due to the fact that none of these three polysaccharides is as shear thinning as xanthan gum at high shear rates, a characteristic that is imparted by the rod-like molecular confirmation of xanthan gum. The steady shear viscosity, oscillatory shear moduli and extensional viscosity of these additional six samples are presented first followed by their sensory properties. The results were then used to test the predictive models

4.3.3.1 Steady shear viscosity

The viscosity curves of the six additional test samples are shown in Figure 4.35 and the viscosity values at both low and high shear rates including the values of the parameters for data fit with the log-log model shown in Table 4.19. The guar gum and methyl cellulose solutions show shear thinning behaviour. The dextran solutions were Newtonian at shear rates up to roughly 10^5 s^{-1}, above which an onset of shear thinning behaviour was observed. Samples of the same polysaccharide at the higher solution concentration showed higher viscosity values over the whole shear rate range investigated. The guar gum and MC solutions show low shear viscosity plateaus which are characteristics of the random coil solution structure of these two polysaccharides. The viscosities of the 0.8 % (w/w) guar gum solution and the 0.9 % (w/w) MC solution were matched at approximately 50 s^{-1} at value of 0.6 Pa.s. At same level of concentration, designed sample P4 (0.83% xanthan only) was more shear thinning compared with guar and MC solutions which indicated the

solutions containing 0.5 %(w/w) guar gum, 0.5 (w/w)% MC or 17 %(w/w) dextran were matched roughly at the lower viscosity of 0.1 Pa.s measured at 50 s^{-1}.

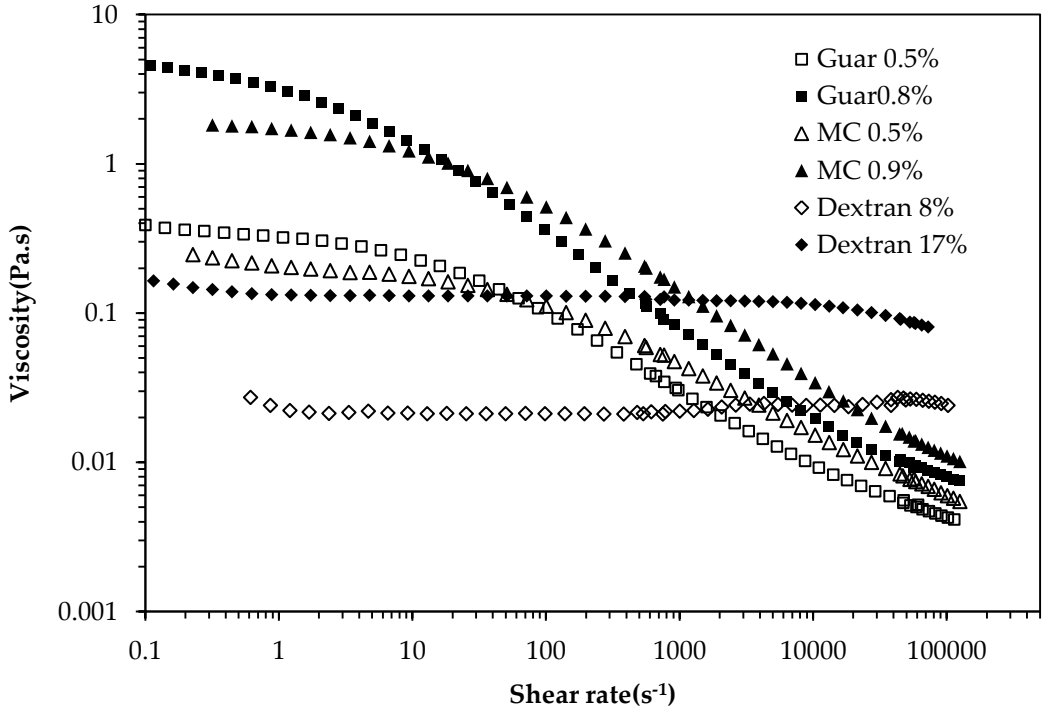

Figure 4.35: Viscosity curves for six model testing samples. Measured using PP-50 at gap height of 500μm, 50μm and 30 μm (corrected for gap error and non-Newtonian behaviour (only for guar and MC samples)). The standard deviations are less than 0.1% in all cases. All measurements were conducted at 20 °C.

Table 4.19: Viscosities values of different polymer solutions at low and high shear rates.

Polymer concentrations %(w/w)	η_L Pa*s	η_H Pa*s	α	β	γ	δ
Guar low(0.5%)	0.136	0.004	2.233	-2.985	-1.007	-2.611
Guar high(0.8%)	0.572	0.008	-3.327	2.146	0.830	0.836
DX low(8%)	0.011	0.011	-	-	-	-
DX high(17%)	0.116	0.116	-	-	-	-
MC low(0.5%)	0.130	0.006	-2.000	3.510	0.979	-0.612
MC high(0.9%)	0.698	0.011	-2.820	3.024	0.912	0.369

4.3.3.2 Dynamic properties

The dynamic moduli of the additional guar gum and MC polysaccharide samples were also evaluated in dynamic oscillatory shear. The dextran solutions were not considered for this rheological test due to their Newtonian nature. The results of the amplitude sweep conducted at 10 rad.s^{-1} are shown in Figure 4.36 and Figure 4.37. The storage modulus G′ of both guar gum solutions was slightly higher than the loss modulus G″ within the LVE which indicate the viscoelastic nature of guar gum solutions. However for both solutions of MC, it was found that G′ dominated over G″ within the LVE which indicated liquid characteristics. Figure 4.37 shows the angular frequency dependency of G′ and G″ of these samples. In the case of guar gum solutions, they showed a low to moderate frequency dependency: the G″ predominated over G′ and both of them increased with frequency. At higher frequency the G″ was crossed over by G′ which indicated that the viscoelastic characteristic approach those of a permanently cross-linked network. However, for MC solution, G′ was higher than G″ at low frequency which indicated that at low frequency the MC showed elastic properties but with increased frequency, G′ was crossed over by G″ which indicated the viscous behaviour at higher frequency.

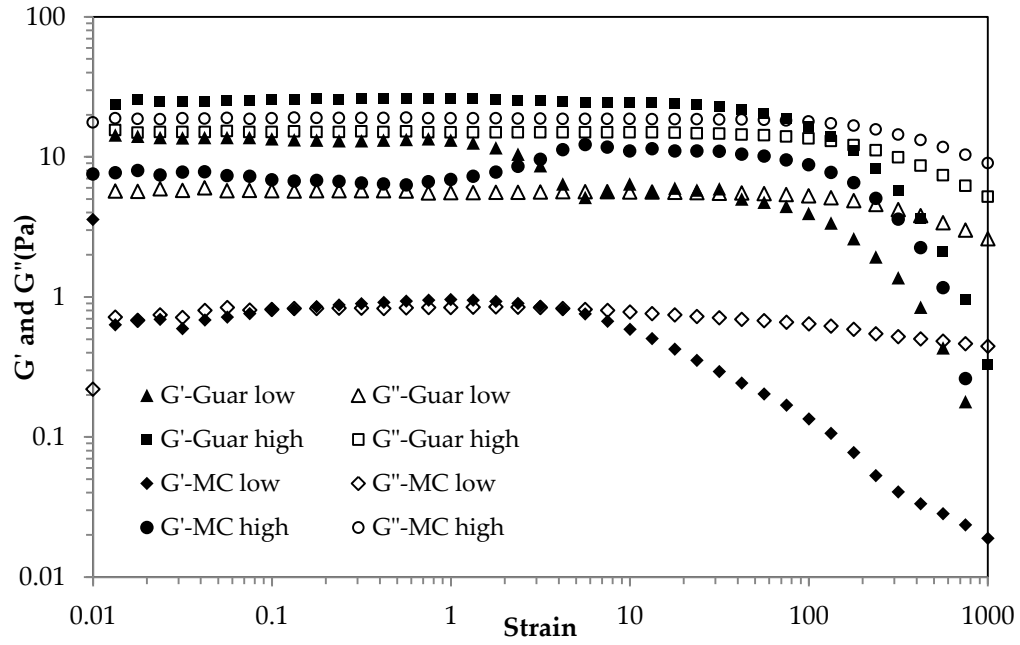

Figure 4.36: Storage modulus (G′) (filled symbols) and loss modulus (G″) (open symbols) as a function of strain at constant angular frequency of 10 rad.s^{-1}. All measurements were conducted at 20 °C

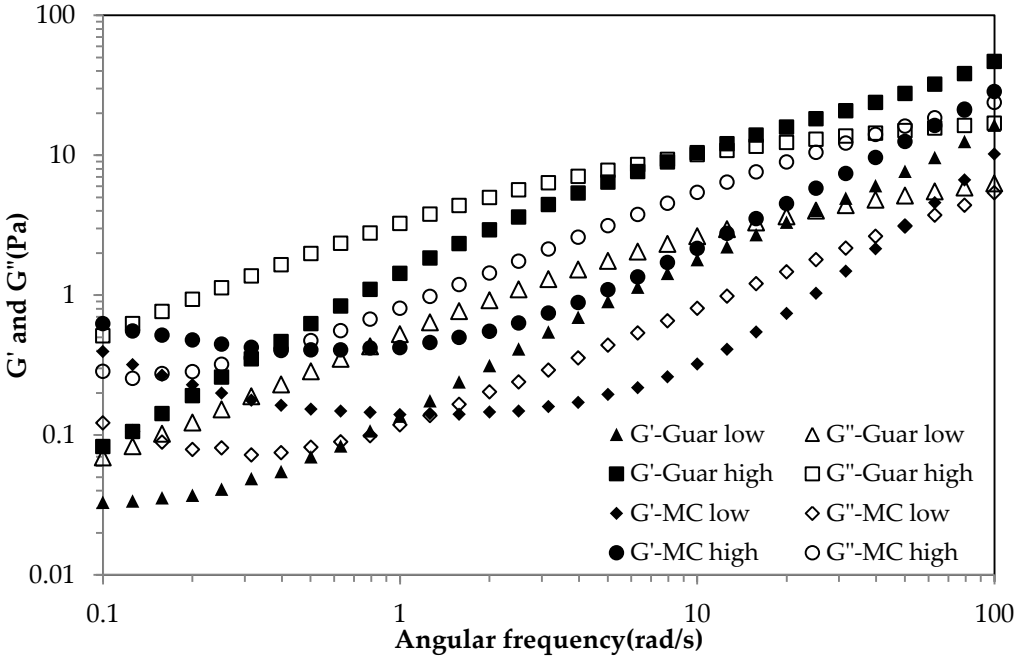

Figure 4.37: Storage modulus (G′) (filled symbols) and loss modulus (G″) (open symbols) as a function of frequency at a constant strain of 1%. All measurements were conducted at 20 °C.

4.3.3.3 Extensional flow properties

The extensional flow behaviour of these additional six samples was analysed using the same filament thinning experiment as for the main study samples. The results for the decay of the normalised diameter versus time for the additional six samples are shown in Figure 4.38. As the time scale of breakup for the higher concentrated methylcellulose solution was longer than the rest of samples, therefore the results for both MC solutions are shown in a separate plot in Figure 4.38. The values of breakup time, relaxation time (see Equation 2.29) and the extensional viscosity (Equation 2.30) of these samples are displayed in Table 4.20.

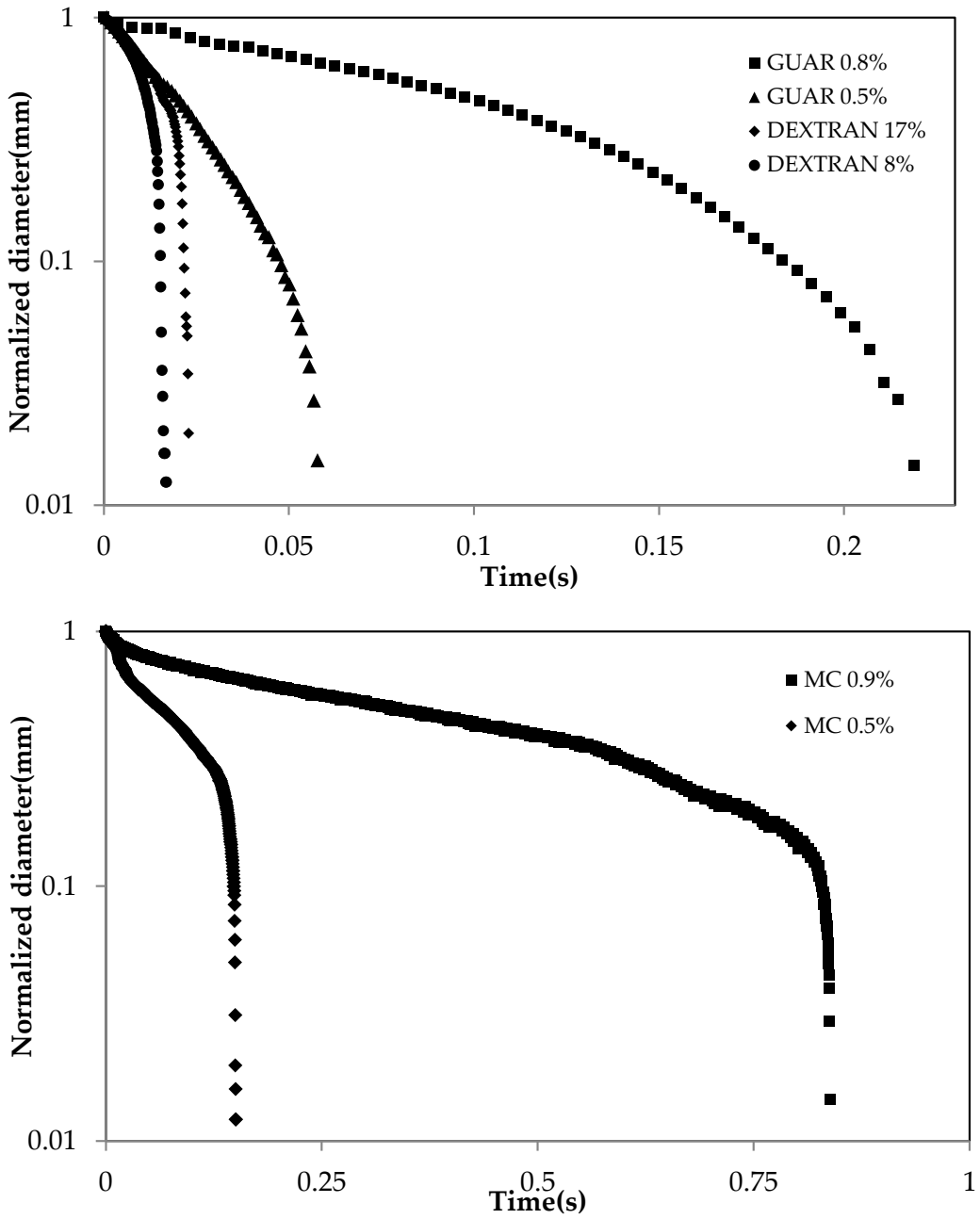

Figure 4.38: Evolution of the normalised filament mid-point diameter for model testing samples. The standard deviation was within 10% in all cases. (Measured at 20 °C). Note the different time scale in the plots.

Table 4.20: The breakup time, relaxation time and extensional viscosities of model testing samples.

Polymers %	t_B s	λ s	η_E Pa.s
Dextran 8%	0.017	-	0.033
Dextran 17%	0.027	-	0.348
Guar 0.5%	0.058	0.0083	6.57
Guar 0.8%	0.228	0.047	17.75
MC 0.5%	0.15	0.033	18.43
MC 0.9%	0.839	0.21	81.81

As expected, the breakup time, relaxation time and extensional viscosities of samples increased with increasing concentration. It was found that these samples differed appreciably in their extensional flow behaviour. The normalised diameter of both dextran gum solutions was found to decay linearly with time which is due to their Newtonian/inelastic behaviour. This is also why Table 4.20 does not show a relaxation time for these two samples and why breakup times and extensional viscosity are the lowest among these six samples. For the two lower as well as the two higher solution concentrations of guar gum and MC, it was found that the MC solution took longer to breakup than the guar gum solutions. This means that at similar concentration the MC solutions utilised in this research were more elastic than then guar gum solution. Also, when comparing these additional samples, it was found that at similar polymer concentration, the breakup time for P4 (0.83% xanthan) was much lower than high concentration of MC. These results indicated that probably more entanglements occurred between MC polymer molecules in solution

than for guar and xanthan and therefore when extensional flow is encountered, more time is needed for the MC filament to breakup.

4.3.3.4 Sensory results and models testing

4.3.3.4.1 Thickness attributes

Table 4.21 shows the sensory results for the "Initial thickness and Thickness in mouth" for the six additional samples. The sensory scores showed that these six samples were widely spread over the whole scale. ANOVA results revealed that these samples were significantly different from each other for both Initial thickness and Thickness in mouth. Both 'Thickness' perceptions of the higher concentration polysaccharide solutions for all three sample pairs were perceived as significantly higher than the lower concentration counterparts. This result is not unexpected. Comparing the two solutions of approximately similar viscosity at 50 s^{-1} the 0.9 % (w/w) MC solution was perceived as significantly higher in both 'Initial thickness' and 'Thickness in mouth' than the 0.8 % (w/w) guar gum solution. These two samples were also compared with P4 of the main sample set containing 0.83 % (w/w) of xanthan gum. It showed that sample P4 were given the lowest scores for perceived thickness. At equivalent low shear viscosity, 17% dextran was perceived higher in both thickness perceptions than 5% MC and 0.5% guar solutions. These

results further proved that viscosity at higher shear rate affected the mouthfeel perceptions.

Table 4.21: ANOVA *p*-value and mean sample scores for two thickness attributes of six model testing samples. Samples coded with the same letter in any one column are not significantly different (*p*>0.05)

		Initial thickness	Thickness in mouth
p-values	Product	<0.0001 ***	<0.0001 ***
	Panellists	<0.0001 ***	<0.0001 ***
	Products*Panellists	0.0005 ***	0.0306 *
Mean Sample score	Dextran 8%	0.92 *f*	0.85 *f*
	Dextran 17%	5.33 *c*	5.54 *c*
	Guar 0.5%	2.55 *e*	2.29 *e*
	Guar 0.8	7.03 *b*	6.66 *b*
	MC 0.5%	4.14 *d*	3.81 *d*
	MC 0.9%	9.41 *a*	9.32 *a*

The scores for both thickness mouthfeel attributes were then predicted with the predictive models (see Table 4.16) for these two attributes using the models considering low and high shear viscosity only as model input parameters. These simple models were the only ones tested here because including further rheological parameters did not improve model performance. It is worth stressing that the models were developed based on samples containing dextran and/or xanthan gum. The actual sensory scores from panel analysis and the predicted values are displayed in Table 4.22. The large discrepancies between the actual and predicted values are clear at first sight.

Table 4.22: The actual value and predicted value from models including both low and high shear viscosities for model testing samples for Initial thickness and Thickness in mouth.

	Initial thickness		Thickness in mouth	
	Actual	**Predicted**	**Actual**	**Predicted**
Guar high(0.8%)	7.03	9.59	6.66	9.09
Guarr low(0.5%)	2.55	1.89	2.29	1.56
DX high(17%)	5.33	-4.12	5.54	-4.83
DX low(8%)	0.92	0.85	0.85	0.67
MC high(0.9%)	9.41	12.04	9.32	11.52
MC low(0.5%)	4.14	2.09	3.81	1.79

It can be seen that there are some discrepancies between the actual sensory scores and the predicted values from the models. For high concentrations of guar gum and MC, the predicted values were larger than the actual values, but for lower concentration of guar gum and MC, the predicted values were lower than the actual values. The possible reason could be that for high concentration of guar gum and MC, the low shear viscosities were slightly higher than the values that were used for developing the models, therefore the predicted values were slightly out of the designing spaces. The predicted values for 8 %(w/w) dextran were found to be close to the actual values, but it was not the case for 17 %(w/w) dextran It is clear that the attempt to validate the predictive models for the thickness mouthfeel attributes based on low and high shear viscosity as input parameters failed here. This may be due to the fact that the predictive models were developed based on samples containing xanthan gum. Xanthan gum has a unique solution conformation compared to the other polysaccharides utilised in this research. It is a rigid rod

molecule whereas the dextran, guar gum and methylcellulose form random coils in solutions as evidenced by the rheological results presented in this research supported by literature (Norton and Foster, 2002). However, the models can still be used as a roughly guidance for comparing the thickness perceptions of different samples. It also worth noting that the models should be used carefully for Newtonian fluids as the models were designed based on shear thinning samples.

4.3.3.4.2 Stickiness and mouthcoating

Table 4.23 shows the sensory results for stickiness and mouthcoating perceptions for the six model testing samples. ANOVA results indicated that most of these samples were significantly different from each other. The results showed that the stickiness and mouthcoating of the higher concentration polysaccharide solutions for all three sample pairs were perceived as significantly higher than the lower concentration counterparts. For guar and MC solutions, samples with higher extensional viscosities were given higher scores for stickiness and mouthcoating. However, it was not the case for dextran solutions. It is worth noting that although with lower extensional viscosities and breakup time, the 17% dextran were perceived even higher than 0.8% guar solutions for stickiness and mouthcoating. It is unclear why it would be this case. One possible reason could be the mucoadhesive properties of dextran (Vimal Kumar Yadav et al., 2010).

Table 4.23: ANOVA *p*-value and mean sample scores for two stickiness attributes and mouthcoating of six model testing samples. Samples coded with the same letter in any one column are not significant different (p>0.05)

		Stickiness on lips	Stickiness in mouth	Mouth coating
p-values	Product	<0.0001 ***	<0.0001 ***	<0.0001 ***
	Panellists	0.0010 ***	0.0034 **	<0.0001 ***
	Products*Panellists	0.0797	<0.0001 ***	0.0285 *
Mean Sample score	Dextran 8%	2.05 e	1.28 f	2.1 e
	Dextran 17%	7.03 b	7.49 b	8.25 b
	Guar 0.5%	3.09 d	2.33 e	2.4 e
	Guar 0.8%	6.85 b	6.35 c	6.22 c
	MC 0.5%	4.34 c	3.63 d	4.47 d
	MC 0.9%	9.21 a	9.22 a	9.18 a

The actual sensory scores were compared with predicted values from models (see Table 4.17) including both low shear viscosities and extensional viscosities, as shown in Table 4.24.

Table 4.24: The actual value and predicted values from models including both low and extensional viscosities for model testing samples for Stickiness and Mouthcoating.

	Stickiness on lips		Stickiness in mouth		Mouthcoating	
	Actual	Predicted	Actual	Predicted	Actual	Predicted
Dextran 8%	2.05	1.52	1.28	0.65	2.1	0.46
Dextran 17%	7.03	2.51	7.49	1.73	8.25	1.61
Guar 0.5%	3.09	2.94	2.33	2.24	2.4	2.14
Guar 0.8%	6.85	7.43	6.35	7.2	6.22	7.42
MC 0.5%	4.34	3.36	3.63	2.77	4.47	2.67
MC 0.9%	9.21	11.16	9.22	11.68	9.18	11.98

As can be seen from the results the predicted values for guar, MC and also 8% dextran were relatively close to actual values. For MC 0.9, the predicted value is slightly over actual value. This is due to that MC has a slightly higher viscosity value at 50 s^{-1} than the value used in model building. However, as expected, the predicted values for 17% dextran were largely different from the actual values. The results proved that models including low shear and extensional viscosities can be convincing predictors for perceptions of stickiness and mouthcoating for samples with shear thinning behaviours. However more samples need to be tested to find out if these models are also applicable for Newtonian samples.

4.3.3.4.3 Taste and flavour attributes

ANOVA results for "Overall fruity, Sweetness and Musty/Fusty" perceptions showed that there are significant differences between panellists. Also there are significant interaction between products and panellists for musty/fusty which indicated cross-over effect for this attributes. For overall fruity flavour, the scores ranged from 3.47 to 5.43 and in addition it was found that all low concentrations were scored higher than higher concentrations. Post-hoc test showed that there were no significant differences between guar solutions and MC solutions but significant differences were found for dextran groups. For the musty/fusty attribute, only 17% dextran and MC samples were scored above 5 and MC high was scored the highest value of 8.44 across all the sample sets. It has been discussed previously that this

musty/fusty attribute was added when these 6 samples were introduced. Apparently it was mainly due to MC and DX that the panel picked up the musty/fusty attributes.

Table 4.25: ANOVA *p*-value and mean sample scores for taste and flavour attributes of six model testing samples. Samples coded with the same letter in any one column are not significantly different ($p>0.05$)

		Overall fruity flavour	Overall sweetness	Musty/Fusty
p-values	Product	<0.0001 ***	<0.0001 ***	<0.0001 ***
	Panellists	<0.0001 ***	<0.0001 ***	<0.0001 ***
	Products*Panellists	0.3882	0.6039	0.0007 ***
Mean sample score	Dx low(8%)	5.43 *a*	4.78 a	2.78 c
	DX high(17%)	3.47 *b*	4.2 a	5.17 b
	Guar low(0.5%)	5.8 *a*	3.16 b	1.55 c
	Guar high(0.8%)	5.4 *a*	3.04 b	1.83 c
	MC low(0.5%)	3.76 *b*	2.36 c	5.26 b
	MC high(0.9%)	2.69 *b*	1.63 d	8.44 a

Overall sweetness perceptions for model testing samples ranged from 1.63 to 4.78, and all higher concentrations of polymers solutions were given lower scores of sweetness compared with lower concentrations. ANOVA tests showed that there were no significant differences between low and high concentrations for guar and dextran, but significant differences did existed between low and high concentrations of MC solutions. It was found that at similar concentration or equivalent low shear viscosities, sweetness perceptions were least affected by dextran, and followed by guar. MC solutions were found affect the overall sweetness perceptions the most. It has now become widely accepted that the sweetness perceptions are affected by the

mixing properties of polymers: the overall sweetness is more affected if the thickeners have a poor mixing efficiency. The poor mixing efficiency of polymers maybe due to the less shear thinning behaviour: at the similar concentration, guar gum were given the highest scores for sweetness compared with MC. Some researchers argued that it is the nature of the hydrocolloid rather than the viscosity of polymers that affect the perceived sweetness, and guar gum has been found to affect sweetness perception more than CMC and oat gum (Malkki et al., 1993)

4.4 Friction behaviour and sensory properties

In this section, the friction properties of the ten designed samples as well as the six additional samples were studied and the results are presented. In addition, the relationship between friction behaviour of hydrocolloid solutions and their sensory properties are explored.

4.4.1 Friction properties of all study samples

The Stribeck curves for the main study samples of Group 1 and Group 2 are shown in Figure 4.39 and Figure 4.40, respectively. Each Figure shows two plots, the upper plot reports the results for an a normal load of 1.5 N applied during the measurement. The second plot refers to data acquired under 3 N normal force. The relevance of applying two different normal loads was to explore how this would affect the prediction of sensory perceptions based on friction properties. Both levels

of normal force are within the range normally used in food tribology as outlined in Section 2.3.3.

The results clearly show that with increased speed, the friction coefficient was reduced to a minimum and then increased. Unlike typical Stribeck curves, an obvious boundary regime was not observed for either set of samples or normal loads applied. It is worth noting that the rheological properties of the samples were well reflected by their friction behaviours, especially their high shear rheological properties. As for samples of Group 1 which have similar low shear viscosities, their friction behaviours were largely different. The samples that have higher viscosities at high shear rate were found to have higher friction coefficients in the hydrodynamic regime, and also the transition from mixed to hydrodynamic regime occurred at a lower speed. This finding was further proved by samples of Group 2. As expected their approximately equal high shear viscosity meant that the Stribeck curves were superposed. This effect of high shear viscosity on friction coefficient was also reported by Stokes et al. (2011). They suggested that it was the viscosity values at 10^4 s^{-1} that determined the friction coefficient at hydrodynamic regime.

It can be seen that as with increased normal load, the friction coefficients were reduced, especially at the hydrodynamic regime. In addition, the speed at which transition from mixed to hydrodynamic regimes occurs was slightly postponed. This can be expected as with increased normal load, the contacting surfaces are increased. Therefore it requires more polymer molecules to be entrained into the

contacting zone in order to reduce the friction and thus postponed the transition into hydrodynamic regime.

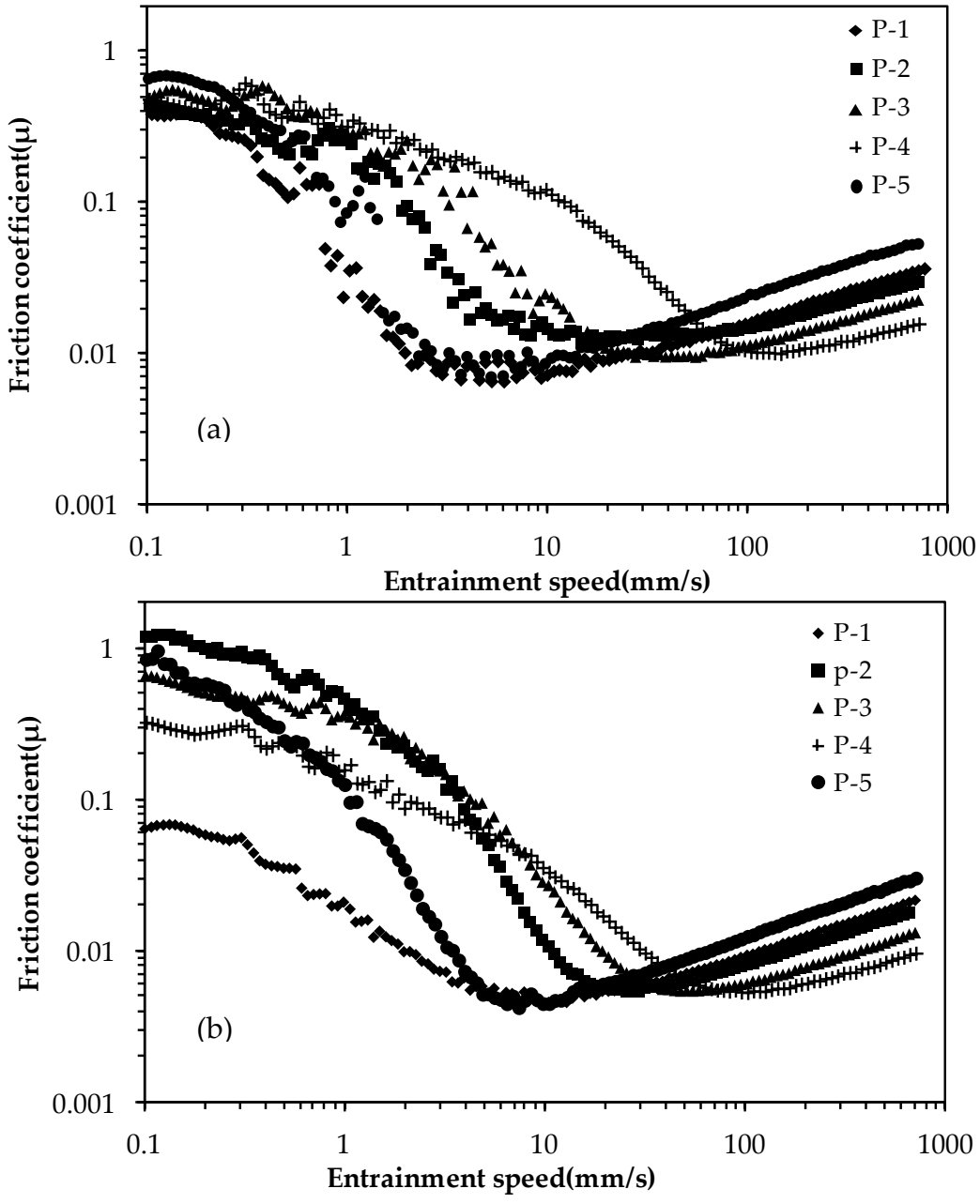

Figure 4.39: The Stribeck curves for Group 1 samples at normal load (F_L) of (a):1.5N and (b) 3N. The testing speed increased from 0.1 to 700 mm/s logarithmically in 5 minutes. All measurements were conducted in PDMS/Steel contact at 35°C.

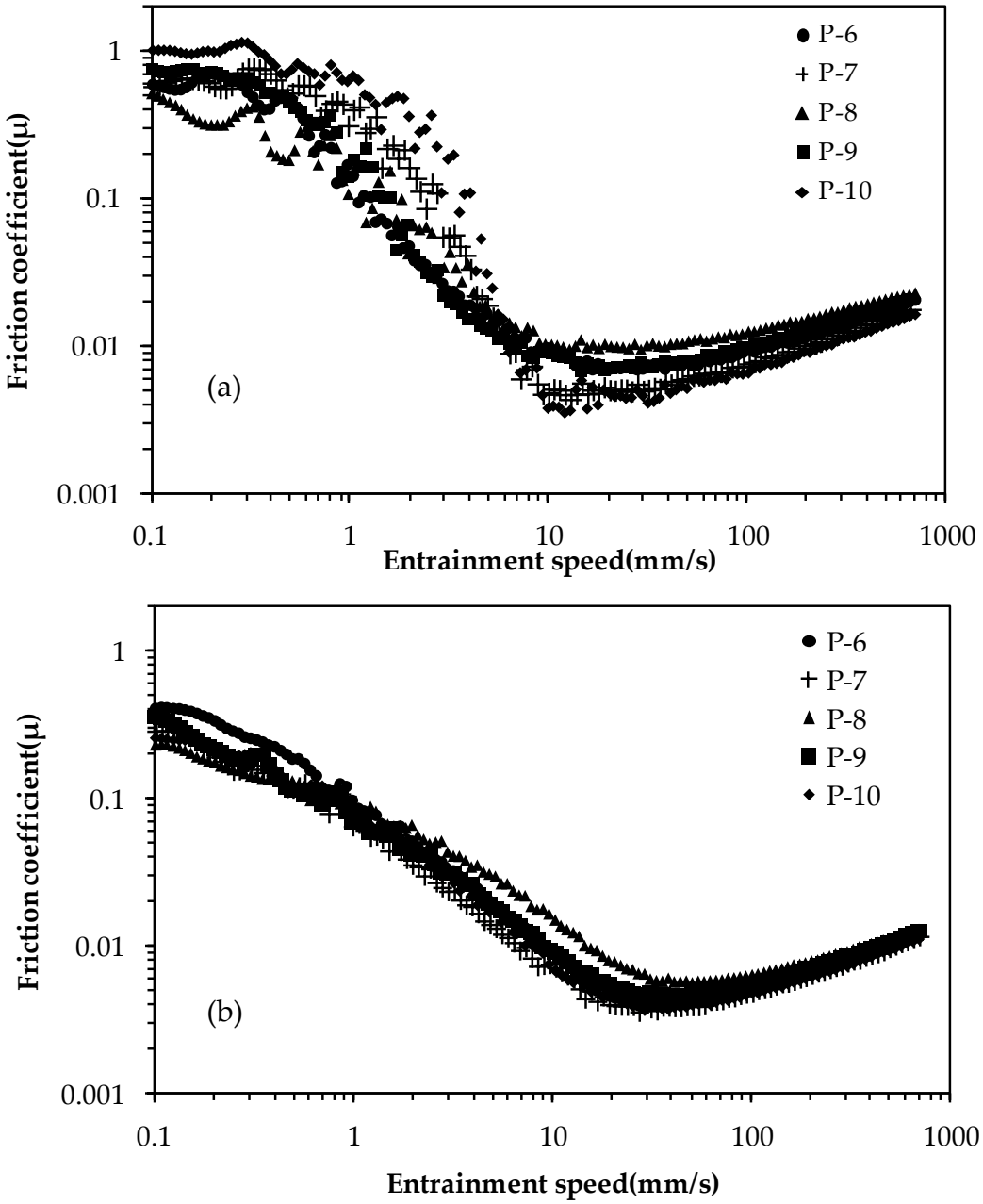

Figure 4.40: The Stribeck curves for Group 2 samples at normal load (F_L) of (a):1.5N and (b) 3N. The testing speed increased from 0.1 to 700 mm/s logarithmically in 5 minutes. All measurements were conducted in PDMS/Steel contact at 35°C.

The friction behaviours of prediction model testing samples were also explored and the results are shown in Figure 4.41. It was found that for all polymer solutions, as

with increased concentration, the friction coefficients were reduced in the mixed regime and also the transition points from mixed to hydrodynamic regime were reduced. Similar results were found by other researchers (Cassin et al., 2001, de Vicente et al., 2005). The friction coefficients at hydrodynamic regimes for all high concentrations of polymers were found higher than low concentrations. Again it was due to the higher viscosities values at high shear rate for higher concentrations of polymers.

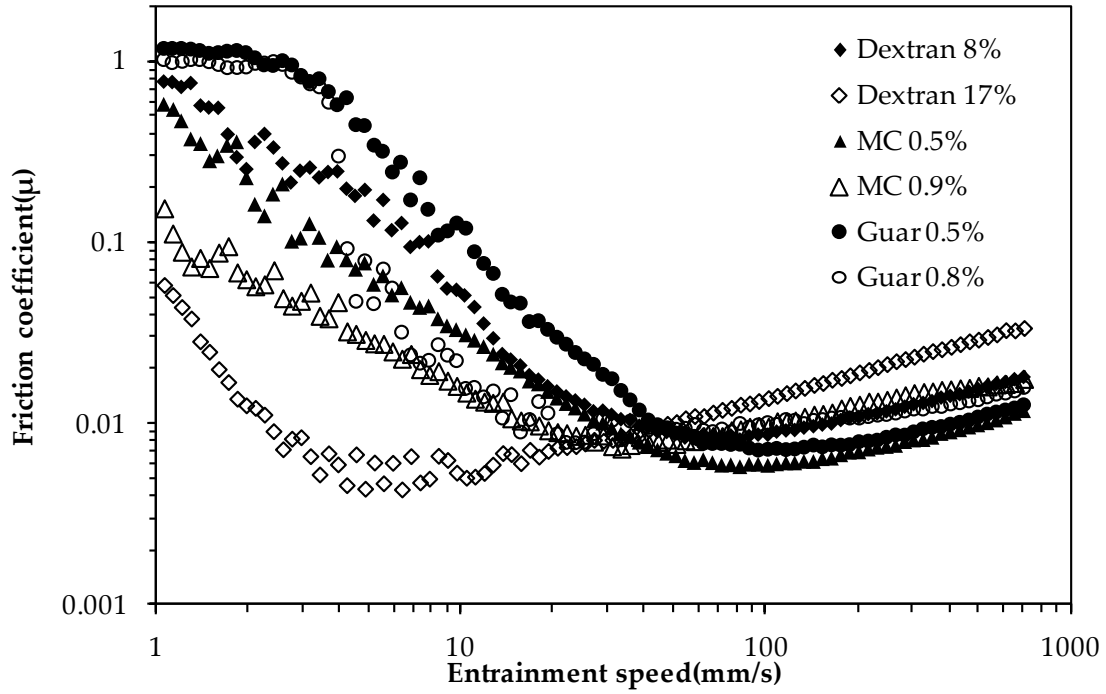

Figure 4.41: The Stribeck curves for prediction model testing samples at normal load (F_L) of 3N. The testing speed increased from 0.1 to 700 mm/s logarithmically in 5 minutes. All measurements were conducted in PDMS/Steel contact at 35°C.

4.4.2 Friction behaviour and sensory perceptions

The friction coefficients at all entrainment speeds were correlated with the sensory scores that were previously acquired from Descriptive Analysis (DA) (see Table 4.8, Table 4.9 and Table 4.10). The results for the correlation coefficients against all entrainment speeds are shown in Figure 4.42. All of the mouthfeel attributes correlate better with friction coefficients at an entrainment speed between 40 and 100 $mm.s^{-1}$. The best correlation has been found for a speed of around 50 $mm.s^{-1}$ ($r=0.90$). The two attributes overall flavour and sweetness are negatively correlated at entrainment speed between 10 and 30 $mm.s^{-1}$ with the best correlation around 20 $mm.s^{-1}$ ($r=-0.85$).

For the additional six samples it was found that the correlation between the friction coefficient at any entrainment speed and scores of any of the sensory attributes were low ($r<0.5$). However, the correlations were largely increased if the two dextran solutions were not considered in this analysis. The correlation coefficients that only include guar and MC solutions are shown in Figure 4.43.

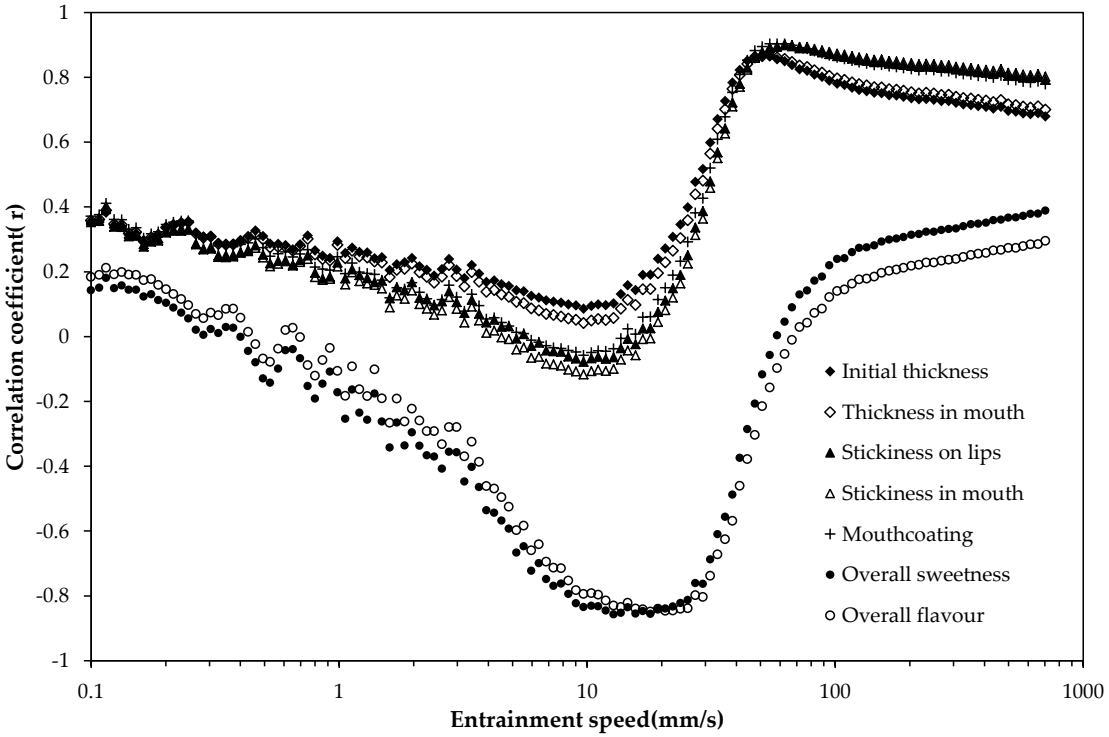

Figure 4.42: The correlation coefficients between friction coefficients and sensory scores plotted against entrainment speed.

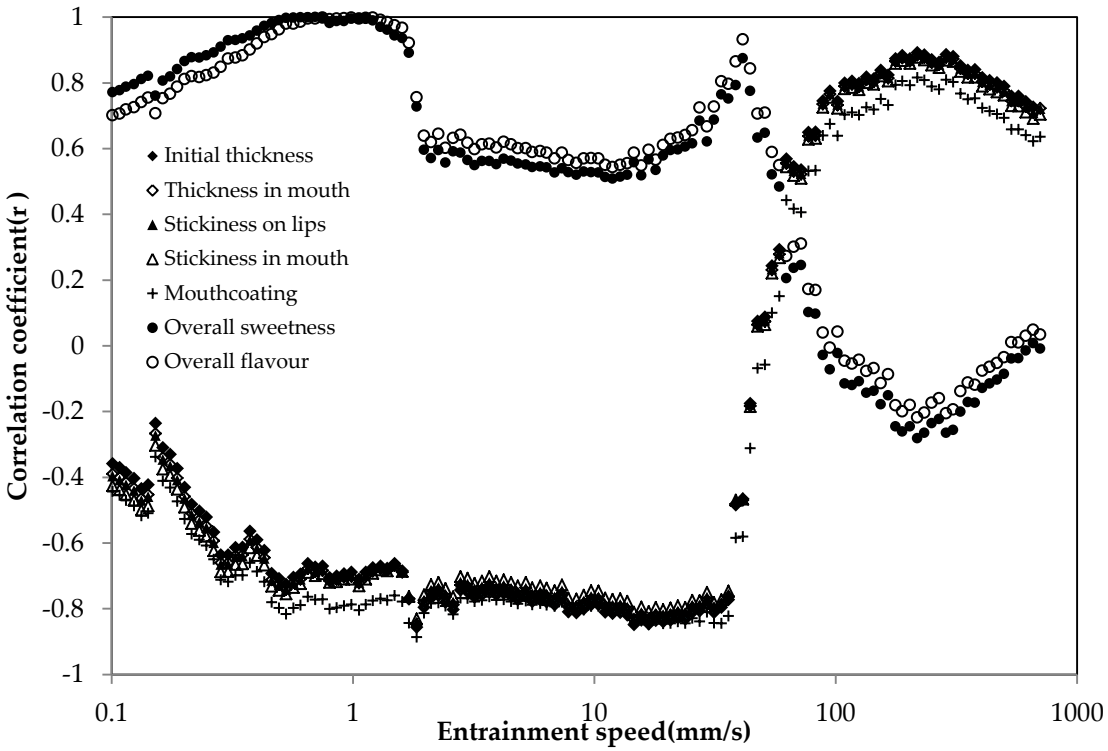

Figure 4.43: The correlation coefficients between friction coefficients and sensory scores against entrainment speed for guar and MC solutions.

The results indicated that for guar and MC solutions, the mouthfeel perceptions were better correlated with friction coefficients at two speed ranges: 10-30 $mm.s^{-1}$ and 100-400 $mm.s^{-1}$. The mouthfeel perceptions were negatively correlated with friction coefficients between 10 and 30 $mm.s^{-1}$ which indicated that higher mouthfeel scores were given to lower friction coefficients at this speed range. The mouthfeel perceptions were also highly correlated with friction coefficients at speed between 100 and 400 $mm.s^{-1}$ with the best correlation at a speed of 218 $mm.s^{-1}$ (r=0.90). For the overall flavour and sweetness, the sensory scores were found highly correlated with the friction coefficients at speed of 1 $mm.s^{-1}$ (r=0.99) and 40 $mm.s^{-1}$ (r=0.93).

The results from this research indicate that the friction behaviour of hydrocolloid solutions could be used as an effective predictor for their sensory perceptions. The correlation for designed samples was found to be best in the speed range of 40 to 100 $mm.s^{-1}$. The results are in agreement with results from Malone et al. (2003) who found that, for a series guar gum solutions, the mouthfeel perception of 'slipperiness' was highly correlated with friction coefficients at speed range from 10 to 100 $mm.s^{-1}$ which represented the mixed regime. However, the results from this research show that the speed regime that relates to mouthfeel perceptions not only covers the mixed regime, but it extends to the hydrodynamic regime. This is probably due to the different contact surfaces used that induce the different lubrication properties. As the friction coefficient is a system property, therefore to use friction coefficient from a certain range of speed to predict the mouthfeel perceptions in other systems is likely to fail. As for guar gum and MC solution, the speed range that related to mouthfeel perceptions was found even more related to the hydrodynamic regime. The difference in terms of speed ranges that related to mouthfeel perceptions for different polymers is probably due to their different molecular confirmations (Garrec and Norton, 2012). As for rigid-rod polymers such as xanthan gum, the molecule is more likely to be aligned to the flow and therefore easily entrained into the contacting zone, and hence the minimum friction is more likely to occur at an early stage. However, for random-coil polymers such as guar gum and MC, it takes longer for the molecule to enter the contacting zone and therefore the transition from mixed

to hydrodynamic happens at a later stage. This could probably explain why for guar gum and MC, the friction coefficients at a higher speed were more related to mouthfeel perceptions.

As discussed previously, the overall flavour and sweetness were negatively correlated with friction coefficients for the 10 designed samples (see Figure 4.42) with the highest correlation coefficients occurred at speed range of 10-30 $mm.s^{-1}$. The results indicated that higher scores were given to samples with lower friction coefficients at this speed range. The reason for this could be that as with increased speed, more polysaccharide molecules were entrained into contacting zone and thus caused less friction. For samples with lower friction coefficients, there could be more polysaccharide molecules that clustered at the contacting zone and therefore fewer molecules around the surroundings which could release more free water to carry tastants to taste receptors.

4.5 Flow behaviour and lubrication properties of saliva

4.5.1 Introduction

In this section, all the results related to saliva work are reported. As mentioned in section 2.2.3.4, saliva plays a crucial role in the sensory perception of foods. The aim of this chapter was to understand its function from the perspective of rheology and tribology. Initially the flow rate of saliva under different stimulation conditions was explored and followed with the reporting and discussion of flow behaviour studies of stimulated saliva including shear and extensional flow. Finally the lubrication properties of stimulated saliva and its effect on lubrication properties of hydrocolloids solutions were explored.

4.5.2 Results and discussion

4.5.2.1 Flow rate of saliva under different stimuli

The flow rate of saliva following the introduction of different taste stimuli at different concentrations as outlined in Table 3.2 was measured for 3 subjects. To begin with unstimulated flow rate of saliva was determined. The averaged results based on 3 repeat measurements are presented in Figure 4.44. Unstimulated saliva flow rate ranged from 0.63 to 0.82 $g.min^{-1}$, which is narrow compared to the previously reported range of 0.15 to 1.68 $mL.min^{-1}$ with a mean value of 0.53$mL.min^{-1}$ (Yamamoto et al., 2009). Statistical analysis showed that the unstimulated saliva flow rates of the three selected subjects were not significantly different from each other (p>0.05)

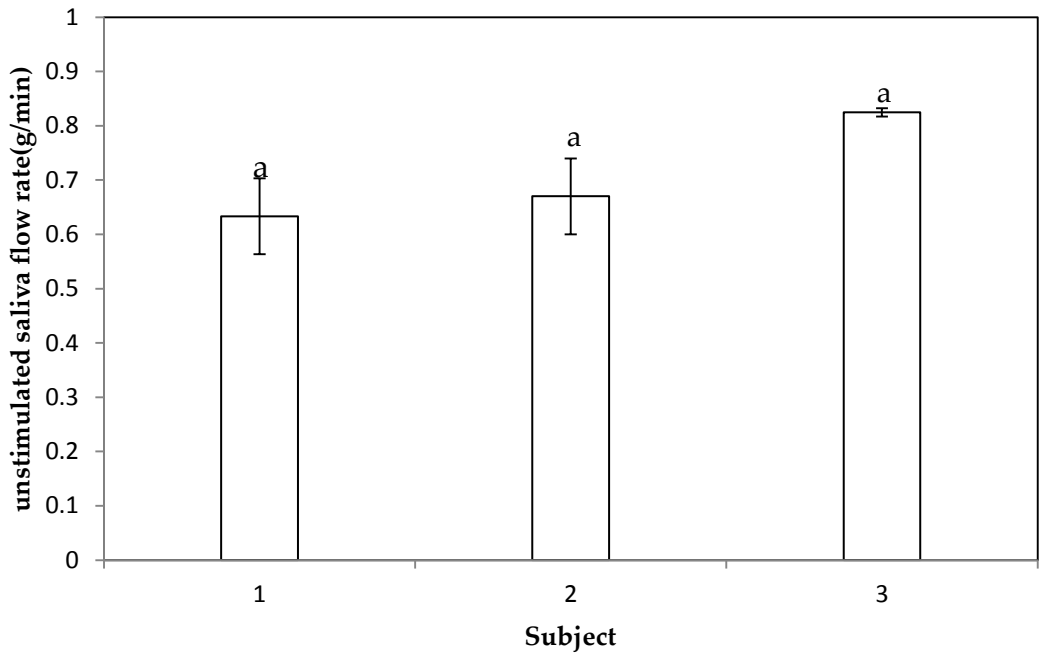

Figure 4.44: Unstimulated saliva flow of the selected three subjects. The same letter 'a' indicates the insignificance between subjects (Tukey HSD, p>0.05).

The overall flow rates of stimulated saliva are shown in Figure 4.45 and Table 4.26. The values were significantly higher than for unstimulated saliva except for the bitterness stimulus caffeine. The flow rate of citric acid stimulated saliva was found to be significantly higher than that of others followed by the sodium chloride stimulated saliva. Also the flow rate of citric acid stimulated saliva varied more compared with other stimuli. The values for sweetness and umami stimulated saliva were slightly lower than that of salty stimulated saliva, although statistical analysis shows they are not significantly different. In case of stimulation with caffeine, the flow rates of saliva were not significantly different from unstimulated saliva. It has been reported by some researchers that the overall order of saliva flow rate in

response to the five basic tastes from highest to lowest is citric acid>MSG>sodium chloride >sucrose> magnesium sulphate (Hodson and Linden, 2006). This sequence is in broad agreement with studies that consider this by comparing the dose-response curves with respect to sour, salt and sweet representatives (Chauncey and Shannon, 1960, Feller et al., 1965, Speirs, 1971b, Froehlich et al., 1987b). The results from the present study show the order of saliva flow rate was in accordance with previous studies except for the umami taste. In fact, the effect of MSG on saliva flow rate is still not clear. Pangborn and Chung (1981) found that generally the flow rate of saliva stimulated by NaCl is higher than MSG and a mixture of the two stimuli which has been found here. The mechanism of secretion of saliva is well studied (Turner and Sugiya, 2002, Catalan et al., 2009). It involves two stages: (1) acinar endpieces produce an isotonic plasma-like saliva and then this NaCl-rich fluid is modified during its passage along the ductal epithelium, where most of the NaCl is reabsorbed, while K^+ is usually secreted. Because ductal epithelium is poorly permeable to water, the final saliva is usually hypotonic. It is known that the pattern and magnitude of the salivary response demonstrated to be dependent on both the type and level of stimulation suggesting that taste stimuli could activate the afferent pathways and send impulses to the brain where efferent secremotor impulses are generated and sent to the effector organ such as the parotid gland (Froehlich et al., 1987a). The high flow rate of saliva caused by citric acid was suggested to be a

dilution mechanism by the human body as a protection of the oral mucosa (Emmelin and Holmberg, 1967).

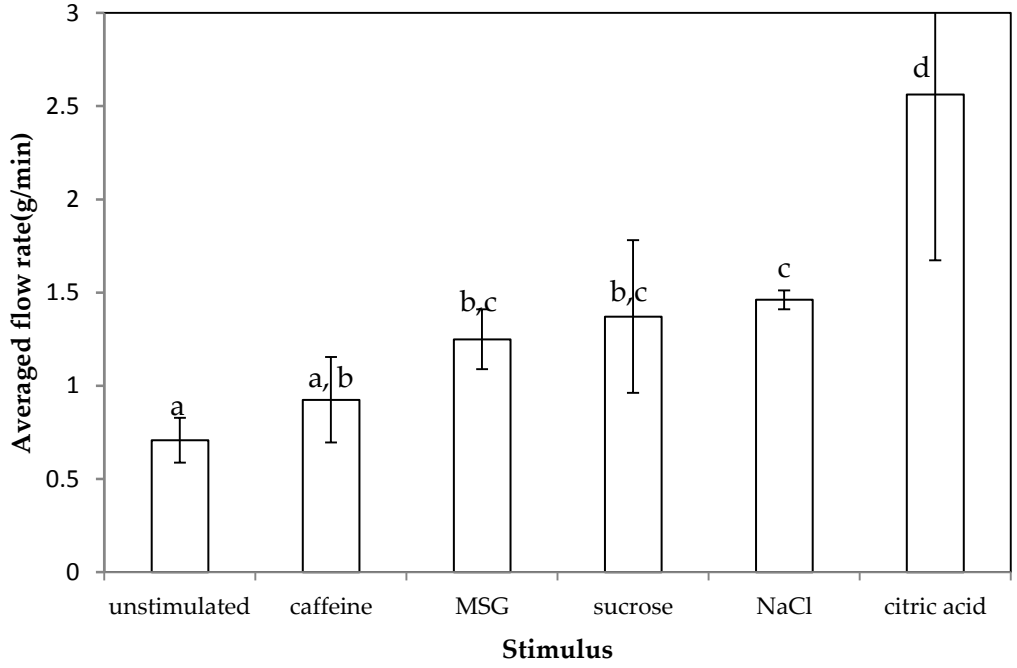

Figure 4.45: Average flow rate of saliva under different stimulation. Columns with the same letters indicate they are not significantly different (Tukey HSD, p>0.05).

Table 4.26: ANOVA of average saliva flow rates for different stimuli (p<0.05)

Stimuli	Range g.min^{-1}	Mean±SD g.min^{-1}	Subset
Unstimulated	0.52-0.83	0.70±0.12	a
Bitterness	0.73-1.4	0.93±0.23	a,b
Umami	1.02-1.61	1.25±0.16	b,c
Sweetness	0.87-2.45	1.37±0.41	b,c
Salty	1.25-1.63	1.46±0.05	c
Sourness	1.55-4.0	2.56±0.89	d

Following evaluation of averaged saliva flow rate for each stimulus, the impact of various concentrations was investigated and results are illustrated in Figure 4.46, and details of the values are displayed in Table 4.27. Saliva flow rates were increased with concentration except for caffeine. The overall saliva flow rates in response to citric acid were significantly higher than to any of the other stimuli. Caffeine produced the lowest saliva flow, and also the flow rate decreased and then increased in response to increasing stimulus concentration. It has been reported by some researchers that magnesium sulphate and quinine, as alternative bitterness stimuli, produce the lowest saliva flow rate among the basic tastes (Chauncey and Shannon, 1960, Neyraud et al., 2009).

ANONA results showed that saliva flow rates were not significantly different for different concentrations of caffeine and sucrose tested, see Table 4.27. The possible reason could be that for these two stimuli, the variation was high compared with other stimuli; also the small number of subjects could be another reason for the insignificance (p>0.05).

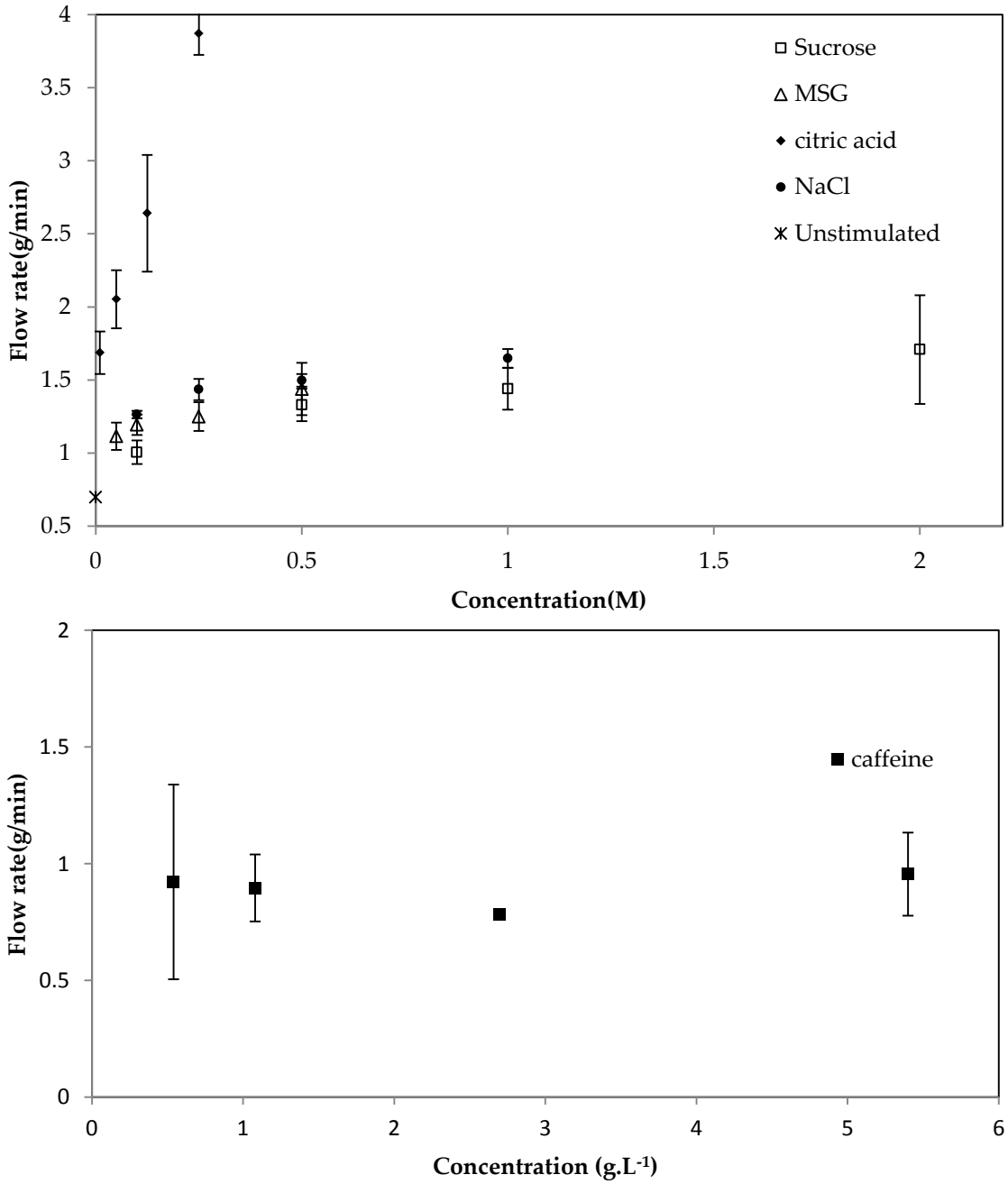

Figure 4.46: The flow rate of saliva under five basic tastants for varied concentrations.

Table 4.27: Comparisons of mean flow rate of saliva for different stimuli under different concentrations and post hoc test groupings for flow rate at different concentrations. The samples with different letters indicate the significant differences (Tukey HSD,$p<0.05$).

	Saltiness		Sweetness		Sourness		Umami		Bitterness	
Concentration	Range	Mean±SD	Range	Mean±SD	Range	Mean±SD	Range	Mean±SD	Range	Mean±SD
C1	1.25-1.3	1.26±0.026 ^{a}	0.87-1.14	1.01±0.14 ^{a}	1.55-1.84	1.69±0.15 ^{a}	1.02-1.21	1.12±0.09 ^{a}	0.74-1.4	1.07±0.5 ^{a}
C2	1.36-1.5	1.41±0.072 ^{b}	1.12-1.51	1.33±0.19 ^{a}	1.83-2.2	2.05±0.2 ^{a}	1.12-1.26	1.20±0.07 ^{a,b}	0.73-1.0	0.84±0.16 ^{a}
C3	1.47-1.5	1.51±0.042 ^{b}	1.18-1.68	1.44±0.25 ^{a}	2.4-3.1	2.64±0.4 ^{b}	1.16-1.36	1.25±0.1 ^{a,b}	0.77-0.8	0.8±0.02 ^{a}
C4	1.60-1.72	1.65±0.064 ^{c}	1.3-2.45	1.71±0.64 ^{a}	3.7-4.0	3.87±0.15 ^{c}	1.26-1.61	1.44±0.18 ^{b}	0.75-1.03	0.89±0.2 ^{a}

4.5.2.2 Shear rheological properties of saliva

4.5.2.2.1 The effect of centrifugation

To test viscosity and first normal stress difference for saliva as collected and following centrifugation, 1 M sucrose stimulated WHS was randomly chosen. Half of the collected saliva was immediately transferred into 2mL centrifuge tubes and centrifuged for 5 minutes at 10,000 g at 37 °C (Fresco 21, Thermo, Germany) and both the supernatant and precipitate were used for the rheological measurements. The other half of the collected saliva was transferred to the rheometer and measured immediately without delay. The measurements of the saliva were completed within 30 minutes of collection. The shear rheology properties including the viscosity as well as the first normal stress difference N_1 for freshly collected and centrifuged WHS are illustrated in Figure 4.47. The viscosity values of WHS samples at the lowest and the highest shear rate, and also N_1 at 100 s^{-1} are displayed in Table 4.28.

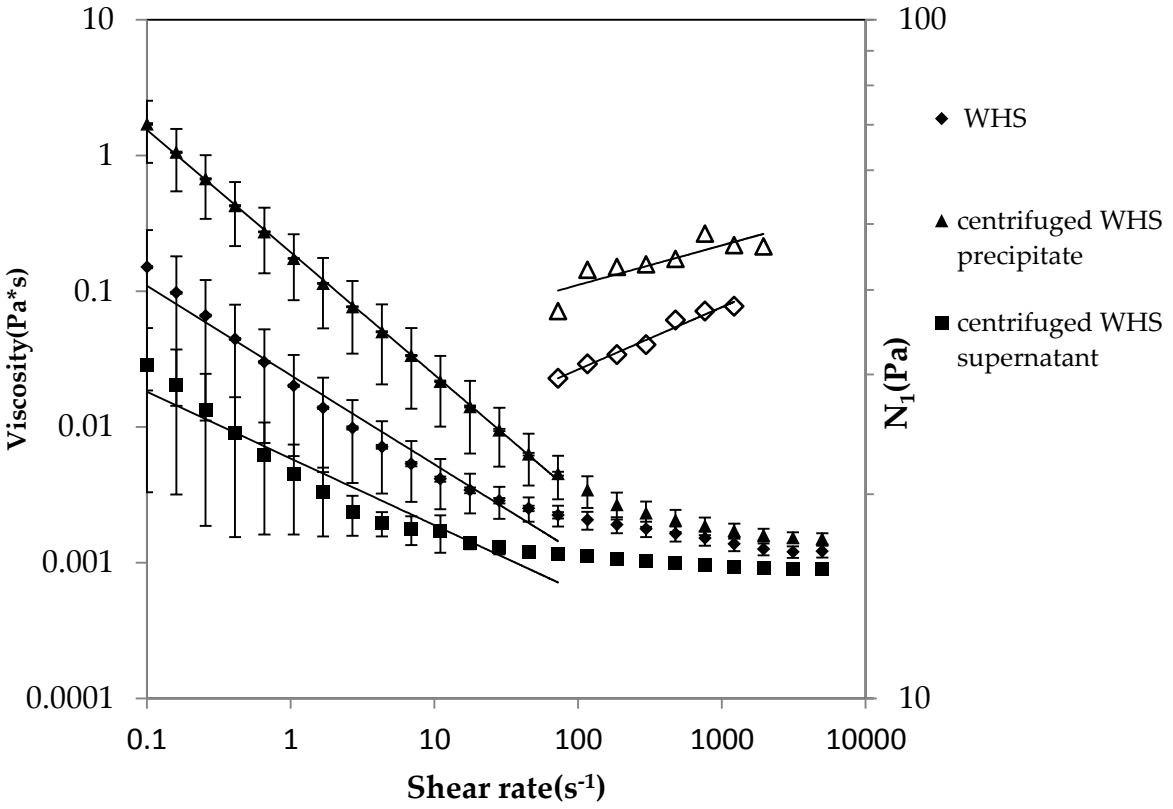

Figure 4.47: Shear rheological properties of freshly collected and centrifuged saliva: filled symbols are viscosity curves and open symbols are indicating N_1. Measurements were all conducted at 35 °C.

Table 4.28: The viscosity of saliva samples before and after centrifugation

	η at 0.1 s^{-1} Pa.s	**η at 5000 s^{-1} Pa.s**	**N_1 at 100s^{-1} Pa**	**Power law index**
WHS	0.15	0.001	30	0.66
Supernatants	0.0285	0.001	40	0.49
Precipitate	1.71	0.002	N/A	0.903

Freshly collected and centrifuged WHS samples all showed shear thinning behaviour. Samples from precipitate of centrifuged WHS showed the highest

viscosity and was the most shear thinning among the three samples followed by supernatants of centrifuged WHS and freshly collected WHS.

A first normal stress difference (N_1) was detected for both centrifuged precipitate and whole saliva samples (WHS) demonstrating the elastic nature of these two samples. As can be seen from Figure 4.47 , N_1 of the centrifuged precipitate is higher than that of WHS. For the supernatant, there was no N_1 detected which means that the sample was not elastic. The precipitate contains a large amount of aggregated buccal epithelial cells, see Figure 4.48. The confocal laser scanning microscopy (CLSM) image of Rhodamine B stained saliva shown in Figure 4.49 confirms that protein is present in the saliva. It has been reported that saliva contains more than 1050 different types of proteins and peptides with molecular mass varying from a few kDa to more than 1000 kDa such as polymeric mucin MUC5B (Silletti et al., 2008). Of all the components presented in saliva, the gel forming mucin MUC5B has by far the highest molecular weight of a reported 2-40MDa and is many micrometres in length (Kesimer and Sheehan, 2008). Also mucin was found to be a somewhat stiffened random coil with a radius of gyration around 100nm (Harding, 1989, Bansil et al., 1995, Fiebrig et al., 1995, Bansil and Turner, 2006). The structure of the mucin explains pronounced shear thinning behaviour. During centrifugation, the large molecular weight mucins sediments at the bottom, leaving the supernatant to be almost pure water. This explains the increased viscosity and elastic nature of the precipitate compared with WHS.

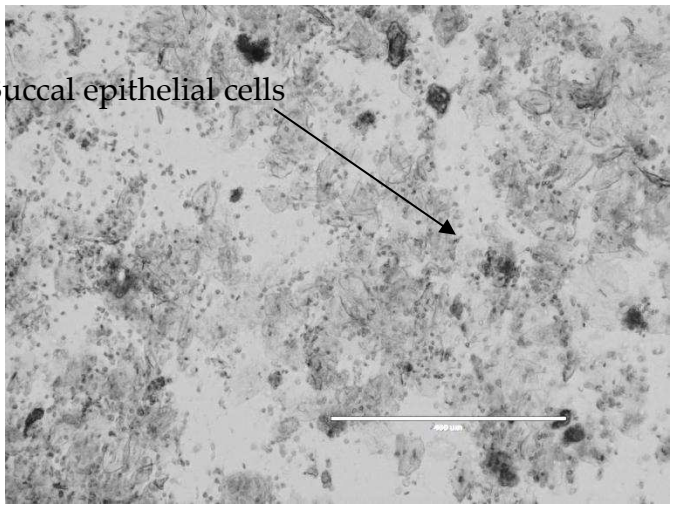

Figure 4.48: Microstructure of centrifuged precipitate of WHS. Scale bar represents 400 µm.

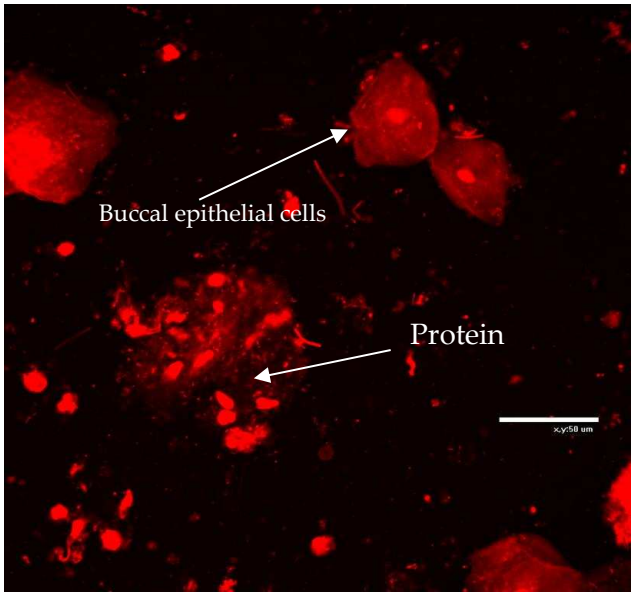

Figure 4.49: CLSM image of freshly collected saliva of which the proteins have been stained with Rhodamine B. Scale bar represents 50 µm.

4.5.2.3 The effect of different stimuli on saliva rheology

As discussed previously saliva plays an important role in mouthfeel and flavour perception. It is therefore essential to understand how rheological properties of saliva change under different taste stimuli as it may consequently influence how the food is perceived. In this section, the influence of the five basic tastes on the rheological properties of saliva is studied. It is worth stressing that the saliva samples are expected to be not containing any stimulus as per collection protocols, see 3.1.2. The saliva properties are the response to stimulation following complex biochemical processes. Therefore an in-depth discussion of the reasons for observed impact of stimuli is provided.

The shear rheological properties of saliva that collected after stimulation at the highest concentration of each stimuli used are illustrated in Figure 4.50.

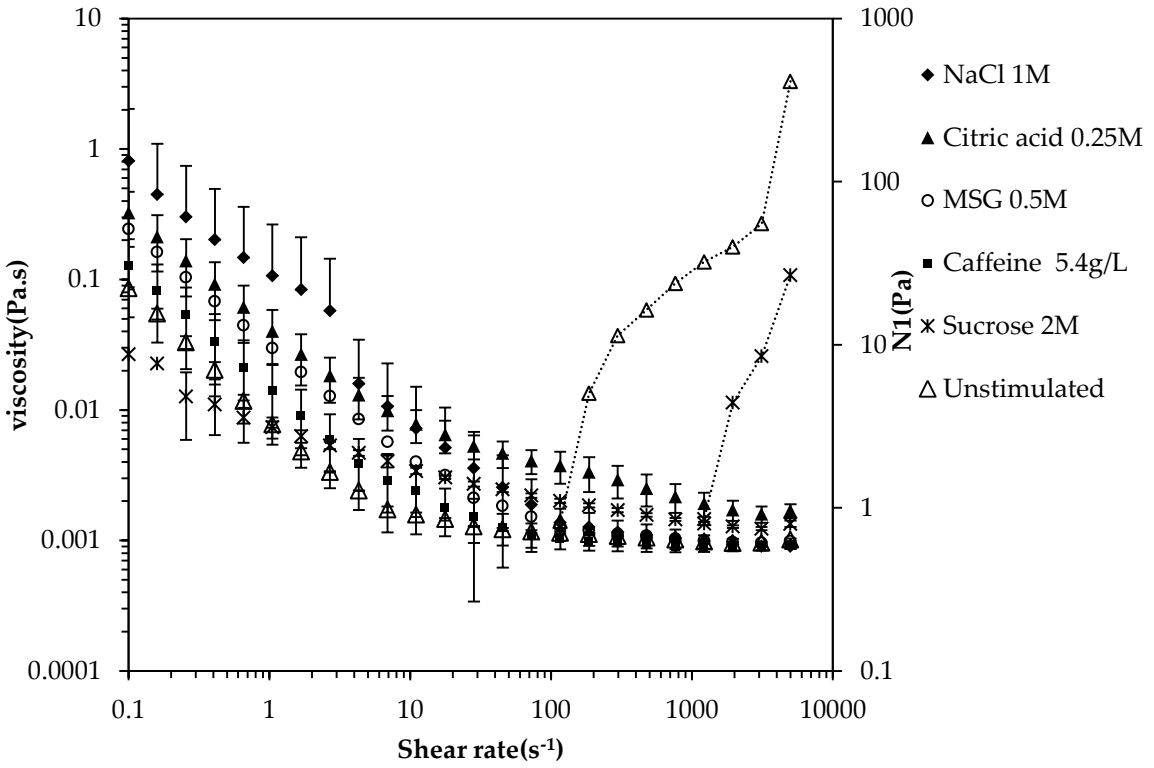

Figure 4.50: Mean shear rheological properties of WHS stimulated by five basic tastes at the highest concentration used. Error bars represent one mean standard deviation. All measurements were conducted at 35 °C.

As can be seen that for unstimulated saliva, there was an observed shear thinning behaviour which is well documented in the literature (Schwarz, 1987b) and the main reason for shear thinning is the presence of large glycoproteins like mucins which caused the weak gel characteristic of saliva (Veerman et al., 1989). The shear rheological properties of saliva are clearly affected by the types of stimulus. Also, there are large error bars which indicates the large variation between saliva samples. Just as unstimulated saliva, all of these samples show shear thinning behaviour. NaCl stimulated saliva had the highest in viscosity at low shear rate (1 s^{-1}) but citric acid stimulated saliva was highest in viscosity at high shear rate of (5000 s^{-1}). In

terms of elasticity, only saliva samples stimulated by citric acid and sucrose generated N_1 values. Citric acid stimulated saliva was found to be most elastic among these samples. The details of the effect of concentration of each stimulus on shear rheological properties of WHS are presented as following.

The effect of stimulus concentration on the shear rheological properties of WHS of a single subject is shown in Figure 4.51 to Figure 4.55. To facilitate comparison between the different stimuli, all the y-axis was set to have the same scales. Also the viscosity values at both low (1 s^{-1}) and high (5000 s^{-1}) shear rate are reported in Table 4.29.

Table 4.29: Comparison of shear rheological properties of WHS stimulated by different stimuli at different concentrations.

	Saltiness			Sweetness			Sourness			Umami			Bitterness		
		η_L	η_H		η_L	η_H		η_L	η_H		η_L	η_H		η_L	η_H
Concentration	Conc.	mPa.s	mPa.s	Conc.	mPa.s	mPa.s	Conc.	mPa.s	mPa.s	Conc.	mPa.s	mPa.s	Conc.	mPa.s	mPa.s
C1	0.1M	9.547	0.845	0.1M	5.277	0.921	0.01M	13.800	1.290	0.05M	34.350	0.947	0.54 $g.L^{-1}$	55.5	1.037
C2	0.25M	26.267	0.961	0.5M	1.087	8.917	0.05M	26.800	2.100	0.1M	33.975	0.937	1.08 $g.L^{-1}$	29.000	0.996
C3	0.5M	55.367	1.019	1M	24.427	1.177	0.125M	63.167	3.117	0.25M	22.050	1.037	2.7 $g.L^{-1}$	20.433	0.920
C4	1M	106.733	0.902	2M	7.395	1.343	0.25M	40.267	1.693	0.5M	29.700	0.986	5.4 $g.L^{-1}$	14.003	0.913
Unstimulated	0M	7.745	1.014	0M	7.745	1.014	0M	7.745	1.014	0M	7.745	1.014	0 $g.L^{-1}$	7.745	1.014

η_L and η_H represents viscosity at 1 s^{-1} and 5000s^{-1}, respectively.

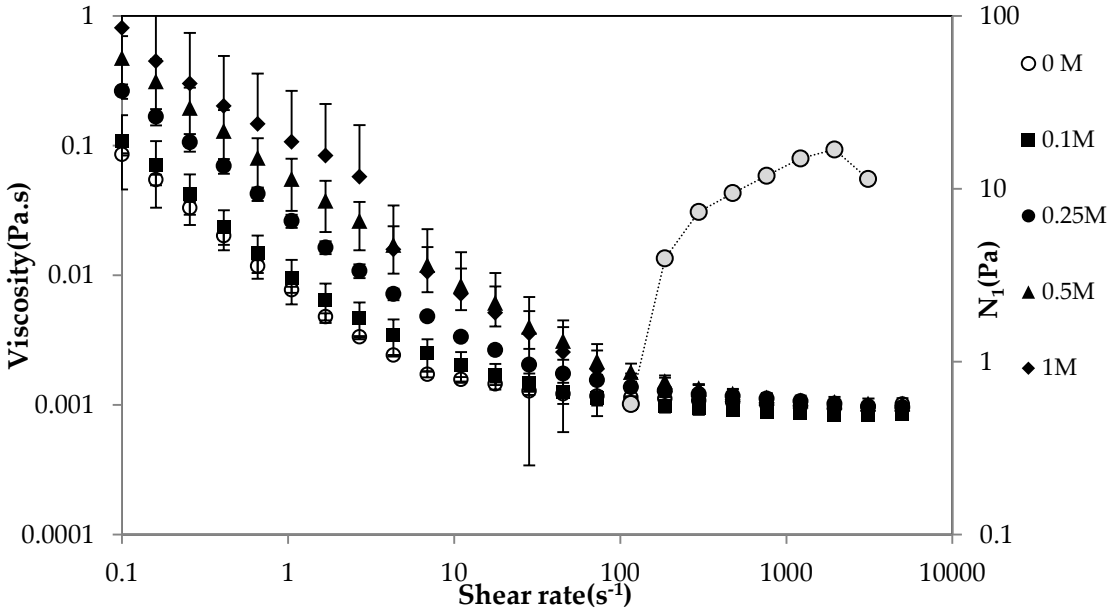

Figure 4.51: Shear rheological properties of WHS stimulated by NaCl at different concentrations. The open symbols represent the detected N_1.

In the case of NaCl stimulated WHS, see Figure 4.51, viscosity at low shear increase proportionally with NaCl concentration. However, the viscosity value at high shear rate of 5000 s^{-1} was almost identical for all samples and close to the value found for unstimulated saliva which was around 1 mPa.s. The shear thinning behaviour of NaCl stimulated WHS was more pronounced with increasing concentration. Elastic behaviour was only found for the stimulus concentrations of 0.25M NaCl. The first normal stress difference for 0.25M stimulated WHS was detected around 100 s^{-1} and increased with shear rate.

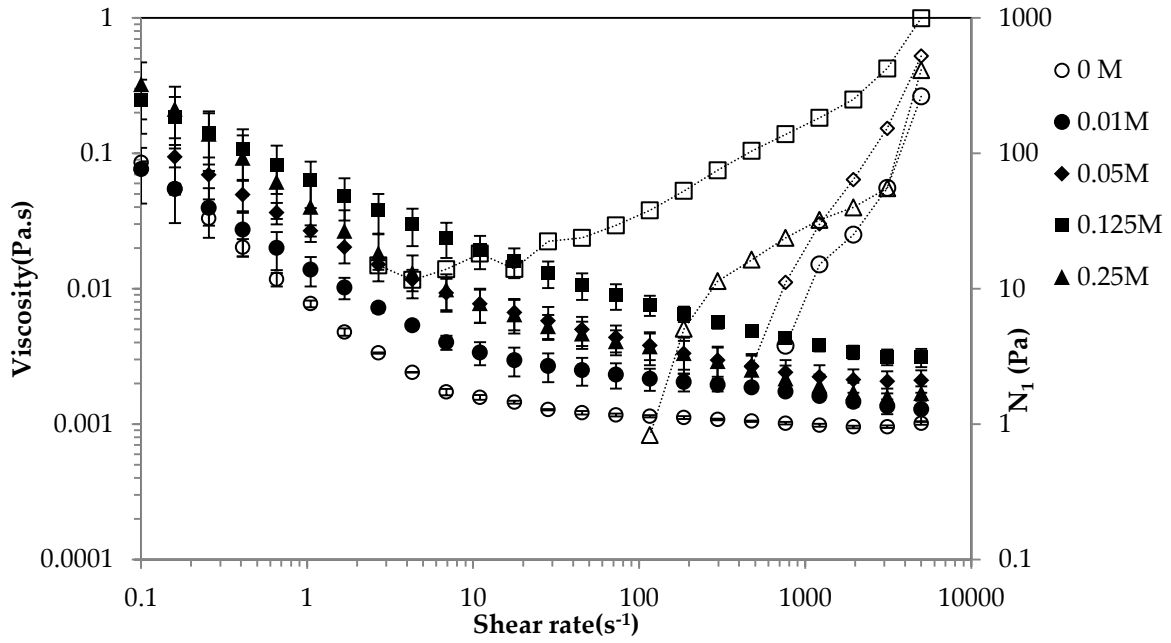

Figure 4.52: Shear rheological properties of WHS stimulated by citric acid at different concentrations. The open symbols represent the detected N_1.

Figure 4.52 shows the shear rheological properties of WHS stimulated by citric acid from 0.01 to 0.25M. The shear viscosity values for citric acid stimulated WHS were all significantly higher than that of unstimulated saliva for both η_L and η_H (see Table 4.29). All of the samples were highly shear thinning with no obvious plateau at high shear rate as it was observed for the other stimuli. It was found that for both η_L and η_H, the viscosities were increased with concentration from 0.01 to 0.125M. However, for the highest concentration of 0.25M, the viscosity at both low and high shear rate dropped to the same level as 0.05M citric acid and it was also the same case for N_1. The first normal stress difference for all samples increased with shear rate and was found to be much higher than in other stimuli. As discussed previously, the rheological properties of saliva are mainly determined by the presence of large

glycoprotein like mucins. It was also reported that viscosity of mucin is pH dependent and greatest at pH 4 (Schipper et al., 2007). This may explain why the viscosity of highest concentration of citric acid stimulated saliva was reduced. The pH of the citric acid solutions was not measured here but it is likely that pH of highest concentration citric acid is less than 4 and thus caused the reduction of viscosity.

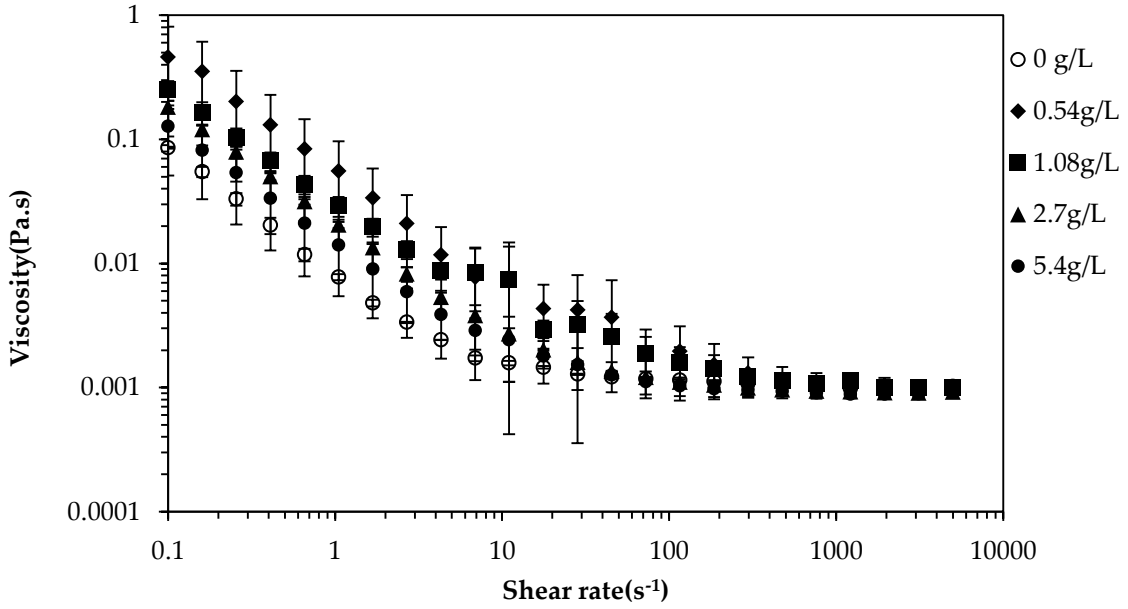

Figure 4.53: Shear rheological properties for caffeine stimulated WHS at different concentrations.

Figure 4.53 shows the viscosity of caffeine stimulated WHS at low shear rate is higher than that of unstimulated WHS but has similar high shear viscosity as unstimulated WHS. It should be noted that the η_L of caffeine stimulated WHS decreased with concentration, which was different compared with other stimuli. As

already discussed, the saliva flow rate of caffeine stimulated WHS followed an unsteady pattern with concentration, indicating a complex effect of caffeine on saliva secretion behaviour. Caffeine stimulated WHS was also the only exception for which no N1 was detected for samples at all concentrations. The effect of caffeine on secretion of saliva and its rheological properties has not been widely studied. However is has been reported that caffeine could selectively inhibit agonist-mediated rise in human gastric epithelial cells which may affect the mucin secretion (Hamada et al., 1997). It is unknown though if caffeine could also inhibits the secretion of salivary mucins using the same mechanism.

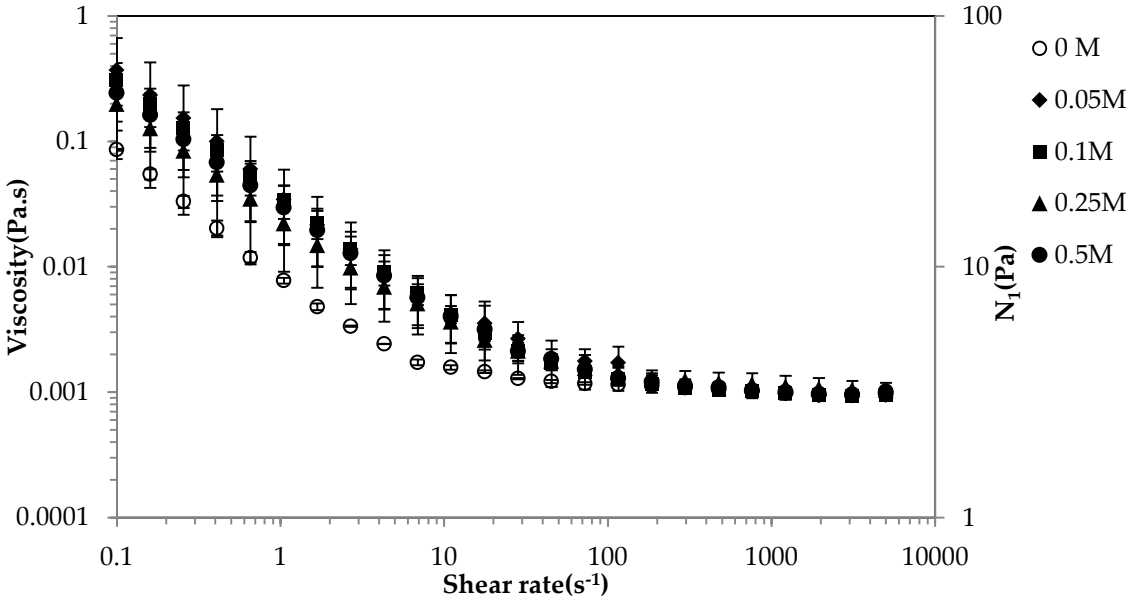

Figure 4.54: Shear rheological properties for WHS stimulated with MSG at different concentrations. The open symbols represent the detected N_1.

Figure 4.54 shows the shear rheological properties of MSG stimulated WHS at a range of concentrations. The saliva samples from MSG all demonstrated shear thinning behaviour, and the viscosities curves overlapped. There was no N1 detected for all the saliva samples stimulated by different concentrations of MSG.

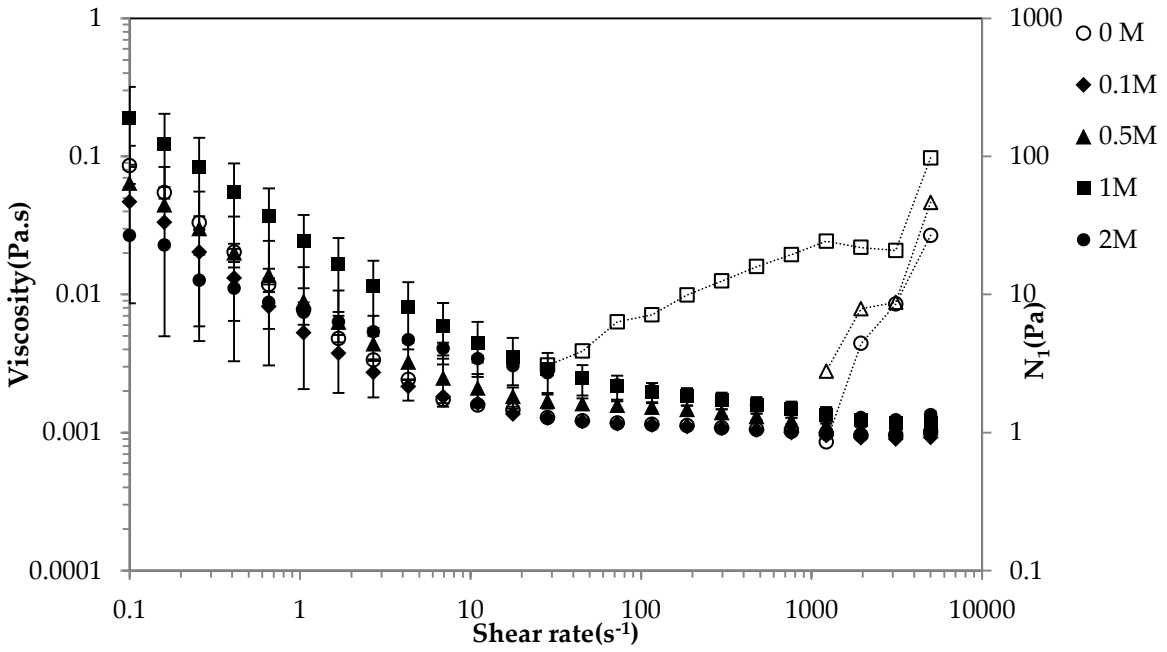

Figure 4.55: Shear rheological properties for WHS stimulated with sucrose at different concentrations. The open symbols represent the detected N_1.

Figure 4.55 shows shear rheological properties of WHS stiumulated with different concentrations of sucrose. It was found that the viscosity of samples was increased with concentration from 0.1 to 1M. However, at concentration of 2M, the viscosity of saliva was not the highest. The first normal stress difference was only detected from 0.5M. Interestingly, N_1 for 2M sucrose stimulated WHS was lower than that of 0.5M and 1M stimulated WHS.

4.5.2.4 The effect of stimuli on extensional properties of WHS

The effect of stimulus on the extensional rheology of WHS is reported in this section. Figure 4.56 to Figure 4.60 show the evolution of the normalised filament mid-diameter for WHS stimulated by different concentrations of stimulus. For each type of stimulus the result from unstimulated WHS was also presented as a comparison. It is worth noting that the time scales are quite different for the different stimuli. All the results were averaged from 5 replicates with standard deviation less than 1%. An exponential model was applied to samples where applicable to determine the relaxation time as shown in Equation 2.29. The calculated relaxation times based on fitting Equation 2.29 to the diameter data and breakup time, are reported in Table 4.30. To compare the difference between the filament breakup times of WHS stimulated by different concentration of tastants, Figure 4.61 has been included. The breakup time of citric acid stimulated HWS is not included in this figure as the scale time scale is much larger compared with the rest of samples.

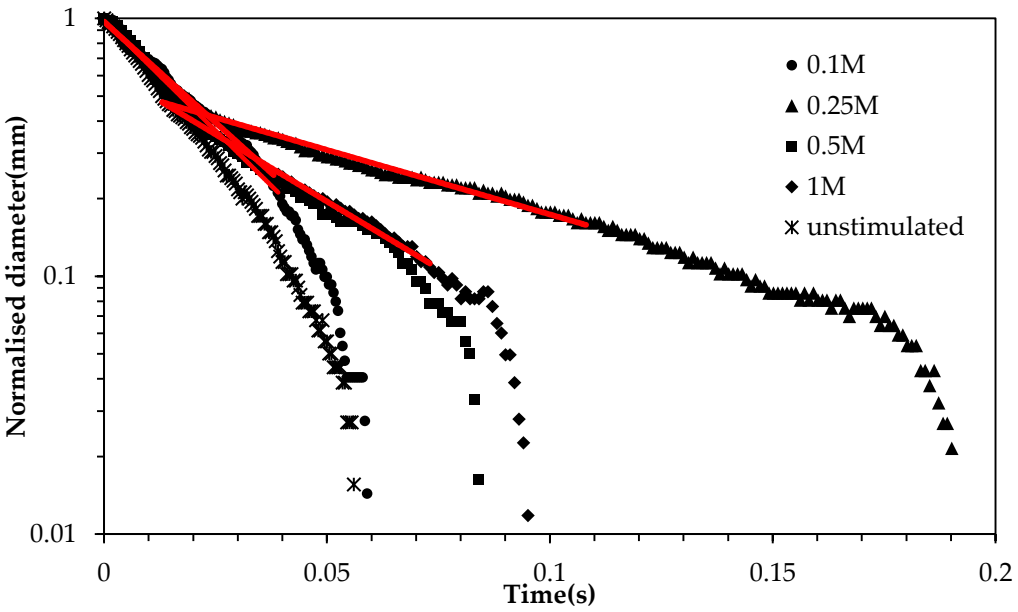

Figure 4.56: Evolution of normalised filament mid-point diameter for WHS stimulated with different concentrations of NaCl. Red lines represent the exponential models fitted (Measured at 35 °C).

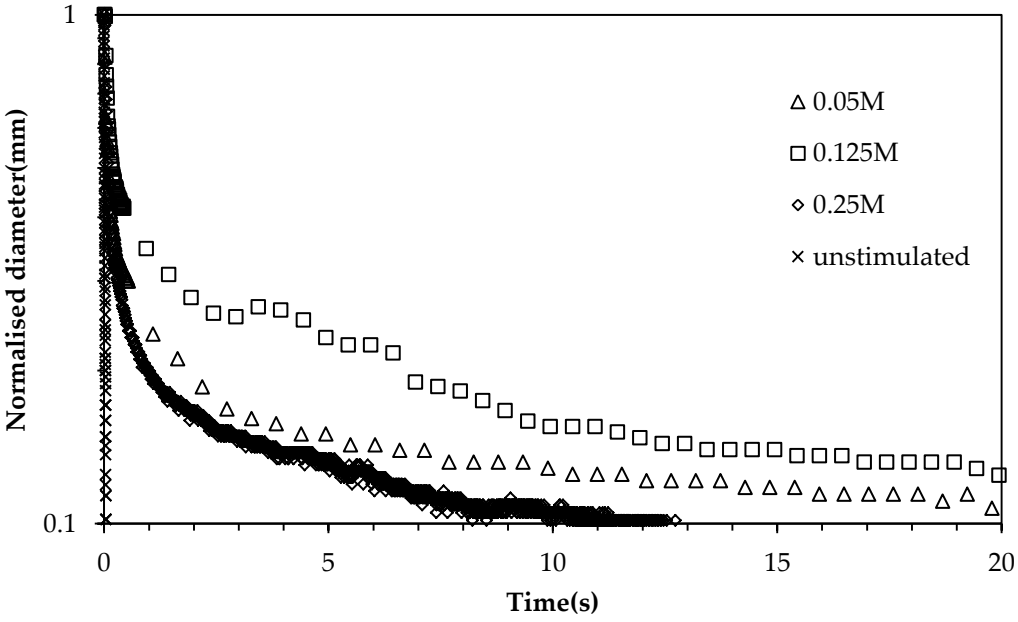

Figure 4.57: Evolution of normalised filament mid-point diameter for WHS stimulated with different concentrations of citric acid (Measured at 35 °C).

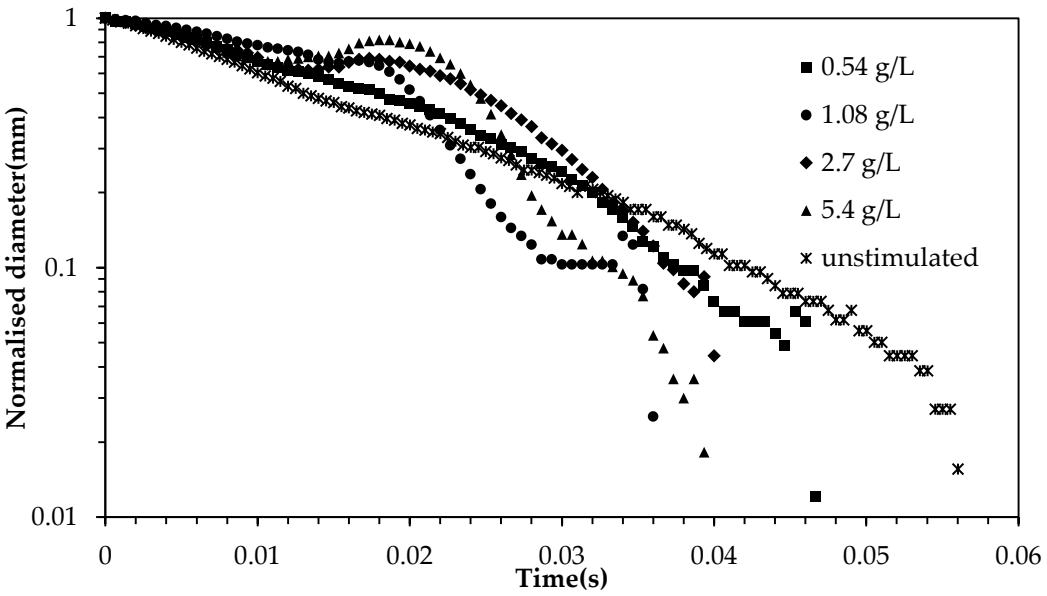

Figure 4.58: Evolution of normalised filament mid-point diameter for WHS stimulated with different concentrations of caffeine. Red lines represent the exponential models fitted (Measured at 35 °C).

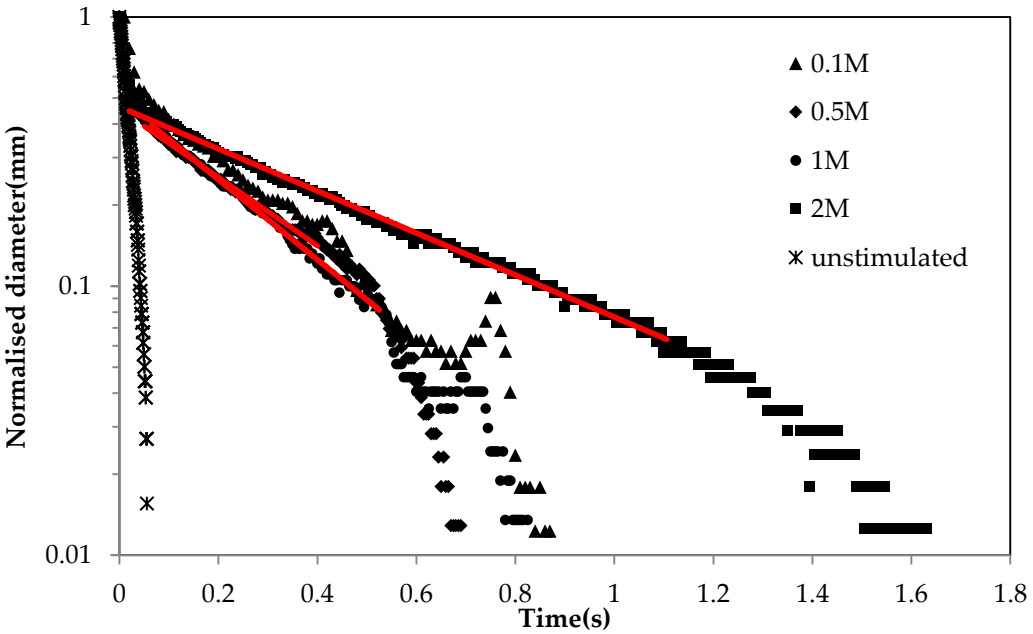

Figure 4.59: Evolution of normalised filament mid-point diameter for WHS stimulated with different concentrations of sucrose. Red lines represent the exponential models fitted (Measured at 35 °C).

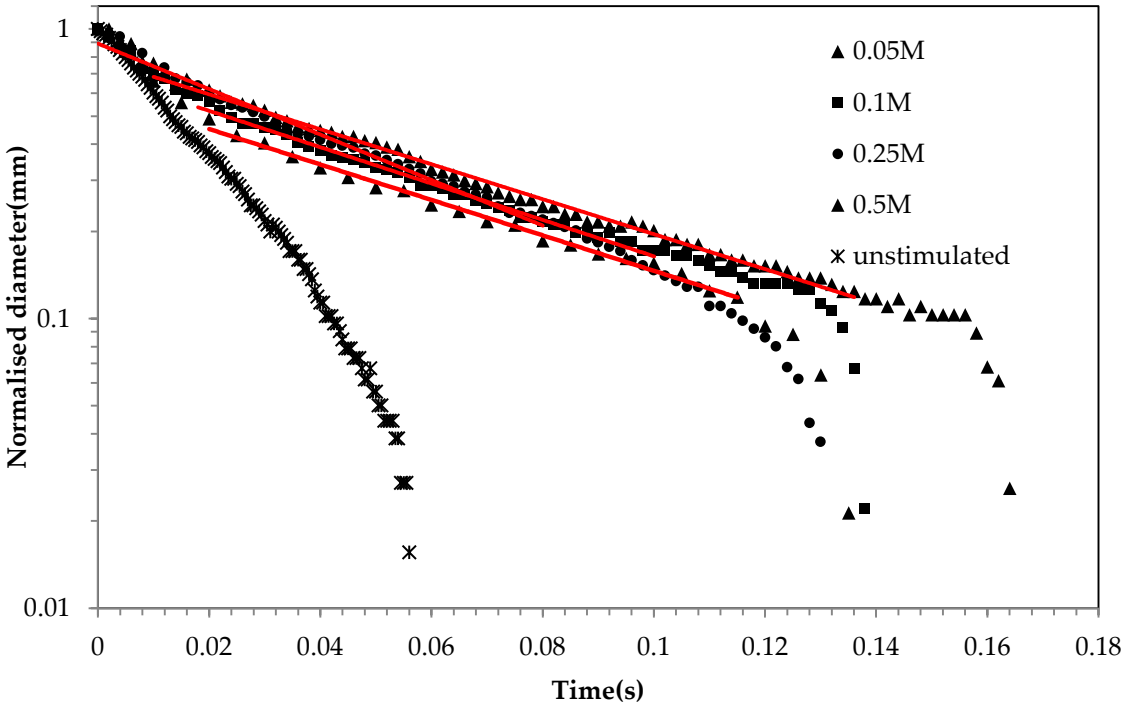

Figure 4.60: Evolution of normalised filament mid-point diameter for WHS stimulated with different concentrations of MSG. Red lines represent the exponential models fitted (Measured at 35 °C).

Table 4.30: Relaxation time and breakup time for WHS under different stimuli concentraions.

Stimuli	Conc.	Relaxation time(λ) s	Breakup time s
Unstimulated		0.007	0.056
Salty (NaCl)	0.1M	0.01	0.06
	0.25M	0.023	0.19
	0.5M	0.019	0.084
	1M	0.014	0.095
Sweetness (Sucrose)	0.1M	0.11	0.97
	0.5M	0.114	0.67
	1M	0.299	0.825
	2M	0.186	1.58
Umami	0.05M	0.024	0.110

(MSG)	0.1M	0.023	0.13
	0.25M	0.018	0.13
	0.5M	0.024	0.166
Bitterness (Caffeine)	0.54g/L	-	0.047
	1.08g/L	-	0.036
	2.7g/L	-	0.04
	5.4g/L	-	0.04
Sourness (Citric acid)	0.05M	-	25
	0.125M	-	40
	0.25M	-	12.5

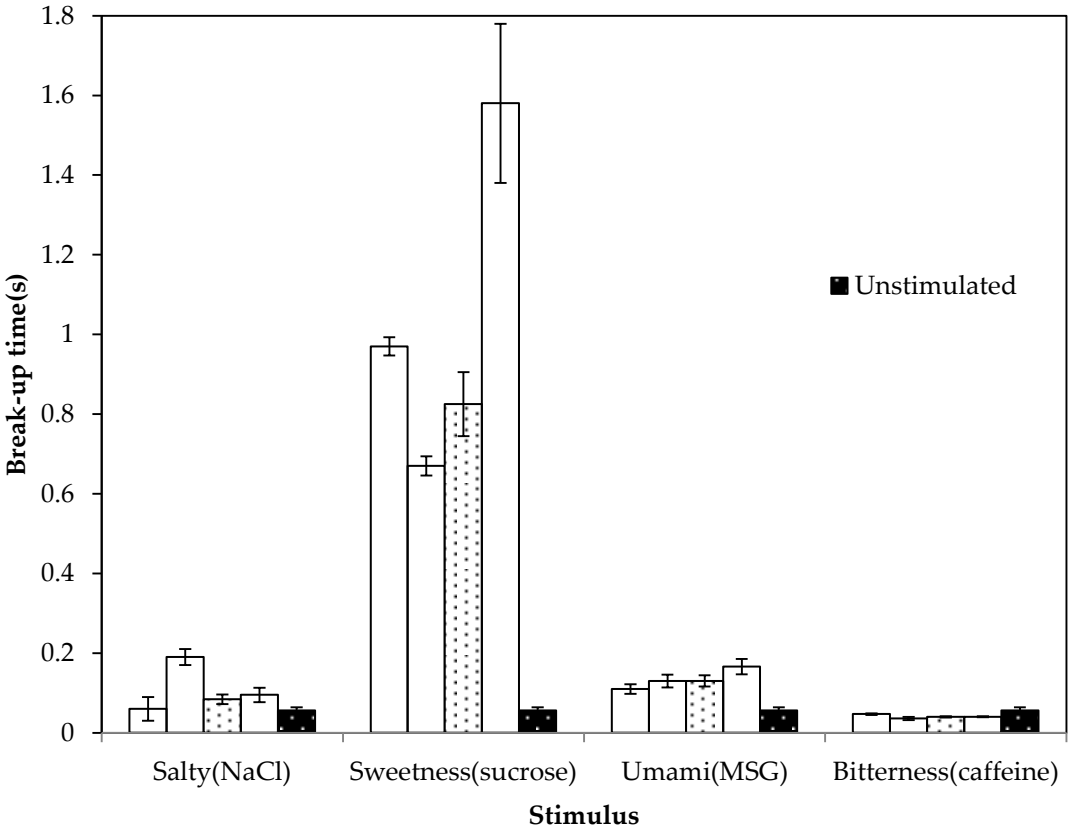

Figure 4.61: Filament breakup time for HWS stimulated by stimulus at different concentrations. The breakup time for unstimulated was included as a reference.

As can be seen from Figure 4.56-4.60 that the extensional rheological behaviour of WHS stimulated by different tastes followed different trend with increased

concentration. Also the breakup time for unstimulated WHS was found shorter than most of the stimulated ones except for caffeine stimulated WHS.

It was found that for NaCl stimulated WHS, see Figure 4.56, the relaxation time and breakup time initially increased with concentration but then dropped at the highest concentration. The breakup time for all concentrations was higher than for unstimulated WHS. Compared with NaCl stimulated WHS, the relaxation time and breakup time for MSG stimulated WHS, see Figure 4.60, was slightly longer, although the concentration of MSG seemed to have little effect on the breakup time.

The breakup time for sucrose stimulated WHS increased with concentration. Interestingly, for the sample stimulated with 1M sucrose solution, the relaxation time was longest although with a shorter breakup time compared with 2M stimulated WHS samples. This result is similar to the N_1 in shear rheology for 1M stimulated samples which was higher than 2M simulated samples.

It was found that for caffeine stimulated WHS, the concentration did not have significant effect on the breakup time. For all samples stimulated with caffeine, less time was taken for breakup to occur than unstimulated saliva which indicated that these samples were less elastic than unstimulated saliva. Also the filament breakup curves showed the classical 'beads on a string effect' which was an indication for low viscosity elastic fluids (Rodd et al, 2004). The filament breakup results are in accordance with the shear rheology results: for both unstimulated and caffeine stimulated WHS, there were no detected first normal stress differences which

indicated that these two samples are less elastic compared with other samples. As discussed previously it was probably due to the inhibition effect of caffeine on secretion of proteins such as mucins and therefore reduced the elasticity of saliva. Also there was an 'astringency' mouthfeel reported from the subjects when stimulated with caffeine solutions which could be another clue for the reduction of protein secretion. It may be relevant in future studies to investigate the protein concentration of saliva stimulated caffeine and also to find out if other bitterness tastants have similar kind of effect on saliva.

Citric acid stimulated WHS produced the longest relaxation and breakup time across all the samples tested. It can be seen from Figure 4.57 that the filament diameter initially dropped to a certain value, but then remained almost constant for a long time. It has been observed that for 0.125M citric acid stimulated WHS, it took more than 120 s to break up. It was also found that 0.125M stimulated WHS took longer to breakup compared with 0.05M and 0.25M citric acid stimulated samples. This is again in agreement with what the shear rheology results (see Figure 4.52) that 0.125M citric acid was highest in both shear viscosity and N_1. The highly elastic properties of citric acid stimulated saliva could be aroused as a defence for oral cavity against acid erosion on teeth in order to form salivary pellicle. Moreover the highly elastic saliva was found to be related to mouthfeel of 'thick' due to the less spreading of saliva (Stokes and Davies, 2007; Davies et al, 2009).

Based on the relaxation and breakup time, the order for the elasticity of WHS under different stimuli is citric acid> sucrose>MSG>NaCl>caffeine. Literature on the extensional rheology of stimulated saliva is scarce and the only paper that can be used to compare the present data was published by Zussman et al. (2007). They used an elongational rheometer to study the viscoelasticity of both unstimulated saliva and 2% citric acid stimulated saliva, and found that the relaxation times for unstimulated and citric acid stimulated saliva were 0.001 s and 0.00346 s, respectively, which is much lower than the results found in this study. One reason for the difference could be the different concentrations of citric acid used. Since the concentration used in this research was higher compared with the other study and therefore could lead to more secretion of proteins and higher concentrations of polymers will normally lead to a longer relaxation time. The relaxation time of saliva was also studied using shear rheology. Stokes and Davies (2007) found that the relaxation time for citric acid stimulated saliva could reach up to 76.2 s by fitting the shear rheology of saliva with a finitely extensible non-linear elastic (FENE-P) dumbbell model. Haward et al. (2011) found that the relaxation time for the longest salivary mucin macromolecules was around 0.005s by using a modified extensional flow oscillatory rheometer (EFOR).

To summarize the main findings in this part, the effect of different stimuli and their concentrations on the breakup and relaxation time of WHS can be divided into three categories: (1) for caffeine stimulated saliva , the breakup time was shorter at all

concentrations which indicated lower elasticity than unstimulated saliva. Also the breakup time of caffeine stimulated saliva was independent on the concentration. (2) The breakup and relaxation time for WHS stimulated by different concentrations of NaCl and MSG were within same order of magnitude with MSG stimulated samples slightly higher than NaCl stimulated samples. In terms of relaxation time, higher values were found for moderate concentrations of NaCl while the concentration of MSG had little effect on the relaxation time. (3) When stimulated with sucrose or citric acid, the breakup and relaxation time of WHS was largely increased to several orders higher compared with other tastants stimulated samples. The effect of different concentration of stimulus on both relaxation and breakup time of saliva may have some implication to mouthfeel perception such as the 'thick' perception after citric acid has been used to stimulate the oral cavity and 'astringency' mouthfeel stimulated by caffeine.

4.5.2.5 The lubrication properties of WHS

As already mentioned in the literature review, see section 2.2.3, one of saliva's key functions in the oral cavity is lubrication (Carpenter, 2012). During oral processing of foods, the oral cavity is exposed to different kinds of stimulation such as mechanical, tastants and temperature etc., which could in turn change the properties of saliva and further change its lubrication properties. In this section, the aging effect on lubrication properties of saliva, and lubrication properties of stimulated saliva itself as well as mixing with polysaccharides are studied.

4.5.2.5.1 The effect of aging on the lubrication properties of WHS

The effect of aging on the lubrication properties of WHS is reported in this section. This test was a preliminary study to find out whether the aging of both stimulated and unstimualted WHS has an effect on the measurement results in the following experiment. 1M sucrose stimulated WHS was randomly selected as the stimulated WHS and was measured immediately, 15 and 30 minutes after collection. The Stribeck curves for 1M sucrose stimulated WHS and unstimulated WHS at different time points are shown in Figure 4.62.

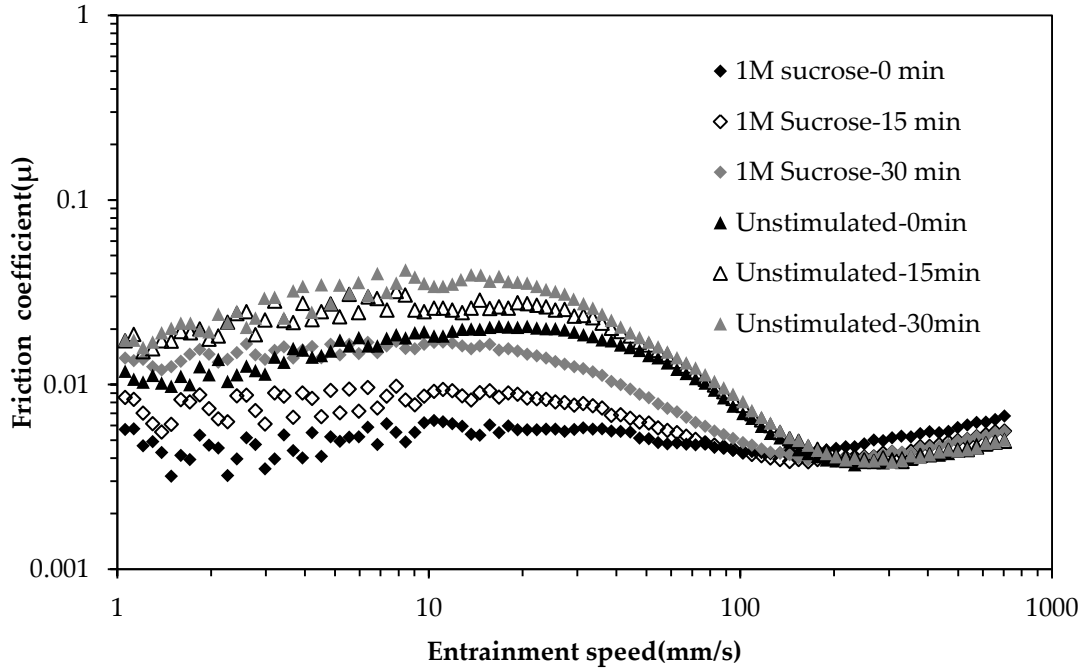

Figure 4.62: Stribeck curves for 1M sucrose stimulated WHS and unstimulated WHS measured at 37 °C immediately after collection (0 min), 15 min and 30 min after collection.

Rather than a plateau in the boundary regime of a typical Stribeck curve, the friction coefficient increased in the boundary regime. This effect has been reported

elsewhere (de Vicente et al., 2006, Gabriele et al., 2010) for polysaccharide samples. Gabriele et al. (2010) suggested that the upward slope at low entrainment speed is similar to that of the hydrodynamic regime and believed that a micro-hydrodynamic regime occurs for the continuous phase before the film thickness is large enough to allow for bulk entrainment. The researchers also gave another possible explanation based on the fact that they investigated a suspension system: for particles larger than the roughness of friction surface dimensions, they are excluded from entrainment and therefore accumulated around the contact with increasing speed thus depriving the contact of lubricant. Other researchers also observed this increase of friction coefficient with speed in the boundary regime for water which they believed was due to the increased shear stress with sliding velocity (Chugg and Chaudhri, 1993, Cassin et al., 2001).

Possible reasons for the increased friction coefficient of saliva samples could be: (1) It was the buccal epithelial cells in the WHS that were excluded from the entrainment during boundary regime which prevented the saliva from entering the contact surface. (2) It was the buccal epithelial cells as well as large molecular proteins such as mucin that caused this effect. It has been demonstrated that the initial slope is absent in both centrifuged and aged WHS (Bongaerts et al., 2007a, Macakova et al., 2011). As for both centrifuged and aged WHS, there are very few large molecular weight proteins present, therefore it should be the proteins, e.g. mucin that caused the initial slope.

In terms of the aging effect on the lubrication properties of saliva, as can be seen from the results, the friction coefficients of WHS for both stimulated and unstimulated WHS changed rapidly after collection. The friction coefficients of both stimulated and unstimulated WHS were increased after 15 and 30minutes of collection in the boundary regime and part of the mixed regime. It has been reported that the friction coefficient of unstimulated WHS was constant at the entrainment speed of 5mm/s for more than 1 hour (Bongaerts et al., 2007a). However, this was not the case here and similarly other researchers have reported that the lubrication property of saliva reduced significantly over time during eight hours of storage (Vardhanabhuti et al., 2011). Also it was found in this research that the effect of time on the lubrication properties was even larger for stimulated than for unstimulated WHS, see Table 4.31. The possible reason for the reduction in lubrication, i.e. increase in friction coefficient, of saliva could be the reduction of elasticity. It has been shown previously that although the shear viscosity of WHS was consistent, the elasticity was reduced quickly with time (Stokes and Davies, 2007). Another possible reason could be the degradation of saliva protein, e.g. mucins during aging. It is known that the adsorption of polymers to the contact surface could significantly reduce the friction coefficients in the boundary and the mixed regime (Selway and Stokes, 2013). Therefore, the increased coefficients in the boundary and the mixed regime could be an indication of reduced amount of surface-adsorbing polymers in aging saliva.

Table 4.31: The effect of time on friction coefficient for unstimulated and 1M sucrose stimulated WHS at sliding speeds of 5mm/s and 10mm/s.

Sliding speed mm/s	WHS samples	Friction coefficient(μ) 0min	15min	30min
5mm/s	Unstimulated	0.0174	0.0233	0.0346
	1M sucrose	0.00493	0.00703	0.0145
10mm/s	Unstimulated	0.0183	0.026	0.034
	1M sucrose	0.00638	0.00919	0.0169

To summarise, aging has a significant effect on the lubrication properties of both stimulated and unstimulated WHS. Therefore freshly collected WHS should always be used for analysis.

4.5.2.5.2 The lubrication properties of stimulated WHS

In this section, the lubrication properties of WHS stimulated by different tastants are reported. The five basic tastants at the second highest concentration were used to collect the stimulated WHS. Also unstimulated WHS, water and dry surfaces were used as references. The Stribeck curve for different WHS as well as dry surfaces and water are illustrated in Figure 4.63.

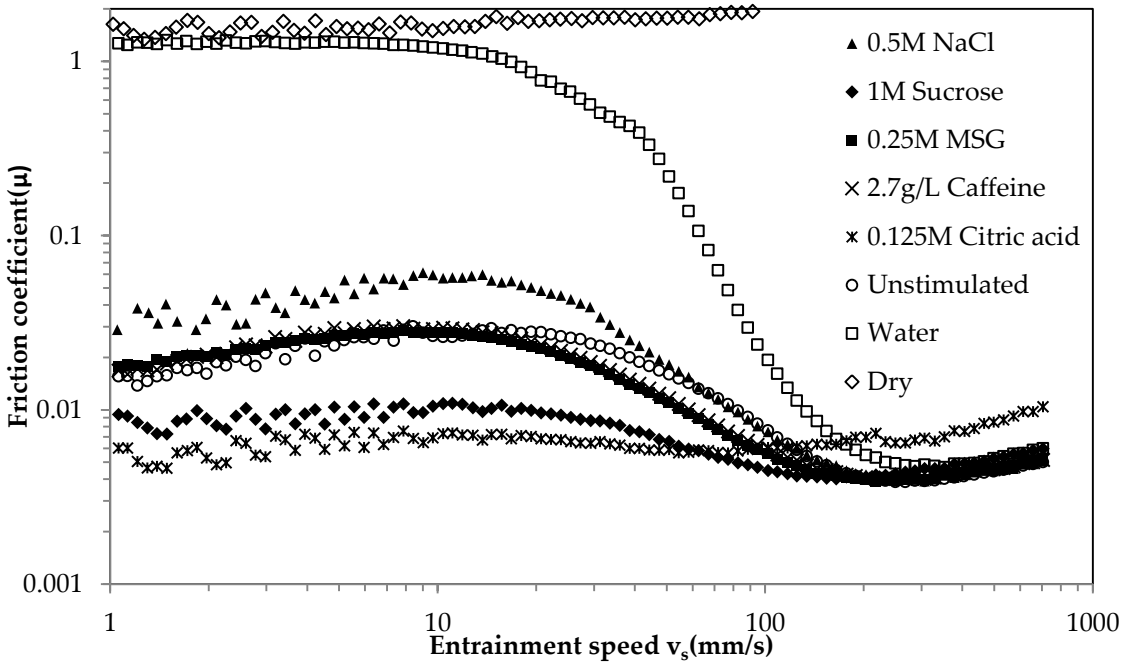

Figure 4.63: The Stribeck curves for five basic tastes stimulated WHS, unstimulated WHS, water and dry surface. Measured at 37 °C.

As can be seen from Figure 4.63, the friction coefficient for the dry surface was independent of the sliding speed and at the Normal Load of 3N, the friction coefficient of the dry surface was around 1.5 at the speed of 10mm/s. For water and WHS samples, the friction coefficient depended on the entrainment speed. For water, there was a plateau in the Stribeck curve at low speed between 1 and 10 mm/s which indicated boundary lubrication. As friction in the boundary regime is mainly influenced by the surface properties of the friction partners, the result here indicates that water did not change the properties of the PDMS surface. With increased speed, the friction coefficient decreased, reaching a minimum of 0.0045 at a speed of around 300mm/s which indicates the end of the mixed regime. Then the fiction coefficient increases with increasing speed in the hydrodynamic regime.

For all WHS samples, the friction coefficient in the boundary regime was dramatically reduced when compared with the dry surface and water. A slight increase in the friction coefficient with increasing entrainment speed was observed for all WHS samples in the mixed regime. Except for citric acid stimulated WHS, the Stribeck curves converge at the same point of minimum friction at speed of 300 mm/s, representing the transition from mixed to elasto-hydrodynamic lubrication where only the fluid's rheology determines the tribological response. The citric acid stimulated WHS was found to reach the lowest friction coefficient at the much lower speed of around 60mm/s, although the minimum friction coefficient was slightly higher.

When comparing the friction coefficient of the samples in boundary and mixed regime, it was found that citric acid stimulated WHS produced the lowest friction coefficient followed by the sucrose stimulated WHS. MSG and caffeine stimulated WHS are found not significantly different compared with unstimulated WHS in the boundary regime(p<0.05). However, the unstimulated WHS produced slightly higher friction coefficients in mixed regime compared with MSG and caffeine stimulated WHS. NaCl stimulated WHS was seen to produce the highest friction coefficient in the boundary regime among all of the WHS samples. The reason for the remarkable reduction of the friction coefficient in the boundary regime for WHS samples could be several: it has been reported that boundary and mixed regimes are more related to surface interactions. The boundary lubrication is generally obtained

through molecules that interact with the contact surfaces. However, for large, non-adsorbing molecules, the friction coefficient was only reduced in the mixed regime. Also the researchers found that for non-adsorbing molecules such as guar gum solution, as with increased concentration, the friction coefficient in the boundary-to-mixed regime decreases (Cassin et al., 2001). It is known that mucin tends to be adsorbed on the hydrophobic surface to form a monolayer film of about 4-6 nm (Shi and Caldwell, 2000). The presence of the adsorbed salivary film renders the hydrophobic surfaces hydrophilic and reduces the boundary friction coefficient between these surfaces in aqueous media. The mechanism behind this is discussed in detail by Macakova et al (2010 &2011): the saliva adsorbs to the hydrophobic surface to form a heterogeneous film which is highly hydrated and viscoelastic. This film consists of an anchoring sublayer, which contains small salivary proteins and nonglycosylated parts of glycoproteins and a lubricious outer layer consisting of glycosylated hydrated chains of the glycoproteins. It has been suggested that the observed low friction in the boundary regime can be understood in the context of other highly hydrated polyelectrolyte structures in good solvents. For surfaces that are lubricated by these polymers, the low boundary friction is due to the strong anchoring of the polymer onto the contacting surfaces and their ability to support applied loads. As with increase of the applied load, the osmotic pressure within the interpenetration zone of the absorbed polymer is increased and acts against the load. Therefore the effective load is decreased and so are the friction coefficients (Macakova et al., 2010, 2011).

It should also be noted that despite the differences in the friction coefficient in the boundary and mixed regime, the friction coefficients in the hydrodynamic regime are almost identical for the WHS samples except for citric acid stimulated WHS. It is known that the friction coefficient in the elasto-dydrodynamic is related to the viscosities of fluids at very high shear rate such as 10^4 s^{-1} (Stokes et al., 2011, Selway and Stokes, 2013). Therefore the results indicate that all the WHS samples have the similar high shear viscosities except for citric acid stimulated WHS. The results from shear viscosities of these samples are actually in accordance with lubricant behaviour: the viscosity of 0.125M stimulated saliva at shear rate of 5000 was almost three times higher than WHS stimulated by other tastants (see Table 4.28).

4.5.2.5.3 The effect of saliva on the lubrication properties of hydrocolloid solutions

The lubrication properties of hydrocolloids solutions as well as the relationship with sensory perception were previously studied in section 4.4. It is however unknown how the lubrication properties of hydrocolloids were changed due to the aid of stimulated saliva during oral processing. In this section, the lubrication properties of designed samples P1-P10 mixed with both taste and flavour stimulated WHS are studied. A solution containing 3% (w/w) sucrose and 100 p.p.m. IAA was used as the stimulus because these are also the same concentrations of taste and flavour used in the designed samples. The stimulated WHS and polysaccharide samples were added to the tribology cell at the same time at the weight ratio of 1:5. For each

measurement, the stimulated saliva was freshly collected and added to the solution without delay. Also water was added to the polysaccharide solutions at the same ratio as a control. To mimic the oral mixing, a ten second pre-shear at the speed of 100mm/s at 3N was applied. The results are shown in separate figures for the sample, the sample mixed with water and the sample mixed with WHS. Figure 4.64- 4.66 are showing results for samples of Group 1 and Figures 4.67-4.69 are showing results from samples of Group 2.

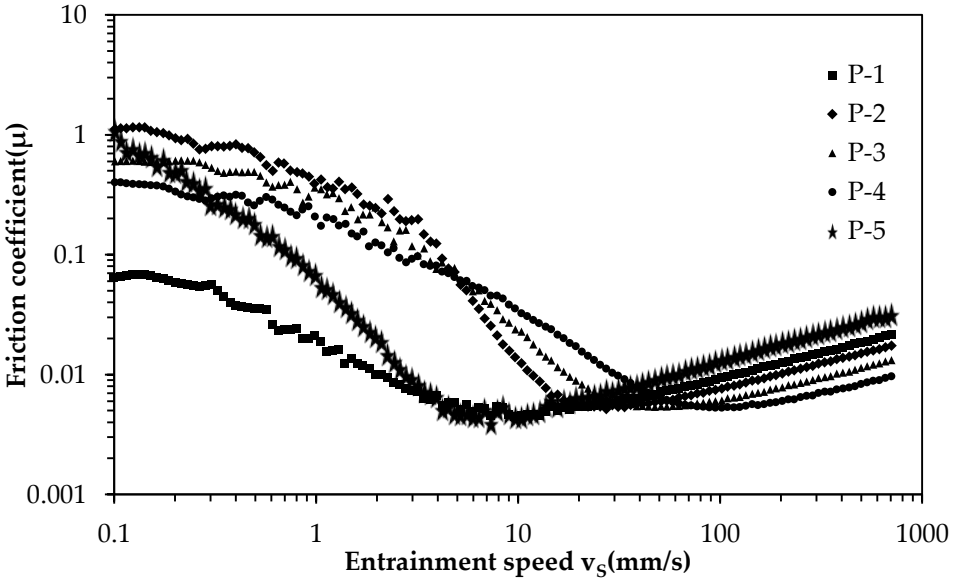

Figure 4.64: The Stribeck curves for Sample P1-P5 (Measured at 37 °C)

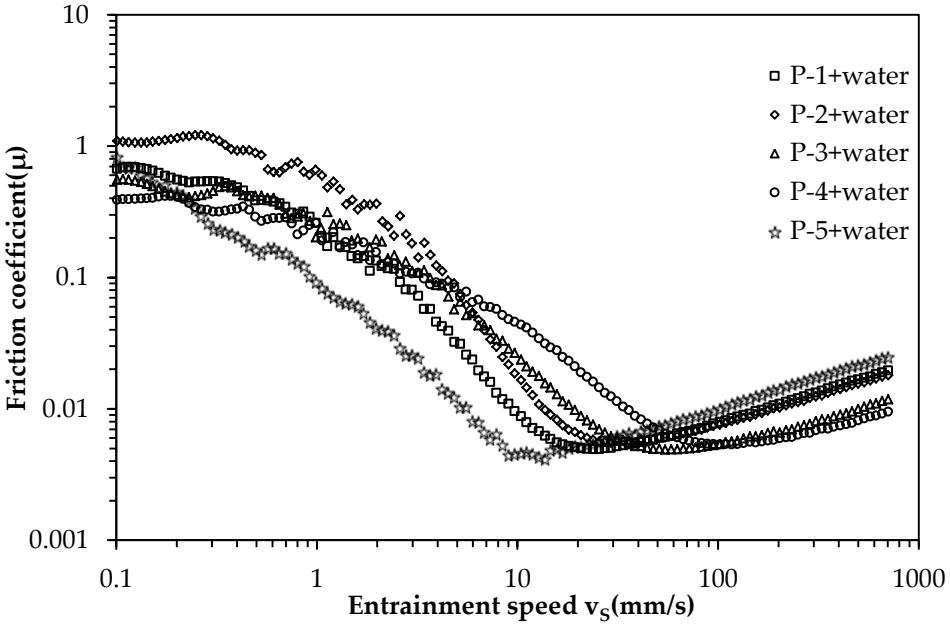

Figure 4.65: The Stribeck curves for Sample P1-P5 mixed with water (Measured at 37 °C)

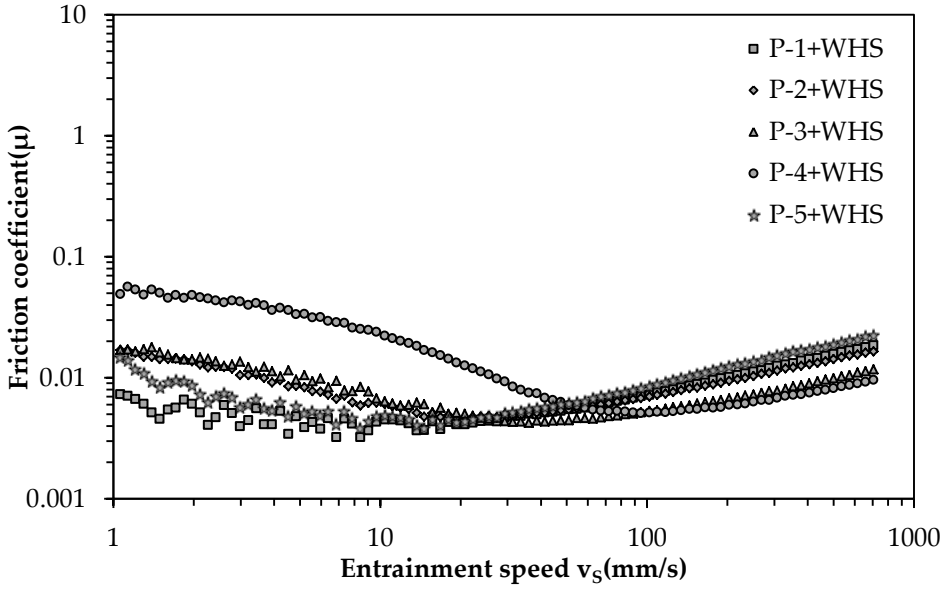

Figure 4.66: The Stribeck curves for Sample P1-P5 mixed with 3% sucrose and 100 p.p.m. IAA stimulated saliva (Measured at 37 °C)

Figure 4.64 shows the friction coefficient of samples P1-P5 as a function of the entrainment speed. The friction coefficient decreases to a minimum and then increases with entrainment speed which indicates the mixed and hydrodynamic regimes, respectively. There are short boundary regimes for samples P1-P4. However for P5, there is no obvious boundary regime and only the mixed and hydrodynamic regime is observed. Also it should be noted that the friction coefficient reaches the lowest value at different entrainment speed and the samples with higher viscosities at high shear rate tend to reach the lowest friction at lower entrainment speed. In terms of friction coefficient at low entrainment speed, most samples show a value of 1 at the entrainment speed of 0.1 mm/s. However, the friction coefficient for P1 at speed of 1 mm/s is about 1 order of magnitude lower.

Figure 4.65 shows that when mixing the polysaccharide samples with water at the ratio of 5:1, the friction coefficients for most of samples stay unchanged except for sample P1. The friction coefficient for P1 is increased by almost one order of magnitude in the mixed regime and slightly decreased in the hydrodynamic regime. Also, the minimum friction coefficient is reached at a higher entrainment speed.

It is shown in Figure 4.66 that when mixing polysaccharide samples with stimulated saliva, the friction coefficients in the mixed regime are reduced by at least one order of magnitude compared with polysaccharide only results. However, in terms of the transition point from mixed to hydrodynamic regime as well as the friction

coefficient in the hydrodynamic regime, there are no significant difference between polysaccharide samples and added saliva samples.

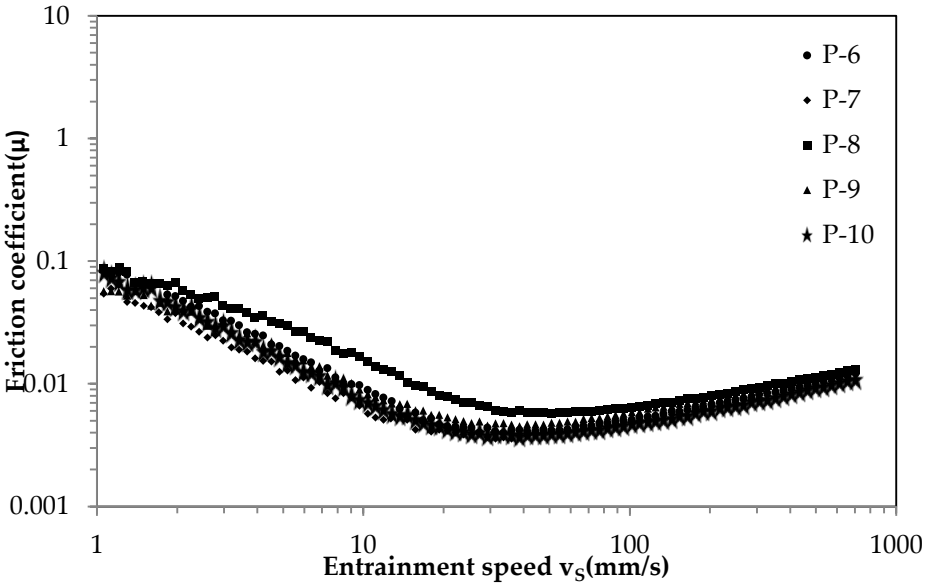

Figure 4.67: The Stribeck curves for Sample P6-P10 (Measured at 37 °C)

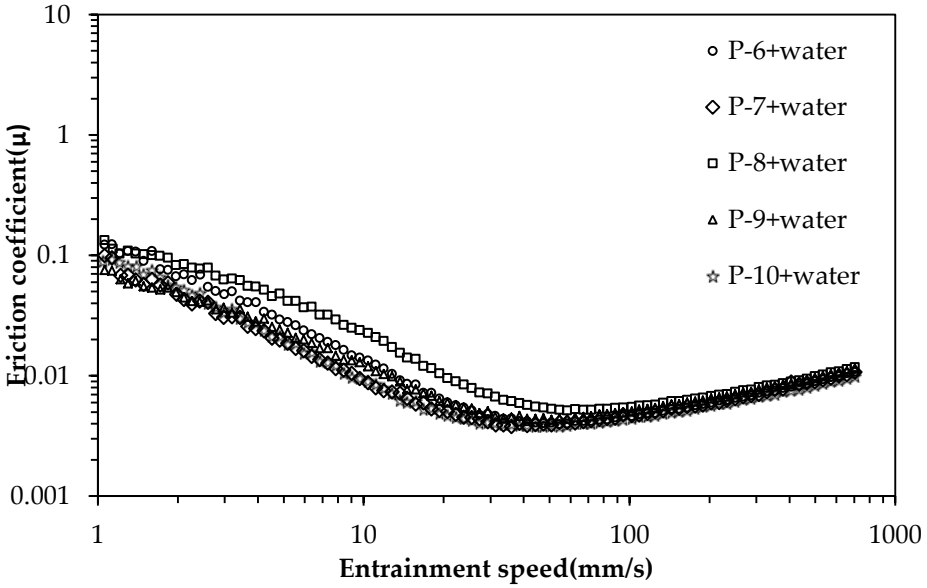

Figure 4.68: The Stribeck curve for Sample P6-P10 mixed with water in (Measured at 37 °C)

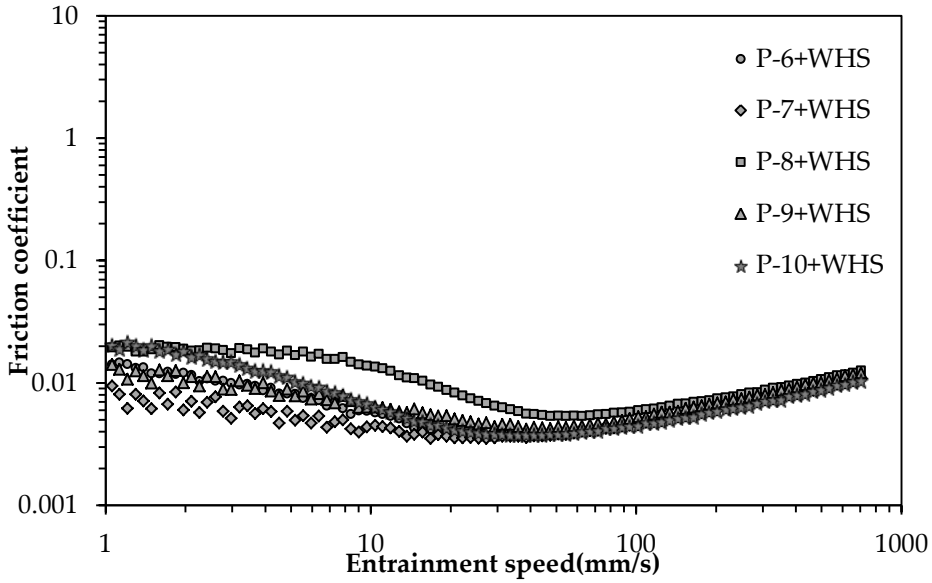

Figure 4.69: The Stribeck curve for Sample 6-10 mixed with 3% sucrose and 100 p.p.m. IAA stimulated saliva (Measured at 37 °C)

For group 2 samples which have similar high shear viscosity but different low shear viscosities, the friction coefficient was almost overlapped in the hydrodynamic regime as expected. It also worth noting that P8 has higher fiction coefficients in the mixed regime compared with the other samples, see Figure 4.67. Again, no obvious boundary regime can be identified based on the present set of data. The transition point from mixed to hydrodynamic regime for most samples occurs at the entrainment speed of around 30mm/s except for sample P8 for which it is around 50 mm/s. As can be seen from Figure 4.68, when water is added to the polysaccharide solutions of Group 2, the friction coefficients are almost unchanged which is similar to the circumstance for samples of Group 1. When samples of Group 2 are mixed with stimulated WHS, the friction coefficients are significantly reduced by about one

order of magnitude in the low entrainment speed range of below 10 mm/s for all samples, see Figure 4.69. Also most of the samples showed boundary regimes.

When comparing the two groups of samples, it was found that for Group 1 samples which have similar viscosities at shear rate of 50 s^{-1} but different viscosities at 10^5 s^{-1}, have higher friction coefficients at low entrainment speed than the samples of Group 2 which have similar high shear viscosities, except for sample P1. It seemed that the lower friction coefficients were mainly due to the higher viscosities at low shear rates as Group 1 samples have higher low shear viscosities than that of Group 2 samples. However, this was not the case for P1 and P8. Although P1 has higher low shear viscosities than most of the samples in Group 2, its friction coefficient at low entrainment speed was identical to the samples in Group 2. On the contrary, although P8 has higher low shear viscosities than the rest of samples in Group 2, its friction coefficient in the mixed regime was similar to the other samples.

The high friction coefficients for Group 1 samples may be due to the confirmation and concentration of the polymer in these samples. It has been suggested that for polymers with random coil secondary structure, they could retain their entanglements even at high shear rate in concentrated solutions. However, for less concentrated solution, the polymer structure is more expanded at such high shear rate (Garrec and Norton, 2012). This structure may attribute to the friction in the boundary and mixed regime of lubrication. In less concentrated solution, the polymer structures are more expanded and therefore more easily entrained into the

contact zone than more concentrated solution. This is may explain the effect that for most samples of Group 1 the friction coefficients in boundary and mixed regimes are higher than that of samples in Group2.

In addition to the conformation of the polysaccharide solution, it has been suggested that the main reason that may cause differences in the tribological profiles are those not viscosity-related such as surface related properties such as adhesion, wettability and molecular adsorption (Selway and Stokes, 2013). Moreover, the mixed regime was found to depend on the hydrated adsorbed polymer mass and the adsorbed film storage modulus and the transition point was found to be directly related to the wet mass of adsorbed polymer (Stokes et al., 2011). The origins of boundary lubrication have been reported by researchers as: (1) physisorption due to van der Waals and London dispersive interactions of the polymers on the surfaces that produces a change in the composition of the fluid in the contact zone; (2) molecular ordering due to the presence of the solid surfaces that produce immobile, solid- like layers and (3) confining effects by which the polymer concentration in the contact zone increases (Cassin et al., 2001).

It has been suggested that the friction behaviour of polysaccharides in the hydrodynamic regime is mainly due to the differences in viscosities at shear rates in the order of 10^4 s^{-1} (Stokes et al., 2011). This is in agreement with this research and moreover, it was found that samples with higher viscosities at high shear rate tend to reach their transition point from mixed to hydrodynamic at lower entrainment

speed. Furthermore, for samples with higher viscosity at high shear rate, the friction coefficients were higher in the hydrodynamic regimes.

When mixing with water, the friction coefficients for both samples in the two groups stayed unchanged except for sample P1 and P5. The friction coefficients of sample P1 and P5 in boundary and mixed regime increase, and also the entrainment speed at which transition point occurred increases slightly. For other samples, the addition of water does not change their friction coefficients. The possible reason could be the dextran concentrations in these two samples which have the highest and second highest concentration of dextran. Thoreau et al. (2005) suggested that dextran adsorption was increased with either the hydrophobic character of the substrate or the concentration of dextran. This could be the reason for the increase of friction coefficients for P1 and P5 in boundary and mixed regimes. As these two samples have the highest dextran concentration, the addition of water may significantly change the concentration of dextran compared with other samples, and therefore significantly changed the adsorption of dextran to the hydrophobic surfaces.

For both groups of samples, when mixed with stimulated saliva, the friction coefficients in the boundary and the mixed regime are largely reduced and the boundary regimes are extended to higher entrainment speed. As discussed previously, due to the adsorbing biopolymers such as mucin, saliva could change the properties of hydrophobic surfaces and hence considerably reduce the friction coefficients in boundary and mixed regimes (Shi and Caldwell, 2000, Bongaerts et al.,

2007b, Macakova et al., 2011). Also it should be noted that for sample P4 and P8, the drop in friction coefficients in the boundary and mixed regime is not as large as for the other samples. When checking the composition of polysaccharides in these two samples, it is found that these two samples have the highest concentration of xanthan gum. The possible reason for the relatively higher friction coefficient could be that the high concentration of xanthan restricts the mixing of saliva with the polysaccharide solution and therefore salivary proteins cannot reach the contacting surface as efficiently as they are in the samples with lower concentrations of xanthan. The lubrication properties of polysaccharides solutions mixed with saliva has been studied elsewhere using starch and locust bean gum (LBG)(Zinoviadou et al., 2008). It was found that the friction coefficients of starch mixed with saliva was increased but remained unchanged for saliva treated LBG solutions. The researchers suggested it was due to the reduced viscosity of saliva treated starch that caused the increase of friction coefficients.

5 CONCLUSIONS AND FUTURE WORK

The main purpose of this research was to understand both mouthfeel and flavour perceptions of hydrocolloid thickened systems, through the study of their flow and lubrication behaviour. As hydrocolloids are widely used in foods as thickeners, it is essential for food product developers to understand the impact of these ingredients on sensory perception. In contrast to time-consuming and expensive sensory tests, food researchers have tried to use instrumental methods to predict consumer sensory perception. In this context, rheology, especially shear rheology, has been most extensively studied to-date.

This research started with one question that has been debated for many years, but still has no definitive answer: which shear rate(s) is most appropriate to apply to viscosity analysis of liquid and semi-liquid foods to correlate to sensory perception? In order to answer this question, two groups of samples with either identical shear viscosities at a shear rate of 50 s^{-1} or at 10^5 s^{-1} were developed by varying the concentrations of two polymers: shear thinning xanthan gum and Newtonian dextran. These samples were analysed for their flow behaviour in shear, uniaxial extension and in small deformation oscillatory shear, as well as their lubrication behaviour with the aim to expand the current understanding of oral processing of liquid and semi-liquid foods. The samples were flavoured with equal levels of sucrose and banana flavour (IAA) to explore how flow and tribological behaviour of samples may affect flavour perception. The samples were evaluated by trained

panellists in terms of both mouthfeel and flavour attributes. The results from both physical and sensory analysis were comprehensively explored to identify the relationships between the two. These relationships were further validated using additional hydrocolloids. The main conclusions with regard to these objectives are summarized in the three following sections: 5.1 Flow behaviour and sensory perception, 5.2 Lubrication behaviour and sensory perception, and 5.3 Saliva related work.

5.1 Flow behaviour and sensory perception

- **A method was developed to design samples with identical low or high shear viscosity.**

Two groups of samples with desired shear rheological properties were developed by varying the concentration of xanthan gum and dextran, with the low shear viscosity mainly decided by the concentration of xanthan gum while high shear viscosities were most influenced by the concentration of dextran. The samples with higher concentrations of dextran were also more elastic with higher first normal stress differences detected in shear flow and longer relaxation and breakup time in the filament breakup measurements. The concentration of xanthan gum had a strong effect on the dynamic properties under small deformation. Samples with higher concentrations of xanthan gum were more viscoelastic and the viscoelastic moduli were less frequency dependent within the LVE domain.

- **Samples with similar viscosity values at 50 s^{-1} or 10^5 s^{-1} were perceived significantly different for mouthfeel perceptions.**

Despite having similar viscosity at 50 s^{-1} or 10^5 s^{-1}, perceived mouthfeel perception was significantly different in terms of thickness, stickiness and mouthcoating perception. The results indicated that both viscosities at low and high shear rate are related to mouthfeel perception.

- **Viscosity at 50 s^{-1} was most related to mouthfeel perception, but a better prediction model for 'thickness' perception was achieved by including both viscosities at 50 s^{-1} and 10^5 s^{-1}.**

Viscosity at 50 s^{-1} was better correlated with mouthfeel perceptions, but models built only including viscosity at 50 s^{-1} were not as good as those including both viscosity values at 50 s^{-1} and 10^5 s^{-1}. This indicated a wide range of shear rates operate in the mouth and contribute to mouthfeel. The models however, should be used with caution for other hydrocolloids and only as a general guidance for thickness perception from shear thinning solutions unless one has verified that the rheological fingerprint falls within the design space of the samples evaluated in this research.

- **Stickiness and mouthcoating perceptions were better predicted through a model including viscosity at 50 s^{-1} and extensional viscosity.**

Stickiness and mouthcoating were more related to extensional viscosity than shear viscosity. Models including viscosity at 50 s^{-1} and also extensional viscosity were used to predict the perceptions of 'stickiness and mouthcoating'. The models were also found to be valid for other hydrocolloids showing shear thinning behaviour

but not valid for Newtonian solutions. This result indicates that perceptions of 'Stickiness and Mouthcoating' are a combination of both shear and extensional flow in oral processing and that the rate dependency of the flow behaviour has a role to play.

- **Mouthfeel perception is related to complex viscosity at angular frequency of 100 rad.s^{-1}.**

The correlation between mouthfeel perceptions and complex viscosity increased with angular frequency and reached the highest correlation at the angular frequency of 100 rad.s^{-1}. This implies that during oral processing, foods may also undergo small deformation. This information can be used to facilitate the understanding of oral processing of liquid and semi-solid foods: there are not only shear flows during oral processing, but also small deformations as well.

- **Sweetness perception is affected by the degree of shear thinning.**

Sweetness perception is reduced with increased viscosity. When hydrocolloids have similar low shear viscosity at 50 s^{-1}, the overall sweetness perception is less affected for samples that are less shear thinning.

- **Flavour and sweetness perception interact.**

In-vivo flavour release indicated that there were no significant differences between designed samples for the maximum flavour intensity and total flavour release during samples evaluation. However, sensory scores for overall sweetness and flavour were highly correlated with each other. Since sweetness is strongly affected

by viscosity of samples, therefore it is the interaction between viscosity, sweetness and flavour that affect the final perception of samples.

5.2 Lubrication and sensory perception

- **The lubrication properties of hydrocolloids in mixed and hydrodynamic regime were determined by their high shear viscosity at 10^5 s^{-1}.**

The friction coefficients of hydrocolloids with higher viscosity at 10^5 s^{-1} were lower in mixed regime but higher in the hydrodynamic regime with transition from mixed to hydrodynamic regime occurring at a lower speed.

- **Mouthfeel perceptions were correlated with friction coefficients at speed range from 40-100 mm/s with the highest correlation occurring at 50 mm/s. Overall sweetness and flavour perceptions were correlated with friction coefficients at speeds of 10-30 mm/s with the highest correlation at speed of 20 mm/s.**

Mouthfeel perception was related to the lubrication behaviour of the designed samples in the hydrodynamic regime. The same applied to the other hydrocolloids such as guar, MC and dextran, although the hydrodynamic regime commenced at higher speeds. Overall sweetness and flavour perception for the designed samples were negatively correlated with friction coefficients at speeds of 10-30 mm/s.

5.3 Preliminary study of saliva

- **Stimulated saliva flow rate followed the order of citric acid > NaCl > sucrose > MSG > caffeine.**

The flow rate of saliva was dependent on stimulus concentration. For citric acid, NaCl, sucrose and MSG stimulated saliva flow rate increased with concentration.

However, the flow rate of saliva when stimulated with caffeine showed a more complex concentration dependence.

- **Stimulated saliva is shear thinning and degree of elasticity depends on stimulus.**

Stimulated saliva was shear thinning. When stimulated with different tastants, the elasticity is dramatically changed. Citric acid stimulated saliva showed the highest elasticity evidenced by the highest value for the first normal stress difference measured in large deformation steady shear as well as the highest filament breakup time determined in capillary break-up tests. The filament breakup time of citric acid stimulated saliva was several orders higher than following stimulation with any of other stimuli. The elasticity of sucrose stimulated saliva was the second highest followed by MSG and NaCl stimulated saliva. Caffeine stimulated saliva was less elastic compared with unstimulated saliva. This is probably related to the astringency mouthfeel reported by the subjects.

- **Saliva significantly reduced the friction in boundary and mixed regime.**

Saliva largely reduced the friction in the boundary and mixed regime by up to two orders of magnitude which is likely to be achieved by the presence of surface adsorbing proteins, e.g. mucins. Different stimulated saliva had different lubrication properties: citric acid and sucrose stimulated salvia led to the lowest friction, followed by caffeine and MSG stimulated saliva. NaCl stimulated saliva caused the highest friction among all the stimulated saliva.

- **The friction coefficient of hydrocolloid solutions mixed with saliva was reduced in both boundary and mixed regime, but not in the hydrodynamic regime.**

When mixing hydrocolloid solutions with saliva at a ratio relevant to oral processing, a boundary regime, absent for hydrocolloid solutions, was identified in the friction curves and friction coefficients were reduced by up to two orders of magnitude in the mixed regime. However, the friction in hydrodynamic regime is not changed. As mouthfeel perception was related to friction coefficients at speeds of 40-100 mm/s which were not changed after mixing the saliva, the lubrication properties of hydrocolloids that related to mouthfeel perceptions were not changed after mixing with saliva.

5.4 Overall conclusions and future work

To summarise, this research presents a novel study concerning the sensory perception of liquid and semi-solid foods using model hydrocolloid systems and a series of rheological and tribological methods. The results from this research confirmed the fact that oral processing is a complex procedure including different parameters, not only physical ones such as flow and friction behaviour, but also biological ones such as mixing with stimulated saliva. A better understanding and prediction of sensory perception can be achieved by combining these parameters. In order to further explore in this area, a few recommendations for future work are discussed in the following.

In the current research, the study of sensory perception was based on xanthan and dextran model system. This food-grade system has distinct characteristics due to the unique rheological properties of xanthan (highly elastic and shear thinning). Therefore the sensory prediction models developed from this system are limited with regard to application to other hydrocolloid samples. It might be useful to apply the same method to an even wider range of hydrocolloids, to determine whether this investigation method is still valid. Also, it would be useful to apply the method to liquid or semi-liquid foods with increasing complexity of microstructure, e.g. emulsions.

In the present study, the lubrication properties of samples were studied in a PDMS-steel contact. It would be useful to study the hydrocolloid samples in PDMS-PDMS contacts just as a comparison to find out if two soft contacts can be used to represent the oral surface better and further increase the correlation between friction behaviour and sensory perception. In addition, the current research has investigated the impact of the conformation of hydrocolloids on their lubrication properties and sensory perception based on limited types of hydrocolloids. Therefore, it would be valuable to investigate more hydrocolloid types in order to understand how conformation affects lubrication properties and moreover influenced sensory perceptions. In addition, the lubrication properties of the designed hydrocolloid samples were only linked to a limited list of sensory attributes. There could be other attributes related to lubrication properties in other hydrocolloid samples or other

food systems that require further investigation. Therefore it would be worthy to broaden this study in terms of sensory attributes including other hydrocolloid or food systems such as emulsions.

In terms of flavour and taste perception, the Napping® method has been proved to be an effective way to distinguish between samples. However, it is difficult using this technique to draw conclusions as to the reasons why samples are different in such way. One hypothesis that could be tested is that, for hydrocolloid thickened solutions, the intensity of flavour and taste maybe released at different rates. Therefore, it would be useful to carry out the Time Intensity or Temporal Dominance of Sensations Evaluation for the flavour and taste perception of samples. Together with the results from Descriptive Analysis and Napping, a better understanding of how thickeners may affect the flavour and taste release can be obtained. Moreover, it has been postulated in this research that different efficiency of 'mixing' during oral processing affected flavour and taste perception. It would be useful to study the mixing properties of different hydrocolloids with saliva during oral processing. This could be achieved by observing oral processed dyed hydrocolloid samples.

In order to better understand the effect of stimulus on saliva properties such as flow rate, rheological and tribological properties, it would be useful to have more subjects to generate more reliable results. Also, the effect of mixed stimulus on saliva secretion would be more useful because in real foods it is more common to have several stimuli, e.g. sour, sweet, aroma and mechanical etc, mixed together. To be in

a better position to interpret the rheological properties of saliva, it would be useful to compositionally analysis the saliva. Focus should be on the protein fraction and in particular the larger molecular weight mucin such as MUC5B. Appropriate analysis methods include GC-MS as well as the Analytical Ultracentrifugation (Harding, 2006). It would also be relevant to investigate the molecular interaction between different hydrocolloids and saliva or purified MUC5B using the same methods. This will aid in the understanding of the flow properties of the liquid foods during oral processing and may provide some guidance for the development of future food hydrocolloids from, for example sustainable sources such as waste or cellulose.

The effect of saliva on lubrication properties of hydrocolloids in this research was studied by *ex-vivo* mixing of flavour and stimulated saliva with hydrocolloid samples. However, during oral processing of hydrocolloid samples, there is combined stimulation such as mechanical jaw movement, viscosity stimulation from samples and flavour and taste stimulations. Therefore, in future work, it might be useful to study the lubrication properties as well as the rheological properties of the actually oral processed hydrocolloid samples. This will further facilitate the understanding of the role of saliva in sensory perception of different hydrocolloid thickened foods from both their flow and lubrication behaviour.

6 REFERENCES

Abdel-Halim, E. S. and S. S. Al-Deyab (2011). "Hydrogel from crosslinked polyacrylamide/guar gum graft copolymer for sorption of hexavalent chromium ion." Carbohydrate Polymers 86(3): 1306-1312.

Abdi, H. and L. J. Williams (2010). "Principal component analysis." Wiley Interdisciplinary Reviews: Computational Statistics 2(4): 433-459.

Abdi, H., L. J. Williams and D. Valentin (2013). "Multiple factor analysis: principal component analysis for multitable and multiblock data sets." Wiley Interdisciplinary Reviews: Computational Statistics 5(2): 149-179.

Abson, R., S. R. Gaddipati, J. Hort, J. R. Mitchell, B. Wolf and S. E. Hill (2014). "A comparison of the sensory and rheological properties of molecular and particulate forms of xanthan gum." Food Hydrocolloids 35(0): 85-90.

Ahmed, R. Z., K. Siddiqui, M. Arman and N. Ahmed (2012). "Characterization of high molecular weight dextran produced by Weissella cibaria CMGDEX3." Carbohydrate Polymers 90(1): 441-446.

Anna, S. L. and G. H. McKinley (2001). "Elasto-capillary thinning and breakup of model elastic liquids." Journal of Rheology 45(1): 115-138.

Baek, I., R. S. T. Linforth, A. Blake and A. J. Taylor (1999). "Sensory perception is related to the rate of change of volatile concentration in-nose during eating of model gels." Chemical Senses 24(2): 155-160.

Baines, Z. V. and E. R. Morris (1987). "Flavour/taste perception in thickened systems: the effect of guar gum above and below c." Food Hydrocolloids 1(3): 197-205.

Baines, Z. V. and E. R. Morris (1988). Effect of polysaccharide thickeners on organoleptic attributes. Gums and Stabilisers for the Food Industry 4. G. O. Phillips, P. A. Williams and D. J. Wedlock. Oxford, IRL Press: 192-201.

Bansil, R., H. E. Stanley and J. T. Lamont (1995). "Mucin Biophysics." Annual Review of Physiology 57: 635-657.

Bansil, R. and B. S. Turner (2006). "Mucin structure, aggregation, physiological functions and biomedical applications." Current Opinion in Colloid & Interface Science 11(2-3): 164-170.

Bardow, A., D. Moe, B. Nyvad and B. Nauntofte (2000). "The buffer capacity and buffer systems of human whole saliva measured without loss of CO2." Archives of Oral Biology 45(1): 1-12.

Barnes, H. A., J. F. Hutton and K. Walters (1989). An introduction to rheology. Amsterdam ; New York, Elsevier : Distributors for the U.S. and Canada, Elsevier Science Pub. Co.

Baxter, N. J., T. H. Lilley, E. Haslam and M. P. Williamson (1997). "Multiple interactions between polyphenols and a salivary proline-rich protein repeat result in complexation and precipitation." Biochemistry 36(18): 5566-5577.

Bazilevsky, A. V., V. M. Entov and A. N. Rozhkov (1990). Liquid Filament Microrheometer and Some of Its Applications. Third European Rheology Conference and Golden Jubilee Meeting of the British Society of Rheology. D. R. Oliver, Springer Netherlands: 41-43.

Bezdek, J. C., C. Coray, R. Gunderson and J. Watson (1981). "Detection and Characterization of Cluster Substructure .1. Linear Structure - Fuzzy C-Lines." Siam Journal on Applied Mathematics 40(2): 339-357.

Bhushan, B. (1999). Principles and applications of tribology. New York, John Wiley.

Bhushan, B. (2001). Modern tribology handbook. Boca Raton, FL, CRC Press.

Bhushan, B. and I. Ebrary (2013). Principles and applications of tribology [electronic resource]. Hoboken Chichester, West Sussex, John Wiley & Sons Inc.

Bongaerts, J., D. Rossetti and J. Stokes (2007a). "The Lubricating Properties of Human Whole Saliva." Tribology Letters 27(3): 277-287.

Bongaerts, J. H. H., D. Rossetti and J. R. Stokes (2007b). "The lubricating properties of human whole saliva." Tribology Letters 27(3): 277-287.

Bousfield, D. W., R. Keunings, G. Marrucci and M. M. Denn (1986). "Nonlinear-Analysis of the Surface-Tension Driven Breakup of Viscoelastic Filaments." Journal of Non-Newtonian Fluid Mechanics 21(1): 79-97.

Breer, H. (2003). "Olfactory receptors: molecular basis for recognition and discrimination of odors." Analytical and Bioanalytical Chemistry 377(3): 427-433.

Cardenas, M., T. Arnebrant, A. Rennie, G. Fragneto, R. K. Thomas and L. Lindh (2007). "Human saliva forms a complex film structure on alumina surfaces." Biomacromolecules 8(1): 65-69.

Carpenter, G. (2012). Role of Saliva in the Oral Processing of Food. Food Oral Processing, Wiley-Blackwell: 45-60.

Cassin, G., E. Heinrich and H. A. Spikes (2001). "The Influence of Surface Roughness on the Lubrication Properties of Adsorbing and Non-Adsorbing Biopolymers." Tribology Letters 11(2): 95-102.

Catalan, M. A., T. Nakamoto and J. E. Melvin (2009). "The salivary gland fluid secretion mechanism." J Med Invest 56 Suppl: 192-196.

Chamberlain, E. K. and M. A. Rao (1999). "Rheological properties of acid converted waxy maize starches in water and 90% DMSO/10% water." Carbohydrate Polymers 40(4): 251-260.

Chatraei, S., C. W. Macosko and H. H. Winter (1981). "Lubricated Squeezing Flow - a New Biaxial Extensional Rheometer." Journal of Rheology 25(4): 467-467.

Chaudhari, N. and S. D. Roper (2010). "The cell biology of taste." Journal of Cell Biology 190(3): 285-296.

Chauncey, H. H. and I. L. Shannon (1960). "Parotid Gland Secretion Rate as Method for Measuring Response to Gustatory Stimuli in Humans." Proceedings of the Society for Experimental Biology and Medicine 103(3): 459-463.

Chen, J., M. Feng, Y. Gonzalez and L. A. Pugnaloni (2008). "Application of probe tensile method for quantitative characterisation of the stickiness of fluid foods." Journal of Food Engineering 87(2): 281-290.

Chen, J. and J. R. Stokes (2012). "Rheology and tribology: Two distinctive regimes of food texture sensation." Trends in Food Science & Technology 25(1): 4-12.

Chen, J. S. (2009). "Food oral processing - A review." Food Hydrocolloids 23(1): 1-25.

Choppe, E., F. Puaud, T. Nicolai and L. Benyahia (2010). "Rheology of xanthan solutions as a function of temperature, concentration and ionic strength." Carbohydrate Polymers 82(4): 1228-1235.

Christensen, C. M. (1979). "Oral perception of solution viscosity." Journal of Texture Studies 10(2): 153-164.

Christensen, C. M. (1980). "EFFECTS OF SOLUTION VISCOSITY ON PERCEIVED SALTINESS AND SWEETNESS." Perception & Psychophysics 28(4): 347-353.

Christensen, C. M., J. G. Brand and D. Malamud (1987). "Salivary changes in solution pH: A source of individual differences in sour taste perception." Physiology & Behavior 40(2): 221-227.

Chugg, K. J. and M. M. Chaudhri (1993). "Boundary Lubrication and Shear Properties of Thin Solid Films of Dioctadecyl Dimethyl Ammonium-Chloride (Ta100)." Journal of Physics D-Applied Physics 26(11): 1993-2000.

Connelly, R. K. and J. L. Kokini (2004). "The effect of shear thinning and differential viscoelasticity on mixing in a model 2D mixer as determined using FEM with particle tracking." Journal of Non-Newtonian Fluid Mechanics 123(1): 1-17.

Cook, D. J., T. A. Hollowood, R. S. T. Linforth and A. J. Taylor (2003). "Oral shear stress predicts flavour perception in viscous solutions." Chemical Senses 28(1): 11-23.

Cowart, B. J. and G. K. Beauchamp (1986). 2 - Factors Affecting Acceptance of Salt by Human Infants and Children. Interaction of the Chemical Senses with Nutrition. R. K. Morley, Academic Press: 25-44.

Cox, W. P. and E. H. Merz (1958). "Correlation of Dynamic and Steady Flow Viscosities." Journal of Polymer Science 28(118): 619-622.

Cross, M. M. and A. Kaye (1987). "Simple procedures for obtaining viscosity/shear rate data from a parallel disc viscometer." Polymer 28(3): 435-440.

Cutler, A. N., E. R. Morris and L. J. Taylor (1983). "ORAL PERCEPTION OF VISCOSITY IN FLUID FOODS AND MODEL SYSTEMS." Journal of Texture Studies 14(4): 377-395.

Da Silva, P. M. S., J. C. Oliveira and M. A. Rao (1998). "Rheological properties of heated cross - linked waxy maize starch dispersions." International Journal of Food Properties 1(1): 23-34.

Dahl, T. and T. Naes (2004). "Outlier and group detection in sensory panels using hierarchical cluster analysis with the Procrustes distance." Food Quality and Preference 15(3): 195-208.

Davidson, J. M., R. S. T. Linforth, T. A. Hollowood and A. J. Taylor (1999). "Effect of sucrose on the perceived flavor intensity of chewing gum." Journal of Agricultural and Food Chemistry 47(10): 4336-4340.

Davies, G. A. and J. R. Stokes (2008). "Thin film and high shear rheology of multiphase complex fluids." Journal of Non-Newtonian Fluid Mechanics 148(1-3): 73-87.

Davies, G. A., E. Wantling and J. R. Stokes (2009). "The influence of beverages on the stimulation and viscoelasticity of saliva: Relationship to mouthfeel?" Food Hydrocolloids 23(8): 2261-2269.

Davis, S. S. (1971). "The rheological properties of saliva." Rheologica Acta 10(1): 28-35.

de Vicente, J., J. R. Stokes and H. A. Spikes (2005). "Lubrication properties of non-adsorbing polymer solutions in soft elastohydrodynamic (EHD) contacts." Tribology International 38(5): 515-526.

de Vicente, J., J. R. Stokes and H. A. Spikes (2006). "Soft lubrication of model hydrocolloids." Food Hydrocolloids 20(4): 483-491.

de Wijk, R. A., L. Engelen and J. F. Prinz (2003). "The role of intra-oral manipulation in the perception of sensory attributes." Appetite 40(1): 1-7.

De Wijk, R. A., J. F. Prinz and A. M. Janssen (2006). "Explaining perceived oral texture of starch-based custard desserts from standard and novel instrumental tests." Food Hydrocolloids 20(1): 24-34.

Dea, A., D. Eves, E. R. Kilcast and Morris (1989). Relationship of electromyographic evaluation of semi-fluid model food systems with dynamic shear viscosity. Gums and stabilisers for the fodd industry. G.O.Phillips, D.J. Wedlock and P. A. Williams. Oxford, 4IRL ltd: 241-246.

Debruijne, D. W., H. A. C. M. Hendrickx, L. Alderliesten and J. Delooff (1993). "Mouthfeel of Foods." Food Colloids and Polymers : Stability and Mechanical Properties 113: 204-213.

Denson, C. D. (1973). "Implications of extensional flows in polymer fabrication processes." Polymer Engineering & Science 13(2): 125-130.

Desbrieres, J., M. Hirrien and S. B. Ross-Murphy (2000). "Thermogelation of methylcellulose: rheological considerations." Polymer 41(7): 2451-2461.

Dickie, A. M. and J. L. Kokini (1983). "An Improved Model for Food Thickness from Non-Newtonian Fluid-Mechanics in the Mouth." Journal of Food Science 48(1): 57-&.

Dodds, M. W. J., D. A. Johnson and C.-K. Yeh (2005). "Health benefits of saliva: a review." Journal of Dentistry 33(3): 223-233.

Dresselhuis, D. M., E. H. A. de Hoog, M. A. Cohen Stuart, M. H. Vingerhoeds and G. A. van Aken (2008a). "The occurrence of in-mouth coalescence of emulsion droplets in relation to perception of fat." Food Hydrocolloids 22(6): 1170-1183.

Dresselhuis, D. M., E. H. A. de Hoog, M. A. C. Stuart and G. A. van Aken (2008b). "Application of oral tissue in tribological measurements in an emulsion perception context." Food Hydrocolloids 22(2): 323-335.

du Toit, D. F. (2003). "The tongue: structure and function relevant to disease and oral health." SADJ 58(9): 375-376, 380-373.

Emmelin, N. and J. Holmberg (1967). "Impulse Frequency in Secretory Nerves of Salivary Glands." Journal of Physiology-London 191(1): 205-&.

Engelen, L. (2012). Oral Receptors. Food Oral Processing, Wiley-Blackwell: 15-43.

Engelen, L., R. A. de Wijk, J. F. Prinz, A. M. Janssen, A. van der Bilt, H. Weenen and F. Bosman (2003). "A comparison of the effects of added saliva, alpha-amylase and water on texture perception in semisolids." Physiology & Behavior 78(4-5): 805-811.

Engelen, L., A. Fontijn-Tekamp and A. v. d. Bilt (2005). "The influence of product and oral characteristics on swallowing." Archives of Oral Biology 50(8): 739-746.

Entov, V. M. and E. J. Hinch (1997). "Effect of a spectrum of relaxation times on the capillary thinning of a filament of elastic liquid." Journal of Non-Newtonian Fluid Mechanics 72(1): 31-53.

Ertmer, C., S. Rehberg, H. Van Aken and M. Westphal (2009). "Relevance of non-albumin colloids in intensive care medicine." Best Practice & Research Clinical Anaesthesiology 23(2): 193-212.

Escofier, B. and J. Pagès (1994). "Multiple factor analysis (AFMULT package)." Computational Statistics & Data Analysis 18(1): 121-140.

Feller, R. P., I. M. Sharon, H. H. Chauncey and I. L. Shannon (1965). "Gustatory Perception of Sour Sweet and Salt Mixtures Using Parotid Gland Flow Rate." Journal of Applied Physiology 20(6): 1341-&.

Ferguson, D. B., Ed. (1999). Oral Bioscience, Edinburgh: Churchill Livingstone.

Ferry, A. L., J. Hort, J. R. Mitchell, D. J. Cook, S. Lagarrigue and B. V. Pamies (2006a). "Viscosity and flavour perception: Why is starch different from hydrocolloids?" Food Hydrocolloids 20(6): 855-862.

Ferry, A. L., J. Hort, J. R. Mitchell, S. Lagarrigue and B. V. Pamies (2004). "EFFECT OF AMYLASE ACTIVITY ON STARCH PASTE VISCOSITY AND ITS IMPLICATIONS FOR FLAVOR PERCEPTION." Journal of Texture Studies 35(5): 511-524.

Ferry, A. L. S., J. R. Mitchell, J. Hort, S. E. Hill, A. J. Taylor, S. Lagarrigue and B. Valles-Pamies (2006b). "In-mouth amylase activity can reduce perception of saltiness in starch-thickened foods." Journal of Agricultural and Food Chemistry 54(23): 8869-8873.

Fiebrig, I., S. E. Harding, A. J. Rowe, S. C. Hyman and S. S. Davis (1995). "Transmission electron microscopy studies on pig gastric mucin and its interactions with chitosan." Carbohydrate Polymers 28(3): 239-244.

Fischer, U., R. B. Boulton and A. C. Noble (1994). "Physiological factors contributing to the variability of sensory assessments: Relationship between salivary flow rate and temporal perception of gustatory stimuli." Food Quality and Preference 5(1–2): 55-64.

Fitzpatrick, P., J. Meadows, I. Ratcliffe and P. A. Williams (2013). "Control of the properties of xanthan/glucomannan mixed gels by varying xanthan fine structure." Carbohydrate Polymers 92(2): 1018-1025.

Foster, T. J. (2010). "Technofunctionality of Hydrocolloids and Their Impact on Food Structure." Gums and Stabilisers for the Food Industry 15: 103-112.

Froehlich, D. A., R. M. Pangborn and J. R. Whitaker (1987a). "The Effect of Oral-Stimulation on Human-Parotid Salivary Flow-Rate and Alpha-Amylase Secretion." Physiology & Behavior 41(3): 209-217.

Froehlich, D. A., R. M. Pangborn and J. R. Whitaker (1987b). "The effect of oral stimulation on human parotid salivary flow rate and alpha-amylase secretion." Physiology & Behavior 41(3): 209-217.

Funami, T. (2011). "Fundamental Properties and Food Application of Hydrocolloids." Journal of the Japanese Society for Food Science and Technology-Nippon Shokuhin Kagaku Kogaku Kaishi 58(4): 137-149.

Gabriele, A., F. Spyropoulos and I. T. Norton (2010). "A conceptual model for fluid gel lubrication." Soft Matter 6(17): 4205-4213.

Garcia-Ochoa, F., V. E. Santos, J. A. Casas and E. Gomez (2000). "Xanthan gum: production, recovery, and properties." Biotechnology Advances 18(7): 549-579.

Garrec, D. A. and I. T. Norton (2012). "The influence of hydrocolloid hydrodynamics on lubrication." Food Hydrocolloids In Press, Corrected Proof.

Giasson, S., J. Israelachvili and H. Yoshizawa (1997). "Thin Film Morphology and Tribology Study of Mayonnaise." Journal of Food Science 62(4): 640-652.

Gibson, J. and J. A. Beeley (1994). "Natural and synthetic saliva: a stimulating subject." Biotechnol Genet Eng Rev 12: 39-61.

Gilbertson, T. A., S. Damak and R. F. Margolskee (2000). "The molecular physiology of taste transduction." Current Opinion in Neurobiology 10(4): 519-527.

Glendinning, J. I. (1992). "Effect of Salivary Proline-Rich Proteins on Ingestive Responses to Tannic-Acid in Mice." Chemical Senses 17(1): 1-12.

Guinard, J.-X. and R. Mazzucchelli (1996). "The sensory perception of texture and mouthfeel." Trends in Food Science & Technology 7(7): 213-219.

Guinard, J. X., C. ZoumasMorse, C. Walchak and H. Simpson (1997). "Relation between saliva flow and flavor release from chewing gum." Physiology & Behavior 61(4): 591-596.

Hamada, E., T. Nakajima, Y. Hata, H. Hazama, K. Iwasawa, M. Takahashi, S.-i. Ota and M. Omata (1997). "Effect of caffeine on mucus secretion and agonist-dependent Ca2+ mobilization in human gastric mucus secreting cells." Biochimica et Biophysica Acta (BBA) - Molecular Cell Research 1356(2): 198-206.

Hand, D. J., H. Mannila and P. Smyth (2001). Principles of data mining. Cambridge, Mass., MIT Press.

Harding, S. E. (1989). The Macrostructure of Mucus Glycoproteins in Solution. Advances in Carbohydrate Chemistry and Biochemistry. R. S. Tipson and H. Derek, Academic Press. Volume 47: 345-381.

Harding, S.E. (2006). "Trends in mucoadhesive analysis." Trends in Food Science & Technology, **17**(5): p. 255-262.

Härdle, W. and L. o. Simar (2012). Applied multivariate statistical analysis. Heidelberg ; New York, Springer.

Harte, F., S. Clark and G. V. Barbosa-Cánovas (2007). "Yield stress for initial firmness determination on yogurt." Journal of Food Engineering 80(3): 990-995.

Haward, S. J., J. A. Odell, M. Berry and T. Hall (2011). "Extensional rheology of human saliva." Rheologica Acta 50(11-12): 869-879.

Heath, M. R. (2002). "The oral management of food: the bases of oral success and for understanding the sensations that drive us to eat." Food Quality and Preference 13(7-8): 453-461.

Hewson, L., T. Hollowood, S. Chandra and J. Hort (2008). "Taste-aroma interactions in a citrus flavoured model beverage system: Similarities and differences between acid and sugar type." Food Quality and Preference 19(3): 323-334.

Heyer, P. and J. Lauger (2008). "A flexible platform for tribological measurements on a rheometer." Xvth International Congress on Rheology - the Society of Rheology 80th Annual Meeting, Pts 1 and 2 1027: 1168-1170.

Hiiemae, K. (2004). "MECHANISMS OF FOOD REDUCTION, TRANSPORT AND DEGLUTITION: HOW THE TEXTURE OF FOOD AFFECTS FEEDING BEHAVIOR." Journal of Texture Studies 35(2): 171-200.

Hill, M. A., J. R. Mitchell and P. A. Sherman (1995). "The Relationship between the Rheological and Sensory Properties of a Lemon Pie Filling." Journal of Texture Studies 26(4): 457-470.

Hodson, N. A. and R. W. A. Linden (2006). "The effect of monosodium glutamate on parotid salivary flow in comparison to the response to representatives of the other four basic tastes." Physiology & Behavior 89(5): 711-717.

Hollowood, T., S. Bayarri, L. Marciani, J. Busch, S. Francis, R. Spiller, A. Taylor and J. Hort (2008). "Modelling sweetness and texture perception in model emulsion systems." European Food Research and Technology 227(2): 537-545.

Hollowood, T. A., J. M. Davidson, L. DeGroot, R. S. T. Linforth and A. J. Taylor (2000). Taste release and its effect on overall flavor perception, San Francisco, Ca, Amer Chemical Soc.

Hollowood, T. A., R. S. T. Linforth and A. J. Taylor (2002). "The effect of viscosity on the perception of flavour." Chemical Senses 27(7): 583-591.

Hort, J. and T. A. Hollowood (2004). "Controlled continuous flow delivery system for investigating taste-aroma interactions." Journal of Agricultural and Food Chemistry 52(15): 4834-4843.

Huang, A. L., X. K. Chen, M. A. Hoon, J. Chandrashekar, W. Guo, D. Trankner, N. J. P. Ryba and C. S. Zuker (2006). "The cells and logic for mammalian sour taste detection." Nature 442(7105): 934-938.

Humphrey, S. P. and R. T. Williamson (2001). "A review of saliva: Normal composition, flow, and function." Journal of Prosthetic Dentistry 85(2): 162-169.

Hutchings, J. B. and P. J. Lillford (1988). "THE PERCEPTION OF FOOD TEXTURE - THE PHILOSOPHY OF THE BREAKDOWN PATH." Journal of Texture Studies 19(2): 103-115.

Imai, A., M. Tanaka, M. Tatsuta and T. Kawazoe (1995). "Ultrasonographic images of tongue movement during mastication." J Osaka Dent Univ 29(2): 61-69.

Isono, Y. and J. D. Ferry (1985). "Stress-Relaxation and Differential Dynamic Modulus of Polyisobutylene in Large Shearing Deformations." Journal of Rheology 29(3): 273-280.

James, D. F. (2009). "Boger Fluids." Annual Review of Fluid Mechanics 41: 129-142.

James, D. F. and K. Walters (1993). A Critical Appraisal of Available Methods for the Measurement of Extensional Properties of Mobile Systems. Techniques in Rheological Measurement. A. A. Collyer, Springer Netherlands: 33-53.

Janssen, A. M., A. M. van de Pijpekamp and D. Labiausse (2009). "Differential saliva-induced breakdown of starch filled protein gels in relation to sensory perception." Food Hydrocolloids 23(3): 795-805.

Kesimer, M. and J. K. Sheehan (2008). "Analyzing the functions of large glycoconjugates through the dissipative properties of their absorbed layers using the gel-forming mucin MUC5B as an example." Glycobiology 18(6): 463-472.

Khan, N. A. and P. Besnard (2009). "Oro-sensory perception of dietary lipids: New insights into the fat taste transduction." Biochimica Et Biophysica Acta-Molecular and Cell Biology of Lipids 1791(3): 149-155.

Kinnamon, S. C. (1996). "Taste transduction: Linkage between molecular mechanisms and psychophysics." Food Quality and Preference 7(3–4): 153-159.

Kinnamon, S. C. and R. F. Margolskee (1996). "Mechanisms of taste transduction." Current Opinion in Neurobiology 6(4): 506-513.

Koc, H., C. J. Vinyard, G. K. Essick and E. A. Foegeding (2013). "Food Oral Processing: Conversion of Food Structure to Textural Perception." Annual Review of Food Science and Technology, Vol 4 4: 237-266.

Kokini, J. L. (1985). "Fluid and Semi-Solid Food Texture and Texture Taste Interactions." Food Technology 39(11): 86-&.

Kokini, J. L. (1987). "The physical basis of liquid food texture and texture-taste interactions." Journal of Food Engineering 6(1): 51-81.

Kokini, J. L. and E. L. Cussler (1983). "Predicting the Texture of Liquid and Melting Semi-Solid Foods." Journal of Food Science 48(4): 1221-1225.

Kokini, J. L., J. B. Kadane and E. L. Cussler (1977). "Liquid texture perceived in mouth." Journal of Texture Studies 8(2): 195-218.

Kokini, J. L. and K. Surmay (1994). "Steady Shear Viscosity First Normal Stress Difference and Recoverable Strain in Carboxymethyl Cellulose, Sodium Alginate and Guar Gum." Carbohydrate Polymers 23(1): 27-33.

Koliandris, A.-L., C. Morris, L. Hewson, J. Hort, A. J. Taylor and B. Wolf (2010). "Correlation between saltiness perception and shear flow behaviour for viscous solutions." Food Hydrocolloids 24(8): 792-799.

Koliandris, A., A. Lee, A. L. Ferry, S. Hill and J. Mitchell (2008). "Relationship between structure of hydrocolloid gels and solutions and flavour release." Food Hydrocolloids 22(4): 623-630.

Koliandris, A. L., E. Rondeau, L. Hewson, J. Hort, A. J. Taylor, J. Cooper-White and B. Wolf (2011). "Food Grade Boger Fluids for Sensory Studies." Applied Rheology 21(1).

Kool, M. M., H. A. Schols, R. J. B. M. Delahaije, G. Sworn, P. A. Wierenga and H. Gruppen (2013). "The influence of the primary and secondary xanthan structure on the enzymatic hydrolysis of the xanthan backbone." Carbohydrate Polymers 97(2): 368-375.

Kramer, J., J. T. Uhl and R. K. Prudhomme (1987). "Measurement of the Viscosity of Guar Gum Solutions to 50,000 S-1 Using a Parallel Plate Rheometer." Polymer Engineering and Science 27(8): 598-602.

Lauger, J. and P. Heyer (2009). "Temperature-Dependent Rheology and Tribology of Lubrication Greases Investigated with New Flexible Platform for Tribological Measurements on A Rheometer." Advanced Tribology: 61-63.

Lawless, H. T. and H. Heymann (2010). Sensory evaluation of food : principles and practices. New York, Springer.

Lee, H. C. and D. A. Brant (2002). "Rheology of concentrated isotropic and anisotropic xanthan solutions. 2. A semiflexible wormlike intermediate molecular weight sample." Macromolecules 35(6): 2223-2234.

Lucas, P. W., J. F. Prinz, K. R. Agrawal and I. C. Bruce (2002). "Food physics and oral physiology." Food Quality and Preference 13(4): 203-213.

Luengo, G., M. Tsuchiya, M. Heuberger and J. Israelachvili (1997). "Thin Film Rheology and Tribology of Chocolate." Journal of Food Science 62(4): 767-812.

Macakova, L., G. E. Yakubov, M. A. Plunkett and J. R. Stokes (2010). "Influence of ionic strength changes on the structure of pre-adsorbed salivary films. A response of a natural multi-component layer." Colloids and Surfaces B-Biointerfaces 77(1): 31-39.

Macakova, L., G. E. Yakubov, M. A. Plunkett and J. R. Stokes (2011). "Influence of ionic strength on the tribological properties of pre-adsorbed salivary films." Tribology International 44(9): 956-962.

Macosko, C. W. (1994). Rheology - Principles, Measurements and Applications, John Wiley & Sons.

Maina, N. H., L. Virkki, H. Pynnonen, H. Maaheirno and M. Tenkanen (2011). "Structural Analysis of Enzyme-Resistant Isomaltooligosaccharides Reveals the Elongation of alpha-(1 -> 3)-Linked Branches in Weissella confusa Dextran." Biomacromolecules 12(2): 409-418.

Malkin, A. Y. and A. I. Isayev (2012). Rheology - Concepts, Methods, and Applications (2nd Edition), ChemTec Publishing.

Malkki, Y., R. L. Heini and K. Autio (1993). "Influence of oat gum, guar gum and carboxymethyl cellulose on the perception of sweetness and flavour." Food Hydrocolloids 6(6): 525-532.

Mälkki, Y., R. L. Heiniö and K. Autio (1993). "Influence of oat gum, guar gum and carboxymethyl cellulose on the perception of sweetness and flavour." Food Hydrocolloids 6(6): 525-532.

Malone, M. E., I. A. M. Appelqvist and I. T. Norton (2003). "Oral behaviour of food hydrocolloids and emulsions. Part 1. Lubrication and deposition considerations." Food Hydrocolloids 17(6): 763-773.

Mandel, I. D. (1987). "The Functions of Saliva." Journal of Dental Research 66: 623-627.

Mannarswamy, A., S. H. Munson-McGee and P. K. Andersen (2010). "D-optimal designs for the Cross viscosity model applied to guar gum mixtures." Journal of Food Engineering 97(3): 403-409.

Matsuo, R. (2000). "Role of saliva in the maintenance of taste sensitivity." Critical Reviews in Oral Biology & Medicine 11(2): 216-229.

Matz, S. A. (1962). Food texture. Westport, Conn.,, Avi Pub. Co.

Matz, S. A. (1963). "Food Texture - Matz,Sa." Royal Society of Health Journal 83(6): 309-309.

McCurdy, R. D., H. D. Goff, D. W. Stanley and A. P. Stone (1994). "Rheological properties of dextran related to food applications." Food Hydrocolloids 8(6): 609-623.

McKinley, G. H. and A. Tripathi (2000). "How to extract the Newtonian viscosity from capillary breakup measurements in a filament rheometer." Journal of Rheology 44(3): 653-670.

Meullenet, J. F., R. Xiong and C. J. Findlay (2007). Multivariate and probabilistic analyses of sensory science problems. Chicago, Blackwell Pub.

Miller, E., C. Clasen and J. P. Rothstein (2009). "The effect of step-stretch parameters on capillary breakup extensional rheology (CaBER) measurements." Rheologica Acta 48(6): 625-639.

Mitchell, J. R. and B. Wolf (2011). Relationship between Food Rheology and Perception. Practical Food Rheolgy:An Interpretive Approach. I. T. Norton, F. Spyropulos and P. Cox. Oxford, Wiley-Blackwell.

Monsan, P., S. Bozonnet, C. Albenne, G. Joucla, R.-M. Willemot and M. Remaud-Siméon (2001). "Homopolysaccharides from lactic acid bacteria." International Dairy Journal 11(9): 675-685.

Mooi, E. and M. Sarstedt (2011). "A concise guide to market research: the process, data and methods using IBM SPSS statistics." International Journal of Market Research 53(4): 563-564.

Morris, E. R., R. K. Richardson and L. J. Taylor (1984). "Correlation of the perceived texture of random coil polysaccharide solutions with objective parameters." Carbohydrate Polymers 4(3): 175-191.

Morris, E. R. and L. J. Taylor (1982). "ORAL PERCEPTION OF FLUID VISCOSITY." Progress in Food and Nutrition Science 6(1-6): 285-296.

Morris, V. J. (2006). Bacterial Polysaccharides. Food Polysaccharides and Their Applications, CRC Press: 413-454.

Moskowitz, H. R. and P. Arabie (1970). "TASTE INTENSITY AS A FUNCTION OF STIMULUS CONCENTRATION AND SOLVENT VISCOSITY." Journal of Texture Studies 1(4): 502-510.

Næs, T., P. B. Brockhoff and O. Tomić (2010). Statistics for sensory and consumer science. Chichester, West Sussex, Wiley.

Navazesh, M. (1993). "Methods for Collecting Saliva." Annals of the New York Academy of Sciences 694: 72-77.

Negoias, S., R. Visschers, A. Boelrijk and T. Hummel (2008). "New ways to understand aroma perception." Food Chemistry 108(4): 1247-1254.

Neyraud, E., C. I. Heinzerling, J. H. F. Bult, C. Mesmin and E. Dransfield (2009). "Effects of Different Tastants on Parotid Saliva Flow and Composition." Chemosensory Perception 2(2): 108-116.

Nicosia, M. A. and J. Robbins (2001). "The fluid mechanics of bolus ejection from the oral cavity." Journal of Biomechanics 34(12): 1537-1544.

Nomura, H., S. Koda and F. Hattori (1990). "Viscosity of aqueous solutions of polysaccharides and their carboxylate derivatives." Journal of Applied Polymer Science 41(11-12): 2959-2969.

Norton, I. T. and T. J. Foster (2002). "Hydrocolloids in real food systems." Gums and Stabilisers for the Food Industry 11(278): 187-200.

Nyström, B., A.-L. Kjøniksen, N. Beheshti, A. Maleki, K. Zhu, K. D. Knudsen, R. Pamies, J. G. Hernández Cifre and J. García de la Torre (2010). "Characterization of polyelectrolyte features in polysaccharide systems and mucin." Advances in Colloid and Interface Science 158(1–2): 108-118.

Omahony, M. (1979). "Salt Taste Adaptation - Psychophysical Effects of Adapting Solutions and Residual Stimuli from Prior Tastings on the Taste of Sodium-Chloride." Perception 8(4): 441-476.

Omahony, M. and C. Heintz (1981). "Direct Magnitude Estimation of Salt Taste Intensity with Continuous Correction for Salivary Adaptation." Chemical Senses 6(2): 101-112.

Pages, J. (2003). "Direct collection of sensory distances: application to the evaluation of ten white wines of the Loire Valley." Sciences Des Aliments 23(5-6): 679-688.

Pagès, J. (2005). "Collection and analysis of perceived product inter-distances using multiple factor analysis: Application to the study of 10 white wines from the Loire Valley." Food Quality and Preference 16(7): 642-649.

Pangborn, R. M. and C. M. Chung (1981). "Parotid Salivation in Response to Sodium Chloride and Monosodium Glutamate in Water and in Broths." Appetite 2(4): 380-385.

Pangborn, R. M., Z. M. Gibbs and C. Tassan (1978). "Effect of Hydrocolloids on Apparent Viscosity and Sensory Properties of Selected Beverages." Journal of Texture Studies 9(4): 415-436.

Pangborn, R. M. and A. S. Szczesniak (1974). "EFFECT OF HYDROCOLLOIDS AND VISCOSITY ON FLAVOR AND ODOR INTENSITIES OF AROMATIC FLAVOR COMPOUNDS*." Journal of Texture Studies 4(4): 467-482.

Pangborn, R. M., I. M. Trabue and A. S. Szczesniak (1973). "EFFECT OF HYDROCOLLOIDS ON ORAL VISCOSITY AND BASIC TASTE INTENSITIES *." Journal of Texture Studies 4(2): 224-241.

Papageorgiou, D. T. (1995). "On the Breakup of Viscous-Liquid Threads." Physics of Fluids 7(7): 1529-1544.

Park, J. S. and E. Ruckenstein (2001). "Viscoelastic properties of plasticized methylcellulose and chemically crosslinked methylcellulose." Carbohydrate Polymers 46(4): 373-381.

Paulus, K. and E. M. Haas (1980). "The Influence of Solvent Viscosity on the Threshold Values of Primary Tastes." Chemical Senses 5(1): 23-32.

Perrin, L., R. Symoneaux, I. Maître, C. Asselin, F. Jourjon and J. Pagès (2008). "Comparison of three sensory methods for use with the Napping® procedure: Case of ten wines from Loire valley." Food Quality and Preference 19(1): 1-11.

Petrie, C. J. S. (2006). "Extensional viscosity: A critical discussion." Journal of Non-Newtonian Fluid Mechanics 137(1–3): 15-23.

Pfeiffer, J. C., J. Hort, T. A. Hollowood and A. J. Taylor (2006). "Taste-aroma interactions in a ternary system: A model of fruitiness perception in sucrose/acid solutions." Perception & Psychophysics 68(2): 216-227.

Prinz, J. F., R. A. de Wijk and L. Huntjens (2007). "Load dependency of the coefficient of friction of oral mucosa." Food Hydrocolloids 21(3): 402-408.

Prinz, J. F. and P. W. Lucas (1995). "Swallow thresholds in human mastication." Archives of Oral Biology 40(5): 401-403.

Proctor, G. B., S. Hamdan, G. H. Carpenter and P. Wilde (2005). "A statherin and calcium enriched layer at the air interface of human parotid saliva." Biochemical Journal 389: 111-116.

Rao, M. A. (2007). Rheology of fluid and semisolid foods : principles and applications. New York, Springer.

Richardson, R. K., E. R. Morris, S. B. Ross-Murphy, L. J. Taylor and I. C. M. Dea (1989a). "Characterization of the perceived texture of thickened systems by dynamic viscosity measurements." Food Hydrocolloids 3(3): 175-191.

Richardson, R. K., E. R. Morris, S. B. Ross-Murphy, L. J. Taylor and I. C. M. Dea (1989b). "Characterization of the perceived texture of thickened systems by dynamic viscosity measurements." Food Hydrocolloids 3(3): 175-192.

Roberts, K. T. (2011). "The physiological and rheological effects of foods supplemented with guar gum." Food Research International 44(5): 1109-1114.

Rodd, L. E., T. P. Scott, J. J. Cooper-White and G. H. McKinley (2005). "Capillary breakup rheometry of low-viscosity elastic fluids." Applied Rheology 15(1): 12-27.

Roper, S. D. (2007). "Signal transduction and information processing in mammalian taste buds." Pflugers Archiv-European Journal of Physiology 454(5): 759-776.

Ross, C. F. (2009). "Sensory science at the human-machine interface." Trends in Food Science & Technology 20(2): 63-72.

Rossetti, D., G. E. Yakubov, J. R. Stokes, A. M. Williamson and G. G. Fuller (2008). "Interaction of human whole saliva and astringent dietary compounds investigated by interfacial shear rheology." Food Hydrocolloids 22(6): 1068-1078.

Rozin, P. (1982). ""Taste-smell confusions" and the duality of the olfactory sense." Perception & Psychophysics 31(4): 397-401.

Rubinstein, A. (2000). "Natural polysaccharides as targeting tools of drugs to the human colon." Drug Development Research 50(3-4): 435-439.

Sanz, T., M. A. Fernández, A. Salvador, J. Muñoz and S. M. Fiszman (2005). "Thermogelation properties of methylcellulose (MC) and their effect on a batter formula." Food Hydrocolloids 19(1): 141-147.

Schipper, R. G., E. Silletti and M. H. Vinyerhoeds (2007). "Saliva as research material: Biochemical, physicochemlical and practical aspects." Archives of Oral Biology 52(12): 1114-1135.

Schwarz, W. H. (1987a). "The Rheology of Saliva." Journal of Dental Research 66: 660-666.

Schwarz, W. H. (1987b). "The rheology of saliva." J Dent Res 66 Spec No: 660-666.

Selway, N. and J. R. Stokes (2013). "Insights into the dynamics of oral lubrication and mouthfeel using soft tribology: Differentiating semi-fluid foods with similar rheology." Food Research International 54(1): 423-431.

Shama, F., C. Parkinson and P. Sherman (1973). "Identification of stimuli controlling the sensory evaluation of viscosity I:Non-Oral Methods. ." Journal of Texture Studies 4(1): 102-110.

Shama, F. and P. Sherman (1973). "Identification of stimuli controlling the sensory evaluation of viscosity II:Oral Methods. ." Journal of Texture Studies 4(1): 111-118.

Shaw, M. T. and Z. H. Z. Liu (2006). "Single-point determination of nonlinear rheological data from parallel-plate torsional flow." Applied Rheology 16(2): 70-79.

Shi, L. and K. D. Caldwell (2000). "Mucin adsorption to hydrophobic surfaces." Journal of Colloid and Interface Science 224(2): 372-381.

Silletti, E., M. H. Vingerhoeds, W. Norde and G. A. van Aken (2007). "The role of electrostatics in saliva-induced emulsion flocculation." Food Hydrocolloids 21(4): 596-606.

Silletti, E., M. H. Vingerhoeds, G. A. Van Aken and W. Norde (2008). "Rheological behavior of food emulsions mixed with saliva: Effect of oil content, salivary protein content, and saliva type." Food Biophysics 3(3): 318-328.

Song, K. W., Y. S. Kim and G. S. Chang (2006). "Rheology of concentrated xanthan gum solutions: Steady shear flow behavior." Fibers and Polymers 7(2): 129-138.

Speirs, R. L. (1971a). "The effects of interactions between gustatory stimulation the reflex flow-rate of human parotid saliva." Archives of Oral Biology 16(4): 349-365.

Speirs, R. L. (1971b). "The effects of interactions between gustatory stimuli on the reflex flow-rate of human parotid saliva." Archives of Oral Biology 16(4): 351-365.

Stedman, T. L., Ed. (2005). Stedman's Medical Dictionary, Lippincott Williams and Wilkins.

Steffe, J. F. (1996). Rheological methods in food process engineering. East Lansing, MI, Freeman Press.

Stelter, M. and G. Brenn (2000). "Validation and application of a novel elongational device for polymer solutions." Journal of Rheology 44(3): 595-616.

Stokes, J. R. (2012a). 'Oral' Rheology. Food Oral Processing, Wiley-Blackwell: 225-263.

Stokes, J. R. (2012b). 'Oral' Tribology. Food Oral Processing, Wiley-Blackwell: 265-287.

Stokes, J. R., M. W. Boehm and S. K. Baier (2013). "Oral processing, texture and mouthfeel: From rheology to tribology and beyond." Current Opinion in Colloid & Interface Science 18(4): 349-359.

Stokes, J. R. and G. A. Davies (2007). "Viscoelasticity of human whole saliva collected after acid and mechanical stimulation." Biorheology 44(3): 141-160.

Stokes, J. R., L. Macakova, A. Chojnicka-Paszun, C. G. de Kruif and H. H. J. de Jongh (2011). "Lubrication, Adsorption, and Rheology of Aqueous Polysaccharide Solutions." Langmuir 27(7): 3474-3484.

Stone, H. and S. Oliver (1966). "Effect of Viscosity on Detection of Relative Sweetness Intensity of Sucrose Solutions." Journal of Food Science 31(1): 129-&.

Stone, H., J. Sidel, S. Oliver, A. Woolsey and Singleto.Rc (1974). "Sensory Evaluation by Quantitative Descriptive Analysis." Food Technology 28(11): 24-&.

Sworn, G. (2009). "Xanthan gum." Handbook of hydrocolloids.

Sworn, G. (2011). Xanthan Gum – Functionality and Application. Practical Food Rheology, Wiley-Blackwell: 85-112.

Szczesniak, A. S. (2002). "Texture is a sensory property." Food Quality and Preference 13(4): 215-225.

Szczesniak, A. S. and E. Farkas (1962). "Objective Characterization of Mouthfeel of Gum Solutions." Journal of Food Science 27(4): 381-&.

Taylor, A., T. Hollowood, J. Davidson, D. Cook and R. Linforth (2002). Relating taste, aromla and mouthfeel stimuli to overall flavour perception, Beaune, France, Lavoisier - Tec & Doc.

Taylor, A. J., S. Besnard, M. Puaud and R. S. T. Linforth (2001). "In vivo measurement of flavour release from mixed phase gels." Biomolecular Engineering 17(4-5): 143-150.

Taylor, A. J., R. S. T. Linforth, B. A. Harvey and B. Blake (1999). Atmospheric pressure chemical ionisation mass spectrometry for in vivo analysis of volatile flavour release, Udine, Italy, Elsevier Sci Ltd.

Taylor, A. J., R. S. T. Linforth, B. A. Harvey and B. Blake (2000). Atmospheric pressure chemical ionisation mass spectrometry for in vivo analysis of volatile flavour release, Udine, Italy, Elsevier Sci Ltd.

Terpstra, M. E. J., R. H. Jellema, A. M. Janssen, R. A. de Wijk, J. F. Prinz and E. van der Linden (2009). "Prediction of Texture Perception of Mayonnaises from Rheological and Novel Instrumental Measurements." Journal of Texture Studies 40(1): 82-108.

Thoreau, V., L. Boulange and J. C. Joud (2005). "Adsorption from Dextran solutions: influence of stainless steel substrates." Colloids and Surfaces a-Physicochemical and Engineering Aspects 261(1-3): 141-146.

Trouton, F. T. (1906). "On the coefficient of viscous traction and its relation to that of viscosity." Proceedings of the Royal Society of London Series a-Containing Papers of a Mathematical and Physical Character 77(519): 426-440.

Trulsson, M. (2006). "Sensory-motor function of human periodontal mechanoreceptors." Journal of Oral Rehabilitation 33(4): 262-273.

Trulsson, M. and R. S. Johansson (1996). "Encoding of tooth loads by human periodontal afferents and their role in jaw motor control." Progress in Neurobiology 49(3): 267-284.

Turner, R. J. and H. Sugiya (2002). "Understanding salivary fluid and protein secretion." Oral Dis 8(1): 3-11.

Vaisey, M., R. Brunon and J. Cooper (1969). "Some Sensory Effects of Hydrocolloid Sols on Sweetness." Journal of Food Science 34(5): 397-&.

Van der Reijden, W. A., E. C. I. Veerman and A. V. N. Amerongen (1993a). "Shear Rate-Dependent Viscoelastic Behavior of Human Glandular Salivas." Biorheology 30(2): 141-152.

Van der Reijden, W. A., E. C. I. Veerman and A. V. N. Amerongen (1993b). "Shear Rate-Dependent Viscoelastic Behavior of Human Glandular Salivas (Vol 30, Pg 141, 1993)." Biorheology 30(3-4): 301-301.

van Vliet, T. (2002). "On the relation between texture perception and fundamental mechanical parameters for liquids and time dependent solids." Food Quality and Preference 13(4): 227-236.

Vardhanabhuti, B., P. W. Cox, I. T. Norton and E. A. Foegeding (2011). "Lubricating properties of human whole saliva as affected by β-lactoglobulin." Food Hydrocolloids 25(6): 1499-1506.

Veerman, E. C., M. Valentijn-Benz and A. V. Nieuw Amerongen (1989). "Viscosity of human salivary mucins: effect of pH and ionic strength and role of sialic acid." J Biol Buccale 17(4): 297-306.

Vimal Kumar Yadav, A.B. Gupta, Raj Kumar, Jaideep S. Yadav and B. Kumar (2010). "Mucoadhesive Polymers: Means of Improving the Mucoadhesive Properties of Drug Delivery System " Journal of Chemical and Pharmaceutical Research 2(5): 418-432.

Vingerhoeds, M. H., T. B. J. Blijdenstein, F. D. Zoet and G. A. van Aken (2005). "Emulsion flocculation induced by saliva and mucin." Food Hydrocolloids 19(5): 915-922.

Wajrock, S., N. Antille, A. Rytz, N. Pineau and C. Hager (2008). "Partitioning methods outperform hierarchical methods for clustering consumers in preference mapping." Food Quality and Preference 19(7): 662-669.

Ward, J. H. (1963). "Hierarchical Grouping to Optimize an Objective Function." Journal of the American Statistical Association 58(301): 236-&.

Waterman, H. A., C. Blom, H. J. Holterman, E. J. s-Gravenmade and J. Mellema (1988). "Rheological properties of human saliva." Archives of Oral Biology 33(8): 589-596.

Wood, F. W. (1968). Psychophysical studies on the consistency of liquid foods. S.C.I. monograph: Rheology and texture of foodstuffs: 40-49.

Yamamoto, K., M. Kurihara, Y. Matsusue, M. Imanishi, M. Tsuyuki and T. Kirita (2009). "Whole saliva flow rate and body profile in healthy young adults." Archives of Oral Biology 54(5): 464-469.

Yoon, S. J., D. C. Chu and L. R. Juneja (2008). "Chemical and physical properties, safety and application of partially hydrolized guar gum as dietary fiber." Journal of Clinical Biochemistry and Nutrition 42(1): 1-7.

Zell, A., S. Gier, S. Rafaï and C. Wagner (2010). "Is there a relation between the relaxation time measured in CaBER experiments and the first normal stress coefficient?" Journal of Non-Newtonian Fluid Mechanics 165(19–20): 1265-1274.

Zhang, C. (2009). Investigating aroma-taste-texture interactions in model food systems. PhD Thesis, The University of Nottingham.

Zinoviadou, K. G., A. M. Janssen and H. H. J. de Jongh (2008). "Tribological properties of neutral polysaccharide solutions under simulated oral conditions." Journal of Food Science 73(2): E88-E94.

Zirnsak, M. A., D. V. Boger and V. Tirtaatmadja (1999). "Steady shear and dynamic rheological properties of xanthan gum solutions in viscous solvents." Journal of Rheology (1978-present) 43(3): 627-650.

Zussman, E., A. L. Yarin and R. M. Nagler (2007). "Age- and flow-dependency of salivary viscoelasticity." Journal of Dental Research 86(3): 281-285.